Synthesis and Coordination Chemistry of Ligands for Supramolecular Chemistry and Sensing Applications

Hayley Jane Clayton BSc (Hons)

A thesis submitted to the University of Huddersfield in partial fulfilment of the requirements for the degree of Doctor of Philosophy

University of Huddersfield
Department of Chemical & Biological Sciences
July 2008

In loving memory of Ryan Vickers and Frederick Booth.

Contents

Abstract

A series of multidentate N-donor ligands have been synthesised all containing pyridyl and pyridyl/thiazole units and their coordination behaviour is described.
The ligands are classified into four types; i) terpyridine containing pyridyl/thiazole ligands (L^{1-3}); ii) pyridyl/thiazole ligands containing a 3,3′-disubstituted bipyridine core. (L^{4-8}); iii) 2,2′-bipyridine containing a crown ether moiety (L^{9-11}); and iv) a 2,2′-bipyridine derived ligand containing a urea functional group in the 3,3′-positions (L^{12}).

Chapter II describes terpyridyl/pyridyl/thiazole ligands: - the synthesis of (L^{1-3}) is described and the complexes ($[Cu(L^1)][ClO_4]_2$, $[Ni(L^2)][ClO_4]_2$, $[Co(L^2)][ClO_4]_2$, $[Cd_3(L^3)_2][ClO_4]_6$) structurally characterised. Partitioning of the ligands (L^{1-3}) is dependant on the position of the thiazole ring within the ligand chain. This partitioning is found to occur at a position adjacent to that of the thiazole ring in all but the L^2 ligand complexes, where it is partitioned preferentially at a position creating favourable coordination geometry for the metal ion.

Chapter III describes 3,3′-disubstituted pyridyl/thiazole ligands (L^{4-8}): - the novel potentially hexadentate ligands ($L^{4, 5}$), the potentially octadentate ligand (L^6) and the potentially tetradentate ligands ($L^{7, 8}$) have been synthesized and structurally characterised. All ligands are found to partition at the central pyridine unit due to unfavourable steric interactions to form a pyridyl/thiazole/pyridyl-binding domain (L^{4-6}) and the pyridyl/thiazole-binding domain ($L^{7,8}$). The substituents are found to dominate the control of the formation of complexes produced ($[Zn(L^4)][ClO_4]_2$, $[Cd(L^5)][ClO_4]_2$, $[Cd_2(L^6)_2][ClO_4]_2$, $[Cd_2(L^8)_2][ClO_4]_2$).

Chapter IV, Section 1 describes ditopic bipyridine/crown ether ligands: - the synthesis of (L^{9-11}) is described and the Ru (II) complexes (L^{9-11}) structurally characterised. The Ru(II) complexes of these 3,3′-disubstituted crown ether species were found to luminesce. Modulation of the luminescent properties of the ruthenium complex was investigated with a selection of common cations but resulted in little or no response.

Chapter IV: - Section 2- Ditopic bipyridine/urea ligands: - the novel ligand containing urea substituent side chains (L^{12}) has been synthesised and a ligand containing both pyridine and urea substituents has been synthesised and characterised.

A ruthenium complex (X) was synthesised with ligand (L^{12}) and $(bipy)_2RuCl_2$, the resulting structure confirmed via ^{1}H & ^{13}C NMR as well as electrospray mass spectrometry (ESI-MS). Unfortunately no complexes have been structurally characterised due to the instability and decomposition of the complex after a short period of time. The ruthenium complex however was found to luminesce; ligand/anion recognition studies with complex (X) and a selection of common anions showed a marked change, a ten fold increase in the luminescence was observed with the addition of $H_2PO_4^-$ when in a non-aqueous solvent.

Acknowledgements

A special thank you to Dr Craig Rice for all the support and encouragement he has given me over the last four years. For the guidance, tolerance and enthusiasm he has shown while this project has progressed.

To Paul, a big thank you for your support throughout the last 8 years.

To my family for supporting me all these years, from the very first day they left me in university halls, to my graduation and beyond and to some great friends that I made along the way, especially Abbie and Adele.

Thanks to all my fellow post-graduate students who I've worked alongside during my research, especially to Christian, Ryan, Georgios, Lesley Graham and Christina Loukou.

Finally, thank you to the University of Huddersfield for the funding of this doctorate and for the last eight years of my life here at Huddersfield, as an undergraduate student, and now a postgraduate. I have fond memories that I shall take with me wherever I go and whatever I do in the future.

Abbreviations

%	Percentage
δ	Delta (Chemical shift)
(aq)	Aqueous
Anal	Analysis
bipy	Bipyridine
Calc	Calculated
$CDCl_3$	Deuterated Chloroform
cm^3	Centimetre cubed (Measurement)
d	Doublet
dd	Doublet of Doublets
DMF	dimethylformamide
ESI-MS	Electrospray Ionisation – Mass Spectrometry
g	Grams
Hr	Hour
Hz	Hertz
J	Coupling Constant
M+	Molecular Ion
m	Multiplet
m-CPBA	*Meta*-chloroperoxybenzoic acid
MHz	Mega Hertz
mmol	Millimolar
MS	Mass Spectrometry
m/z	Mass to Charge Ratio (MS)
nm	Nanometres
NMR	Nuclear Magnetic Resonance
ppm	Parts per million
py	Pyridine
s	Singlet
S.G	Specific Gravity
t	Triplet
THF	Tetrahydrofuran
TLC	Thin Layer Chromatography
tpy	Terpyridine
tz	Thiazole
UV/Vis	Ultraviolet / Visible spectrophotometry

CHAPTER I

1.0 Introduction

1.1 Supramolecular chemistry

Jean-Marie Lehn introduced the term supramolecular chemistry and its concept in 1978. He defined it in words, as "supramolecular chemistry is the chemistry of the intermolecular bond, concerning the structure and function of the entities formed by the association of two or more chemical species".[1]

As this new field emerges these initial definitions are often reformulated and many other definitions have since been used including, 'chemistry beyond the molecule',[1] which describes supramolecular chemistry as being more complex than molecular chemistry and molecular covalently bonded systems.

Supramolecular chemistry uses non-covalent intermolecular forces to assemble large molecular architectures held together and organised by binding interactions. Components in a non-covalent system are held together reversibly and the term 'non-covalent' encompasses an enormous range of attractive and repulsive forces.[2] These interactions may include electrostatic forces, hydrogen bonding, $\pi - \pi$ stacking interactions, ion-ion, ion-dipole and dipole-dipole interactions, cation- π interactions and Van de Waals forces.[3]

The goal of supramolecular ligand design, both in nature and in artificial systems, is the achievement of selectivity; the discrimination between one guest and another. The power of supramolecular chemistry lies in the combination of a number of relatively weak interactions that allow a summative, reasonably strong and selective recognition of specific guests to be achieved.[3]

Development of this new field of supramolecular chemistry has been rapid and although it may be possible to trace its concepts back to the beginnings of modern chemistry it is mostly defined as dating back to the late 1960's.[3] The development emerged from the initial studies into the binding of alkali metal cations to natural and synthetic macrocyclic based ligands.[1]

Supramolecular chemistry is a multidisciplinary field, which incorporates organic chemistry, physical chemistry and biology as well as inorganic chemistry.[2]
"A whole new world of unusual and unnatural products have been opened up by the fusion of organic and inorganic chemistry into supramolecular chemistry".[4]

1.2 Non-covalent interactions

Intermolecular forces are relatively weak when compared to covalent bonds so that supramolecular species are i) thermodynamically less stable ii) kinetically more labile and iii) dynamically more flexible than covalent molecules. Due to there relatively weak interactions non-covalent bonds are often called soft bonds and their chemistry 'soft chemistry'.[1]

The individual components that make-up a supramolecular architecture can be brought together by any number of the following interactions; electrostatic forces, hydrogen bonding, $\pi - \pi$ stacking, ion-ion, ion-dipole, dipole-dipole interactions, cation- π interactions or Van der Waals forces.[2] Most of these interactions are relatively weak in energy and it is an accumulation of a number of these interactions that give rise to a stable supramolecular species.[1]

Supramolecular species are characterised both by the special arrangement of their components, architecture or superstructure and by the nature of the intermolecular bond that holds them together. Various types of interaction present different degrees of strength, directionality and dependence on distance and angles.[1]

As already mentioned, the term 'non-covalent' encompasses an enormous range of both attractive and repulsive forces but those ion-dipole interactions are the ones most associated with metallosupramolecular chemistry.

1.3 Self-assembly

Self-assembly is a system of self-arrangement, where the system itself is capable of spontaneously generating a supramolecular architecture from the components it contains, under certain specific conditions.[2,3,4] Self-assembly is a term representative of a system where the evolution of molecular recognition is seen through spontaneous interaction of a number of components (two or more species), in that system to produce a species composed of an intermolecular non-covalent nature. The self-assembly process seen with ligand and metal components is of fundamental interest as it is closely related to the formation of architectures seen in nature, of which DNA is the most significant example.[3,2] "The self-assembly of molecular

components to large supramolecular systems capable of performing specific functions is one of the basic principles in biology".[2,3,4,6]

Self-assembly can be further divided into two sections, namely strict self-assembly and self-assembly with covalent modifications. Strict self-assembly involves the use of purely non-covalent interaction, in contrast to self-assembly with covalent modification. In strict self-assembly the final product assembly is produced solely by the spontaneous combination and recognition of different components when mixed (via the correct ratio, in the correct conditions, temperature, pH, concentration). The product must be reversible and represent the thermodynamic minimum, of which DNA is the famous example. The reversibility of supramolecular self-assembly is key to the resulting systems ability to sift through the available components to form the thermodynamically most favourable structure. This incorporates the potential for self-repair and correction of defects, as is seen in biological systems.[2,6]

1.4 Metallosupramolecular chemistry

Recent trends include the use of transition metal centres to control the assembly of novel supramolecular architectures, this is called "metallosupramolecular chemistry".[4]

Although supramolecular chemistry encompasses a large range of non-covalent, intermolecular interactions, the area of metallosupramolecular chemistry is concerned predominantly with the interactions of transition metal ions and polydentate ligands. The transition metal ion is the core around which polydentate ligands orientate themselves. The area of metallosupramolecular chemistry concerns the matching-up of transition metal ions and their inherent characteristics with the bonding properties of polydentate ligands in order to control the assembly of supramolecular complexes. Transition metal ions have a preference of coordination number and coordination geometry, more formerly the number of donor ligands/atoms bonded to the metal and the arrangement of those donor ligands/atoms in space.[5] The individual units and components that undergo self-assembly are given the term '*tector'* from the Greek meaning of builder. Molecular components contain certain information in the form of specific molecular recognition features, as well as their size, shape and symmetry.[1]

The organic polycyclic ligands are synthetically designed to have pre-organised structures, such that the disposition of binding sites within the ligands enable coordination of more than one ligand to a single metal ion. The term pre-organised denotes that the ligand molecule is instructed to bind a metal in a specific manner. The ligand must have binding sites that are of correct electronic character to complement the metal ion in order to bind. Furthermore those binding sites must be distributed on the ligand in such a way as to make it possible for them to interact with the metal ion. If all these criteria are met by the ligand then the ligand and metal ion are described as complementary. What is seen when these two individual entities are mixed is that appropriately designed species in solution controlled by intermolecular forces lead to the reversible assembly of a supermolecule.

There are a long list of highly specific architectures that can be produced from the coordination of transition metal ions and polydentate ligands. In the sections that follow some of these will be discussed in detail. The formation of the helicate complex is where our attention will be focussed, the formation of 'metallohelicates'.[9]

1.5 Host-Guest Chemistry

To understand host-guest chemistry you must first understand that supramolecular chemistry at the basic level involves the interaction or complexation of two species. These two species are formally known as a host and a guest species. The host is commonly a large molecule or aggregate that possesses convergent binding sites (for example hydrogen bond donors etc). The guest on the other hand may be a simple inorganic anion possessing divergent binding sites (for example a hydrogen bond acceptor halide anion). Host-guest complexes can be typified by the following class of compounds; crown ethers, cryptands and spherands molecular hosts for cations. These examples display significant binding in both the solid state and in solution.

a) Crown Ethers

C.J. Pedersen discovered the crown ethers in 1967. The first crown ether – dibenzo[18] crown-6 discovered by accident as a by-product for the synthesis of the linear di-ol shown in *Figure 1.1*.[7] The crown ethers were so called because of the crown-like shape created upon complexation of this species with a potassium ion. The crown ethers consist simply of cyclic arrangements of alternating ether oxygen atoms and organic spacer groups. The crown ethers showed interesting properties, for example their solubility in methanol (MeOH), increased significantly with the addition of alkali metal salts, they have become popular for various uses, in particular cation complexation.

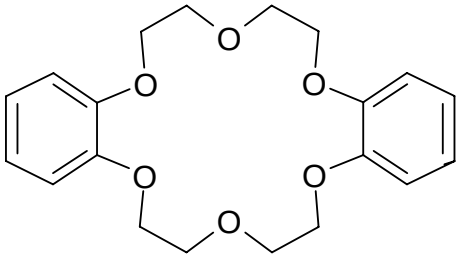

Figure 1.1 Dibenzo [18] crown-6 crown ether

b) Cryptands

Jean-Marie Lehn designed cryptands as a three-dimensional analogue to the crown ether; any such metal ion could be potentially encapsulated within the crown structure. The name cryptand as it suggests is as a result of its mode of action to surround or "entomb" as in a crypt from the Greek "*kruptos*" meaning "hidden".[1] An important compound of this series is the [2.2.2] cryptand, similar in size to the [18] crown-6 species it exhibited selectivity towards the potassium cation and this selectivity was superior to the crown ether. It is believed that this is due to the metal ion being held within a three-dimensional "spherical recognition" cavity.[1]

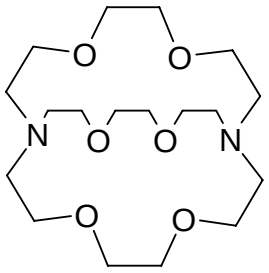

Figure 1.2 [2.2.2] Cryptand

c) Spherands

The third of the host-guest species is that of the spherands developed by Donald Cram. The spherands differ to the former crown ethers and cryptands as they are designed to be inflexible and rigid in structure. By creating this rigid framework the cation binding of oxygen atoms are preorganised and selectivity is increased. The three-dimensional spherand shown below in *Figure 1.3* selectively binds small cations such as Li^+ and Na^+. It is one of the strongest complexants known for Li^+.[6-12]

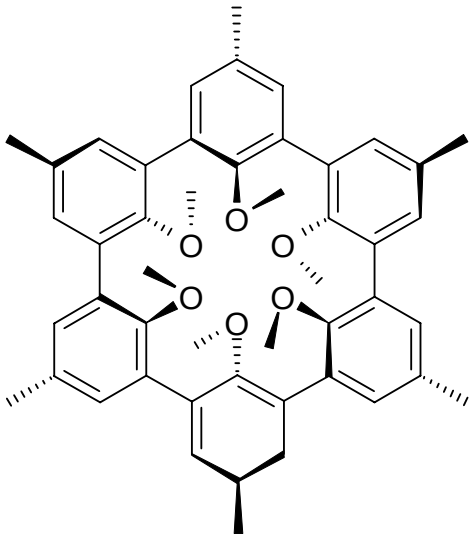

Figure 1.3 3D Spherand

1.6 Grids, ladders, racks and cylinders.

These are lattice motifs that include grid, rack and ladder structures as well as 2D network coordination oligomers/polymer arrays. They incorporate extensive orthogonal or near-orthogonal binding. A characteristic common to all of these motifs is the formation of coordination bonds at alternating right angles to each other.

Grids are generally anchored by a combination of tetrahedrally or octahedrally disposed metal ions with rigid linear ligands that have multiple chelating sites down their length. The presence of these two components ensures a rigid, orthogonal architecture where separate ligands are bound to a single metal ion. Grids are described using the nomenclature [n x n']G, in which ligands having n and n' binding sites respectively combine with n and n' metal ions to form a complex containing [n + n'] ligands in a grid arrangement.[13] A variety of coordination complexes displaying grid secondary structure motifs have been reported. These include 2x2G, 2x3G and 3x3G.

Bidentate heteroaromatic linkers such as pyrimidines or pyridazines have commonly been used, these ligands are characteristically planar and contain linear spacers between their binding sites. The heteroatoms in these spacers typically participate in separate, adjacent binding sites. Tetrahedral metal ions have been widely employed in grid formation, ions such as Ag(I) and Cu(I).[14-17] *Figure 1.4* is a diagrammatic representation of the formation of a grid structure from its components, the ligand strand and metal ions.

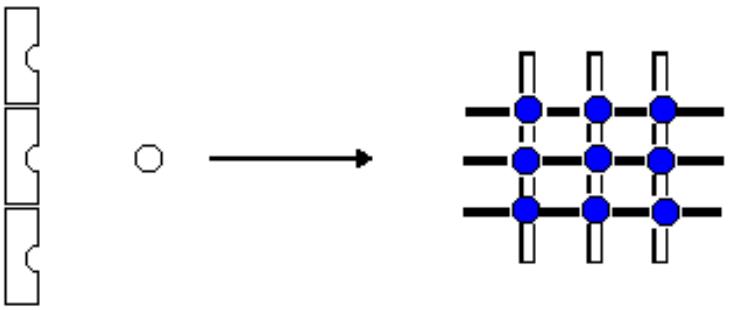

Figure 1.4 Diagrammatic representation of a grid structure

Shown in *Figure 1.5* is an example of a [2x2] grid complex. The work of Timothy E. Glass *et al* indicates the formation of a rigid cavity containing tetra-cobalt (III) with a bis(bipyridine)dimethoxynaphthyridine ligand.[16] Many examples of [2x2] grids are known, here in this example a grid has been constructed with what is thought to be a 'useful' cavity in terms of size.[17]

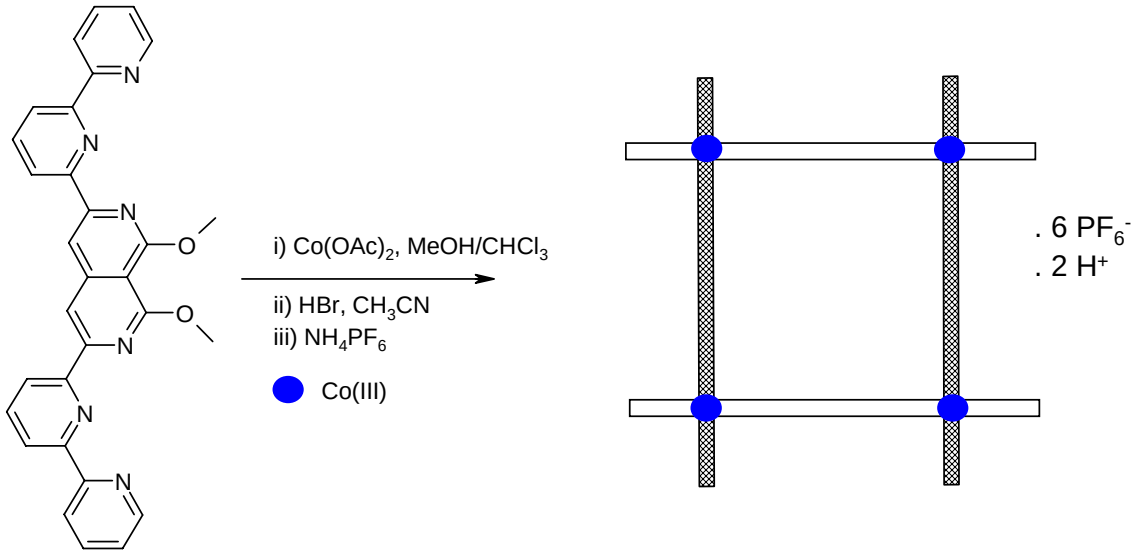

Figure 1.5 An example of a rigid [2x2] grid with 'useful' cavity

Shown in *Figure 1.6* is a specific example of the use of Ag(I) ions to produce a [3x3]G grid. [16]

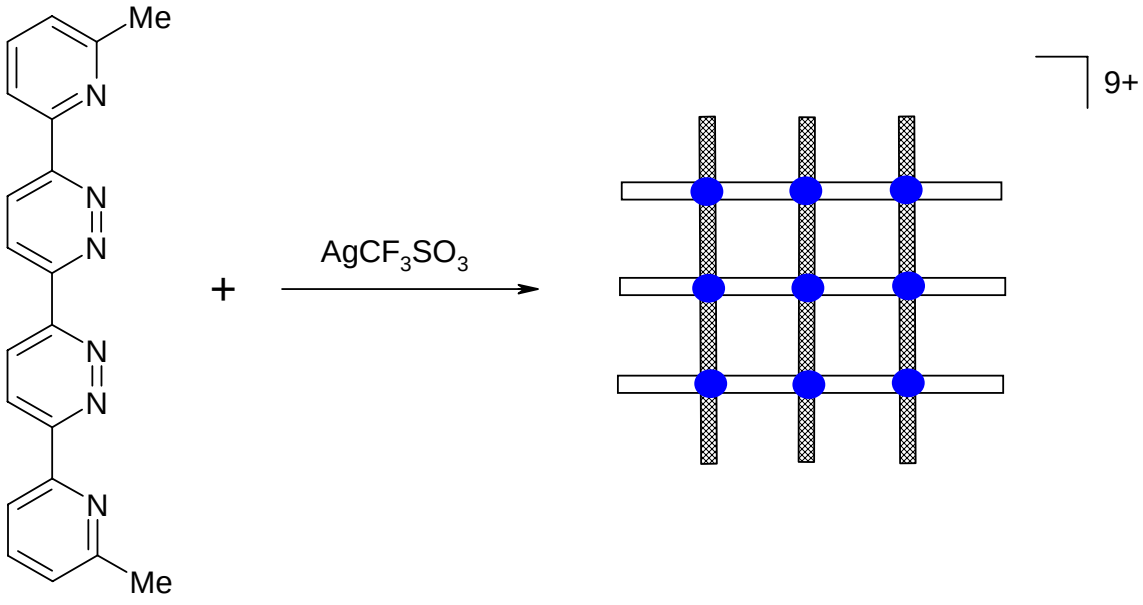

Figure 1.6 An example of a [3x3] grid constructed by Ag(I) metal ions.

More recently however a number of grid-like structures have been created by Stuart Onions *et al.*[17] Through the use of the ligand chain shown below they have produced the unique dodecanuclear copper(II) 'picture frame' which is held in a [4x4] grid-like assembly and recently still, is the production of the hexadecanuclear 'grid of grids', a [4x(2x2)] construction from the spontaneous self-assembly of the tridentate ligand shown in *Figure 1.7* and $Pb(CF_3SO_3)_2$.[15]

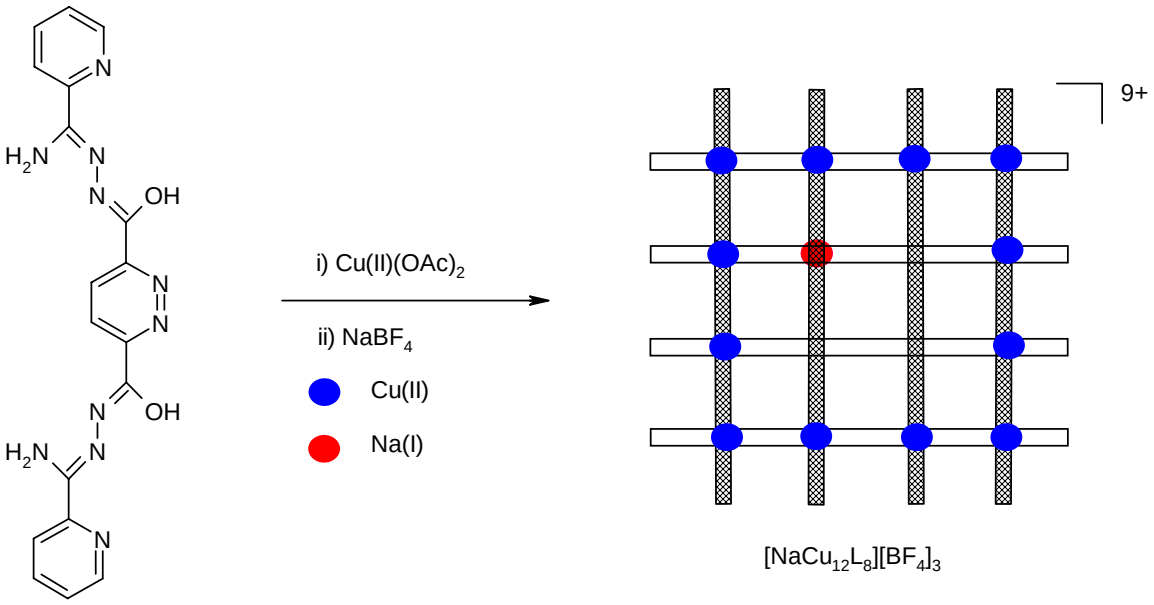

Figure 1.7 A diagrammatic representation of [4x(2x2)] 'grid of grids' utilising a tridentate ligand strand.[15]

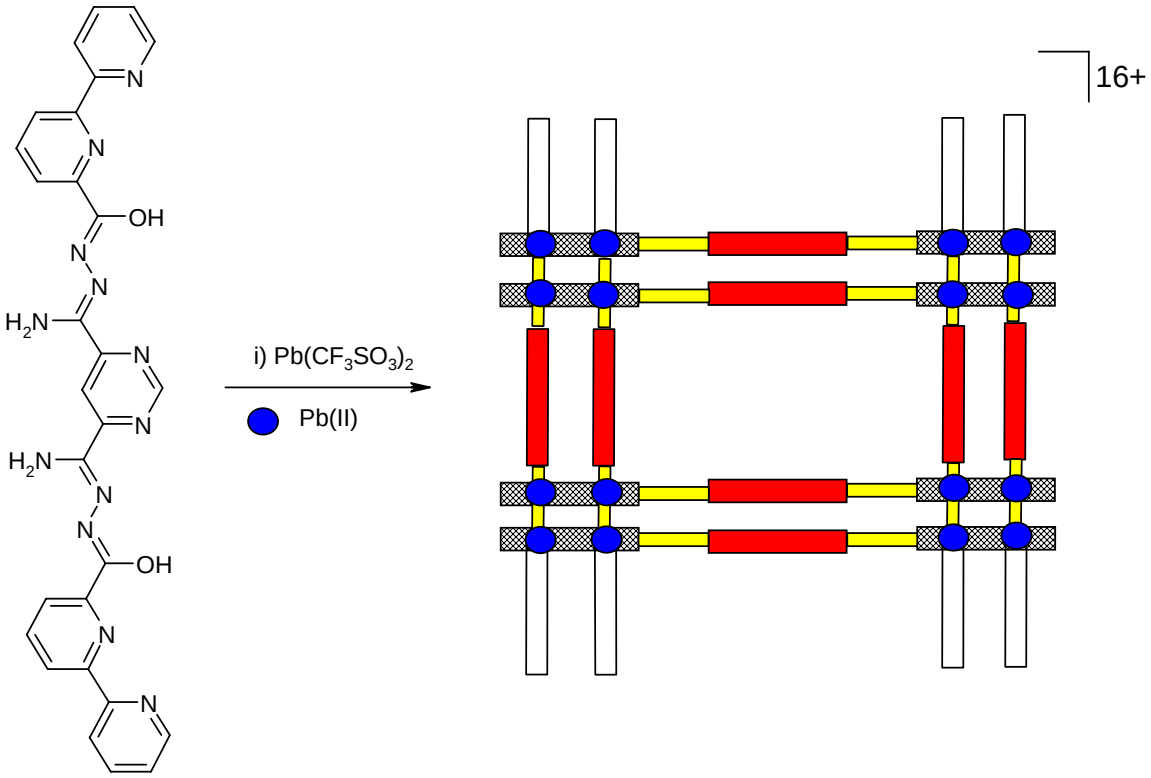

Figure 1.8 A diagrammatic representation of a [4x4] 'picture frame' constructed from the tridentate ligand strand as above.

1.6 a) Racks and Ladders

Racks and ladders are similar to grids in that they have multiple coordination down the length of the polydentate ligand from which they are constructed, but they differ in that they require a second mono or bidentate ligand containing binding sites at one end (in the formation of a rack) and both ends (in the formation of a ladder).

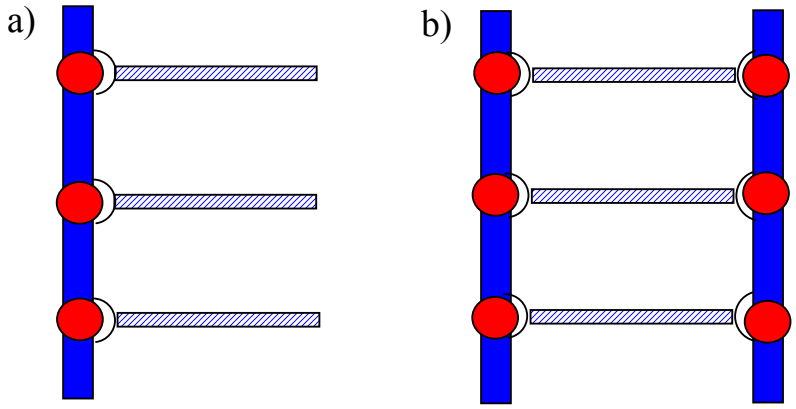

Figure 1.9 Illustration to show the structure of; a) a rack and b) a ladder.

In coordination arrays several rigid ligands having binding sites organised in various right-angled arrangements are usually employed.

Ladders are also structurally rigid and produced as secondary motifs by the thermodynamically self-assembly processes. Ladders are described using the formula [2xn]L, where n is the number of 'rung' ligands present. Several of the [2x2]L, [2x3]L ladder species have been reported.[17-19]

Scheme 1.1 shows synthesis of a [2x2]L, type 1 ladder by Jean-Marie Lehn and co-workers using an oligopyridine ligands (L^A), a bipyrimidine ligand (L^B) and Cu(I) metal ions to form the ladder species, A) $[Cu_4(\mathbf{L^A})_2(\mathbf{L^B})_2]^{4+}$.

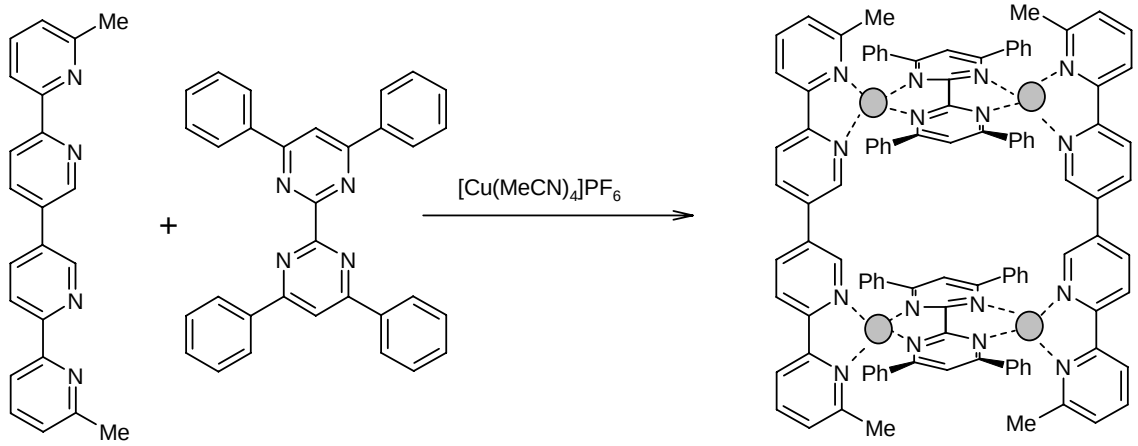

Scheme 1.1 Type 1 ladder example utilising oligopyridine ligands

Racks are described by [n]R, where n refers to the nuclearity of the species. Since racks have only one linear polytopic ligand present they may display structural isomers if linkers of that ligand permit rotational freedom. Several rack compounds having [2]R and [3]R structure have been reported. An example that uses the ruthenium(II) terpyridine moiety to form bi- and trinuclear racks is shown below.[12,18]

Figure 1.10 An example of [2]R and [3]R rack structures

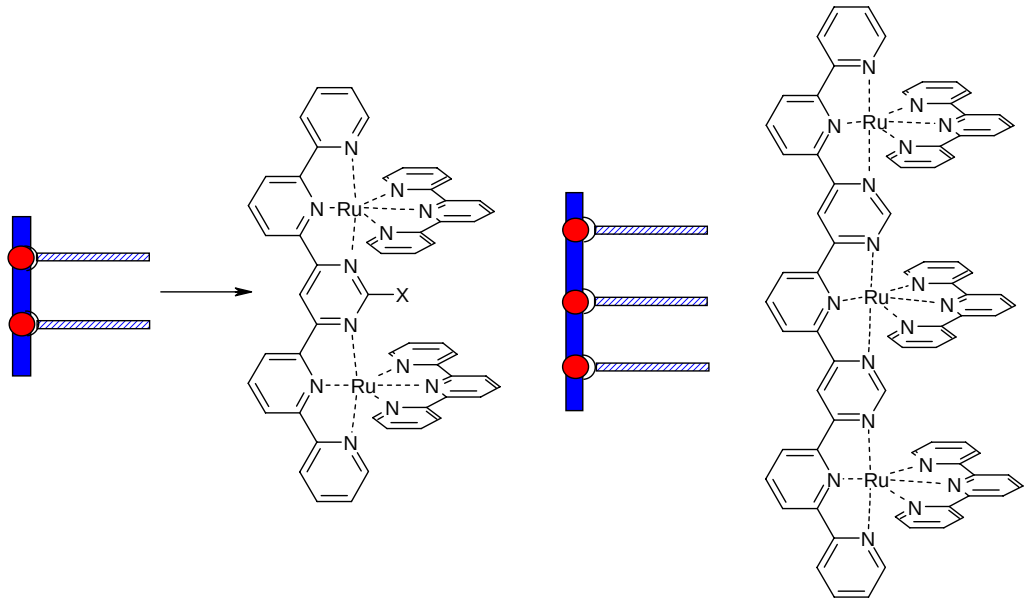

1.6 b) Cylinders

Cylinders are a species, which are self-assembled from appropriate metal ions with two different types of ligand, one planar polytopic ligand and one rigid circular polytopic ligand. A diagrammatic representation is shown below in *Figure 1.11*.

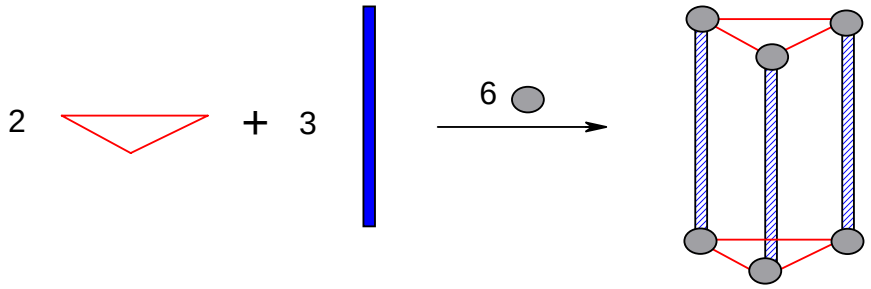

Figure 1.11 The formation of a cylinder

The formation of the molecular cylindrical structure below, *Figure 1.12* is from the interaction of, in this example two cyclic hexaphenylhexaazatriphenylene ligands ($\mathbf{L}^{C}$) and three linear bis(bipyridine) ligands ($\mathbf{L}^{D}$) with six equivalents of $[Cu(CH_3CN)_4][BF_4]$.[13]

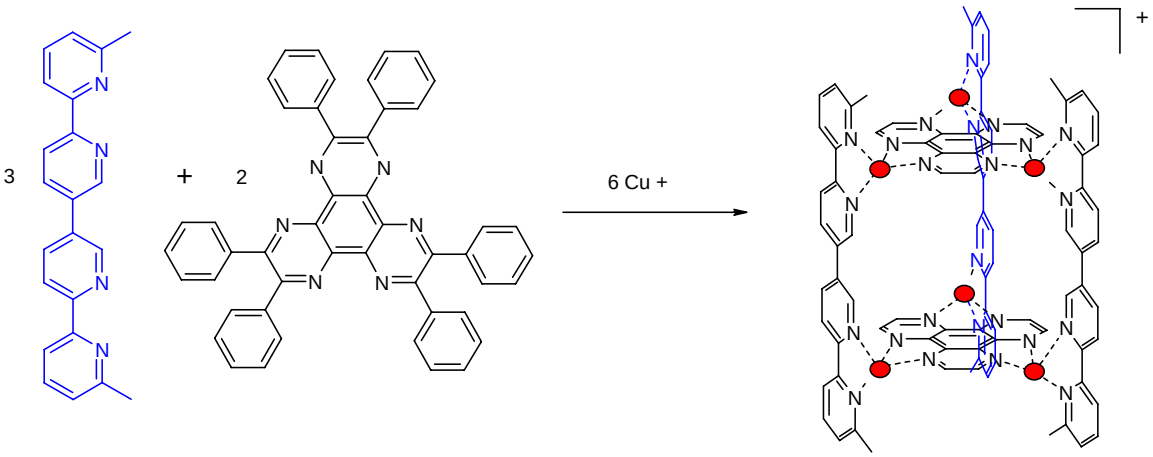

Figure 1.12 An example of a molecular cylinder structure

Figure 1.13 below depicts a larger triple-decker molecular cylinder structure. An example of this utilising ligands $\mathbf{L}^{E}$ and $\mathbf{L}^{C}$ is shown. Here the metal ions can be either Cu(I) or Ag(I).

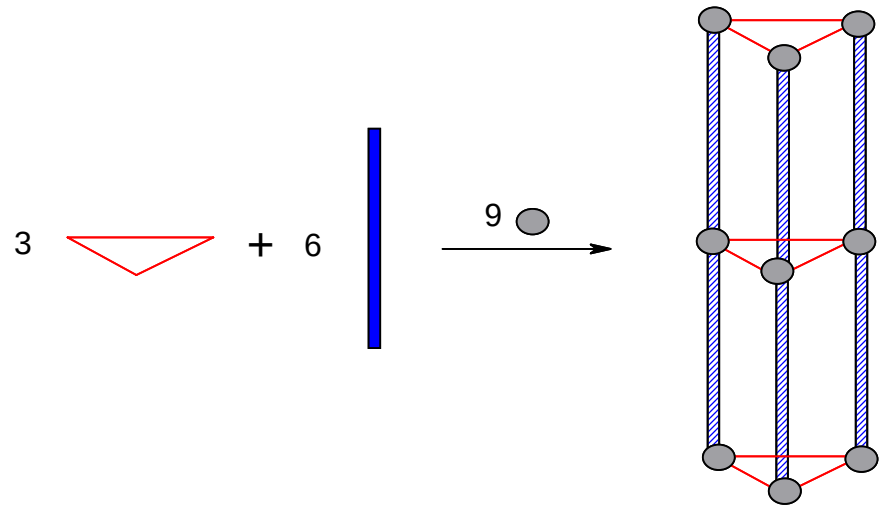

Figure 1.13 A diagrammatical representation of a triple-decker molecular cylinder

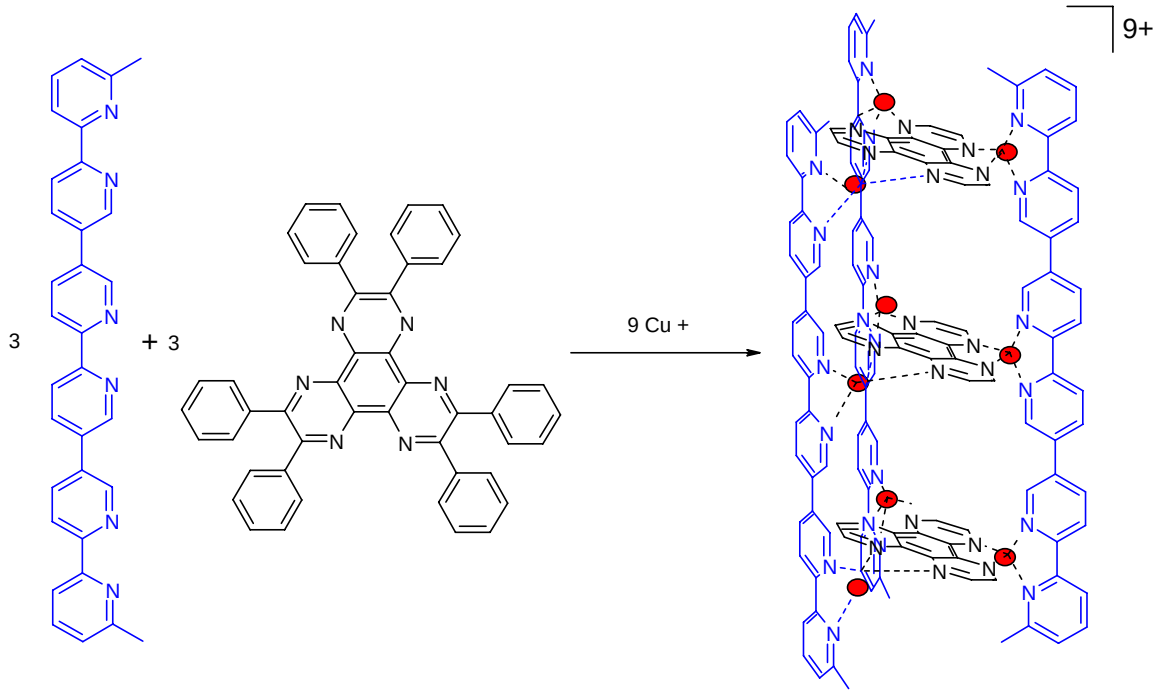

Figure 1.14 An example of the construction of a triple-decker molecular cylinder utilising the ligands in *Figure 1.13*, L^{E} and L^{C} and introduction of either Cu(I) or Ag(I) metal ions

1.7 Rods and Metallodendrimers

Rods and metallodendrimers are two of the most common filamentous motifs. They are strand-like macromolecules separated by coordinated bridging ligands with terminal binding sites. There are two basic building blocks; the spacer or bridging ligand and the terminating ligand.

Rods are filamentous motifs obtained from the self-assembly of metal ions with ligand strands bearing donor sites at each end. The resulting compounds are known as 1D, 2D and 3D linear oligomers. A bidentate ligand with a rigid spacer that separates each individual binding domain is extended to produce a rigid, linear complex as more mono or bi-dentate species are coordinated.

The coordination of a rod motif is achieved via the formation of a complex in which a number of metal ions and ligands are alternately coordinated down the length of the molecular strand. The oligomeric ligands are the main building blocks in the construction of a rod, with spacer ligands at either end of these blocks to form long chains via coordination to transition metal ions, until a terminator ligand is coordinated. This deactivates the complex and the rod motif can no longer grow in structure. Rods are conformationally inflexible and the linear coordination oligomers, metal ions and spacer ligands all lie on a single straight line. The spacers between binding sites in ligand complexes belonging to these rod motifs must be rigidly straight. The metal ions involved in the rod motif are coordinatively unsaturated and can only become saturated with the introduction of what is termed a 'termination species' this effectively binds to or deactivates the remaining binding sites of the macromolecular species.

A substantial number of rods have been reported [13] and many have been used in the study of the photophysical properties of the rod when they contain photoactive metal ions. *Figure 1.15* below depicts the self-assembly of trinuclear molecular rods by the reaction of a ruthenium based ligand complex with labile metal ions, namely Fe(II) and Co(II).

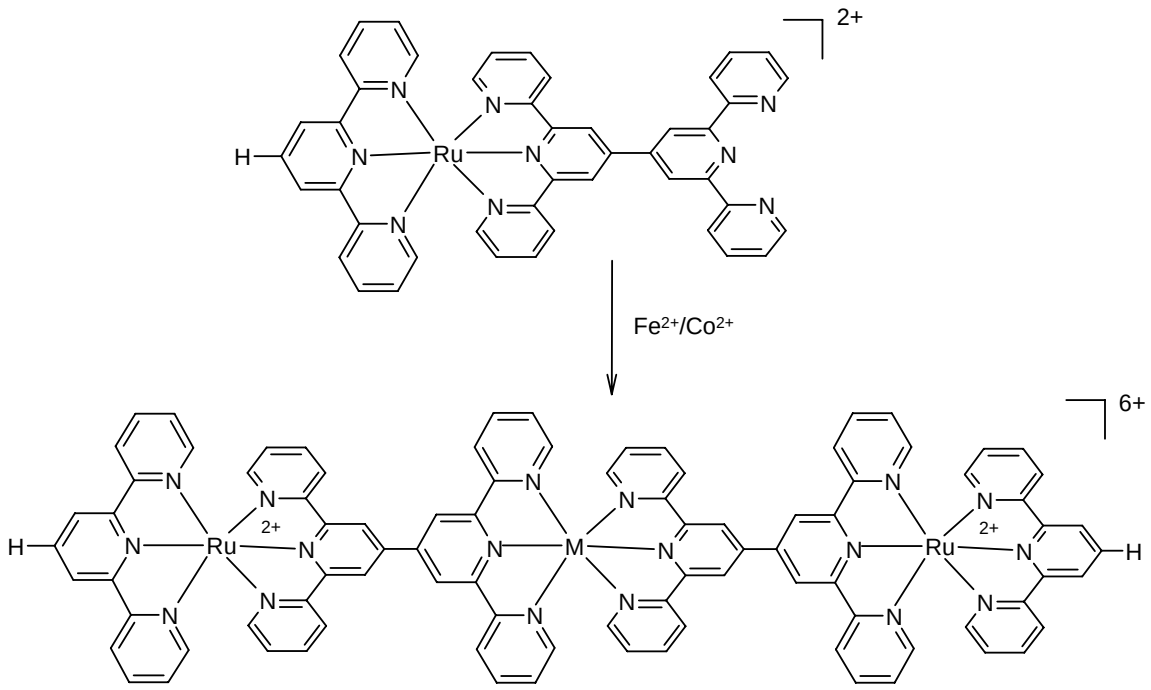

Figure 1.15 Formation of a trinuclear molecular rod utilising a Ru(II) based ligand and either Fe(II) or Co(II) metal ions.[13]

Metallodendrimers are a highly branched species, resulting from the use of ligand at the dendrimer centre. Termination takes place in the same way as rods, via coordination of a capping species that binds to or deactivates any remaining binding site, at which point the full extent of the macromolecule complex ends. A large number of metallodendrimers have been reported, amongst them are those containing the 2,2′:6,2″ terpyridine (tpy) derivative to construct a ruthenium based metallodendrimer.[11] This first generation triruthenium metallodendrimer is created by the reaction of the "triterpyridine" ligand with [Ru(tpy)Cl_3] as shown in *Figure 1.16.* This ligand is composed of a benzene ring substituted by terpyridine in the 1,3, and 5 positions. This example simply illustrates the construction via a branched polytopic ligand.

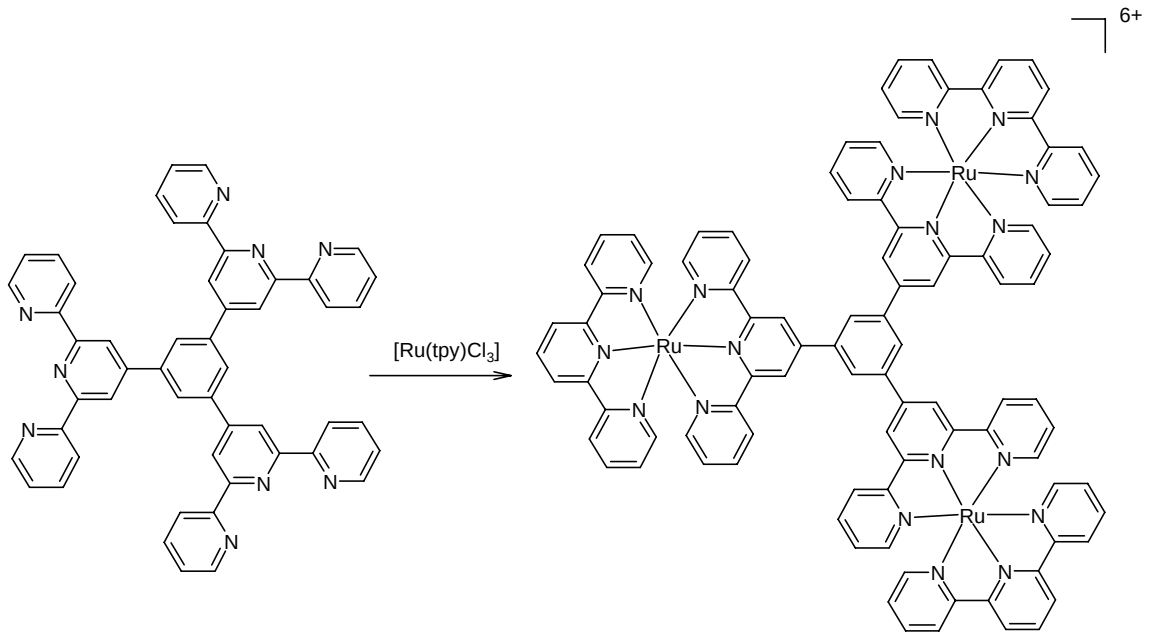

Figure 1.16. An example of a branched metallodendrimer, utilising the 'triterpyridine' ligand.[13]

1.8 Catenanes and Rotaxanes

Catenanes have been termed 'chemical curiosities' since their development 40 years ago. "The potential for such systems for storage and relay of information at a molecular level awaits exploitation"[14,] A lot of effort has gone into the creation of many alternative approaches to their synthesis but in the majority of these the overall yields of these compounds have been significantly low.[2, 20-22]

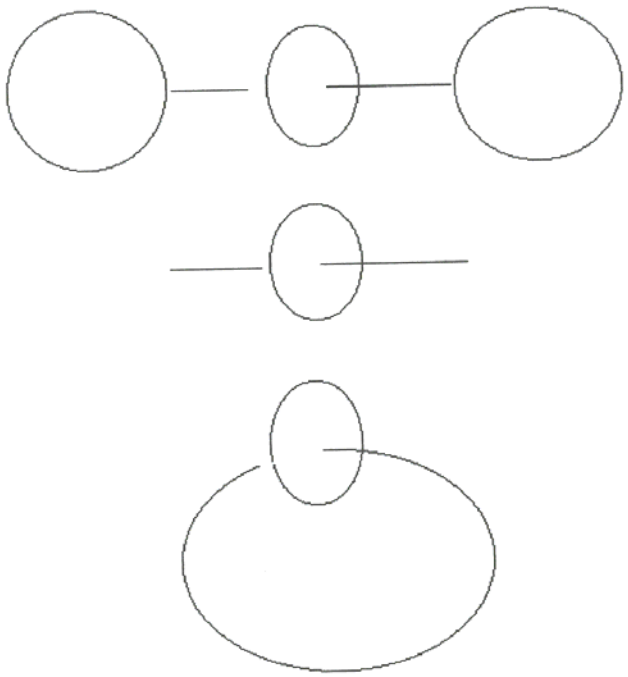

Figure 1.17 shows a diagrammatic representation of (in descending order) a rotaxane, a pseudorotaxane and a catenane.

The production of a catenate involves the interlocking of two cyclic structures. If two such cycles are simultaneously bound to a single metal ion, the resulting motif can be termed a catenate. The nomenclature [n] employed is for simple catenates where 'n', indicates the number of interlocked rings.

In the 1980s Sauvage[21,22] developed a multistep covalently templated synthesis approach that overcame some of the low yielding syntheses. It involved the use of a concept proposed by Sololeov in 1973 proposing the employment of transition metals and appropriate ligands coordinatively bonded in order to template catananes from catenands via demetalation.[23]

Scheme 1.2 shows four simple routes to a template-directed approach to the synthesis of catananes and rotaxanes; a) A second ring 'clipped' onto an already complete ring, b), c) guest is 'capped' covalently by large stoppers and the threading through of the ring-shaped host, d) Guest with stopper attached then converted to ring-shaped host by 'clipping'.[20]

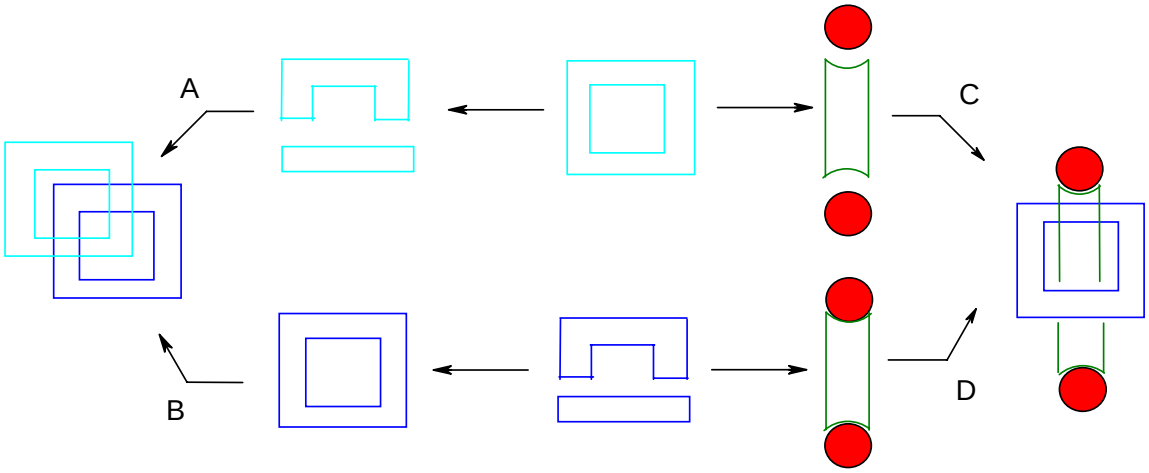

Scheme 1.2 A four-route template-directed synthesis of Catenates and Rotaxanes

Catenates differ by the number of times one ring 'crosses' another in its complete length. Most are singly locked, others with two and four crossings are termed for example 2-crossing or 4-crossing catenates. Multi-ring catenates are termed molecular necklaces, described using the nomenclature [n]MN, where 'n' refers to the number of cycles present.

Metallocatenates are a species that exhibit interlocking ring motifs in which one or more rings have been closed by metal ion coordination, in effect it is the self-assembly of two interlocked metallocycles. In the process of self-assembled catenantes the cycles need to be spontaneously formed and interlocked during the reaction but this is unlikely and statistically rare. The work of Fujita *et al*, has seen exactly this approach used in the self-assembly of several metallocatenates. In this Pd(II) system, the free metallocycles are formed because of the enthalpy of formation of the Pd-N bonds. *Figure 1.18* shows the structural self-assembly of metallocatenates in a palladium system reported by Fujita *et al*.[13]

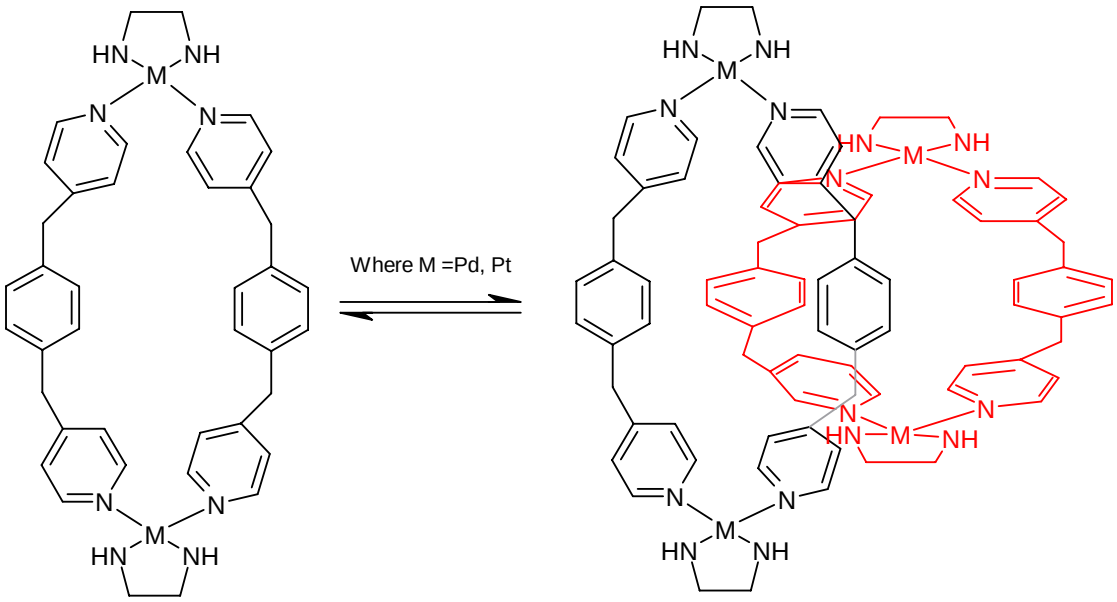

Figure 1.18 Structural self-assembly of a metallocatenate in a palladium or platinum system.

Alternatively, synthesis of a metallocatenate via the manipulation of a pseudorotaxane may take place. A pseudorotaxane, which may have free chelating sites at the termini of the threaded filamentous ligand, then undergoes ring closure by coordination to a single metal ion giving a complex, which is correctly termed a metallocatenate.

1.8 a) Rotaxanes and Pseudorotaxanes

A rotaxane is an interlaced structure in which a filamentous species, stoppered at each end is threaded through a cyclic one. Rotaxanes offer useful frameworks for examining through-space electron transfer in molecules. The use of a filamentous ligand containing several coordination sites along their length makes a reaction of this type and the resultant structures produced hard to predict. The main challenge in the synthesis of rotaxanes is to identify an effective protecting group that would serve as a ‘stopper’. A number of bulky protecting functional groups have been examined in

order to identify a potential protecting group; one contender seen was the use of triisopropyl-silyl ether.[20]

Pseudorotaxanes are not sterically trapped unlike rotaxanes by the presence of bulky stopper groups at the termini of the ligand species. They are physically able to 'dethread' from the rotaxane they are sterically locked to and topologically bound. The nomenclature [n] for a rotaxane and [n] for a pseudorotaxane is employed, where 'n' indicates the nuclearity of the complex.

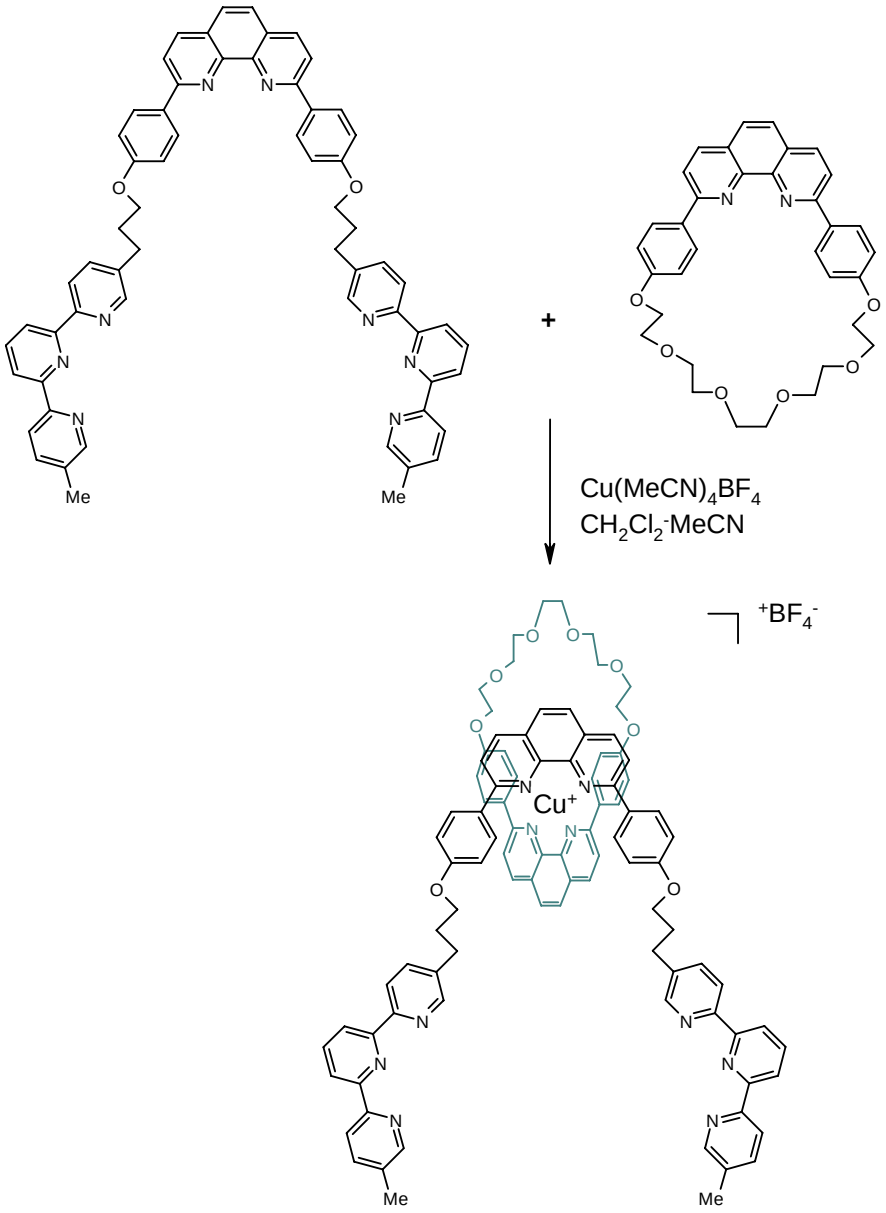

Scheme 1.3 A single-threaded [1] Pseudorotaxane mixed ligand complex

The illustration above in *Scheme 1.3* indicates the production of a [1] pseudorotaxane, a mixed ligand complex self-assembled utilising a tetrahedrally disposed metal ion with a bidentate ligand and a macrocyclic ligand strand.[13]

Pseudorotaxanes can be described as the treatment of a tetrahedrally disposed metal with a mixture of a linear bidentate ligand strand and a macrocyclic bidentate ligand. Coordination sites lie on the inside of the cycle and lead to the mixed ligand complex of a pseudorotaxane structure. Semi-flexible species can be added in between the binding site to prevent multiple chelation to a single metal ion *e.g.* Cu(I) thereby producing a polynuclear pseudrotaxanes. 'The rings and strings' approach (Sauvage *et al*) is an example where the use of more spacers $-(CH_2)_6-$ has led to half stoppered pseudorotaxanes where cyanide is used as a decomplexation reagent.[4, 15-25]

1.9 Molecular Knots

Molecular knots are a class of their own and all knots involve a process of self-assembly, followed by post modification. They have a long and distinguished history of often beautiful designs, such as the Celtic knot shown in *Figure 1.19*

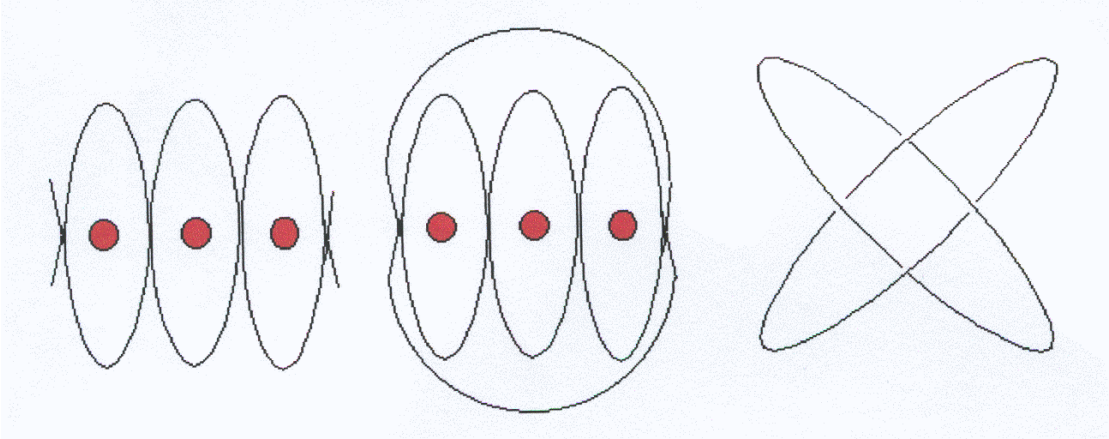

Figure 1.19. Diagram of a Celtic knot.

Knots are a species in which a single strand alternately passes over and under itself several times in a continuous loop. Knot motifs are named according to the number of times the strand crosses itself. Knots, having a singly structural motif, such as the trefoil knot are known as prime knots, while those with more than one knotted motif are called composite knots. These are usually formed by connecting opposite ends of the two ligands in a double stranded helicate to form a single continuous, intertwined ligand strand about the metal ion. They are termed multiply interpenetrated complexes. They are similar to catenates due to their interlocking links, yet catenates, unlike the molecular knots are based on a single stranded loop.[2,13,21]

As a general rule, it may be shown with the preparation of molecular knots (in the way described) that if the number of metal centres is even, the number of crossings of the molecular loop will be odd. This diagram illustrates the two metal centred structures that produce a trefoil knot.[13] This is an example of where an trefoil knot structure can be prepared from a self-assembled helicate thus the reaction of the ligand with Cu(I) generates the helicate shown which in turn is treated with $[ICH_2(CH_2OCH_2)_5CH_2I]$ ($CsCO_3$, DMF, 60˚C)[13] *Scheme 1.4* below.

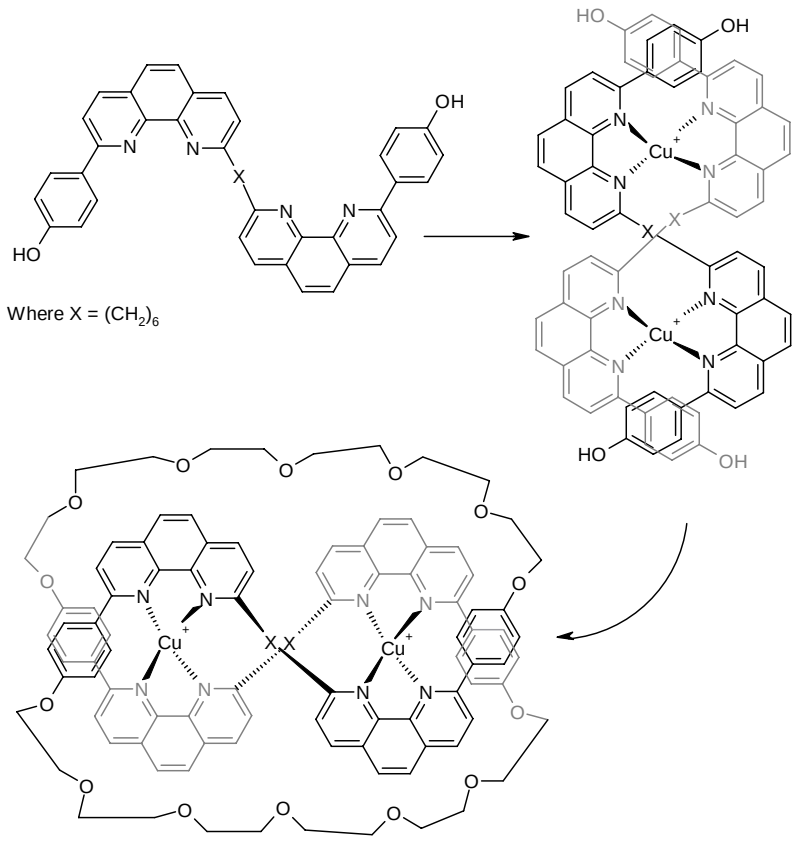

Scheme 1.4 Self-assembly of one example of the Trefoil Knot[13,27]

Where four metal centres results in a pentafoil knot, six metal centres results in a heptafoil knot. Therefore an odd number of metal centres will generate an even numbers of crossings and give rise to doubly interlocked catenates and even numbers of metal centres will generate odd numbers of crossings.

The helicate within this self-assembly process provides the twisting of the ligand strand that is essential to the formation of a multiply intertwined knot structure. The

number of metal ions, and the pitch of the helicate will govern the type of knot obtained.

1.10 Helicates

The term "Helicate" was first introduced by Jean-Marie Lehn and co-workers in 1987, as a "polymetallic helical double-stranded complex".[1] The word helicate is a reduction of the word helix, from the Greek meaning spiral or winding and the suffix "ate" referring to host-guest complexes between metal ions and preorganised receptors.

From their first discovery much detailed research began into helicates which explored the control of these complicated architectures and the synthesis of selective designs. At the moment of their discovery, the spontaneous generation of the helix was perceived to be a self-assembly process similar to that seen in biology.[1,2,6] Since that time helicates have been an area of great interest.

The importance of helicates stems from a culmination of the development and understanding of those self-processes involved in supramolecular chemistry. Four main concepts were established and believed to be crucial in further development of this new field of supramolecular chemistry. They included; i) molecular recognition, the selective interaction between two or more components in a self-process; ii) self-organisation, a system capable of spontaneously generating well defined supramolecular architectures from complimentary components under a certain set of conditions; iii) self-assembly, an elemental step in a self-organisation process; iv) supramolecular programming, incorporation of instructions into components of a self-assembly.[6]

It has been said, "The study of helicate complexes resulting from metal ions and coordinated organic receptors has become a domain of its own".[6]

1.11 Helicate classification

The helicate is a complicated supramolecular complex made-up of one or more covalent organic strands wrapped around and coordinated to a series of ions defining a helical axis. The final metallosupramolecular helicate generated is the result of the interaction between organic ligand strands and metal ions.

The principal behind the self-assembly of a helicate lies in the spontaneous creation of architectures from the molecular recognition properties of individual components. Selectivity of self-assembly depends on two important associations, firstly the stereoelectronic molecular information that each individual constituent has held within its design and secondly other external conditions that are applied to each self-assembly process in the formation of all supramolecular species.

Metal ions (generally cations, although helicates composed of anions are known) are used in helicate self-assembly due to the individual properties they posses. These include; i) specific coordination numbers and stereochemical preferences depending on their individual size, charge and electronic structure; ii) a large variation in binding strength and kinetic stability; iii) the varying affinities for binding units that they comprise; iv) specific magnetic, electronic and spectroscopic properties expressed in the final helicate.[3, 6-9]

An ideal ligand should include to following; i) several binding units along the ligand strand; ii) molecular spacers between binding units that are rigid to a high enough degree to deter the coordination of several binding units of one ligand strand to the same metal ion, but are also flexible enough to be able to undergo the helication process of wrapping around the metal ions producing a complex that is multinuclear and stable.

The synthesis of ligands via covalent interactions results in the generation of an almost unlimited supply of covalent organic ligand strands, which vary in their design and the intrinsic information that a particular receptor may posses. In the extreme case ligand strands that contain spacers that do not allow the formation of helicates leads to the formation of clusters of metal ion combinations, where the lack of flexibility within the ligand strand is insufficient and self-assembly of a helicate species in prevented.[6-9]

1.12 Helicate Terminology and basic helicates

There is a whole range of helicate terminology that has been developed to explain and simplify those terms used in the formation of a helicate complex.
The organic ligand strand that is used in helicate formation is known as a helicand.[2] Helices may be single or multiple stranded and vary in pitch (the distance along the helical axis for the strands to complete a full turn). The wrapping may be controlled by metal ion coordination or other supramolecular non-covalent interactions *e.g.* hydrogen bonding. *Figure 1.20* illustrates the helical screw about an axis. The distance between one turn of the helix and the next.[2]

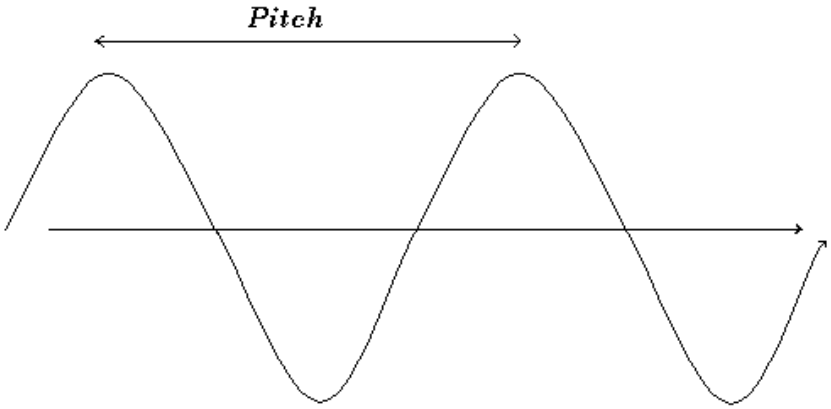

Figure 1.20 Representation of a Helical screw axis

Where those ligands strands are identical they correspond to a homostranded helicate, the following is a diagrammatic representation of a homostranded helicate.

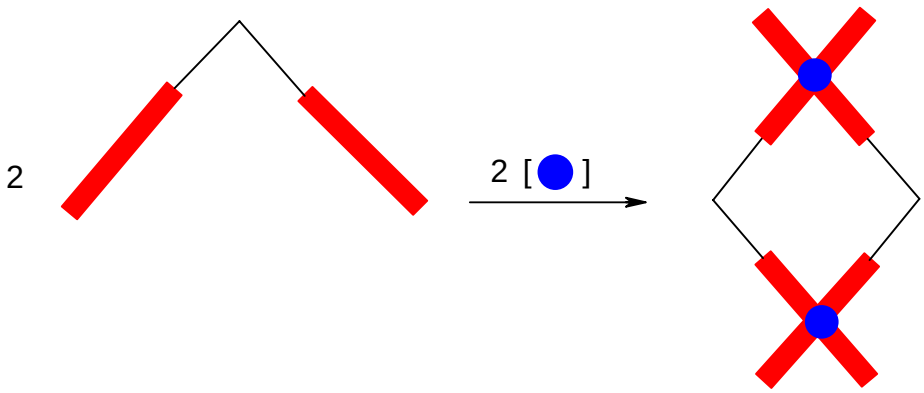

Figure 1.21 Homostranded Helicate

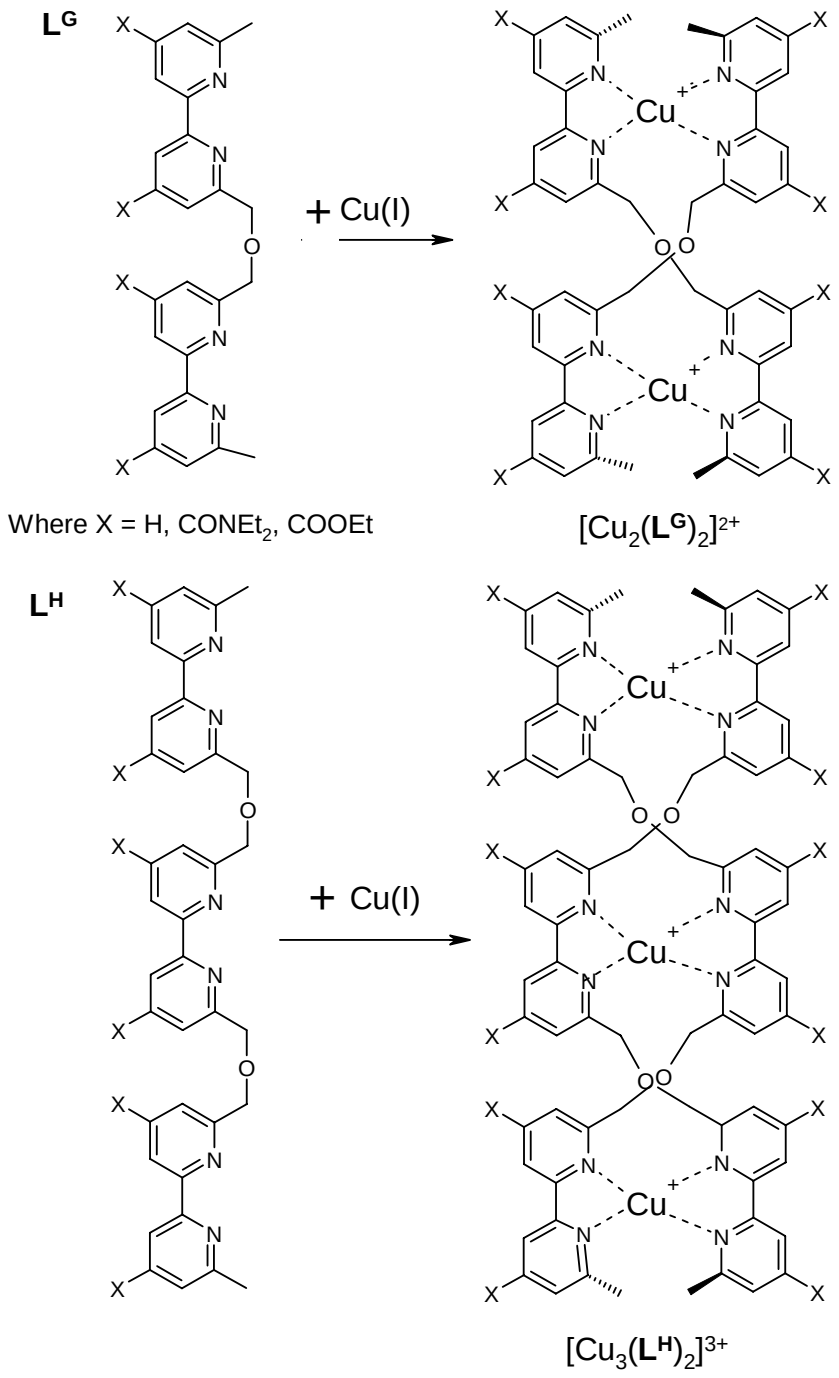

Figure 1.22 Homostranded helicate complex $[Cu_2(\mathbf{L}^{\mathbf{G}})_2]^{2+}$ and $[Cu_3(\mathbf{L}^{\mathbf{H}})_2]^{3+}$

Jean-Marie Lehn and co-workers demonstrated quite eloquently the formation of the homostranded helicate using a series of bipyridyl ligands that contained ether spacer groups. A series of ligands $\mathbf{L}^{\mathbf{F}}$ to $\mathbf{L}^{\mathbf{G}}$ were prepared (herein only $\mathbf{L}^{\mathbf{G}}$ and $\mathbf{L}^{\mathbf{H}}$ are shown) and when mixed with Cu(I) ions were found to produce only the homostranded helicate complexes, shown here in *Figure 1.22* as $[Cu_2(\mathbf{L}^{\mathbf{G}})_2]^{2+}$ and $[Cu_3(\mathbf{L}^{\mathbf{H}})_2]^{3+}$.[27]

On the other hand where those ligands strands are different, they correspond to a heterostranded helicate. *Figure 1.23* illustrates the diagrammatic representation of a heterostranded helicate.

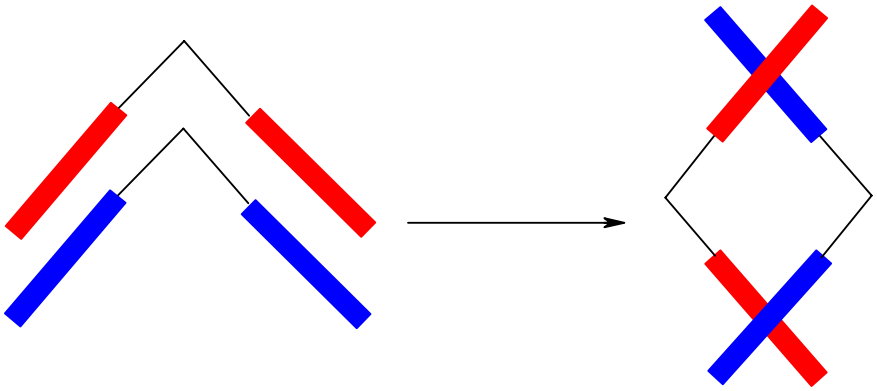

Figure 1.23 Heterostranded helicate

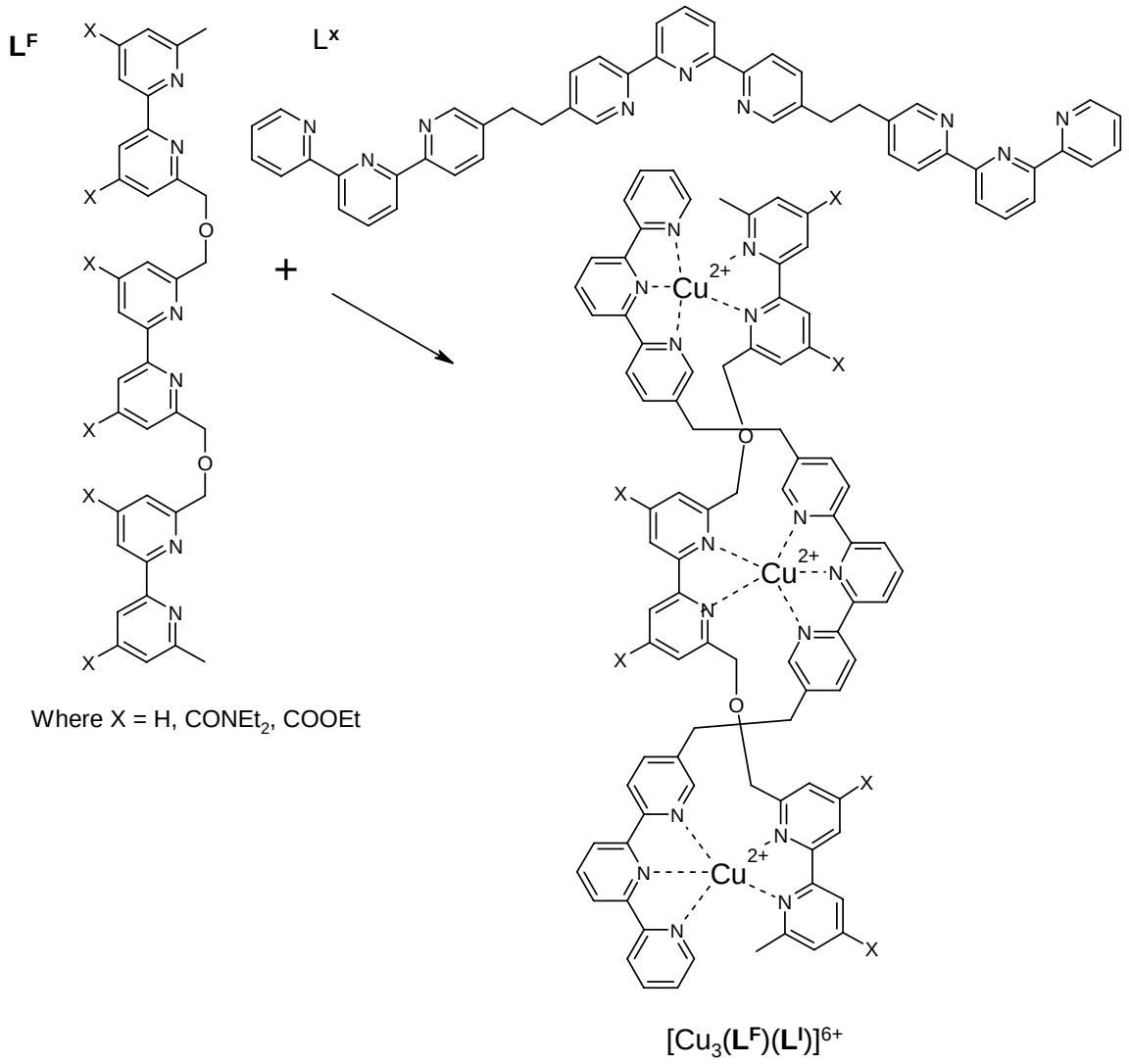

Figure 1.24 Example of a heterostranded helicate

Once again, as shown in *Figure 1.24* Jean-Marie Lehn employed a bipyridyl ligand (seen in the previous example) namely the ligand $\mathbf{L^F}$, and a new ligand $\mathbf{L^I}$, that contains three terpyridine (tpy) units, that when mixed in the presence of Cu(II) ions produced only the heterostranded helicate complex $[Cu_3(\mathbf{L^F})(\mathbf{L^I})]^{6+}$ shown above. Each Cu(II) centre binds to one bipyridine and one terpyridine subunit and no homostranded helicate complexes were generated due to the preference of Cu(II) for a five-coordinate array.[27]

The strands of a helicate can be further segregated into two different types of strand namely homotopic ligand strands, those possessing an identical sequence of binding units along a strand. Conversely, the heterotopic ligand strand is where the sequence of binding units is different, and therefore produces directionality.

This type of strand exist in two isomeric forms of the HH “head to tail” alignment and the HT head to tail” alignment. Shown below *Figure 1.25* is a diagrammatic representation of both [HH] and [HT] helicate complexes.

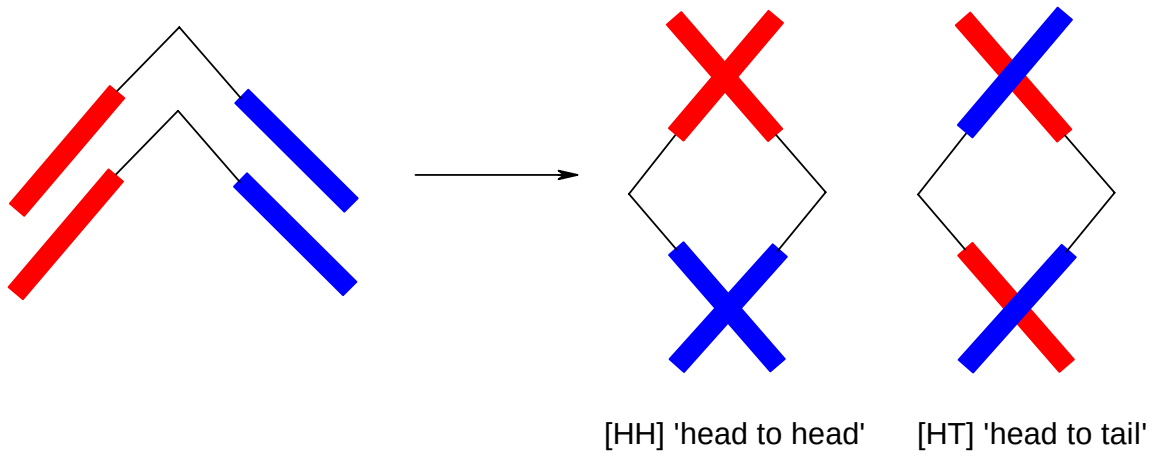

Figure 1.25 Diagrammatic representation of [HH] and [HT] helicate complexes

Another category that a helicate complex can attain is whether a helicate is saturated or unsaturated. A saturated helicate is one whereby each metal ion attains its stereochemical requirements solely through the use of the helicands that surround it. An unsaturated helicate is therefore one which contains metal ions so that the helicands that surround it do not fulfil its stereochemical requirements and therefore needs other supplementary molecules (usually other solvent molecules or anions) to complete its coordination sphere. *Figure 1.26* illustrates both examples of this type of helicate.

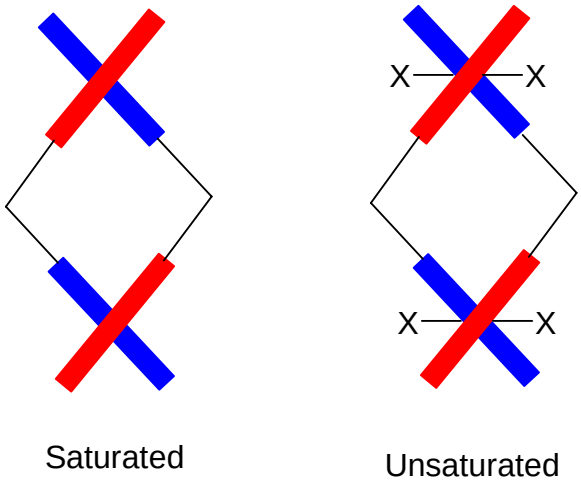

Figure 1.26 Diagrammatic representation of a saturated and unsaturated helicate

If a helicate is viewed down it's helical axis the rotation of the helix may be clockwise and therefore termed a right-handed or *P*(positive) helicate. A helicate that has an anti-clockwise rotation about the helical axis is termed a left-handed or *M*(minus) helicate.[28]

The pre-programming of an organic ligand chain to achieve the action of helication is a large and growing area of supramolecular helicate chemistry. There are many ways in which a ligand can be synthesised so that it contains intrinsic information and therefore its action upon coordination to a number of transition metal ions.[29]

1.13 Ligand recognition

Self or hetero-recognition of ligands can be controlled via a number of ways; one example controls the self-recognition by the number of binding sites a ligand has along its chain. An example of this control by binding sites has been described by Jean-Marie Lehn *et al* which employs a bipyridine derivative and Cu(I) ions, *Figure 1.27*. This bipyridine derivative, containing ether linkages, $\mathbf{L}^{\mathbf{J,K,L,M}}$, only forms homoleptic double-stranded helicates with copper (I) ions during the self-assembly process, namely $[Cu_2(\mathbf{L}^{\mathbf{J}})_2]^{2+}$, $[Cu_3(\mathbf{L}^{\mathbf{K}})_2]^{3+}$, $[Cu_4(\mathbf{L}^{\mathbf{L}})_2]_{4+}$ and $[Cu_5(\mathbf{L}^{\mathbf{M}})_2]^{5+}$;

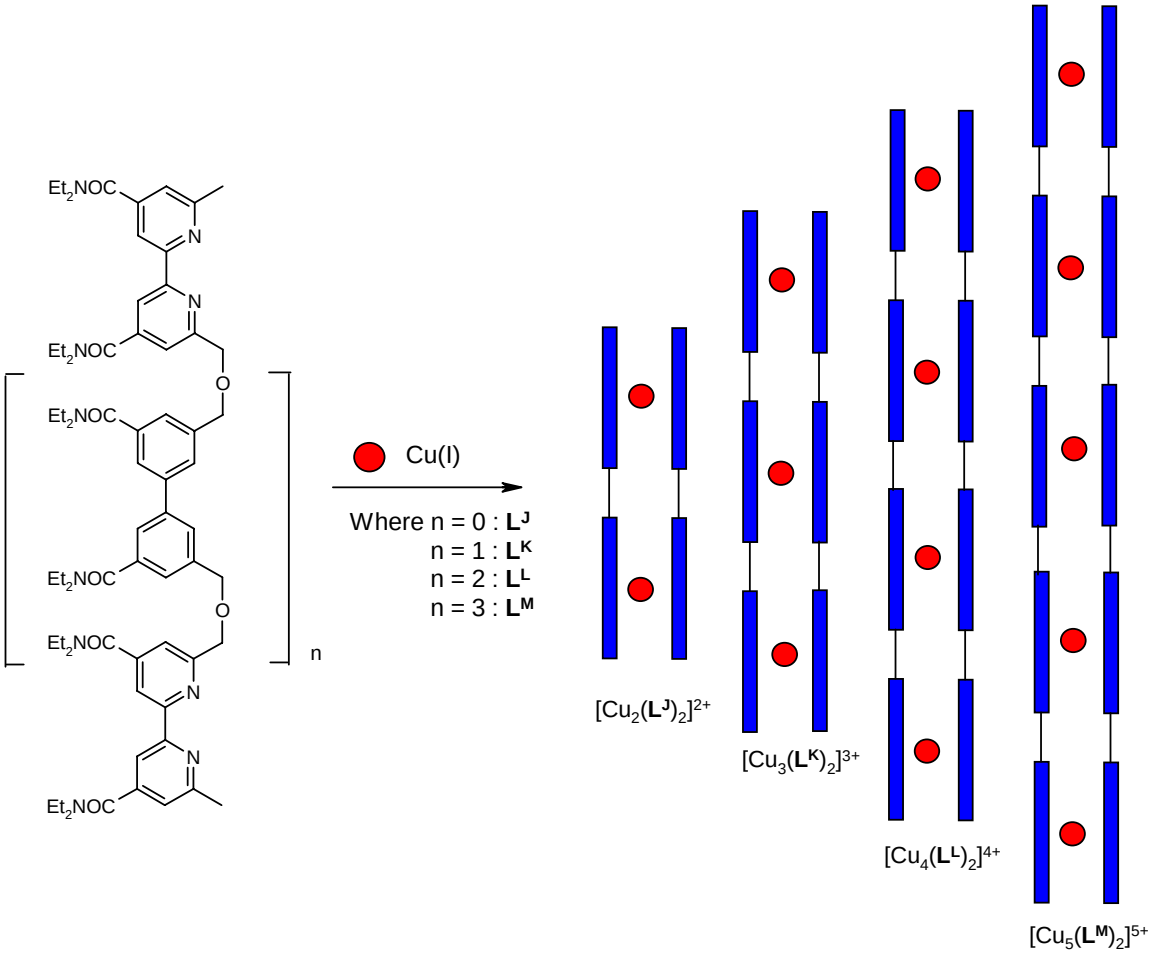

Figure 1.27. Diagrammatic representation of hetero-recognition via control of binding sites.

Another example of control via coordination geometry is seen when ligands with different spacer groups are mixed together in the presence of transition metal ions, the preferred coordination geometry of the metal ion dictates the self-assembled species. An example of this control is shown below in *Figure 1.28.* The work of Jean-Marie Lehn described the self-assembly between ligands $\mathbf{L^N}$ and $\mathbf{L^O}$ with Cu(I) and Ni(II), a mixture of transition metal ions with the resulting complexes formed; the double-stranded copper helicate $[Cu_3(\mathbf{L^N})_2]^{3+}$ and the triple-stranded helicate $[Ni_3(\mathbf{L^O})_3]^{6+}$ are observed and this an example of "homo" self-recognition.

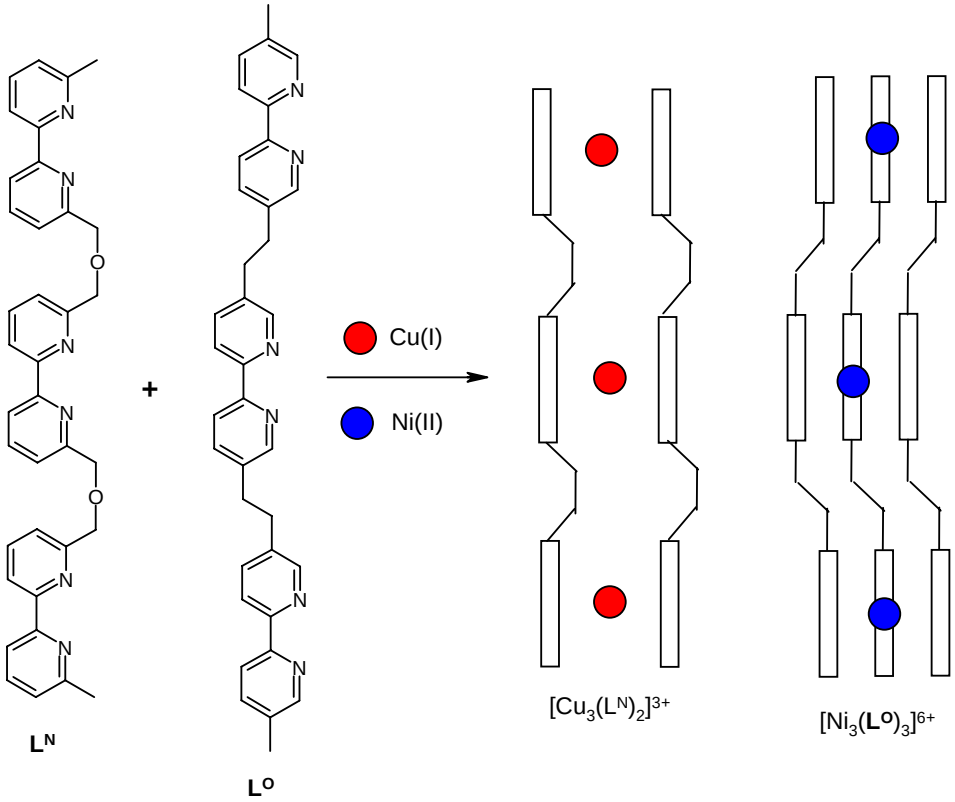

Figure 1.28. Representation of Self-assembly control via coordination geometry[7]

It is therefore also possible to select and observe "hetero" self-recognition occurring. The example given below shows ligands $\mathbf{L^N}$ and $\mathbf{L^P}$ when mixed with Cu(II) leading to the formation of a hetero-double-stranded helicate $[Cu_3(\mathbf{L^N})(\mathbf{L^P})]^{6+}$ due to the preferred coordination number of the Cu(II) metal ion that are wrapped around by the

two different ligands, a tridentate terpyridine unit from one ligand and a bidentate unit from the other thereby creating the desired 5-oordinate array;

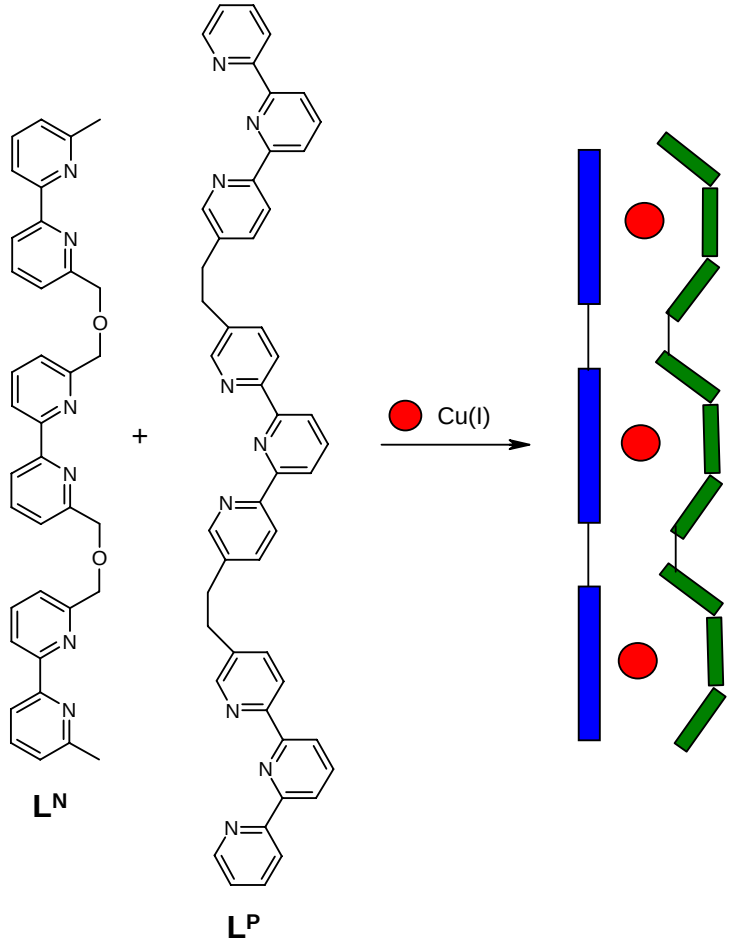

Figure 1.29 A diagrammatic representation of ligand recognition via control of coordination number.[7]

Another example of metal-specific recognition is the use of ligands containing a pyridyl/thiazole ligand (described later in more detail). In this example the position of the thiazole unit within the ligand chain is key to the difference in coordination mode shown by the complexes formed. When complexing a mixture of the ligands $L^{\mathbf{Q}}$ and $L^{\mathbf{R}}$, with transition metal ions, Ni(II) or Cu(II) a mixture of species if formed, $[M_2(L^{\mathbf{Q}})(L^{\mathbf{R}})]^{4+}$, $[M_2(L^{\mathbf{Q}})_2]^{4+}$, and $[M_2(L^{\mathbf{R}})_2]^{4+}$ yet with a Zn(II) metal ions fewer species are produced and what is seen is that self-self-recognition is favoured with this particular metal ion only.[30-33]

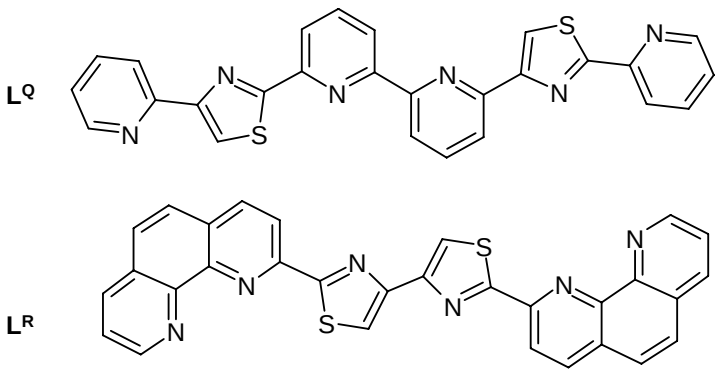

Figure 1.30 Representation of ligands L^{Q} & L^{R}

1.14 Chiral recognition

Self-assembly, self-recognition and replication all may involve chiral components. There are thus general considerations about the role of molecular chirality in supramolecular species. "Chirality is expressed on both the molecular and the supramolecular level".[1] Just as a molecule, a supramolecule, may exist in enantiomeric or diastereomeric forms. Supramolecular chirality results from both the properties of the components and from the way in which they associate. Thus, a supermolecule may be chiral either; i) because at least one component is asymmetric or; ii) when the interaction between chiral components is dissymmetrizing, yielding a chiral association as may occur in crystal growth. Therefore achiral components can associate to chiral supermolecules and chiral components can give an achiral supermolecule.[34,35]

Molecular chirality also affects they way in which self-assembly from chiral components occurs and the nature of the resulting supramolecular architecture. Three methods are distinguished between; i) asymmetric induction in self-assembly of a chiral structure where induction of helicity in a particular helicate can occur from ligand strands containing asymmetric centres; ii) enantioselective self-assembly *i.e.* self-resolution, when two homochiral supermolecules are formed from a mixture of enantiomeric components by spontaneous selection of components of the same

chirality *e.g.* L^S, formation of triple helical strands of opposing helicity, and homochiral supramolecular ribbons from a racemic mixuture of components;[34,35]

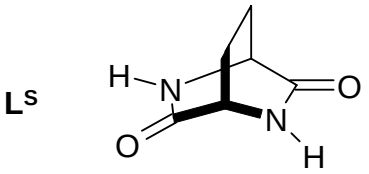

iii) chirality directed self-assembly, in which the architecture of the supramolecular species depends on the chiral features of the components, different superstructures being generated by enantiomerically pure components from racemic mixtures and chirality control of supramolecular entities $\mathbf{L^T}$ formed through formation of four hydrogen bonds yielding either homochiral ring $\mathbf{L^U}$ or heterochiral strand $\mathbf{L^U}$. *Figure 1.31* depicts the structures $\mathbf{L^T}$ and $\mathbf{L^U}$, derived form compound $\mathbf{L^T}$

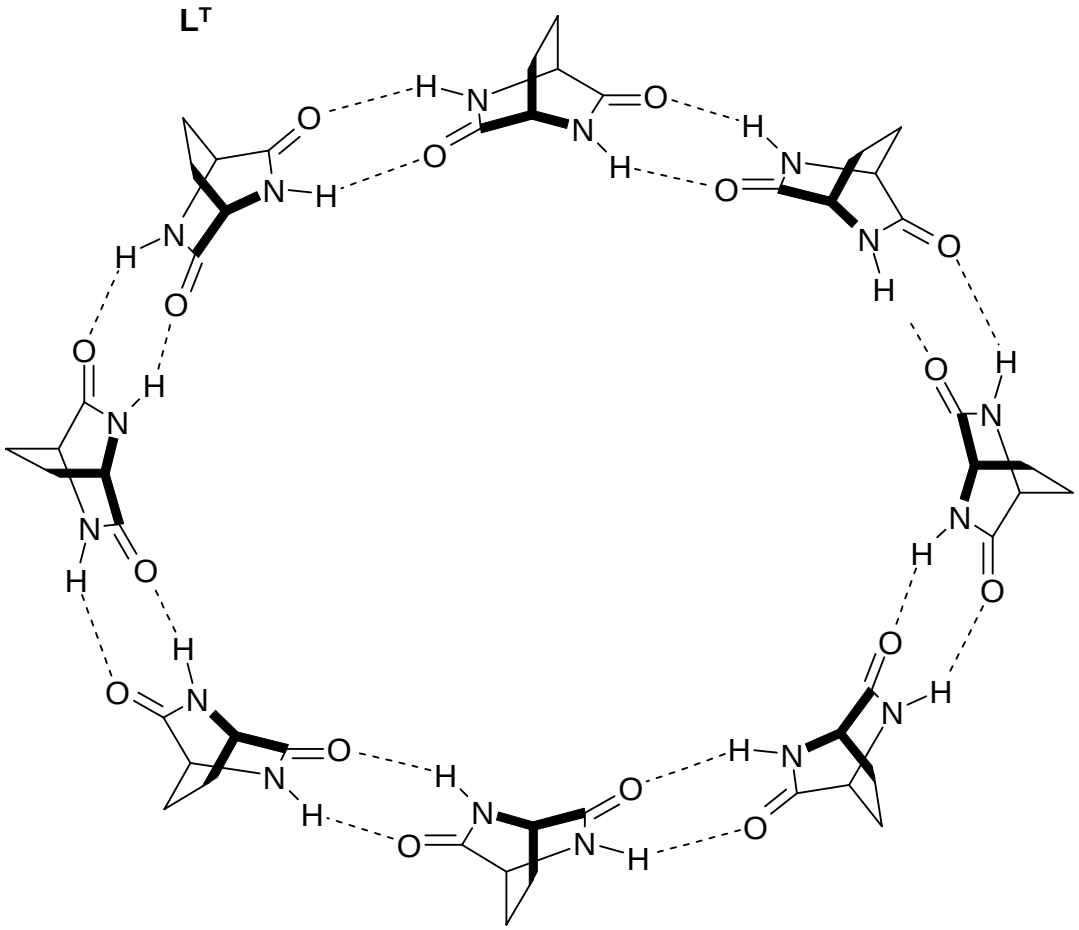

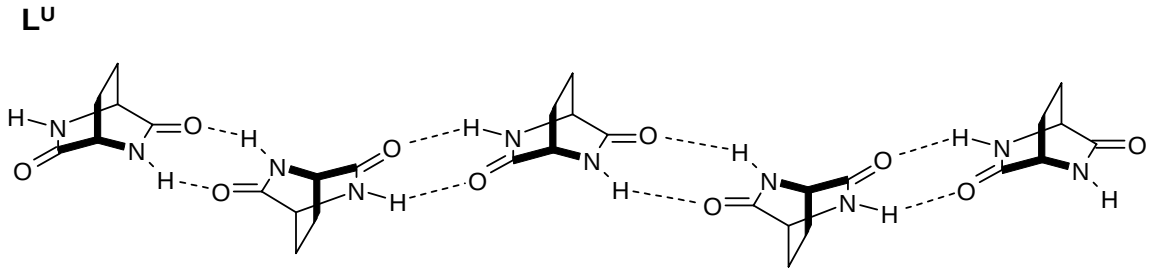

Figure 1.31 Depicting a homochiral ring ($\mathbf{L}^{\mathbf{T}}$) and a heterochiral strand ($\mathbf{L}^{\mathbf{U}}$)

1.15 Circular helicates

Circular helicates are given the general formula $[n]^{m}$cH, where "cH" represents the circular helicate in question, where "n" represents the number of metal ions and where "m" is the helicity *i.e.* "m2" would be equal to 2 for a double helix. Circular helicates have specific features and may be considered as toroidal helices. [35] There are two types of circular helical systems firstly, those helices where self-assembly takes places only in the presence of an anion, therefore acting as a template and secondly, where circular helicates assemble from metal ions and ligands alone.[36] An example of anion-centred circular helicates is shown in *Figure 1.32* below.

Ligand $[\mathbf{5}]^2$ cH33

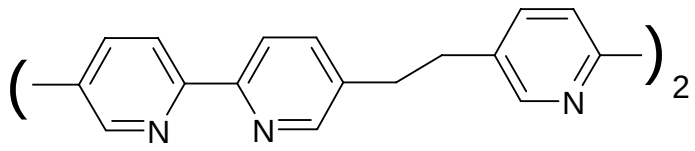

Figure 1.32 Example of a ligand that can produce an anion centered circular helicate

The self-assembly of the first circular helicate was reported by Jean-Marie Lehn and co-workers in 1997, this took the form of a penta-nuclear double helicate closed into a ring. Although a number of transition metal complexes possessing cyclic structures have been described, each circular helicate has its own unique features.[36]

In the example shown below in *Figure 1.33* each ligand extends over three adjacent metal centres and in addition the ligand strands wrap around each other having a double-helical structure and having related itself to that circular double-stranded DNA. A pentagonal shape, enclosing a strongly bound chloride anion tightly fitted into the central cavity.[36]

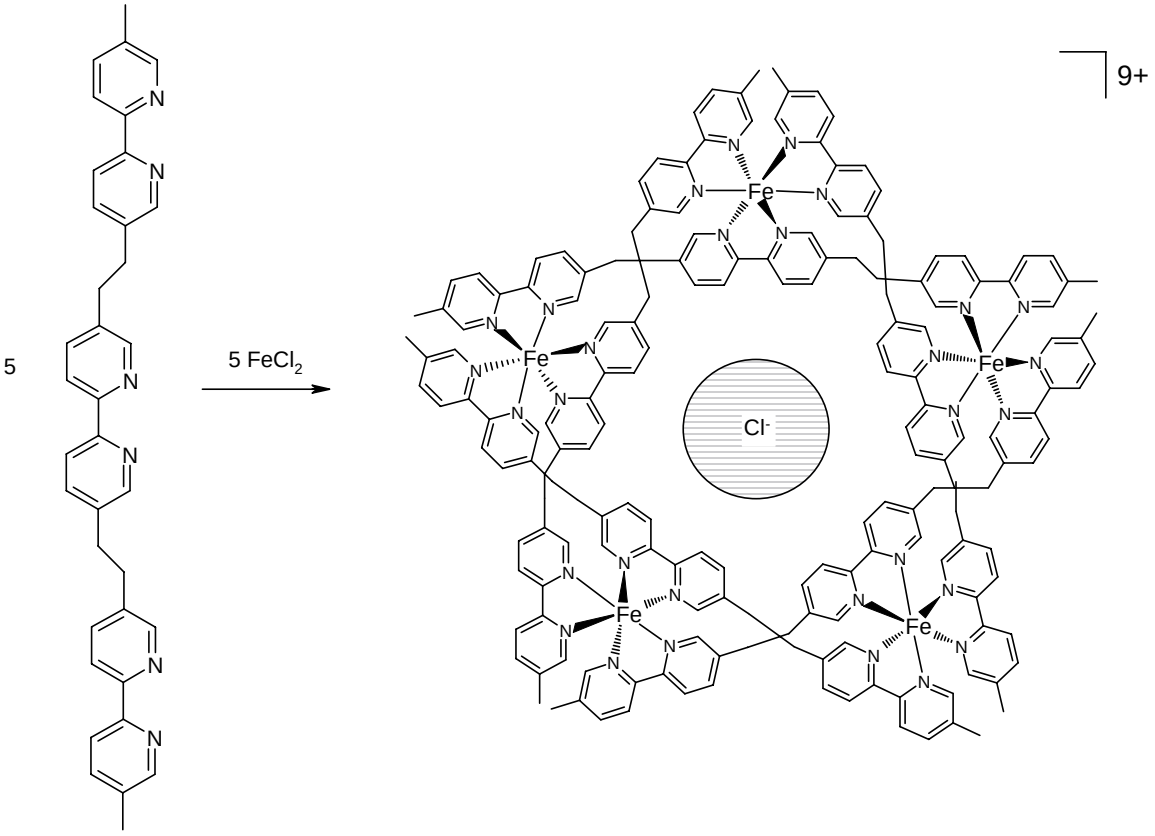

Figure 1.33 An anion-centered circular double helicate

Figure 1.33 represents a circular double helicate with Cl^- incorporated. The self-assembly of the tris-2,2′-bipyridine ligands with a small chloride ion generates the penta-nuclear circular helicate. In this system there is only one optimal structure for the species possible, with all of the ligand binding sites occupied and all of the metal ions being coordinatively saturated. The ligand has three bidentate chelating sites and coordination to metal ions preferring six-coordination gives complexes with a 1:1 metal to ligand stoichiometry. Due to the formation of a variety of definable species this is termed a dynamic combinatorial library.[37-41]

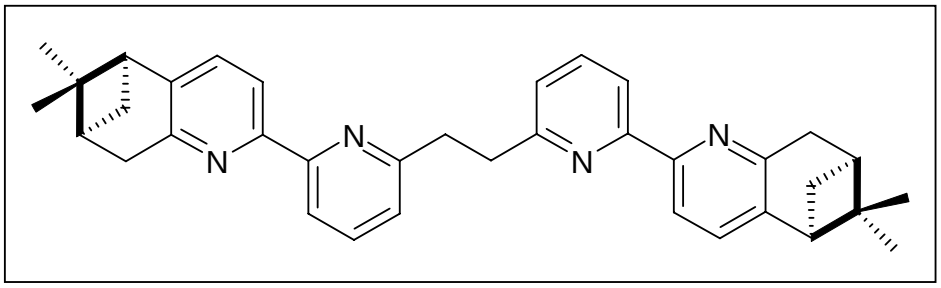

Figure 1.34 An example of a ligand that generates a dynamic combinatorial library of species.

1.16 Oligopyridines

The nomenclature given to the oligopyridine series of ligands corresponds to that given to the polyphenyls series and following the IUPAC rule. This states that the Latin prefixes bi-, ter-, quarter-, quinque-, sexi-, septi-, etc are given to this series of ligands replacing the Greek prefixes of di-, tri-, tetra-, penta-, hexa-, hepta-, etc previously used. An oligopyridine ligand is defined as an aromatic or cyclic system where two or more identical ring systems are named according to the number of units in the chain. The exception to the rule is the use of a benzene ring in a ligand chain, where the polyphenyl prefixes are used.[41-45] The naming of certain oligopyridines can be used in conjunction with α-, β-, γ-, expressions and when numbers are not used in the naming of the oligopyridine in question then it is assumed you are dealing with those with an interpyridine bond in the 2,2′- position.[41-45]

The chemistry of the aromatic pyridine ring is dominated by the interaction of the nitrogen-atom, which is an excellent donor to metal ions. There are a large number of helicates derived from the oligopyridines.[41-45] The formation of helical architectures through the simple mixing of transition metal ions and organic ligand strands reported over the last 25 years has given a wealth of knowledge to the researcher as to the role of those factors affecting the overall formation of a helicate complex. The factors to be examined include; i) the stereoelectronic preference of the metal ion and equally; ii) the disposition of the binding sites along a ligand chain.

Oligopyridines, consisting of pyridine rings linked directly via interannular carbon-carbon bonds have provided much of the early work in this helicate chemistry

field. In particular Jean-Marie Lehn *et al*, and E. C. Constable demonstrated that oligopyridines can behave as helicating ligands with many different binding modes yielding many important structures, some of which will be given as examples to follow.[41-45]

1.17 Bipyridine & terpyridine

2,2′-bipyridine units can behave as discrete units or co-ordination polymers through chelating or bridging metal-ligand interaction.[47,48] It has been seen that di-substituted bipyridines can also be utilised as receptors for certain anions when complexed with metal ions.[47,48] Although on its own it does not form helicates, 2,2′-bipyridine is an important building block in helicating ligands.

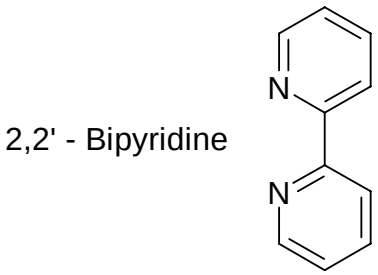

Figure 1.35. 2,2′-Bipyridine

Oligopyridines containing bipyridine units linked by flexible spacers have been synthesised and as long as the spacer is flexible enough they can form double-stranded helicate complexes with transition metal ions.[46] Furthermore, the substitution pattern of the bipyridine ring can determine its use as a helicating ligand. This substitution pattern is further examined in Chapter I,II and III of this thesis. Substituents at the 6,6′-position for example do not allow the formation of trinuclear triple helicates as these substituents would form unfavourable steric interactions.[46] However, bipyridine containing ligands can be used for the preparation of dinuclear double helicates when there are substituents at the 4- and 5- position.[46]

Each of the bipyridine units seen in *Figure 1.36* is capable of coordination to Cu(I) ions, however coordination of the metal centres by two units from the same ligand is prevented by the geometrical constraints of the ether bridging units. Thus to

satisfy the tetrahedral coordination geometry required by the Cu(I) ions a second ligand strand is required, resulting in the formation of a trinuclear double helicate. The substituents present on the 6-position prevent formation of a triple-stranded helicate with metal ions that prefer octahedral coordination geometry.

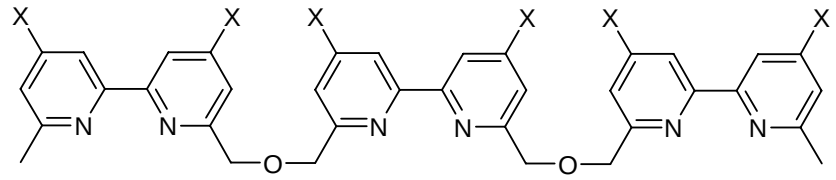

Where X = H, $CONEt_2$, COOEt

Figure 1.36 Example of a 2,2′-bipyridine species linked via fixed bridging ligands.

The nature of the spacer group is crucial for ensuring helical arrays are generated. Much detailed investigation has been performed into changing the bridging unit between two bipyridine ligands. Ligands $\mathbf{L^X}$ and L^Y are examples of ligands with different bridging ligands,[49-52] *Figure 1.37*

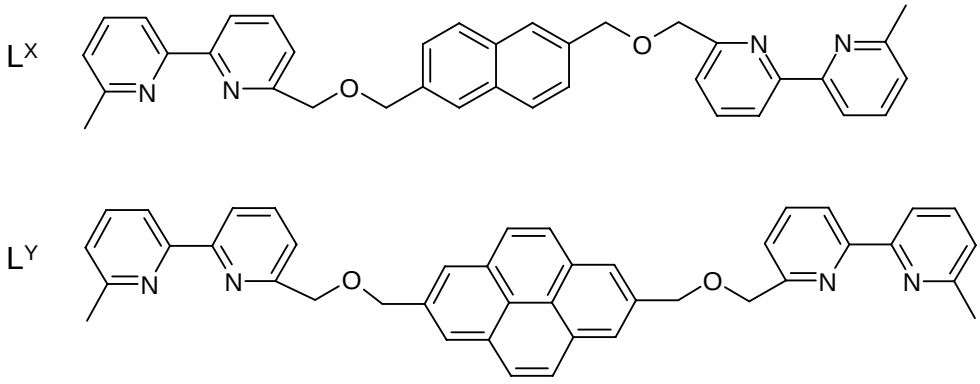

Figure 1.37 Examples of 2,2′-bipyridine units with differing bridging units

When mixed with Cu(I) metal ions both ligands form an equal mixture of helical and mono-nuclear structures, but a change is seen when the metal is exchanged to that of

Zn(II). In the example of ligand $\mathbf{L}^{\mathbf{X}}$, as is observed with Cu(I), a mixture of two specific species is now observed. However with ligand $\mathbf{L}^{\mathbf{Y}}$, the reaction with Zn(II) metal ion results in only the mono-nuclear species to be formed.

While substitution of the bipyridine unit at the 4-, 5- and 6- positions is well known, substitution at the 3- position is less explored, due to the large repulsion observed when the bipyridine unit adopts a *cis* co-planar conformation. Of particular interest (in this thesis) are the di-hydroxy and the di-amino 3,3′-disubstituted bipyridine and pyridyl/thiazole unit, of which many complexes have been shown to form a number of often novel architectures (Chapter III outlines several species).[51,52]

Terpyridine is one of the well known and well studied oligopyridines and it is adaptable and easily functionalised at either end thus allowing a whole plethora of terpyridine based ligands to be synthesized.[46,53-55] Previous research has often focussed on the synthesis of terpyridine derived ligand strands that include the use of spacer groups such as ether or ethyl groups.[46,53-55] These pyridine derivatives are relatively easy to synthesise and functionalise to prepare a wide range of different ligand compounds.

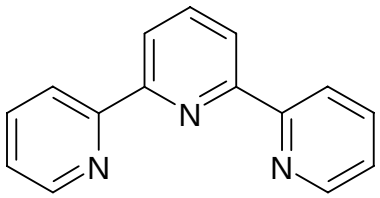

2,2':6,2'' - Terpyridine

Higher analogues of the oligopyridine series

Quaterpyridine is a molecule that can behave in one of four binding modes; i) either as a tetradentate molecule; ii) or a terdentate unit with an uncoordinated pyridine; iii) or a bidentate unit with two non-coordinated pyridines; iv) or as a bis-bidentate donor, which results in the formation of helicates.

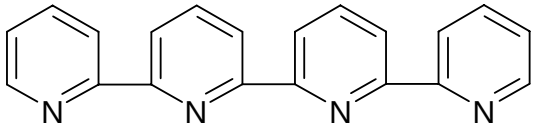

2,2':6',2'':6'',2''' - quaterpyridine

Quaterpyridine can be thought of as consisting of two bipyridine units and their connection at the, 6′,2″ position makes them suitable for double helicate formation. The symmetrical ligand is able to form double stranded helicates with metals that prefer tetrahedral coordination geometry, copper (I) and silver (I). In this mode the ligand acts as a bis-bidentate donor with both terminal bipyridine domains acting as bis-bidentate donors. The introduction of chiral substituents at the terminal of the ligand leads to chiral induced dinuclear double-stranded helicates of which many examples exist; copper (I) and silver (I) helicates $[M_2(\mathbf{L}^{\mathbf{AC}})_2]^{2+}$.[56,57] Initially two stereoisomers are formed in solution and upon crystallisation the enantio-pure diastereoisomers is formed. With the following ligands, $\mathbf{L}^{\mathbf{AC}}$ and $\mathbf{L}^{\mathbf{AC}}$**,** the formation of (*P*)-$[M_2(\mathbf{L}^{\mathbf{AC}})_2]^{2+}$ isomer is formed in favour of the (*M*)-$[M_2(\mathbf{L}^{\mathbf{AC}}$**,**$)_2]^{2+}$ ligand formed with $\mathbf{L}^{\mathbf{AC}}$ ligand.[56,57] *Figure 1.38.*

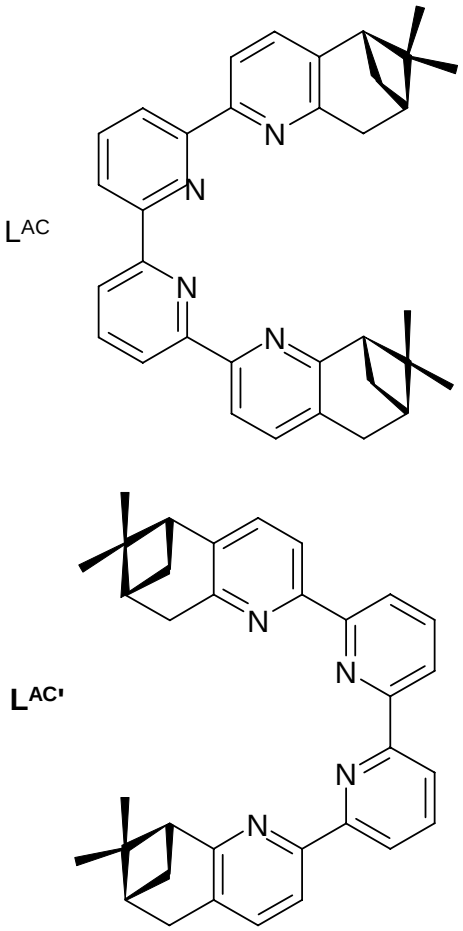

Figure 1.38 An example of ligands used in chiral induced synthesis of dinuclear double helicates.[56,57]

Quinquepyridine

The next ligand in the oligopyridine series is a little more complex and its behaviour has been explained by five different modes of coordination. The ligand is more versatile and is able to partition into both bipyridine, terpyridine and pyridine domains generating a variety of possible coordination modes such as pentadentate, bidentate and tridentate or bis-bidentate coordination domains.

This ligand ($\mathbf{L}^{\mathbf{AD}}$), forms the dinuclear double helicate $\{Pd_2(\mathbf{L}^{\mathbf{AD}})_2]^{4+}$ with palladium (II) ions.[58] *Figure 1.39*

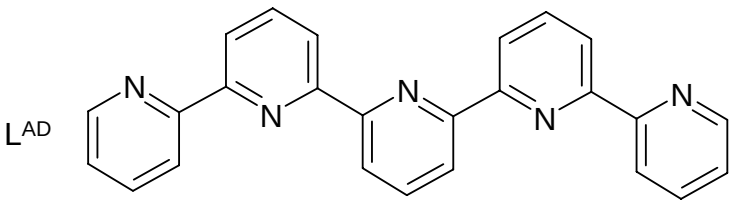

The coordination of the helicate with Pd(II) is seen where the Pd(II) metal ion adopts a five-coordinate geometry and the ligand splits into terdentate and bidentate binding domains with each metal centre coordinated by one terdentate domain from one ligand and a bidentate domain from the other. Also the reaction of quinquepyridine with $RuCl_3 \cdot H_2O$ sees the production of a dinuclear double helicate. Here the ligand acts in a similar manner to that observed with Pd(II). However in this case one of the Ru^{2+} centres is coordinated by a terdentate unit from both ligand strands and the other Ru^{2+} centre through a bidentate domain from each ligand.[46,59] *Figure 1.40.*

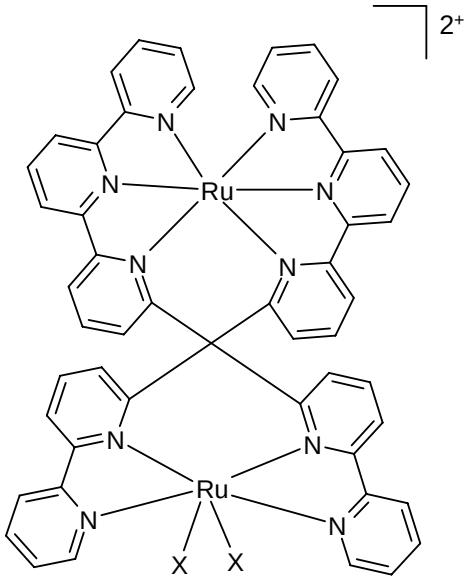

Figure 1.40. Quinquepyridine with $RuCl_3 \cdot H_2O$

Sexipyridine

2,2′:6′,2″:6″,2‴:6‴,2⁗:6⁗,2⁗′:6⁗′,2⁗″-sexipyridine usually coordinates in one of two ways, it can partition into three bidentate units resulting in a tris-bipyridine type arrangement. However, the ligand can also partition into two terdentate units, reminiscent of two terpyridines. There have been many dinuclear double helicates formed and characterised. For example the sexipyridine ligands $\mathbf{L^{AE}}$ and $\mathbf{L^{AF}}$ form dinuclear double helicate species with metal ions that prefer octahedral coordination geometries *e.g.* Fe^{2+}, Co^{2+}, Ni^{2+}, Cu^{2+}. Shown below in *Figure 1.41.*

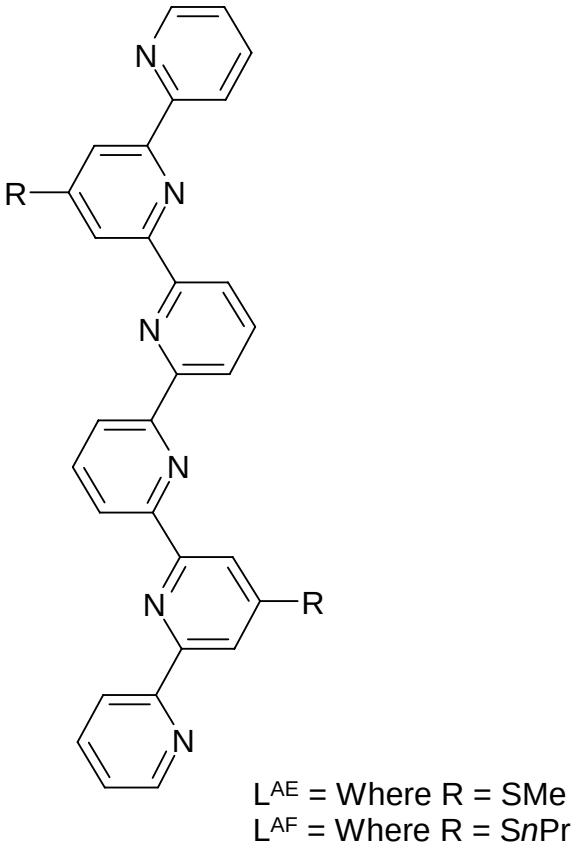

Figure 1.41 Example of Sexipyridine ligand used in synthesis of dinuclear double helicate species with Fe^{2+}, Co^{2+}, Ni^{2+}, Cu^{2+} transition metal ions.[46]

1.18 Pyridyl & thiazole ligands

The synthesis and coordination chemistry of a series of polydentate N-donor ligands based on a mixture of pyridyl and thiazole donors have recently been reported.[60-64] These can be considered as analogues of the well-known polypyridines, but the coordination behaviour of these ligands can be controlled according to the positioning of the thiazole heterocycles units in the linear ligand sequence. Unlike the oligopyridines, these heterocycles have different coordination properties due to the presence of the five-membered thiazole ring, resulting in natural breakages in the ligand backbone into distinct domains. The formation of these complexes highlights the fact that the thiazole group is instrumental in instructing the partitioning of the ligand, which in turn controls the formation of the helicate.[60-64]

There are many examples of pyridyl/thiazole ligand strands, as well as those based on the terpyridine ligand that yield many new derivatives of these species and that show both metal ion helical control and thiazole ligand helical control in the formation of metallosupramolecular helicate complex structures. A number of novel structures will be described herein and the next three chapters will go further to highlighting the usefulness of these species. Many novel compounds produced in the following chapters will include a combination of pyridyl/thiazole ligands with functional groups at the 3,3′-position ligand centre.[60-64]

1.19 Chemical sensor design

"In a chemical context, sensing of a molecular substrate results from a combination of two different and well-defined functions; i) recognition of the substrate; ii) signalling to the outside of the recognition event".[65,66] The design of a molecular sensor involves the coupling of two different components with each performing a particular function. The background to these systems can be found from the 'host-guest' chemistry of the metallocrowns and cryptands – referred to earlier in this introduction; the 'host' component first selectively interacts with a particular substrate, 'guest'. There are a number substrate recognition factors that directly affect the selection, namely the importance of size and shape. Size is discriminative for spherical 'guests' such as positive and negative ions. Shape is particularly important for polyatomic 'guests' such as anions and amino acids, which are more often than

not, larger and more bulky. Energy is also an important factor in the 'host-guest' complementarity as transition metals with similar electrical charges of the same system do not have much difference in size, but have a coordinative behaviour of interaction of very different energies depending upon electronic configurations.[13]

The second component of the sensor device *i.e.* signalling of the recognition event is expected to communicate to the operator the event of the interaction between the receptor and substrate. "The sensing device is expected to put the molecular life in contact with the macroscopic world." [67]

The communication of this interaction can take place through a number of different properties capable of detection via the appropriate instrumentation. A change in the adsorption band, or emission band can be measured in the UV-visible region, while even a shift in an NMR line can be measured. The most notable is the measurement of fluorescence emission, easily studied for a number of reasons; i) high sensitivity and selectivity; ii) possible visible detection by the naked eye (changes in UV-VIS spectra). "Changes seen of the order of 2 magnitudes or more greater than the original". [68,69]

'Semiochemistry' is the name loosely given to an area of supramolecular chemistry concerned with signalling devices. It comes from the term 'semiotics' meaning the study of signs or symbols and their application. The application of semiochemistry is the design of molecular sensors. A species able to both partake in molecular recognition, while signalling at the same time.[1,2,70-72]

Molecular recognition is paramount for the sensing of one analyte from a mixture of analytes. Sensor technology relies upon the optically sensitive host, which is usually immobilised in a device. A signal producing receptor, the host complexes one analyte, the guest and what is seen is that upon binding of the analyte the device changes an intrinsic property, the emission of an optical or electrochemical signal.[1,2,50]

Sensors are devices that "announce" the presence of analytes via reversible real-time signals detectable by one of the human senses. While there is no such thing as a selective sensor, a sensor that is selective to a sufficient degree for that particular application is applied. Sensors can be further classified into biosensors and chemosensors, where a biosensor recognises polypeptides, polysaccarides or polynucleotides and a chemosensor recognises mostly synthetic recognition elements.[72]

1.20 Molecular and supramolecular Devices

Jean-Marie Lehn was once quoted as saying 'The concept of a device is the interaction between the different components and not just the interactions that connect them'.[1,2] Therefore a supramolecular device does not have to be composed of non-covalent interactions, but can be purely covalent in nature and still be termed a supramolecular device as long as it shows characteristics of a supramolecular nature. 'By definition a supramolecular device comprises more than one component'.[2, 73]
The definition of a supramolecular device is somewhat different to the term given by Jean-Marie Lehn for the term supramolecular compound as the combination of non-covalent interactions. "A machine is a functioning entity composed of a number of interacting components that collectively carry out a predefined task for beneficial result". A machine is useful for what it does not just what it is.[2]

The field of molecular recognition deals with all aspects of the way in which two or more molecules associate non-covalently or "bind". Such binding is similar to "bonding" in that the forces involved hold atoms, or groups of atoms near one another despite the entropy cost.[73] Both types of association involve either directional (orbital) or non-directional (polar) components. While "bonding" interactions tend to be stronger in general than binding, this is not absolute, many covalent species (*e.g.* peroxides) break their bonds under conditions under which two complementary strands of DNA continue to bind.[73] However, in the general case covalent bonds do not dissociate spontaneously under ambient conditions, while many reversibly formed non-covalent complexes do.[73]

Common components for a supramolecular device include photoactive compounds capable of absorbing and emitting light and those molecules capable of accepting and donating an electron. "Within the context of supramolecular devices, re-emission of radiation by luminescence is of interest in sensing and signalling applications".[67]

It should be possible to design a photochemical device that is capable of absorbing light at one wavelength and re-emitting at another. The supramolecular device is a modular approach. The light emission processes can be broken down into three parts; i) A = absorbance; ii) ET = the electron transfer and; iii) E = emit-ion. The emission of light is able to cause certain events to take place including the following; charge separation, initiate catalysis or bring about changes to a switching device.

Emission of light (luminescence) is called fluorescence or phosphorescence depending on whether the excited state has the same or different spin compared to the ground state.[74] Luminescence involves radiative decay, in which the promoted electron in its excited state returns to the ground state and this is termed fluorescence. The fluorescent emission is usually of lower energy than the initial absorbed energy, this is due to the electron being promoted to a vibrationally excited state from which it relaxes non-radiatively prior to fluorescing to the electronic ground state.[76-80] Reactions of molecules in their electronically excited state are completely different to those that they may undergo in the ground-state. If no such interaction takes place then the excited state is deactivated, by the emission of a photon of light, (luminescence). Luminescent complexes are particularly useful in this area, the loss of luminescence (quenching) is an obvious sign that the excited state complex is reacting with another species rather than undergoing radiactive decay.

1.21 Chromophores

There are a large number of chromophores "light-absorbing components or photochemically active compounds".[2] Following the adsorption of a photon of light, the chromophore enters a long-lived electronically excited state. Many chromophores are capable of synthetic modification, a common chromophore of such type is the transition metal complex. "It is a fundamental requirement for the incorporation of a chromophore into a supramolecular device that its redox and photochemical behaviour should be stable and reversible." [2] This is due to oxidation and reduction often leading to decomposition or metal-ligand dissociation.

The introduction of chromophores into molecular design also effects the way in which the photoactive compound can behave in terms of sensing, which is dependent on a number of things including the steric orientation, non-covalent interactions and the system environment as a whole. [2]

1.22 Ru(II) polypyridyl complexes

"In particular Ru(II) polypyridyl complexes have played and are still playing a key role in the development of photochemistry, electrochemistry, chemi- and electrochemi-luminescence, and electron and energy transfer."[67]

$Ru(bipy)_3^{2+}$is one of the molecules that has been extensively studied and widely used in research laboratories all over the world in the last twenty years. This molecule has a combination of characteristics that are suitable for studying photochemical and photophysical processes; namely chemical stability, redox properties, excited-state reactivity, luminescence emission at visible wavelengths and a long excited-state lifetime.[76-80] The early interest in $Ru(bipy)_3^{2+}$ photochemistry arose from the possibility of using its long-lived excited state as an energy donor in energy transfer processes. There are a few cases in which energy transfer quenching of $Ru(bipy)_3^{2+}$ has been firmly demonstrated. A clear example is the quenching of $Ru(bipy)_3^{2+}$ by $Cr(CN)_6^{3-}$, where sensitised phosphorescence of the chromium complex has been observed both in fluid solution and in the solid state.[81-85]

In a Ru(II) polypyridines complex Ru^{2+} is a d^6 system and the polypyridine ligands are usually colourless molecules possessing σ-donor orbitals localised on the nitrogen atoms and π donor and π* acceptor orbitals more or less delocalised on aromatic rings. Promotion of an electron from a π_M metal orbital to a π^*_L ligand orbitals gives rise to metal to ligand charge transfer (MLCT) excited states.[81-85]

From a synthetic point of view the modular design of Ru(II) polypyridine allows tuning of the ground and excited state properties by the variation of ligand(s) and coordination geometry. Although the bipyridine ligands in $[Ru(bipy)_3]^{2+}$ are rigid in their pseudo-octahedral conformation, it appears even small adjustments have visibly large effects. In particular steric repulsions between substituents at the 3,3'-position show a species much less emissive than the parent $[Ru(bipy)_3]^{2+}$ due to the distortion of the substituted bipyridyl ring.[81-85]

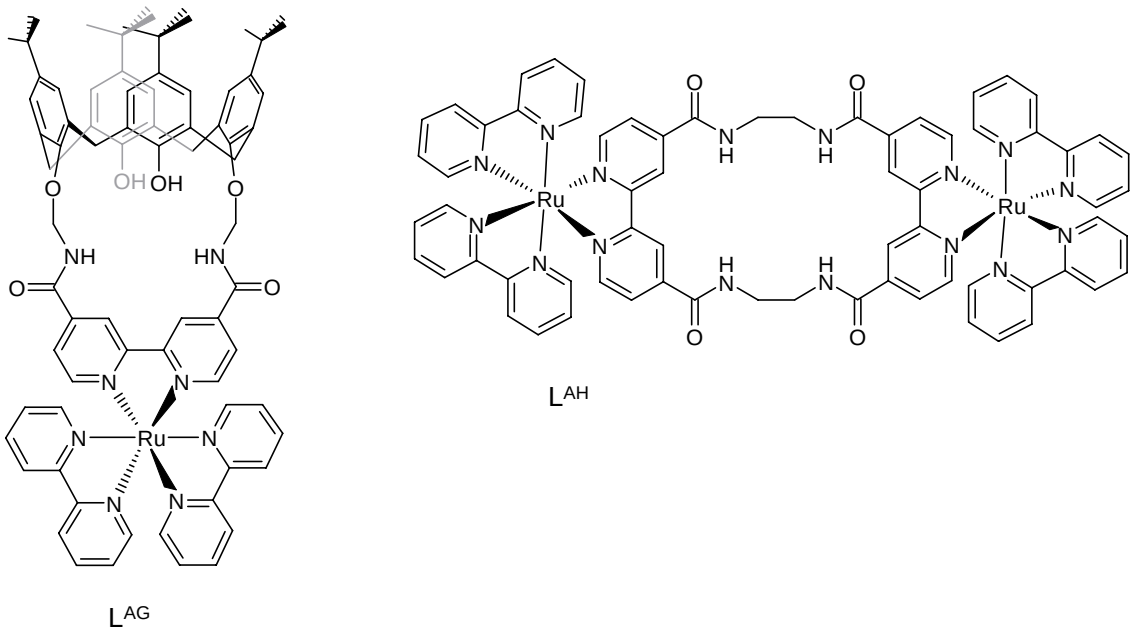

Figure 1.42 Structures L^{AG} & L^{AH} Macrocyclic derivatives of ruthenium(II) bipyridyl

Structures $\mathbf{L^{AG}}$ and $\mathbf{L^{AH}}$ are macrocyclic derivatives of ruthenium(II) bipyridyl, they both allow the sensing of inorganic ions by electrochemical methods. The mode of action of anion binding in both structures is through a combination of electrostatic and hydrogen bonding means. $\mathbf{L^{AG}}$ shows specificity to phosphate anions and the host is able to detect phosphate in a ten-fold excess of sulphate and chloride. Ligand $\mathbf{L^{AH}}$ is specific for chloride ions.

The comparison of macrocyclic $\mathbf{L^{AH}}$ with its acyclic derivative $\mathbf{L^{AI}}$ indicates and difference in the detection of particular anion species. The acyclic host binds strongly to phosphate, more so than chloride, yet in the macrocyclic derivative shows the reverse. The specificity to the individual ions is thought to be down to the rigidity of the macrocyclic structure of $\mathbf{L^{AH}}$, *Figure 1.43*.

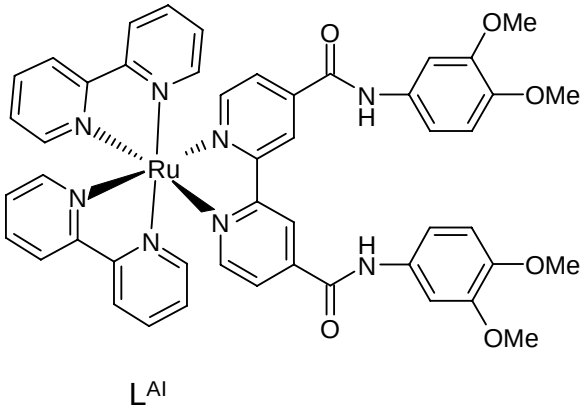

Other ruthenium crown ether hybrids have shown interesting behaviour and luminescent properties.[67]

1.23 Crown Ethers

Charles J Pederson (as mentioned briefly – section 1.5) discovered the group of macrocyclic polyethers named the 'crown ether' in 1967.[7] It was for his work on this new class of ligand that he shared the 1987 Nobel Prize for chemistry, alongside Jean-Marie Lehn and D.J Cram. The first crown that he discovered was the dibenzo[18]crown-6. Charles J Pederson named the crown ethers by the way they looked as a molecular model, with a unique nomenclature designed by Pederson himself in order to remember them with more ease. The nomenclature is made-up of; i) any side ring substituents; ii) the total number of oxygen atoms in the main ring and; iii) the total number of atoms in the ring itself. They are a simple cyclic system of ether oxygen atoms linked by an ethyl organic spacer group. One of the wonders of this class of ligand is that up until their discovery chains and rings of up to 18 atoms would have been deemed quite impossible, the most common ring structures today are those containing either 5, 6 or 7 atoms.

By incorporating 2,2′-bipyridyl or other functions to the novel crown, metal ion binding can then occur at either the macrocyclic or the bipyridyl site.[86-91] Rebek *et al* were able to successfully exploit the 3,3′-substitution positions for the preparation of a novel crown ether derivative which bound transition metal ions at the diamine site, or alkali metal ions at the crown ether.[90,91] In this investigation Rebek *et al* showed how the binding of different metals is a simple model for the allosteric effect. "Allosteric effects; the binding of an effector at a remote, allosteric site can cause conformational changes at the active site, which can alter the reactivity of the enzyme to its substrate".[88,90,91] Rebek noted that there are a number of qualifying requirements in order to construct a system capable of allosteric behaviour; firstly, an active site, secondly an allosteric site and thirdly a mechanism which connects them. Chelation of the metal at the bipyridyl site forces the aromatic bipyridyl rings to an angle of co-planarity thereby restricting the conformational freedom of the macrocycle. The binding properties of crown ethers are sensitive to changes in conformation and effective size. Therefore chelation at the bipyridyl site alters the reactivity of the crown ether's active site.

The work of N.S.Finney and S.A.McFarland has researched the efficiency of Ru(II) luminescence via ion binding-induced conformational restriction of bipyridyl ligands. Conformational restriction by metal ion binding is an extension of their work on conformational-restricted signalling with Ru(II) complex systems.[90,91-100]

They conclude that synthetic modification of the Ru(II) complex is easy due to its 'modular design', where modification is achieved by the introduction of a number of different types of ligand providing a varying overall coordination geometry in the complex. *Figure 1.44*

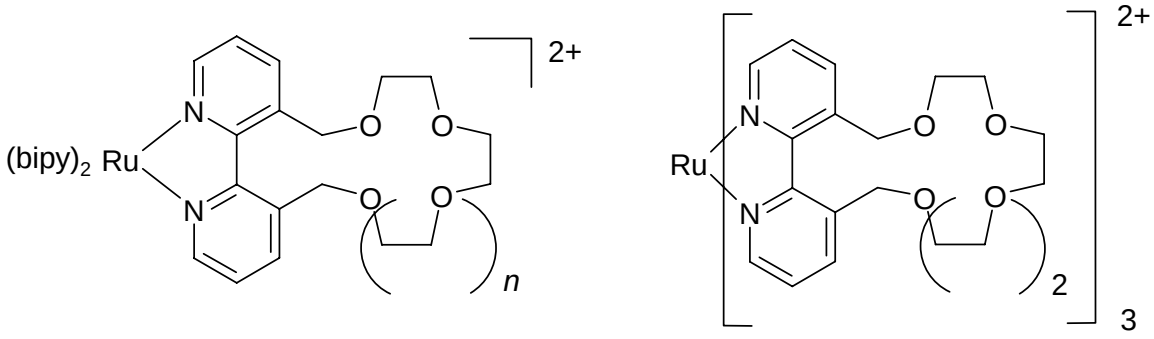

1(n=1) **2**(n=2) **3**(n=3) **4**

Figure 1.44 Diagram representing the ease of synthetic modification of the Ru(II) complex

It is believed steric repulsions between substituents at the 3,3′-positions of the bipyridyl ligand produced a species which is much less emissive than the parent $Ru(bipy)_3^{2+}$. The result of this decrease in emission is due, it is thought to the distortion of the substituted bipyridyl ligand. They prepared a number of $Ru(bipy)_3^{2+}$ based complexes of crown ethers with modified bipyridyl ligands (shown in Figure 1.51), namely an extention of the bipyridyl ligand to include an ethyl linkage between the bipyridyl ligand and that of the crown ether moiety. The emissive response of the addition of a number of different metal ions was investigated. They concluded that complexes 1 and 4 gave no response, whereas complexes 2 and 3 showed a significant increase in response both in the presence of Ca^{2+} and Pb^{2+}. Complex 3 also responded to the addition of Ca^{2+} and Pb^{2+} at submillimolar concentrations and in the presence of other analytes. They are particularly interested in the response corresponding to the addition of lead ion, as it is known that fluorescence is usually quenched by the presence of heavy atoms. They have postulated three hypotheses behind the

luminescent enhancement seen in their research; i) an increase in the energy of the metal e_g orbital; ii) a lowering of the ^{3}MLCT and iii) an increase in the ground state energy of the complex.

There are many other works that have demonstrated similar findings since N.S.Finney and S.A.McFarland. Further to this work is the area of anion and cation binding that may be observed with complexes and structures constructed from metal ion, bipyridyl crown ether complexes, of which there are a vast number in a very fast expanding field of coordination chemistry.[100-105] Chapter IV of this thesis develops some related objectives with interesting results.

CHAPTER II

2. Results & Discussion: Terpyridine containing pyridyl-thiazole ligands

2.0 Synthesis of ligands L^1- L^3

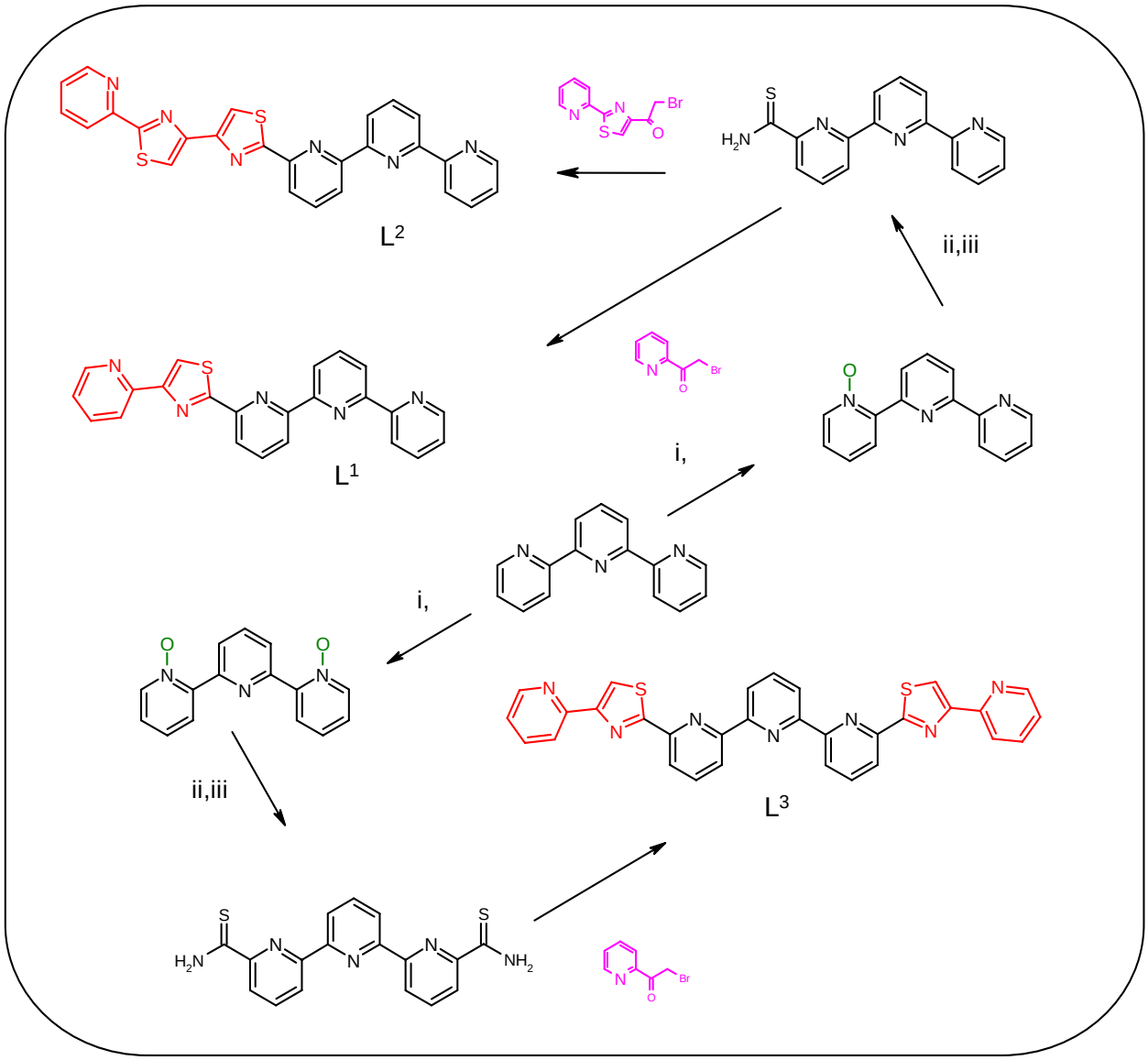

Scheme 2.1 The pyridyl-thiazole multidentate ligands L^1 – L^3

Reagents and conditions; i) $ClC_6H_4CO_3H$, $CHCl_3$; ii) C_6H_5COCl, NaCN, H_2O;

iii) H_2S, EtOH, Et_3N

2.1 Synthesis of mono-substituted terpyridine containing pyridyl-thiazole ligands L^1 and L^2

The potentially pentadentate ligand L^1 and the potentially hexadentate ligand L^2, were prepared from 2,2′:6′,2″-terpyridine-1-oxide, via the incorporation of a nitrile substituent at the C_6 position of pyridine-oxide using standard methods.[46] Conversion of the nitrile unit to a thioamide was achieved by the reaction with hydrogen sulfide gas. Subsequent reaction of the thioamide-functionalised terpyridine with i) 2-(α-bromoacetyl) pyridinium hydrobromide gives ligand L^1; while reaction of the thioamide-functionalised terpyridine-1-oxide with ii) (2′-(pyrid-2-yl) thiazol-4′-yl)ethanone gives ligand L^2. Both reactions are performed in ethanol (EtOH) at reflux with the products precipitating cleanly as their hydrobromide salts. The free ligands are then obtained via neutralisation with aqueous ammonia.

2.1.1 *N*-oxidation

N-oxidation of 2,2′:6′,2″-terpyridine with an equimolar amount of 3-chloroperoxybenzoic acid (*m*-CPBA) affords the mono-substituted 2,2′:6′,2″-terpyridine-1-oxide via precipitation from acetone. The product was identified by ^{1}H NMR and shows 11 different proton environments confirming the unsymmetrical nature of the ligand.

2.1.2 Cyanation

Cyanation of 2,2′:6′,2″-terpyridine-1-oxide was achieved by the reaction of excess benzolyl chloride and sodium cyanide with 2,2′:6′,2″-terpyridine-1-oxide. Recrystallisation from EtOH afforded the 6-cyano-2,2’:6′,2″-terpyridine as a white solid. ^{1}H NMR confirms the formation of 6-cyano-2,2′:6′,2″-terpyridine as the signal corresponding to the proton at the C_2 position is no longer present and a total of 10 signals are observed.

2.1.3 H_2S thioamide addition

Subsequent reaction of 6-cyano-2,2′:6′,2″-terpyridine with hydrogen sulfide gas affords 2,2′:6′,2″-terpyridine-6-thioamide as a yellow crystalline precipitate. The

^{1}H NMR shows a broad singlet at δ 9.62 ppm which is indicative of a thioamide functional group present at the C_2 position.

2.2 Synthesis of di-substituted terpyridine containing pyridyl-thiazole ligand L^3

The potentially septadentate ligand L^3, is synthesised from 2,2′:6′,2″-terpyridine-1,1′-dioxide via the incorporation of a nitrile substituent at the C_6 and $C_{6''}$ position of each pyridine-oxide using standard methods. Conversion of each nitrile unit to a thioamide substituent was achieved by the reaction with hydrogen sulfide gas. Subsequent reaction of the di-thioamide-functionalised terpyridine with 2-(α-bromoacetyl)-pyridinium hydrobromide (in EtOH at reflux) gives L^3 as the hydrobromide salt. Once again the free ligand is obtained via neutralisation with aqueous ammonia.

2.2.1 *N*-oxidation

N-oxidation of 2,2′:6′,2″-terpyridine with two equimolar amounts of *m*-CPBA affords the 2,2′:6′,2″-terpyridine-1,1′-dioxide via precipitation from acetone. Here the ^{1}H NMR shows a symmetrical species with signals substantially shifted when compared to that of the starting material.

2.2.2 Cyanation

Cyanation of 2,2′:6′,2″-terpyridine-1,1′,-dioxide via reaction with excess benzolyl chloride and sodium cyanide followed by recrystallisation from EtOH afforded the solid 6,6″-dicyano-2,2′:6′,2″-terpyridine as a cream solid. Here ^{1}H NMR illustrates that the ligand still retains its symmetrical nature, with only 8 signals observed, as the proton at the C_6 and $C_{6''}$ position δ 8.47 ppm has been replaced with nitrile substituents.

2.2.3 H_2S thioamide addition

Reaction of 6,6″-dicyano-2,2′:6′,2″-terpyridine with hydrogen sulfide gas affords the product 2,2′:6′,2″-terpyridine-6,6″-di-thioamide as a yellow crystalline

precipitate. The ^{1}H NMR of this material shows two signals at δ 10.30 and 10.24 ppm that are indicative of a thioamide functional group. The amine group is most often observed as two individual proton signals due to the degree of double bond character shown by the C-N bond (the two canonical forms are as shown in *Figure 2.1*) and the restricted rotation about that C-N bond gives two unique proton environments.

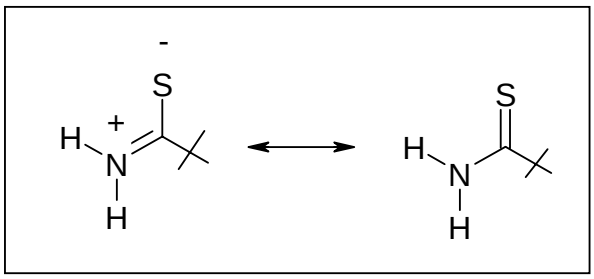

Figure 2.1 A Diagrammatic representation of two resonance canonical forms for a thioamide functional group

2.3 Synthesis and crystal structure of L^1 with $Cu(ClO_4)_2 \cdot 6H_2O$

The potentially pentadentate ligand L^1, as with many similar multidentate pyridyl-thiazole ligands does not dissolve in many common organic solvents. However, L^1 readily dissolves upon reaction with transition metal ions to form soluble complexes in MeCN. Reaction of L^1 with $Cu(ClO_4)_2 \cdot 6H_2O$ in a 1:1 ratio resulted in a clear green solution which produced large green crystals of X-ray quality upon slow diffusion of ethyl acetate into the acetonitrile (MeCN) solution. Analysis of the crystals by electrospray mass spectrometry indicated a dimeric complex cation $[Cu_2(L^1)_2]^{4+}$ *m/z* 521. Elemental analysis was consistent with the empirical formulae $[Cu(L^1)][ClO_4]_2$ with the formation of a dinuclear double helicate confirmed via analysis by X-ray crystallography.

Each copper metal ion was found to be in a five-coordinate environment; that is the coordination geometry about each Cu(II) centre in this complex can be described as essentially square pyradimal, with [N(1)] occupying the axial site. The Cu…Cu separation is 4.37 Å and the Cu…N distances range from 1.926(2) to 2.260(2) Å. The Cu…N distances of the thiazole N-donors are noticeably longer than those N-donors of the pyridyl heterocycles in the ligand chain; 2.086(2) and 2.260(2) Å. The coordination geometry is formed as the ligand splits into two distinct binding domains consisting of a bidentate (pyridyl-thiazole) unit and a tridentate (terpyridyl) unit formed by the partitioning of each ligand. The two ligands in the dinuclear double helicate are said to be "head to tail" [HT] such that each copper centre is coordinated by both a tridentate (terpyridyl) unit from one ligand and a bidentate (pyridyl-thiazole) unit from the other.

The formation of this helicate complex can be said to be controlled by two factors: i) the stereo-electronic preference of Cu(II) ion to form an axially elongated five-coordinate geometry; ii) the tendency of L^1 to partition along the ligand backbone into bidentate and tridentate domains because of the effect of the thiazole ring. The observed twist that partitions this ligand into bidentate and terdentate domains, occurring adjacent to the thiazole ring is in agreement with observed behaviour with other ligands in this series. The alternate binding domain, the tridentate (pyridyl-thiazole-pyridyl) unit is less favoured on geometric grounds as a poor donor, due to the lone pairs on each N atom not being sufficiently convergent.

Figure 2.2 Structures of the complex cation $[Cu_2(L^1)_2]^{4+}$ with a) Capped stick view; b) Ball and stick view; c) a vertical view; and d) space-fill view of the Cu(II) helicate complex

a) Capped stick view

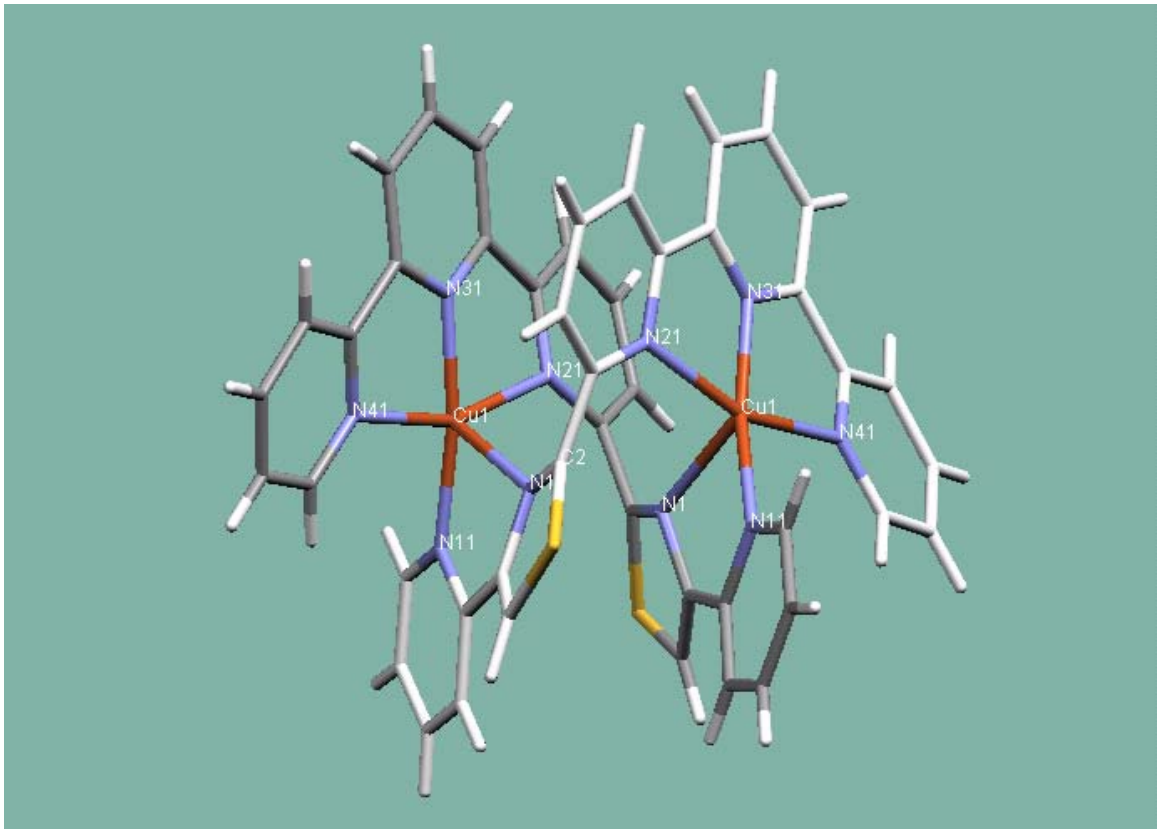

b) Ball & stick view

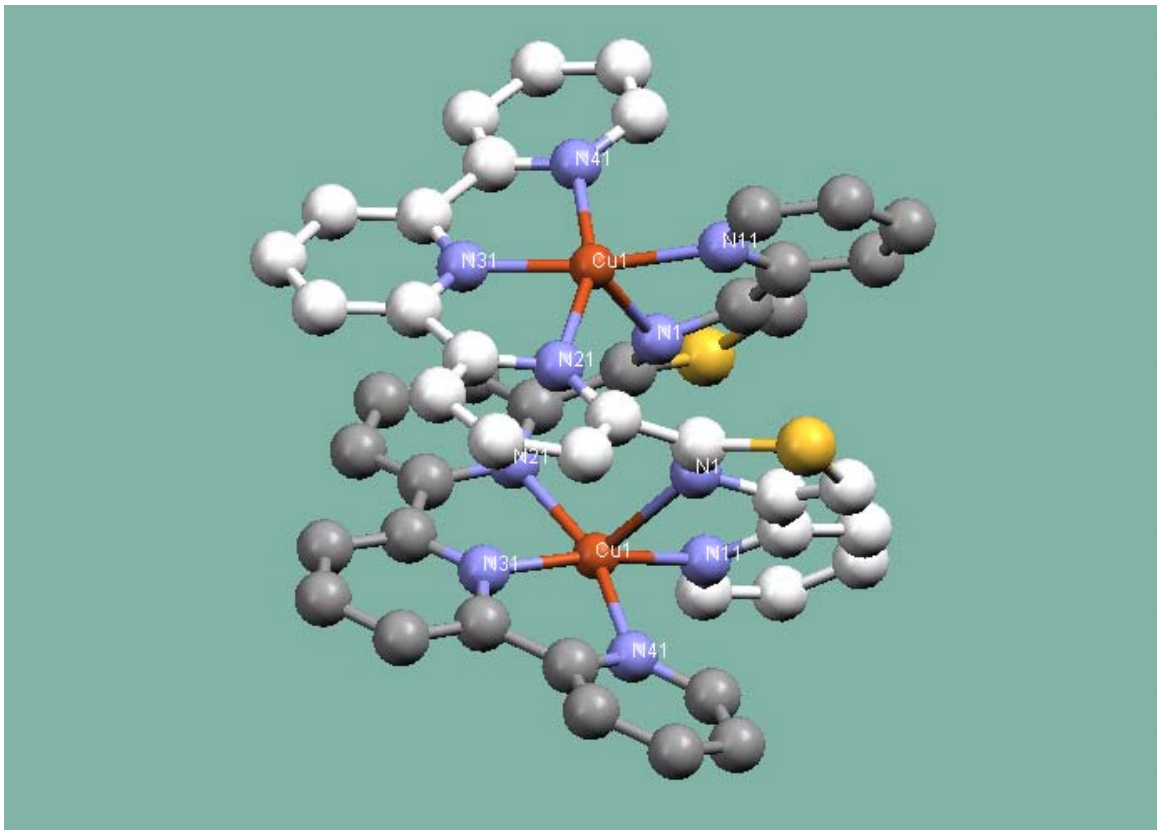

c) Vertical view

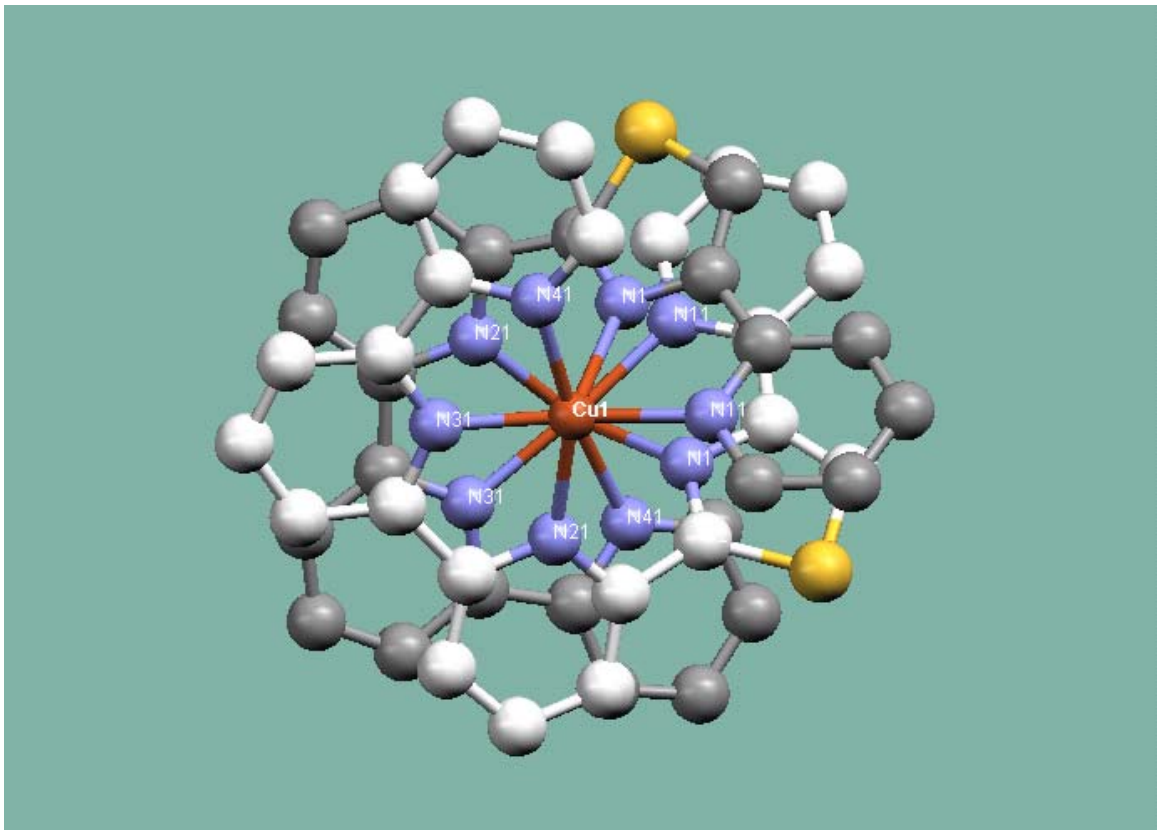

d) Spacefill view

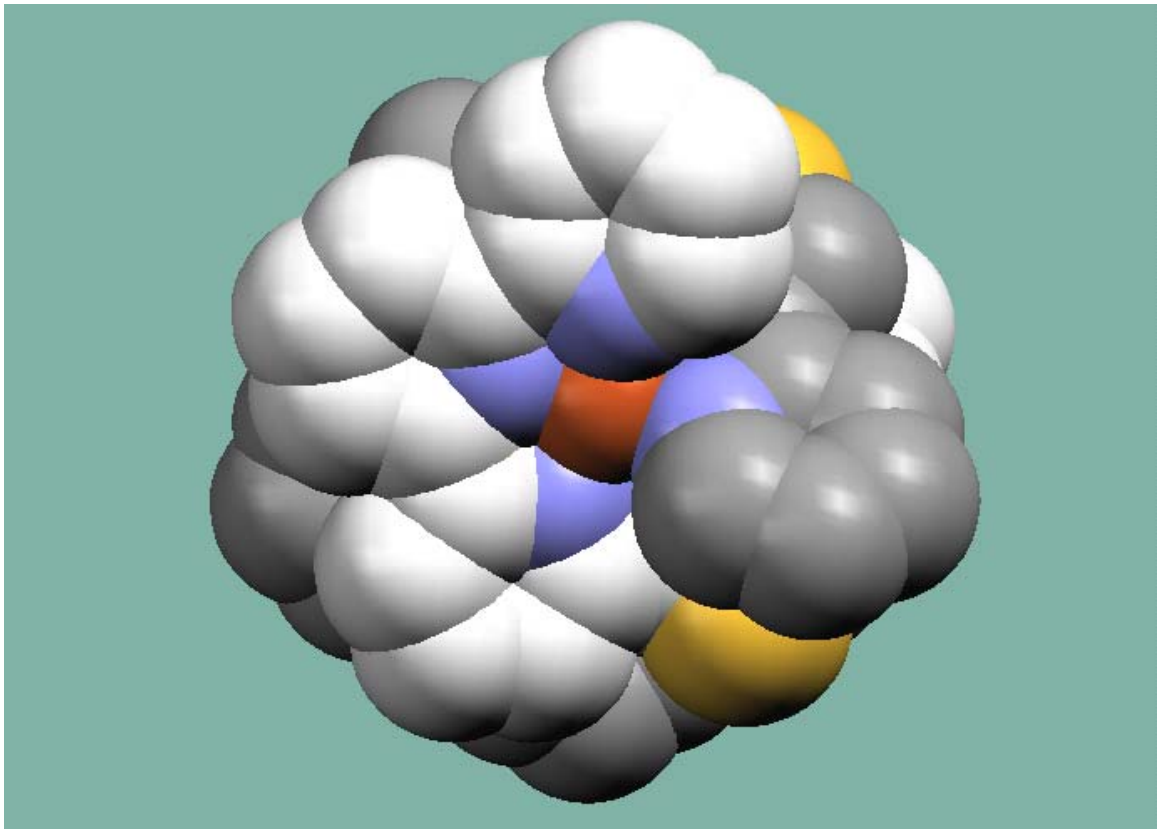

Bond Lengths			
Cu(1) – N(31)	1.926(2)	Cu(1) – N(21)	2.086(2)
Cu(1) – N(11)	1.988(2)	Cu(1) – N(1)	2.260(2)
Cu(1) – N(41)	2.068(2)		
Bond Angles			
N(31) – Cu(1) – N(11)	170.0(8)	N(41) – Cu(1) – N(21)	159.1(7)
N(31) – Cu(1) – N(41)	79.7(7)	N(31) – Cu(1) – N(1)	110.7(7)
N(11) – Cu(1) – N(41)	97.8(7)	N(11) – Cu(1) – N(1)	78.4(7)
N(31) – Cu(1) – N(21)	79.5(7)	N(41) – Cu(1) – N(1)	83.0(7)
N(11) – Cu(1) – N(21)	102 .3(7)	N(21) – Cu(1) – N(1)	106.4(7)

Table 2.1 Selected bond distances (Å) and bond angles (º) for $[Cu_2(L^1)_2][ClO_4]_4$

2.4 Synthesis and crystal structures of L^2 with $Co(ClO_4)_2 \cdot 6H_2O$ and $Ni(ClO_4)_2 \cdot 6H_2O$

Reaction of L^2 with either $Co(ClO_4)_2 \cdot 6H_2O$ or $Ni(ClO_4)_2 \cdot 6H_2O$ gave ions in the electrospray mass spectroscopy corresponding to the formation of a double helicate complex, the complex cation $[Co_2(L^2)_2]^{4+}$ and $[Ni(L^2)_2]^{4+}$ *m/z* 594 and 593 respectively. Elemental analysis was consistent with the empirical formulae $[M(L^2)][ClO_4]_2$ (M = Co or Ni). The formation of a dinuclear double helicate for each complex was confirmed by X-ray crystallography and in both cases the helicates were found to be isostructural.

Each metal ion was found to be in a six-coordinate environment; that is the coordination geometry surrounding each metal centre can be described as a pseudo-octahedral environment. The Co…Co separation is 4.86 Å, while the Ni…Ni separation is 4.91 Å. The Co…N-donor distances range from 2.022(5) to 2.28(6) Å with the longest cobalt to nitrogen bond distances between those of the thiazole heterocycles Co(1)-N(41) 2.248(5) and Co(2)-N(91) 2.280(6) Å, due to the divergent nature of the two thiazole units. The Ni…N-donor distances range from 1.976(5) to 2.256(5) Å and again the longest nickel to nitrogen bond distance between those of the thiazole heterocycles Ni(1)-N(41) 2.234(4) and Ni(2)-N(31) 2.217 Å; this is also as a result of the divergent nature of the thiazole unit.

In both cases the solid state structure reveals that the coordination geometry is split between two tridentate units with the ligand partitioning between the inner thiazole and central pyridine ring of the ligand chain. This creates two inequivalent tridentate binding domains, a tridentate (terpyridyl) unit at one end of the ligand and a second tridentate (pyridyl-thiazole-thiazole) unit at the other. This is unusual because allowing partitioning at this position along the ligand chain creates a tridentate domain that contains two adjacent five-membered thiazole rings that are known to act as a poor bidentate unit as the nitrogen atoms are not sufficiently convergent. Each ligand possesses both a “head” and a “tail” end and gives rise to two possible isomers; in the “head to head” [HH] isomer each metal centre will have a $\{M(terpy)_2\}$ coordination geometry and the other a $\{M(tz\text{-}tz\text{-}py)_2\}$ coordination geometry, where tz = thiazole donor and py = pyridyl donor. In the “head to tail” [HT] isomer the two metal centres are coordinated by the same binding unit, this disorder can be explained as one of the two ligands is perfectly ordered, while the other is not. This second ligand has two possible orientations “head to head” or “head to tail” therefore giving a

complex that overall is disordered. In the Co(II) complex the orientation that gives rise to the two isomeric forms is proportionately different to that of the Ni(II) complex with ligand L^2. Thus, in the Co(II) complex the isomeric ratio is approximately 2:1, whereas in the Ni(II) complex the components are present in equal amounts.

Unlike L^1 and other similar ligands in this series, these two complexes with L^2 are an exception and show that only one factor dominates the way in which these helicate complexes are formed, that of the stereo-electronic preference of the metal ion to form a pseudo-octahedral geometry. This preference does not allow, as seen previously for the partitioning of the ligand to occur between two adjacent thiazole units. Should this have occurred a tetradentate and a bidentate domain would have been created which would be unsuitable for coordination to two octahedral metal ions. Here it is noticeable that as a bi-thiazole unit only one M-N bond is of a typical length, and the other is much larger *e.g.* Ni(1) – N(51) (Py – Ni) is 1.995 Å and Ni(1) – N(41) (thia – M) is 2.234 Å. Partitioning in this manner (due to the formation of a thiazole-containing bidentate unit) is the only way that a fully saturated dinuclear double helicate can be formed.

Figure 2.3 Structures of the head to head (H/T) complex cation $[Co_2(L^2)_2]^{4+}$ with a) Capped stick view; b) c) Ball and stick view, vertical and horizontal; and d) space-fill view of the Co(II) helicate complex.

a) Capped stick view

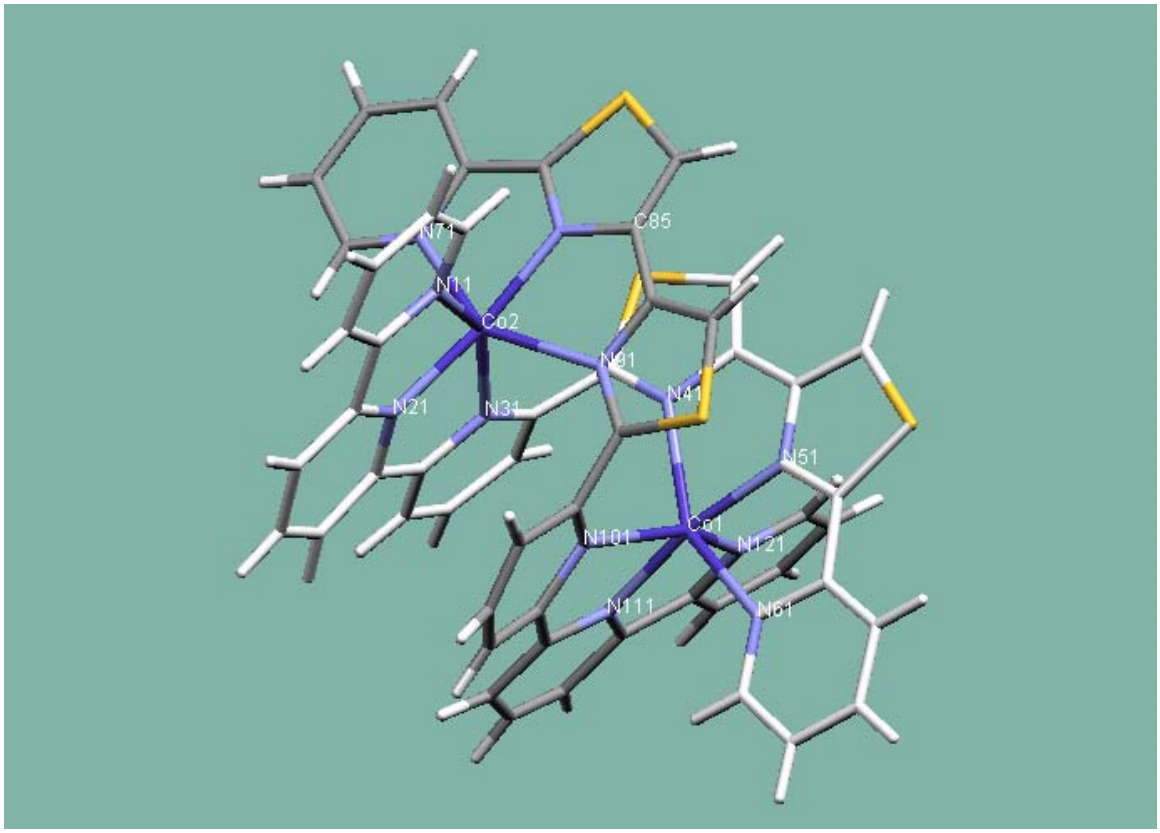

b) Ball and stick view

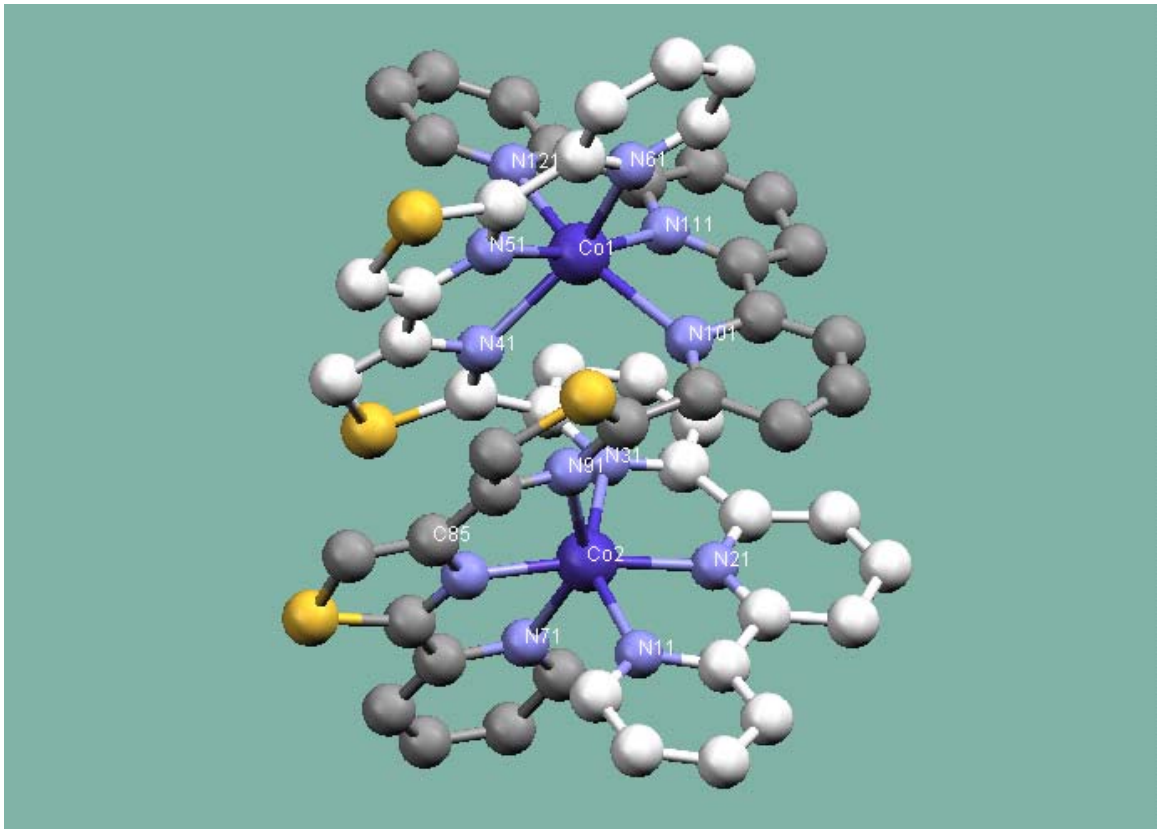

c) Ball and stick view

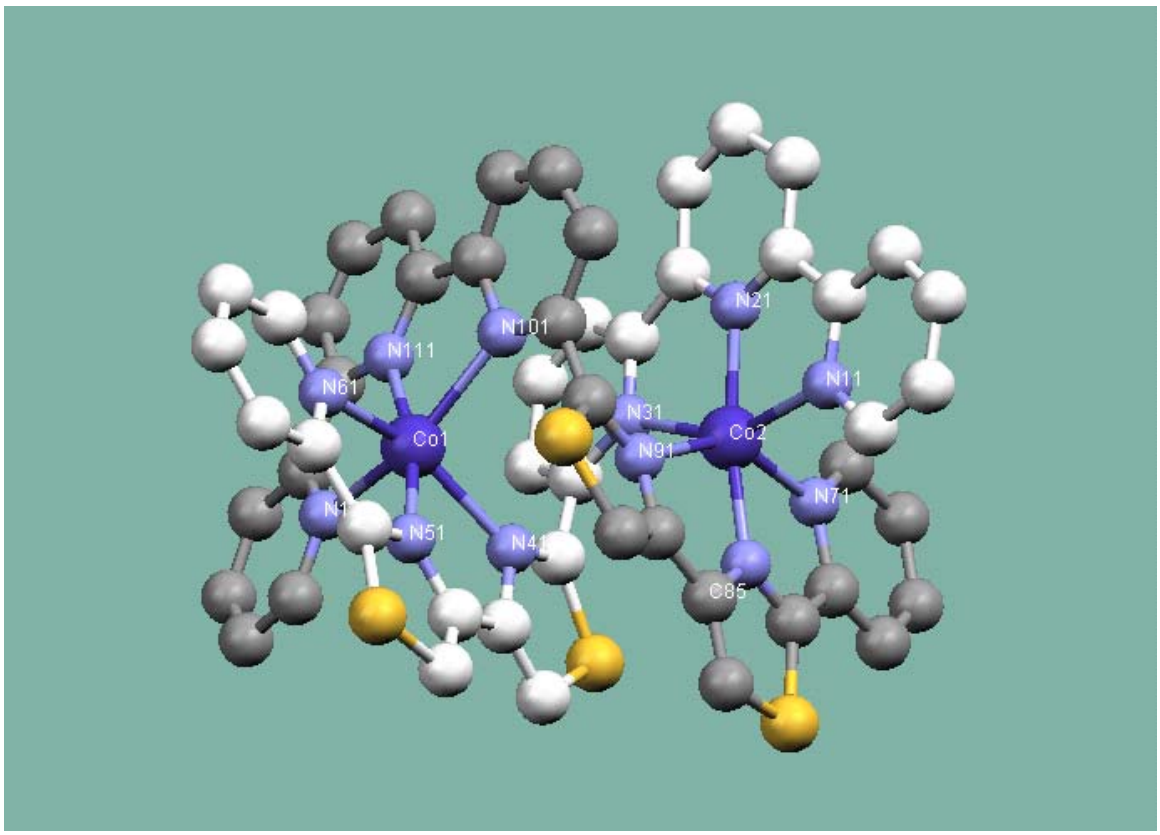

d) Spacefill view

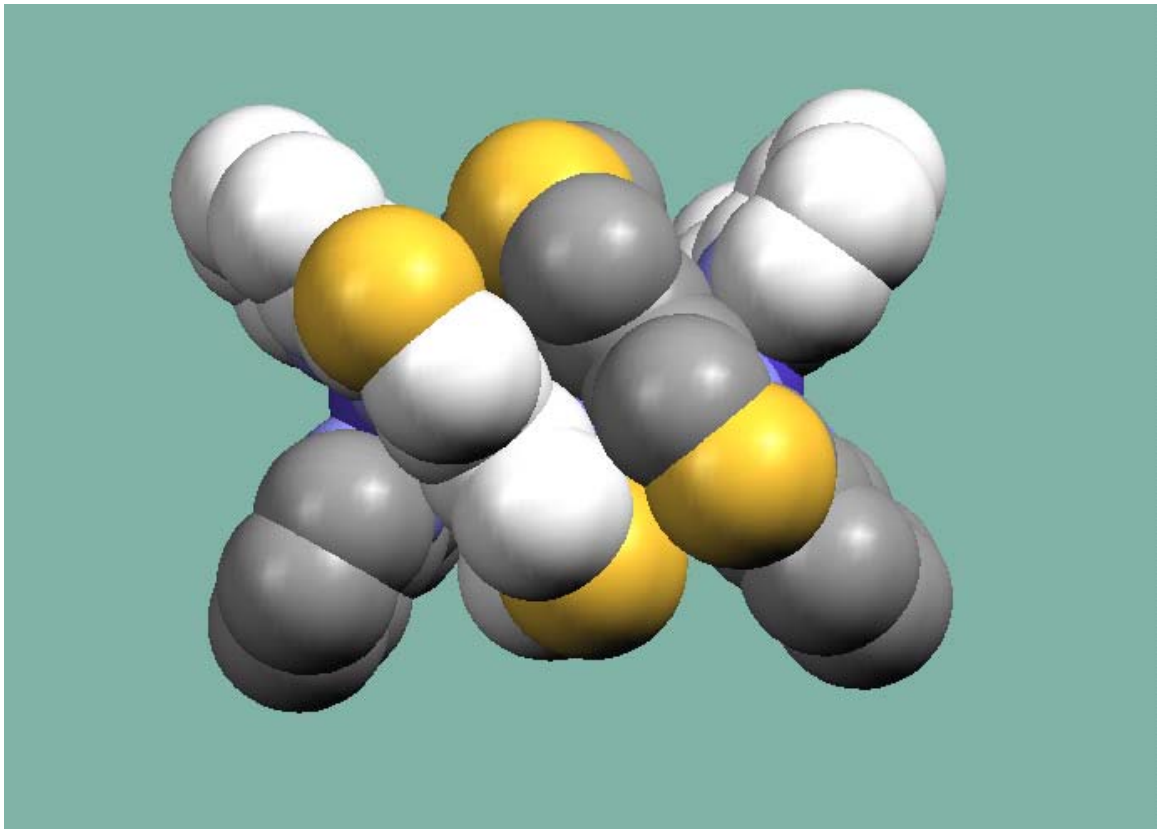

Bond Lengths			
Co(1) – N(51)	2.022(5)	Co(2) – N(81)	2.046(6)
Co(1) – N(111)	2.050(5)	Co(2) – N(21)	2.056(6)
Co(1) – N(121)	2.182(6)	Co(2) – N(11)	2.199(6)
Co(1) – N(61)	2.207(6)	Co(2) – N(31)	2.210(5)
Co(1) – N(101)	2.238(5)	Co(2) – N(71)	2.231(6)
Co(1) – N(41)	2.248(5)	Co(2) – N(91)	2.280(6)
Bond Angles			
N(51) – Co(1) – N(111)	168.2(2)	N(81) – Co(2) – N(21)	169.2(2)
N(51) – Co(1) – N(121)	95.1(2)	N(81) – Co(2) – N(11)	94.0(2)
N(111) – Co(1) – N(121)	76.2(2)	N(21) – Co(2) – N(11)	75.5(2)
N(51) – Co(1) – N(61)	75.1(2)	N(81) – Co(2) – N(31)	115.1(2)
N(111) – Co(1) – N(61)	98.6(2)	N(21) – Co(2) – N(31)	75.6(2)
N(121) – Co(1) – N(61)	102.3(2)	N(11) – Co(2) – N(31)	150.7(2)
N(51) – Co(1) – N(101)	114.3(2)	N(81) – Co(2) – N(71)	74.5(3)
N(111) – Co(1) – N(101)	75.0(2)	N(21) – Co(2) – N(71)	105.0(2)
N(121) – Co(1) – N(101)	150.5(2)	N(11) – Co(2) – N(71)	102.4(2)
N(61) – Co(1) – N(101)	87.8(2)	N(31) – Co(2) – N(71)	89.3(2)
N(51) – Co(1) – N(41)	73.4(2)	N(81) – Co(2) – N(91)	72.7(2)
N(111) – Co(1) – N(41)	113.2(2)	N(21) – Co(2) – N(91)	108.7(2)
N(121) – Co(1) – N(41)	85.3(2)	N(11) – Co(2) – N(91)	87.6(2)
N(61) – Co(1) – N(41)	148.2(2)	N(31) – Co(2) – N(91)	97.6(2)
N(101) – Co(1) – N(41)	100.7(2)	N(71) – Co(2) – N(91)	146.3(2)

Table 2.2 Selected bond distances (Å) and bond angles (º) for $[Co_2(L^2)_2]^{4+}$

Figure 2.4 Structure of the (H/T) complex cation $[Ni_2(L^2)_2]^{4+}$; a) Capped stick view; b) & c) Vertical and horizontal ball and stick view; d) space-fill diagram of the Ni(II) helicate structure

a) Capped stick view

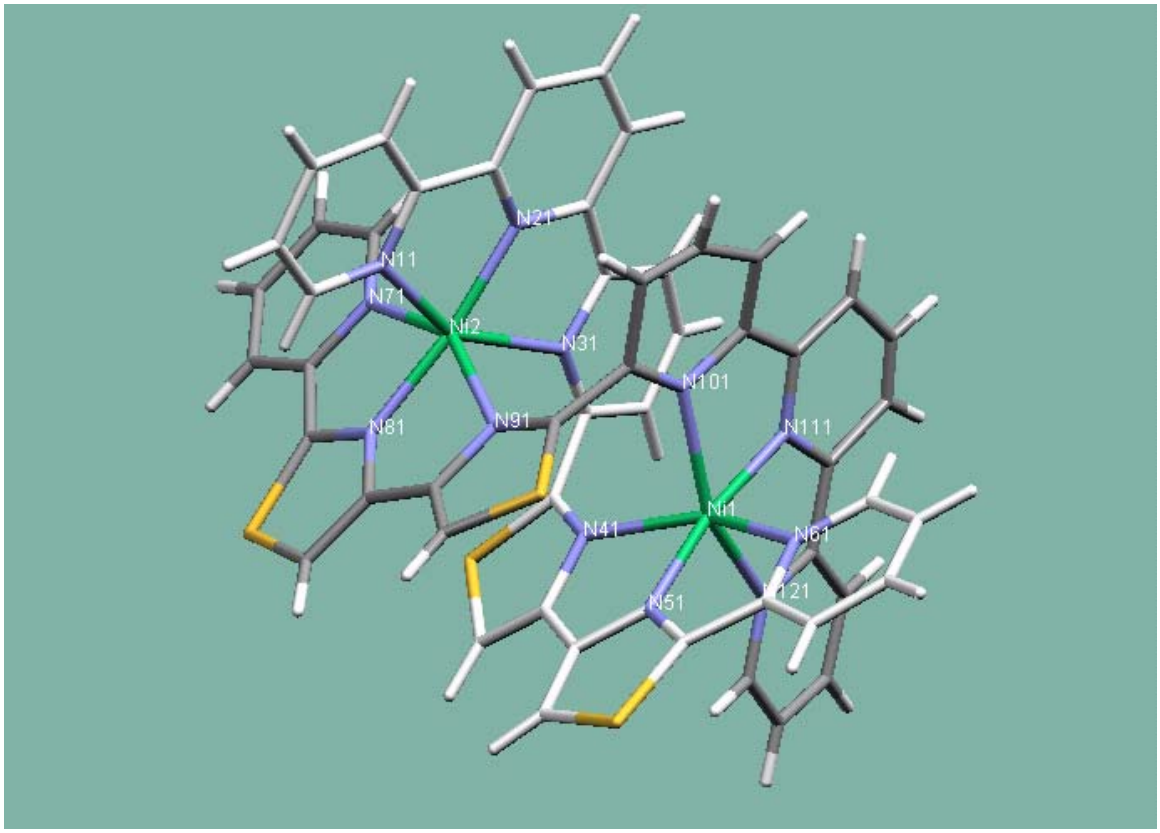

b) Ball and stick view

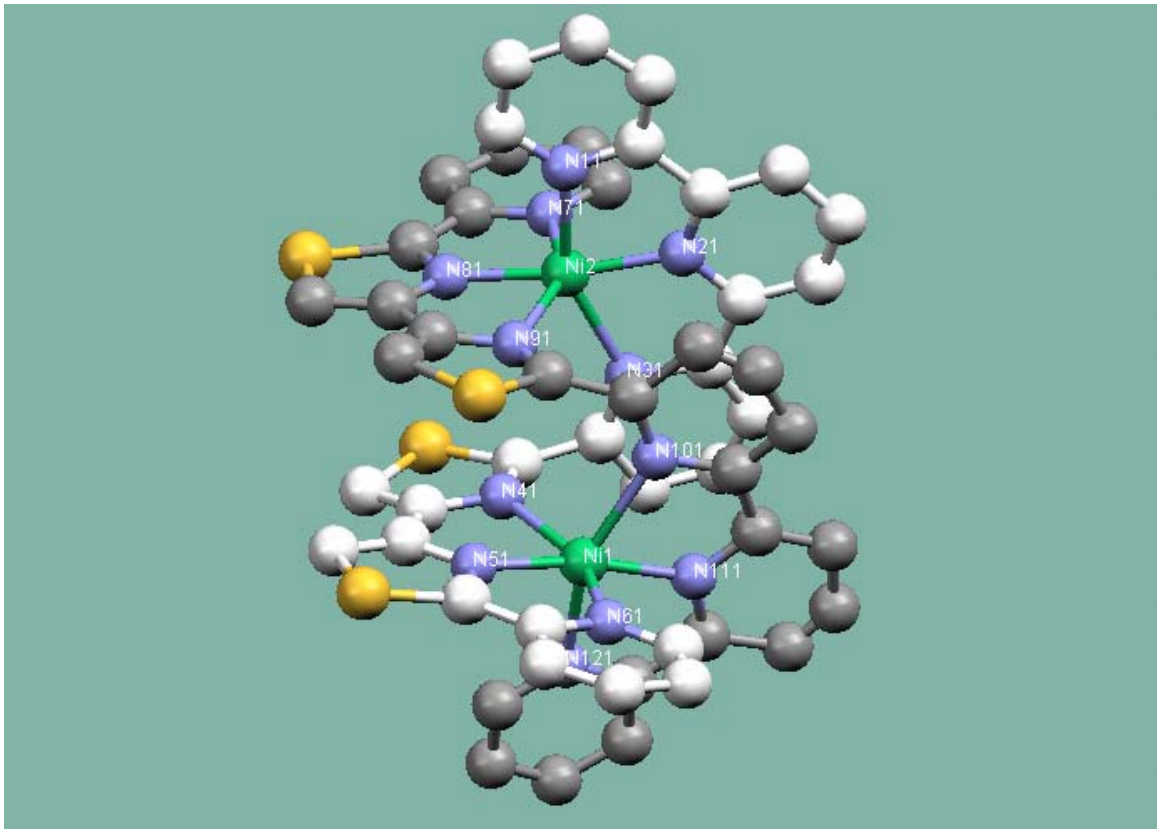

c) Ball and stick view

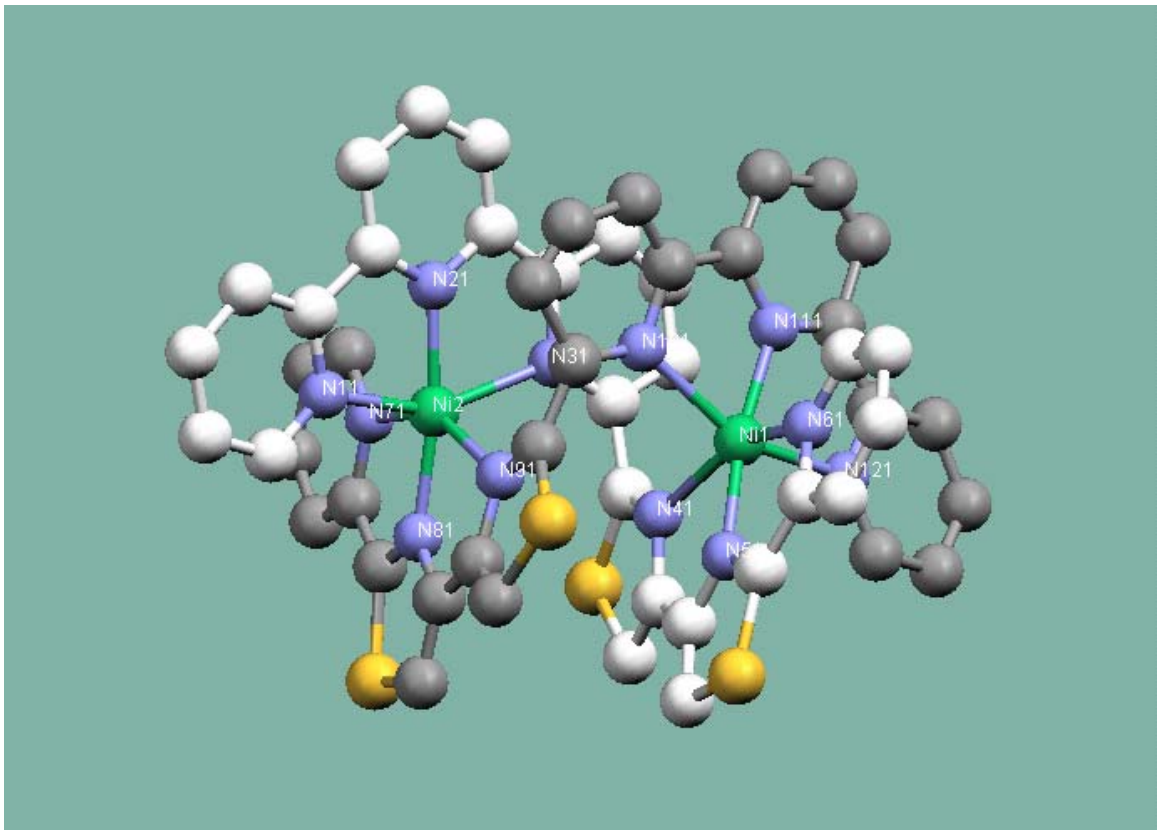

d) Spacefill view

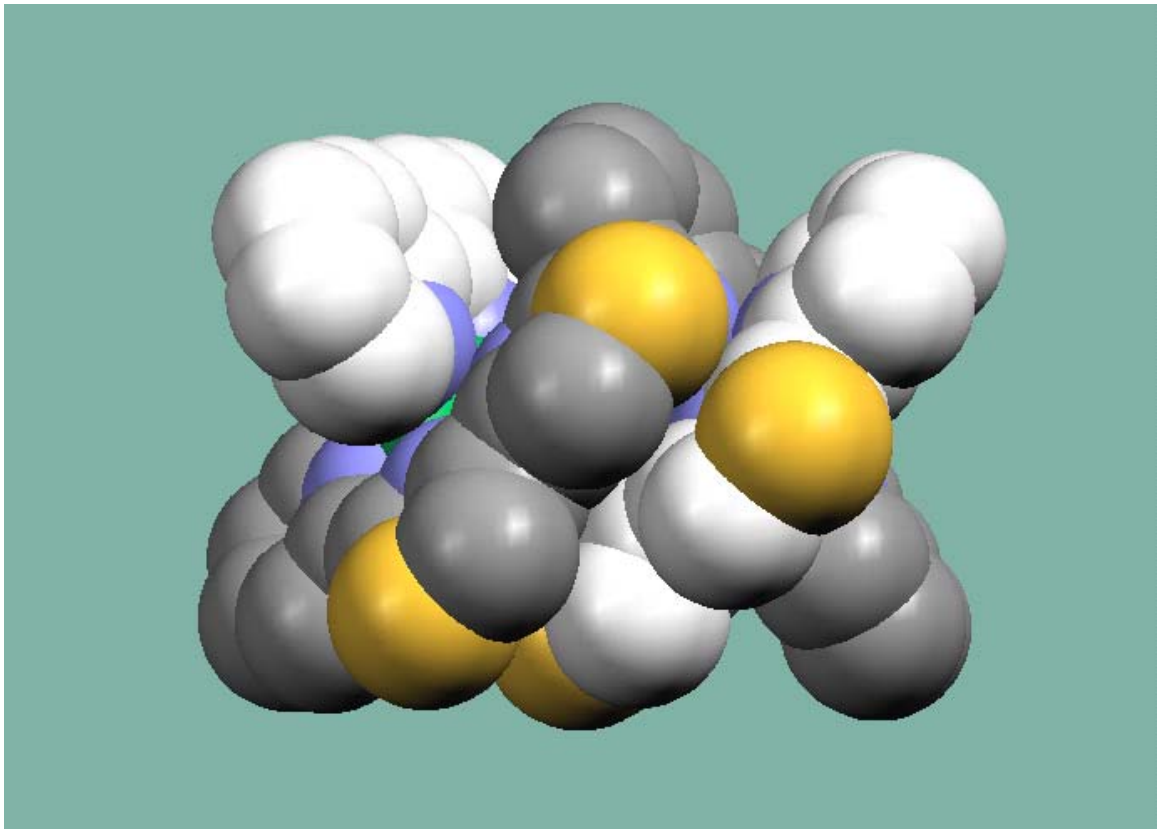

Bond Lengths			
Ni(1) – N(111)	1.989(5)	Ni(2) – N(21)	1.976(5)
Ni(1) – N(51)	1.995(5)	Ni(2) – N(81)	1.984(5)
Ni(1) – N(61)	2.132(5)	Ni(2) – N(11)	2.151(5)
Ni(1) – N(121)	2.143(5)	Ni(2) – N(71)	2.157(5)
Ni(1) – N(41)	2.234(4)	Ni(2) – N(31)	2.217(5)
Ni(1) – N(101)	2.237(5)	Ni(2) – N(91)	2.256(5)
Bond Angles			
N(111) – Ni(1) – N(51)	170.7(2)	N(21) – Ni(2) – N(81)	172.1(2)
N(111) – Ni(1) – N(61)	96.5(2)	N(21) – Ni(2) – N(11)	77.1(2)
N(51) – Ni(1) – N(61)	77.4(2)	N(81) – Ni(2) – N(11)	95.8(2)
N(111) – Ni(1) – N(121)	78.0(2)	N(21) – Ni(2) – N(71)	100.8(2)
N(51) – Ni(1) – N(121)	96.0(2)	N(81) – Ni(2) – N(71)	76.6(2)
N(61) – Ni(1) – N(121)	99.8(2)	N(11) – Ni(2) – N(71)	99.2(2)
N(111) – Ni(1) – N(41)	111.0(2)	N(21) – Ni(2) – N(31)	75.3(2)
N(51) – Ni(1) – N(41)	75.2(2)	N(81) – Ni(2) – N(31)	112.0(2)
N(61) – Ni(10 – N(41)	152.5(2)	N(11) – Ni(2) – N(31)	152.1(2)
N(121) – Ni(1) – N(41)	85.3(2)	N(71) – Ni(2) – N(31)	90.4(2)
N(111) – Ni(1) – N(101)	75.8(2)	N(21) – Ni(2) – N(91)	108.7(2)
N(51) – Ni(1) – N(101)	110.6(2)	N(81) – Ni(2) – N(91)	74.2(2)
N(61) – Ni(10 – N(101)	87.4(2)	N(11) – Ni(2) – N(91)	87.6(2)
N(121) – Ni(1) – N(101)	153.5(2)	N(71) – Ni(2) – N(91)	150.5(2)
N(41) – Ni(1) – N(101)	100.2(2)	N(31) – Ni(2) – N(91)	96.8(2)

Table 2.3 Selected bond distances (Å) and bond angles (º) for $[Ni_2(L^2)_2]^{4+}$

2.5 Synthesis and crystal structure of L^3 with $Cd(ClO_4)_2 \cdot 6H_2O$

Reaction of L^3 with $Cd(ClO_4)_2 \cdot 6H_2O$ in a 2:3 ratio forms a soluble complex in $MeNO_2$ which afforded colourless crystals upon slow diffusion of ethyl acetate into the solution. Analysis of the crystalline material via electrospray mass spectroscopy did not show the molecular ion, but the fragment $[Cd_2(L^3)_2][ClO_4]_3^+$. However, elemental analysis was consistent with the empirical formulae $[Cd_3(L^3)_2][ClO_4]_6$ and ^1H NMR in CD_3NO_2 gave 19 signals in the aromatic region of the spectrum ranging form δ 7.4 to 8.6 ppm indicating symmetry within the ligand was consistent with that of the proposed structure. The formation of the trinuclear double helicate $[Cd_3(L^3)_2]^{6+}$ was confirmed via analysis by X-ray crystallography.

Each Cd(II) metal ion was found to be in an irregular six-coordinate environment. The coordination geometry about two of the three metal ions is identical and coordination around the third is unique. The unique central Cd(II) ion is coordinated by a bis-terpyridyl binding domain and the two identical terminal Cd(II) ions are each coordinated by a bidentate pyridyl-thiazole domain. The six-coordinate environment surrounding these terminal metal ions is completed by coordination of a monodentate perchlorate anion and a monodentate O-donor solvent molecule. In the crystal structure of the O-donor solvent molecule is water for two-thirds of the time and nitromethane for one-third of the time with both occupying the same coordination position. The Cd…Cd metal ion separation within the helicate complex was 4.63 Å and the Cd…N distances range from 2.289(10) to 2.445(12) Å with the longest cadmium to nitrogen bond distance formed by the N-donors of the thiazole rings and the shortest those of the pyridyl and terpyridyl N-donors. Again, the distance is the result of the divergent nature of the thiazole heterocycles.

The coordination geometry that is formed by the ligand splitting into three coordination domains that consist of a central tridentate domain, comprising of a terpyridyl unit and two other terminal bidentate (pyridyl-thiazole) units. The partitioning of the ligand into three separate binding domains follows the sequence of natural breaks along the ligand chain at the point of which adjacent thiazole units are incorporated and this is similar with the succession of natural breaks seen within L^1.

Figure 2.5 Structure of the complex cation $[Cd_3(L^3)_2(MeCN)(ClO_4)_2]^{6+}$ a) Capped stick view; b) & c) Vertical and horizontal ball and stick view; d) space-fill diagram of the Ni(II) helicate structure.

a) Capped stick view

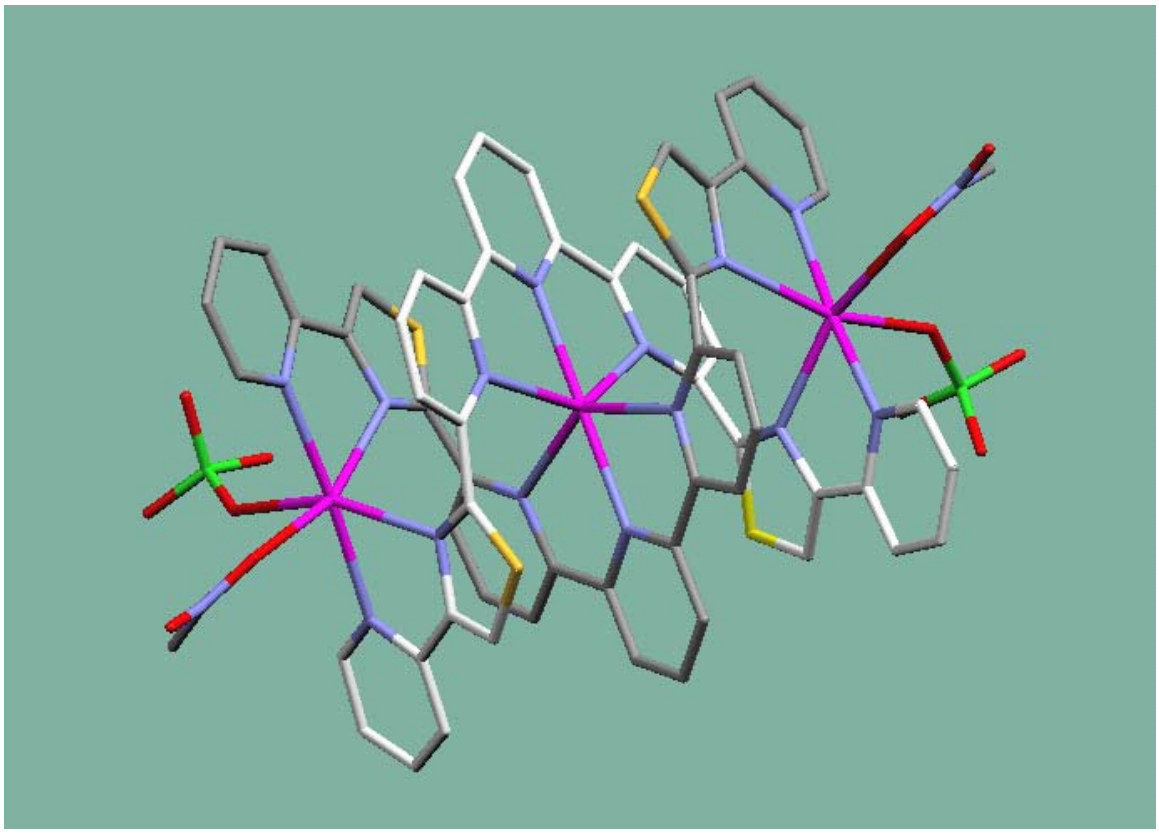

b) Ball and stick view

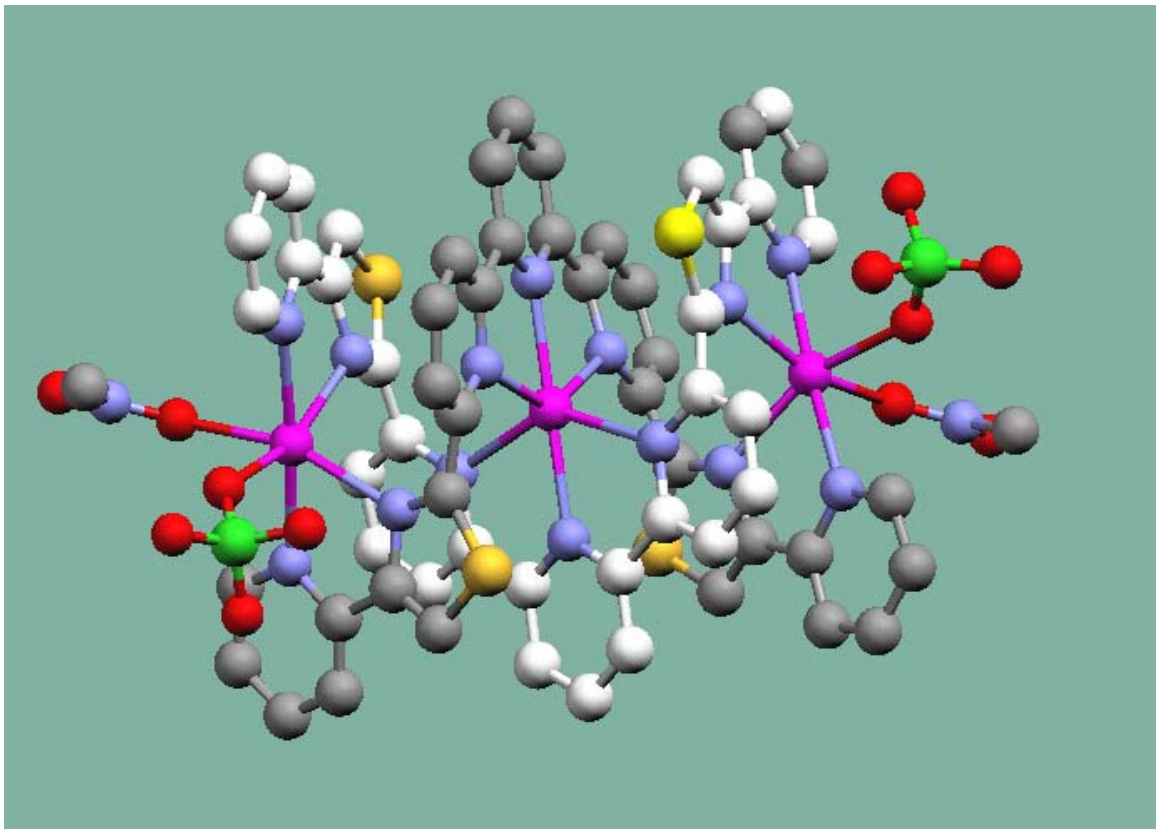

c) Ball and stick view

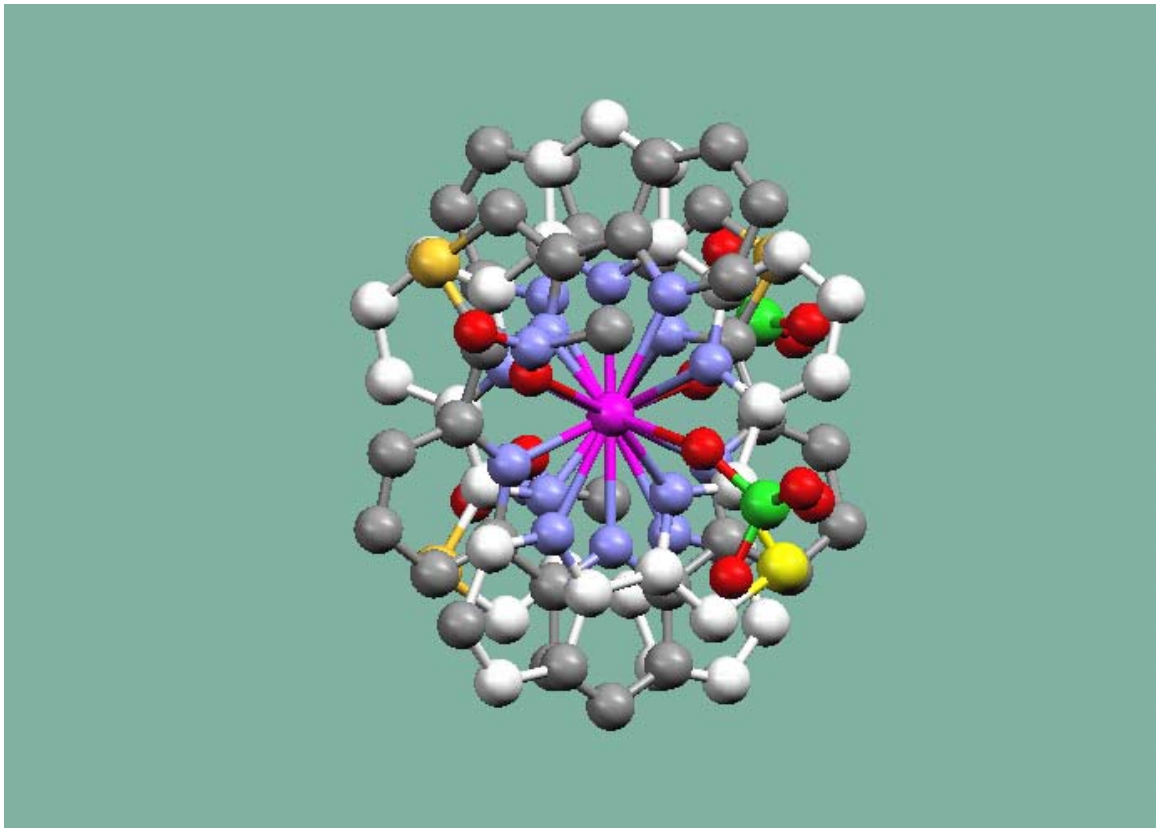

d) Spacefill view

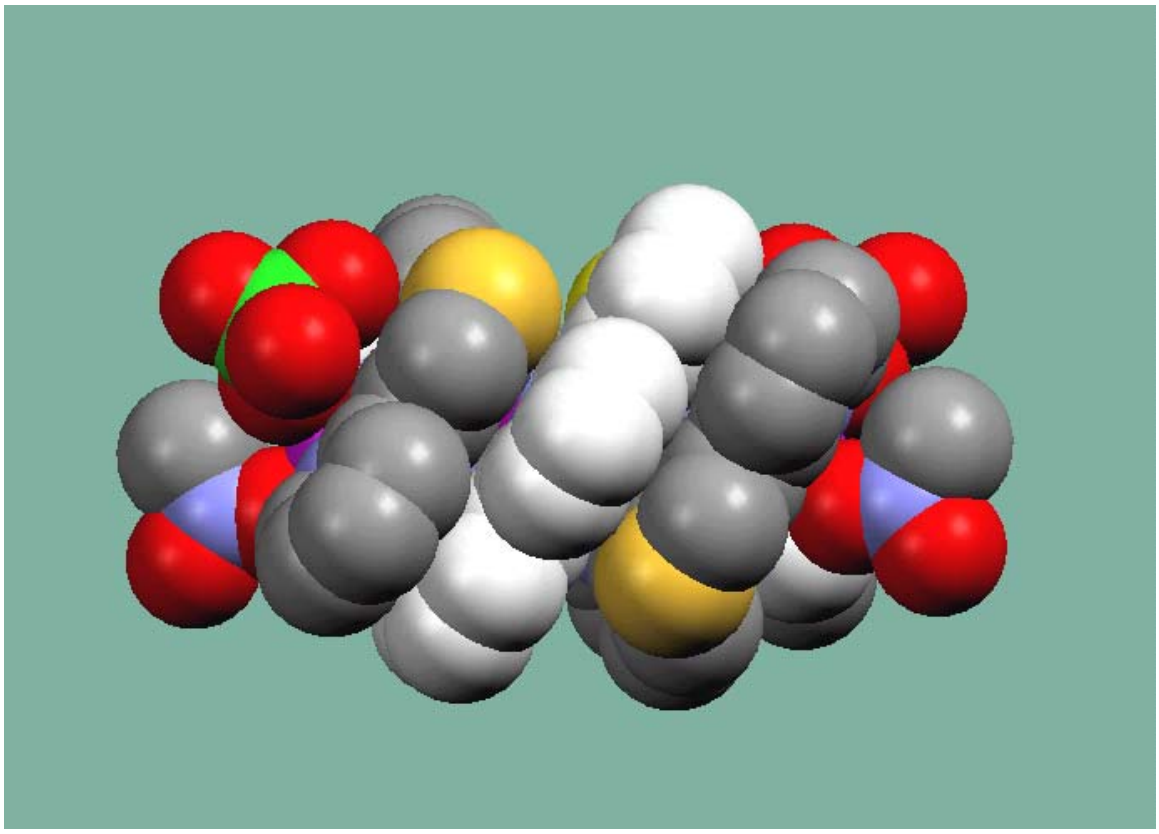

Bond Lengths			
Cd(1) – N(51)	2.29(1)	Cd(2) – N(71)	2.29(1)
Cd(1) – O(93)	2.30(1)	Cd(2) – N(61)	2.43(1)
Cd(1) – O(11)	2.32(1)	Cd(2) – N(31)	2.44(1)
Cd(1) – N(11)	2.32(1)		
Cd(1) – N(41)	2.32(1)		
Cd(1) – N(21)	2.33(1)		
Bond Angles			
N(51) – Cd(1) – O(93)	158.5(4)	N(71) – Cd(2) – N(71)	179.6(6)
N(51) – Cd(1) – O(11)	89.4(4)	N(71) – Cd(2) – N(61)	110.8(4)
O(93) – Cd(1) – N(11)	89.7(5)	N(71) – Cd(2) – N(61)	69.5(4)
N(51) – Cd(1) – N(11)	111.6(4)	N(71) – Cd(2) – N(61)	69.5(4)
O(93) – Cd(1) – N(11)	88 .7(4)	N(71) – Cd(2) – N(61)	110.8(4)
O(11) – Cd(1) – N(11)	85.6(5)	N(61) – Cd(2) – N(61)	87.9(5)
N(51) – Cd(1) – N(41)	71.9(4)	N(71) – Cd(2) – N(31)	110.4(4)
O(93) – Cd(1) – N(41)	87.6(4)	N(71) – Cd(2) – N(31)	69.3(4)
O(11) – Cd(1) – N(41)	92.1(5)	N(61) – Cd(2) – N(31)	138.9(4)
N(11) – Cd(1) – N(41)	175.7(4)	N(61) – Cd(2) – N(31)	106.6(4)
N(51) – Cd(1) – N(21)	99.0(4)	N(71) – Cd(2) – N(31)	69.3(4)
O(93) – Cd(1) – N(21)	89.6(4)	N(71) – Cd(2) – N(31)	110.4(4)
O(11) – Cd(1) – N(21)	157.3(5)	N(61) – Cd(2) – N(31)	106.6(4)
N(11) – Cd(1) – N(21)	71.7(5)	N(61) – Cd(2) – N(31)	138.9(4)
N(41) – Cd(1) – N(21)	110.5(4)	N(31) – Cd(2) – N(31)	87.6(5)

Table 2.4 Selected bond distances (Å) and bond angles (º) for $[Cd_3(L^3)_2]^{6+}$

2.6 Conclusion

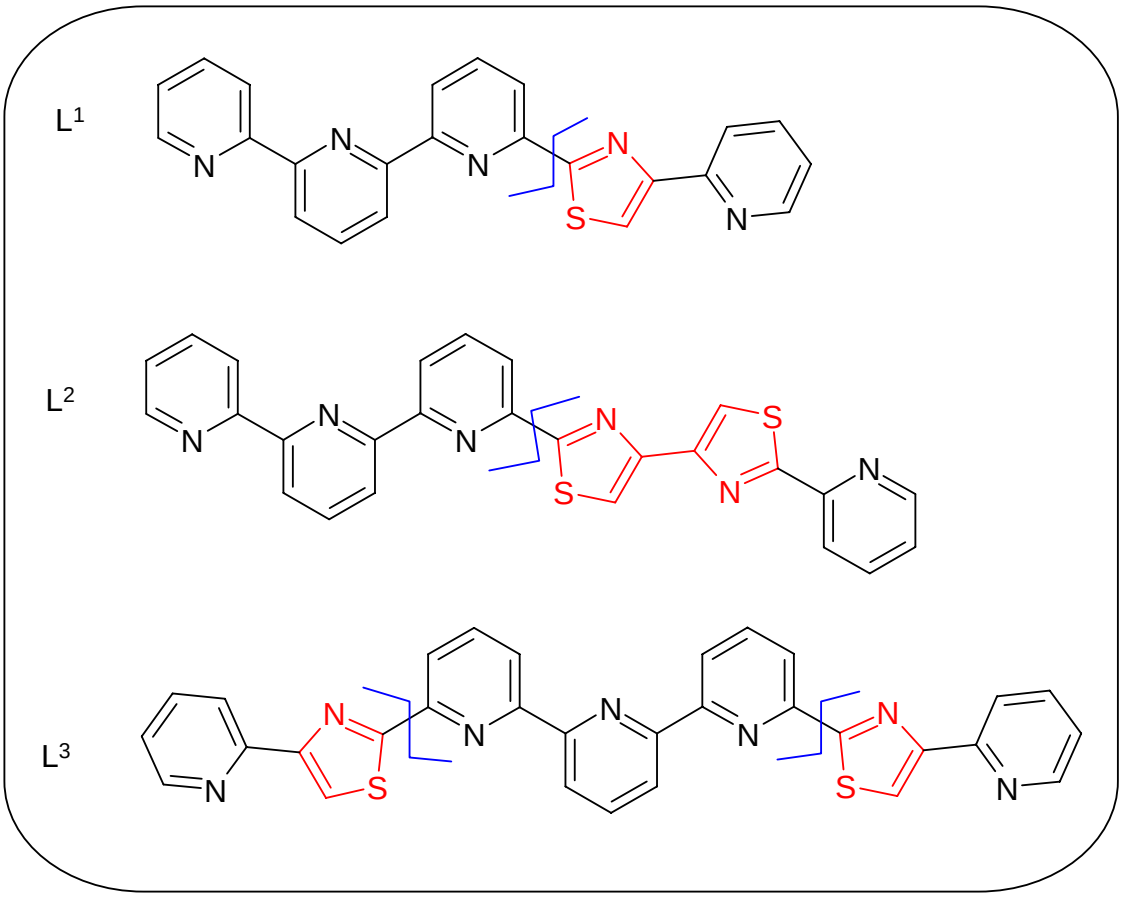

Scheme 2.2 Diagrammatic representation of partitioning in ligand chains L^1-L^3

The ligands L^1, L^2 and L^3 are novel examples of polydentate ligands containing pyridyl, thiazole and terpyridyl N-donor heterocycles. The five-membered thiazole ring demonstrates interesting coordination properties due to its partitioning into different binding domains. L^1 and L^3 have been shown here to partition as observed with other pyridyl-thiazole multidentate ligands whereas L^2 does not follow this observed trend.

Ligand L^1 as shown in Scheme 2.2 illustrates how this ligand partitions at a position adjacent to the thiazole ring, creating a bidentate pyridyl-thiazole binding domain and a tridentate terpyridyl binding domain. This ligand is pre-organised and partitioning in this way allows coordination to the copper metal ion in its preferred geometry, a five coordinate array. Ligand L^3, shown in the same scheme partitions (here at both ends of the ligand) at a position along the ligand chain adjacent to the

thiazole ring in similarity with the succession of natural breaks seen within ligand L^1. In the case of the Cd(II) complex three individual binding domains are created; a central terpyridyl unit and two terminal bidentate units. This ligand is also pre-organised in such a way that partitioning allows coordination to each cadmium metal ion in a pseudo-octahedral environment, the preferred geometry of the metal ion. Ligand L^2, unlike the previous two ligand chains, partitions itself at a position adjacent to the inner thiazole ring creating two tridentate six-coordinate binding domains; a tridentate terpyridyl unit and a tridentate unit consisting of the terminal pyridyl ring and the two inner five-membered thiazole rings. The ligand partitioning at this position creates two binding domains that allow the preferred coordination geometry of the six coordinate Co(II) and Ni(II) metal ions. This is unusual as it would be expected that the ligand would split between the two thiazole rings to create two unique binding domains; i) a tetradentate terpyridyl-thiazole binding domain; ii) a bidentate pyridyl-thiazole binding domain. These complexes are unusual as the two adjacent thiazole rings act as a bidentate unit, which due to their divergent nature is unfavourable. Instead the ligand is driven to partition itself adjacently to the thiazole ring to create two terdentate binding domains consistent with the requirements of the metal ion in solution. This shows how the preferred coordination geometry of the metal ion in each case is the dominating factor in determination of the helicate complex.

In this section we have shown examples where two factors are equally associated with the partitioning of the ligand chain; i) the position of the five-membered thiazole ring along the ligand chain; ii) the preferred coordination geometry of the transition metal ion (seen in L^1 and L^3). This section has also shown where just one dominating factor can effect the way in which these helicate complexes are formed; that is the preferred coordination geometry of the metal ion in each case shown here with ligand L^2 for both Co(II) and Ni(II) complexes.

CHAPTER III

3. Results and discussion: Synthesis of polydentate ligands derived from 3,3′-disubstituted-2,2′-bipyridine

3.1 Synthesis of 3,3′-disubstituted ligands L^4, L^5 & L^6

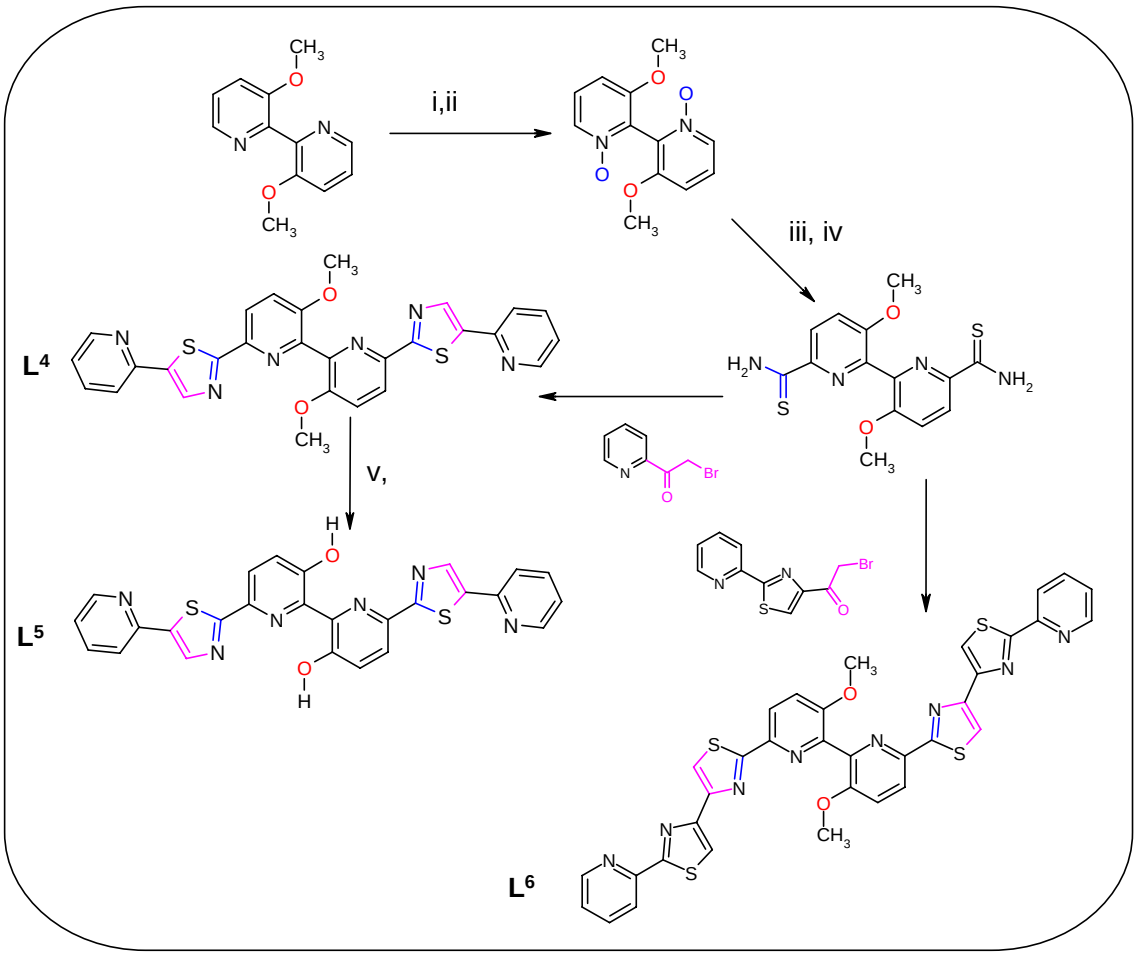

Scheme 3.1 Synthesis of Ligands L^4, L^5 & L^6;
Reagents and conditions; i) CH_3CO_2H; ii) H_2O_2; iii) $(CH_3O)_2SO_2$; iv) NaCN;
v) C_5H_5N, HCl

The potentially hexadentate ligand L^4, the potentially hexadentate ligand L^5 and the potentially octadentate ligand L^6 were prepared from 3,3′-dimethoxy-2,2′-bipyridine-1,1′-dioxide via the incorporation of a nitrile substituent at the C_6 position of bipyridine-1,1′-dioxide using standard methods. Conversion of the nitrile into the 6,6′-dithioamide was achieved by the reaction with hydrogen sulfide gas. Subsequent reaction of the 6,6′-dithioamide with 2-(α-bromoacetyl) pyridinium hydrobromide (in EtOH at reflux) gives ligand L^4 and reaction of the newly prepared L^4 with molten

pyridinium hydrochloride gives ligand L^5. Subsequent reaction of the 6,6′-dithioamide derivative with (2′-(pyrid-2-yl) thiazol-4′-yl)ethanone gives ligand L^6.

3.2 Synthesis of Ligand L^4

3.2.1 Synthesis of 3,3′-dimethoxy-2,2′-bipyridine precursor ligand

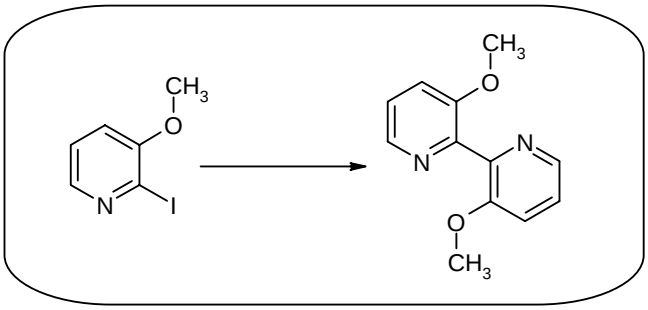

Figure 3.1 Synthesis of 3,3′- dimethoxy-2,2′-bipyridine

The preparation of 3,3′-dimethoxy-2,2′-bipyridine was achieved by reaction of 3-methoxy-2-iodopyridine with $NiCl_2(PPh_3)_2$ in the presence of zinc powder giving 3,3′-dimethoxy-2,2′-bipyridine as a yellow oil. The product was characterised by its ^1H NMR (see experimental section) and the synthesis as previously reported.[24,106,107]Yields were found to be within the range of 20-50%.

3.2.2 *N*-oxidation

N-oxidation of 3,3′-dimethoxy-2,2′-bipyridine with glacial acetic acid and excess hydrogen peroxide afforded 3,3′-dimethoxy-2,2′-bipyridine-1,1′-dioxide. Here the ^1H NMR shows a symmetrical species with all three aromatic protons signals substantially shifted when compared to that of the starting material.

3.2.3 Formation of 6,6′-dicyano-3,3′-dimethoxy-2,2′-bipyridine

Cyanation of 3,3′-dimethoxy-2,2′-bipyridine-1,1′-dioxide via heating in $(MeO)_2SO_2$ overnight at 80˚C, precipitation by the addition of CH_3CO_2Et and subsequent reaction with excess sodium cyanide (solution in H_2O) gave 6,6′-dicyano-

3,3′-dimethoxy-2,2′-bipyridine as a cream coloured solid. The ^{1}H NMR shows that only two aromatic signals are observed. The proton at the C_6 position δ 6.92 ppm is no longer present and has been replaced with a nitrile substituent. Subsequent purification of the product if required can be achieved via column chromatography.

3.2.4 Formation of 3,3′-dimethoxy-2,2′-bipyridine-6,6′-dithioamide ligand

The reaction of the 6,6′-dicyano-3,3′-dimethoxy-2,2′-bipyridine in ethanol with hydrogen sulfide gas affords the yellow crystalline 3,3′-dimethoxy-2,2′-bipyridine-6,6′-dithioamide. The ^{1}H NMR shows two signals at δ 9.25 ppm and 7.48 ppm, which are indicative of the presence of a thioamide functional group, present here at the C_6 position of each pyridine ring.

3.3 Synthesis of 3,3′-disubstituted ligand L^4 and L^6

The potentially hexadentate ligand L^4 and the potentially octadentate ligand L^6 were prepared via reaction of 3,3′-methoxy-2,2′-bipyridine-6,6′-dithioamide in ethanol at reflux with; i) 2-(α-bromoacetyl) pyridinium hydrobromide to produce L^4; and ii) (2′-(pyrid-2-yl) thiazol-4′-yl)ethanone to produce L^6.

3.4 Synthesis of 3,3′-disubstituted ligand L^5

The potentially hexadentate ligand L^5, was prepared via de-methylation of ligand L^4, by reaction of the 6,6′-disubstituted 3,3′-dimethoxy-2,2′-bipyridine ligand with pyridine hydrochloride at 200ºC producing 3,3′-dihydroxy-derivative as a yellow crystalline precipitate. The use of ^{1}H NMR to substantiate the preparation of this material proved difficult due to solubility problems with this ligand. The preparation of this material was confirmed as it is highly luminescent; which is indicative of the presence of a 3,3′-dihydroxy-2,2′-bipyridyl moiety.

3.5 Synthesis and crystal structure of L^4 with $Zn(ClO_4)_2 \cdot 6H_2O$

The potentially hexadentate ligand L^4, as with L^1 – L^3 is insoluble in many organic solvents. However, L^4 readily dissolves upon reaction with transition metal ions to form soluble complexes in $MeNO_2$. Reaction of L^4 with $Zn(ClO_4)_2 \cdot 6H_2O$ in a 1:1 ratio resulted in colourless crystals of X-ray quality, upon slow diffusion of ethyl acetate into the $MeNO_2$ solution. Analysis via electrospray mass spectrometry indicated the complex cation $[Zn_2(L^4)_2(ClO_4)_3]^+$ *m/z* 1209.1 and elemental analysis was consistent with the empirical formula $[Zn(L^4)][ClO_4]_2$. The formation of a dinuclear double helicate was confirmed via X-ray crystallographic analysis.

Each zinc metal ion was found to be in a six-coordinate environment where the coordination geometry about each Zn(II) centre in this complex can be described as pseudo-octahedral. The metal ions in this complex are coordinated to the three N-donors of the two tridentate units, which have formed due to the partitioning of the ligand at its centre. The Zn…Zn separation is 4.682 Å, and the Zn-N distances range from 1.991 – 2.480 Å. The distances between the metal ion and the N-donors of the central bipyridine ring, which contain the substituents, have the longest distances ranging from 2.365 to 2.480 Å. This suggests that the zinc metal ion may sit at a position closer to the terminal pyridyl and thiazole rings.

The solid-state structure reveals that the ligand partitions into two equivalent tridentate binding domains consisting of pyridyl-thiazole-pyridyl units. The ligand partitions at the centre of the bipyridine unit with a N-C-C-N torsion angle of 65.43 and 63.18 Å. The ligand contains di-methoxy substituents at the C_3 position of the bipyridine unit and any unfavourable steric interaction between these two substituents is minimised by the formation of the two terdentate binding domains. These two domains are approaching orthogonality (70˚) reducing any unfavourable steric interactions.

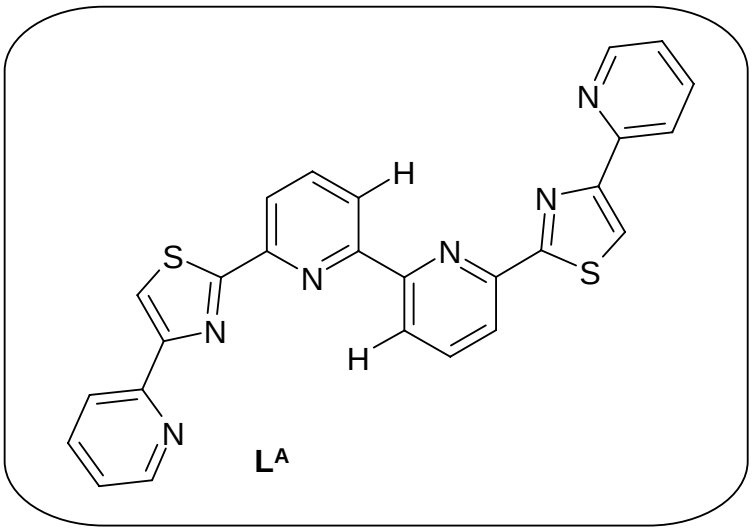

Figure 3.2 Unsubstituted ligand L^A

A similar ligand has already previously been prepared which contains the same array of N-donor atoms but which does not contain any substituents on the central bipyridine unit. This ligand has also been complexed with $Zn(ClO_4)_2 \cdot 6H_2O$ and forms a dinuclear double helicate. However, the interaction of the metal and ligand are quite different in this example.[108] In this case the formation of this helicate complex is controlled by the preferred coordination geometry of the metal ion. In the case of the Zn(II) complex of L^A the metal ion is seen to adopt a four-coordinate geometry and the ligand partitions into three distinct bidentate binding domains with the formation of two terminal pyridyl-thiazole binding domains and with the central bipyridine unit uncoordinated. The mode of action of this ligand is due directly to the divergent nature of the 5-membered thiazole ring which prevents the py-thia-py domain acting as a tridentate unit. This partitioning of the ligand can be clearly seen by the torsion angles formed by the central bipyridine unit. If the ligand had partitioned into two terdentate binding domains the torsion angles would have been closer to 90˚. However, the observed torsion angles of 38˚ and 50˚ indicate that two terdentate units have not formed and the central bipyridine unit is uncoordinated.

Ligand L^4 with its 3,3′-dimethoxy substituents, when complexed with Zn(II) behaves in a very different manner. The ligand partitions into two equivalent bis-tridentate binding domains that consist of a pyridyl-thiazole-pyridyl tridentate unit. The N-C-C-N torsion angle of the centre of the bipyridine unit is closer to 90º, as a

consequence of the steric repulsion between the substituents groups, not otherwise seen in ligand L^A. Ligand L^4, like many other ligands in this series would be expected to partition at a position along the ligand chain adjacent to the thiazole ring thus creating three bidentate binding domains; a unique bidentate bipyridyl (or hypodentate in the case of $[Zn_2(L^{unsub})_2]$) unit at the centre of the ligand chain and two identical bidentate (pyridyl-thiazole) units at either end of the ligand. It is the presence of the substituents at the C_3 position of this unit that significantly alter the way in which the ligand partitions and it is the effect of those substituents that controls the formation of the terdentate domains.

The formation of this helicate complex is thus controlled by two factors; i) the stereo-electronic preference of the Zn(II) metal ion to adopt a six-coordinate pseudo octahedral coordination geometry formed by tridentate binding domains created by the partitioning of the ligand at its centre; ii) the effect of the substituents at the C_3 position of the central bipyridine unit to alter the pre-organised partitioning of the ligand chain

Figure 3.3 Structure of the complex cation $[Zn_2(L^4)_2]^{4+}$ with a) Capped stick view; b), c) Ball and stick view; d) Spacefill view of the Zn(II) helicate complex.

a) Capped stick

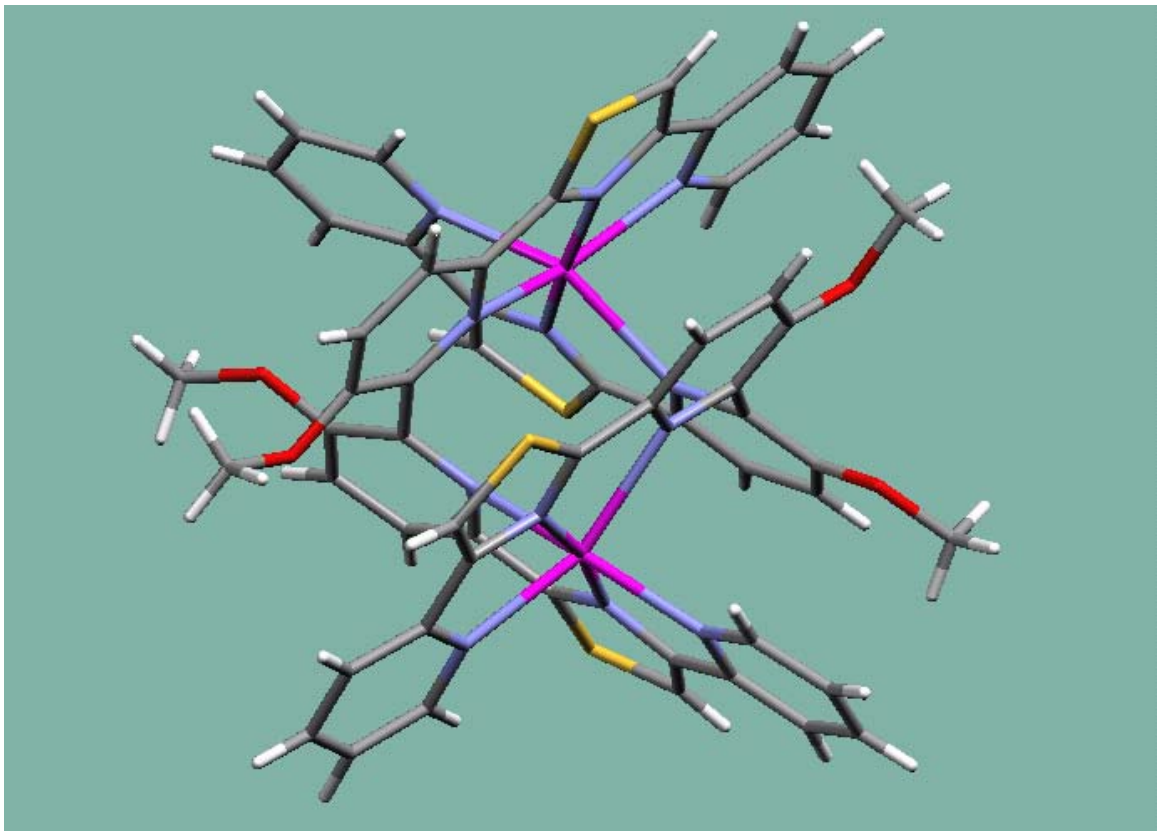

b) Ball and stick view

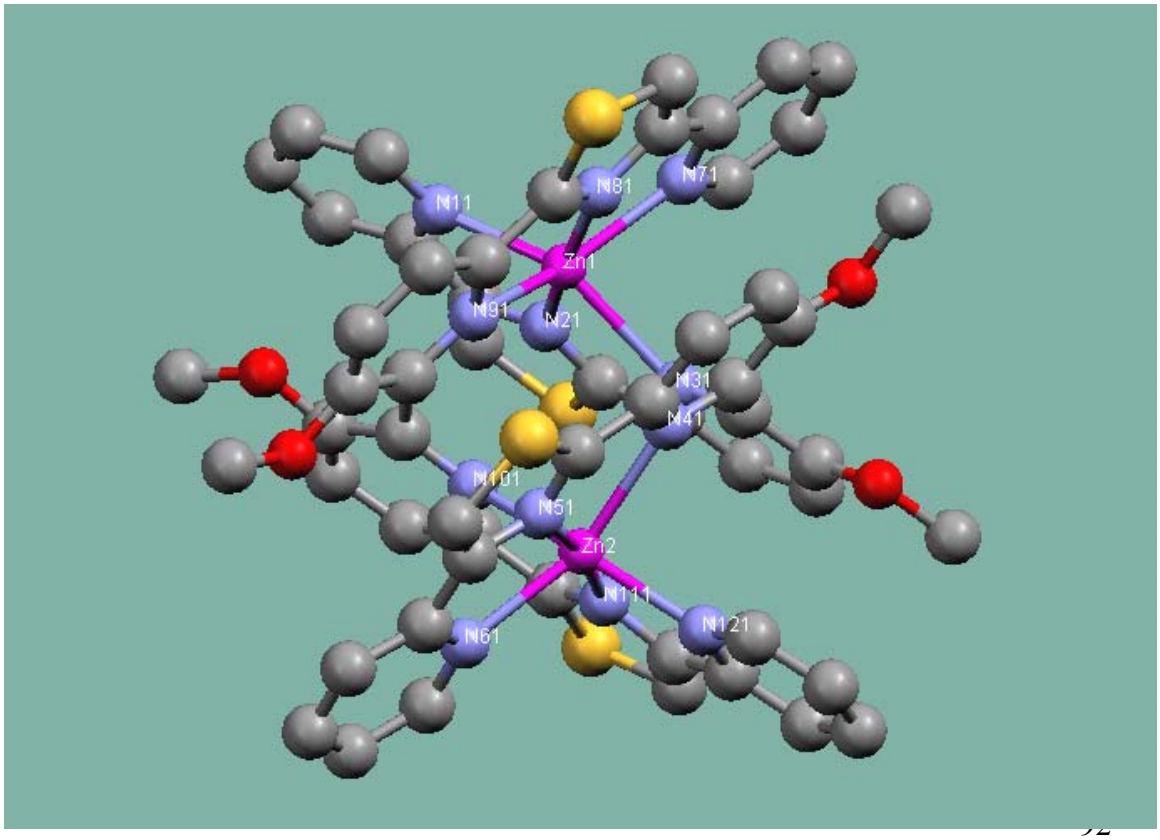

c) Vertical ball and stick view

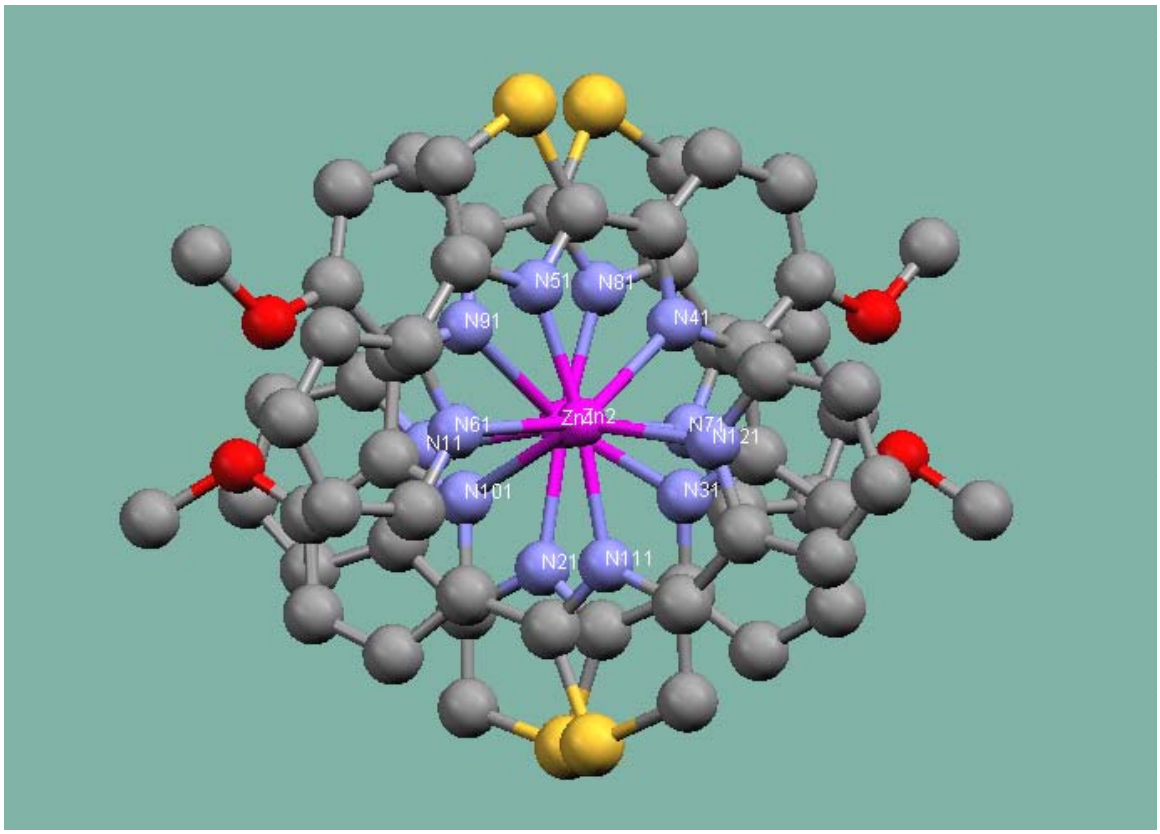

d) Spacefill view

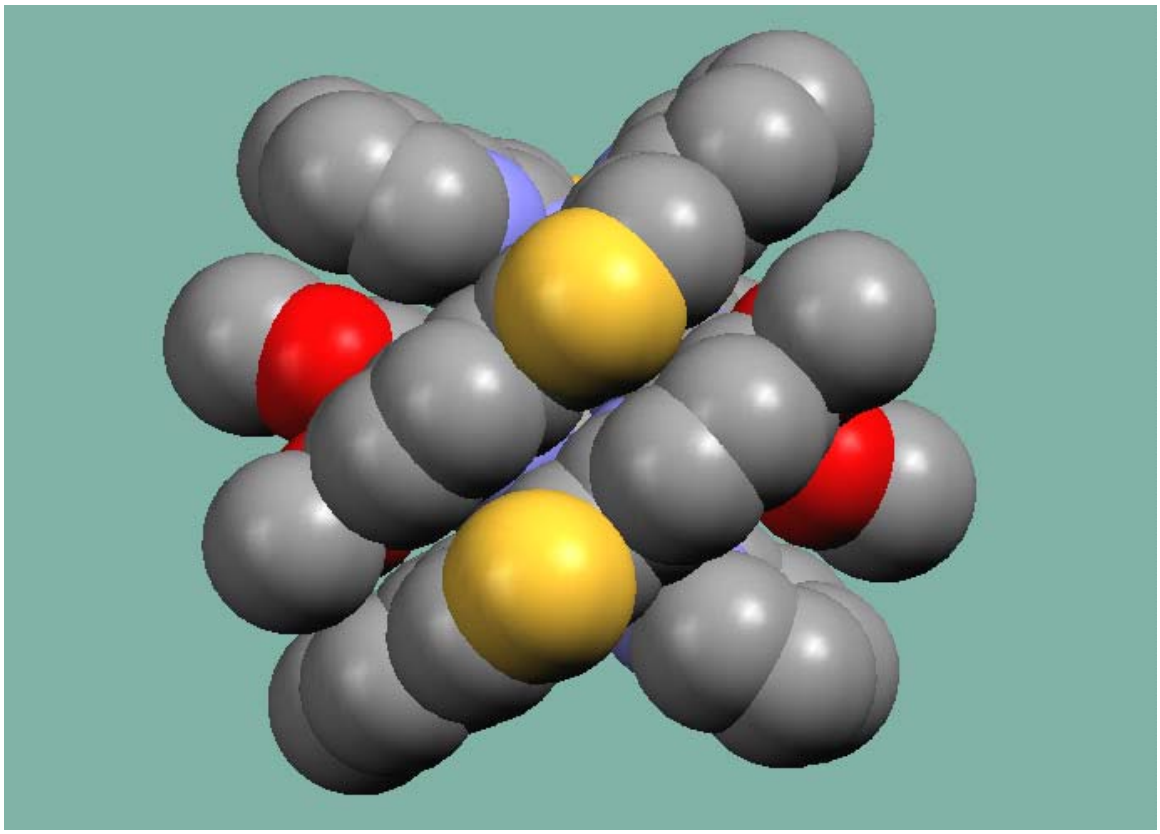

Table 3.1 Selected bond distances (Å) and bond angles (º) for $[Zn_2(L^4)_2]^{4+}$

Bond lengths			
Zn(1) – N(31)	2.472(2)	Zn(2) – N(61)	2.274(3)
Zn(1) – N(21)	2.016(2)	Zn(2) – N(51)	1.995(2)
Zn(1) – N(71)	2.295(3)	Zn(2) – N(41)	2.380(2)
Zn(1) – N(11)	2.210(2)	Zn(2) – N(121)	2.186(3)
Zn(1) – N(81)	1.991(2)	Zn(2) – N(111)	2.013(2)
Zn(1) – N(91)	2.365(2)	Zn(2) – N(101)	2.480(2)
Bond Angles			
N(21) – Zn(1) – N(31)	70.7(9)	N(61) – Zn(2) – N(51)	74.9(1)
N(71) – Zn(1) – N(31)	81.5(8)	N(61) – Zn(2) – N(41)	147.3(9)
N(21) – Zn(1) – N(71)	95.4(9)	N(51) – Zn(2) – N(41)	72.6(9)
N(31) – Zn(1) – N(11)	145.5(8)	N(61) – Zn(2) – N(121)	107.2(9)
N(21) – Zn(1) – N(11)	75.7(9)	N(51) – Zn(2) – N(121)	108.8(1)
N(81) – Zn(1) – N(21)	169.1(1)	N(51) – Zn(2) – N(111)	170.2(1)
N(81) – Zn(1) – N(91)	73.3(9)	N(111) – Zn(2) – N(121)	75.8(1)
N(11) – Zn(1) – N(91)	83.5(8)	N(111) – Zn(2) – N(61)	95.6(9)
N(81) – Zn(1) – N(31)	109.4(9)	N(121) – Zn(2) – N(41)	87.2(9)
N(91) – Zn(1) – N(31)	104.9(8)	N(111) – Zn(2) – N(41)	116.7(9)
N(81) – Zn(1) – N(11)	105.1(9)	N(111) – Zn(2) – N(101)	70.7(9)
N(81) – Zn(1) – N(71)	74.0(9)	N(61) – Zn(2) – N(101)	82.6(8)
N(11) – Zn(1) – N(71)	109.8(9)	N(51) – Zn(2) – N(101)	105.2(9)
N(21) – Zn(1) – N(91)	117.4(9)	N(121) – Zn(2) – N(101)	146.0(9)
N(71) – Zn(1) – N(91)	146.9(9)	N(41) – Zn(2) – N(101)	102.1(8)

3.6 Synthesis and crystal structure of L^5 with $Cd(ClO_4)_2 \cdot 6H_2O$

Reaction of L^5 with $Cd(ClO_4)_2 \cdot 6H_2O$ gave a complex that when analysed via electrospray mass spectrometry was found to contain the complex cation $\{[Cd_2(L^5)_2][ClO_4]_3\}^+$ and $\{[Cd(L^5)][ClO_4]_2\}^{2+}$, *m/z* 1338.5 and 620 respectively. Elemental analysis was consistent with the empirical formula $[Cd(L^5)][ClO_4]_2$ and the formation of a dinuclear double helicate for the complex was confirmed via X-ray crystallographic analysis.

Each metal ion was found to be in a six-coordinate environment and the coordination geometry surrounding each metal centre can be described as pseudo-octahedral. The metal ions in each complex are coordinated to the three N-donors of the tridentate py-thia-py unit from each ligand. The metal-metal separations are 4.378 Å for cadmium with metal-nitrogen bond distances ranging from 2.228 – 2.587 Å for Cd(II).

In this complex the coordination geometry is formed by the partitioning of the ligand into two equivalent tridentate binding domains that consist of pyridyl-thiazole-pyridyl units. The central bipyridine unit has hydroxyl substituents at the C_3, C_3' positions and these substituents force the ligand to partition at the centre in an effort to minimise unfavourable steric interactions.

The L^5 ligand like many other ligands in this series, including L^4, would be expected to partition at a position along the ligand chain adjacent to the thiazole ring thus creating three bidentate binding domains; a unique bipyridyl bidentate unit at the centre of the ligand chain, and two equivalent pyridyl-thiazole bidentate units at either end of the ligand. Interestingly reaction of the unsubstituted derivative of L^4 *i.e.* L^A with Cd(II) metal ions also forms a dinuclear double helicate $[Cd_2(L^A)_2]^{4+}$. However in this species the ligand partitions into a bidentate binding domain consisting of a pyridyl-thiazole unit, a tridenate binding domain inclusive of the central bipyridyl and thiazole unit and the terminal pyridyl ring that is not coordinated. This irregular six-coordinate environment comprises of one tridentate pyridyl-pyridyl-thiazole unit of one ligand, a pyridyl-thiazole unit from the other ligand and a monodentate ligand, MeCN at Cd(1) and a perchlorate anion at Cd(2). The ligand is arranged "head to tail" with the pendant pyridyl units at opposite ends of the helicate. The nitrogen atoms of these are directed to the cadmium centres but with values of 3.15 Å Cd(1) – N(151) and 3.09 Å Cd(2) – N(251) are too long to be considered as bonding interactions.

Thus the formation of this helicate complex with L^5 is controlled by two factors; i) the preference of each metal ion to form a six-coordinate pseudo-octahedral environment; ii) the hydroxyl substituents which due to unfavourable steric interactions force the ligand to increase the bipyridine N-C-C-N torsion angle resulting in the formation of two terdentate domains. Comparison of ligand L^5 with ligand L^A, illustrates that without the presence of these substituents, the mode of complexation is very different and relies upon the partitioning of the ligand backbone into binding domains where the pyridyl-thiazole-pyridyl unit is to be avoided.

Figure 3.4 Structure of the complex cation $[Cd_2(L^5)_2]^{4+}$ with a) Capped stick view; b), c) Ball and stick view; d) Spacefill view of the Cd(II) helicate complex.

a) Capped stick view

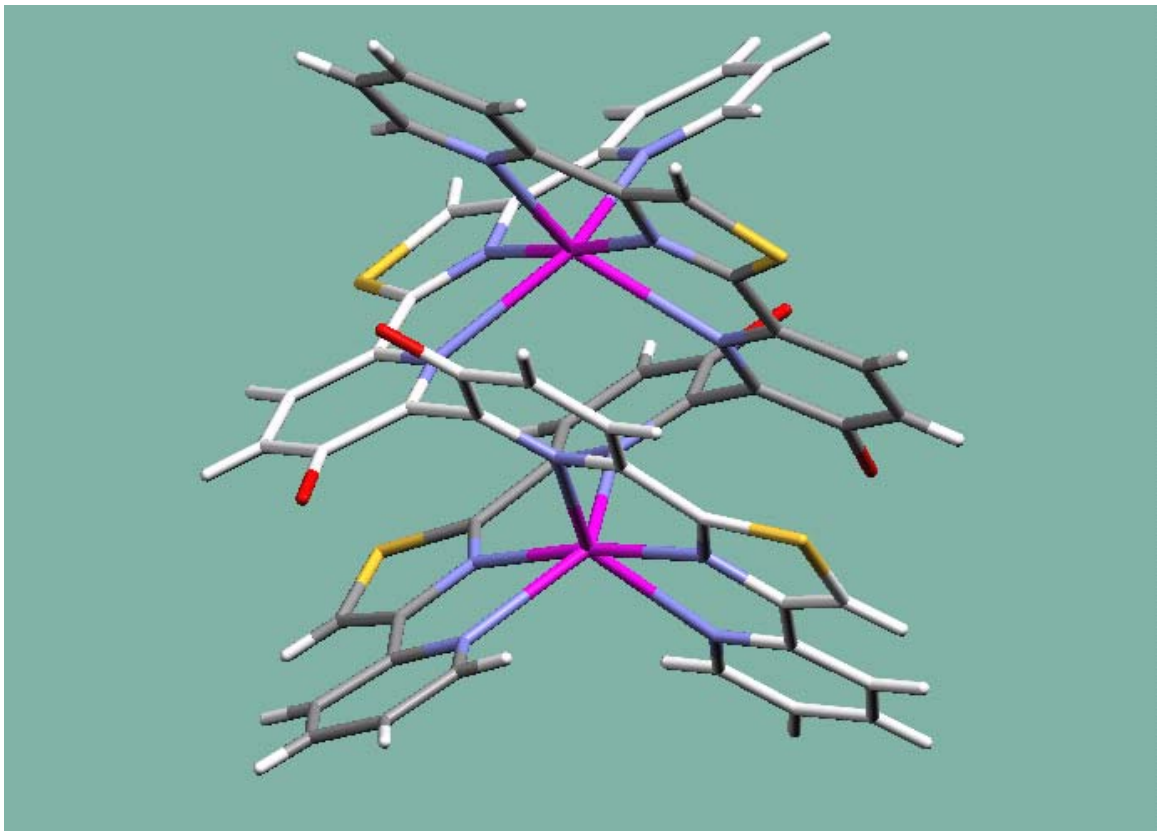

b) Ball and stick view

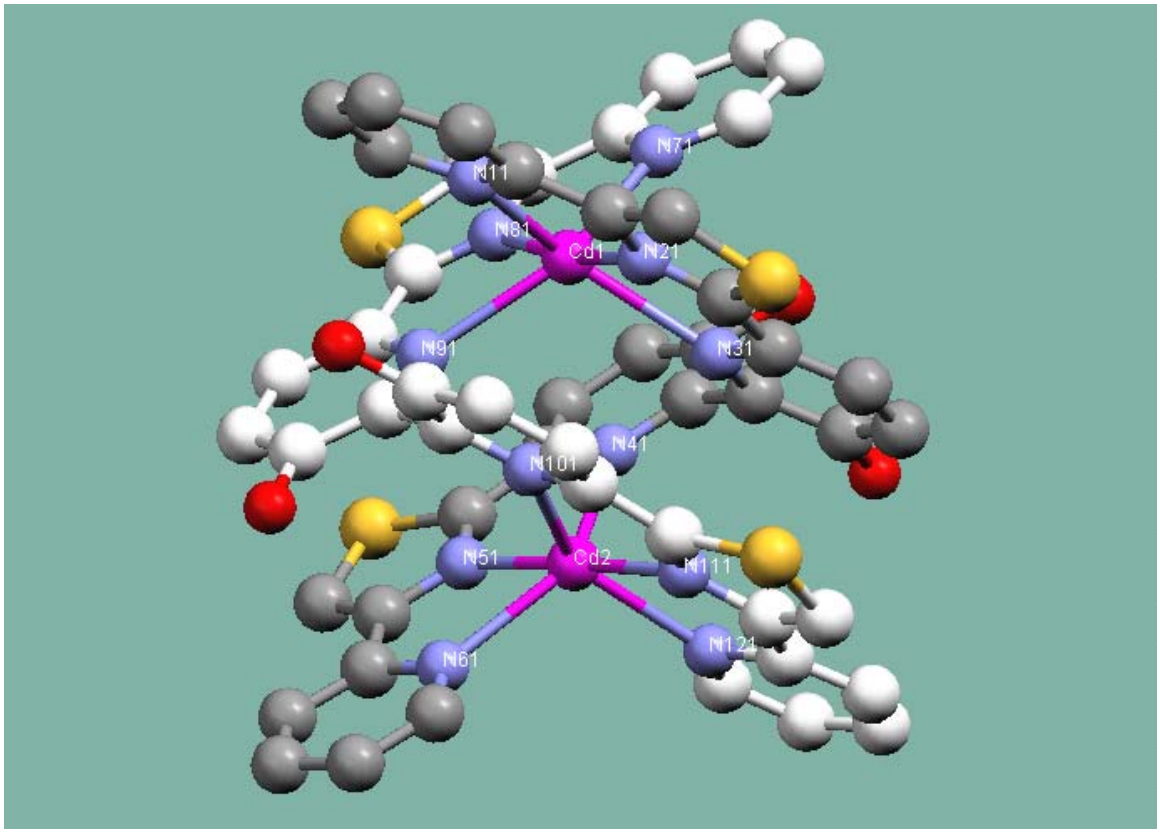

c) Vertical ball and stick view

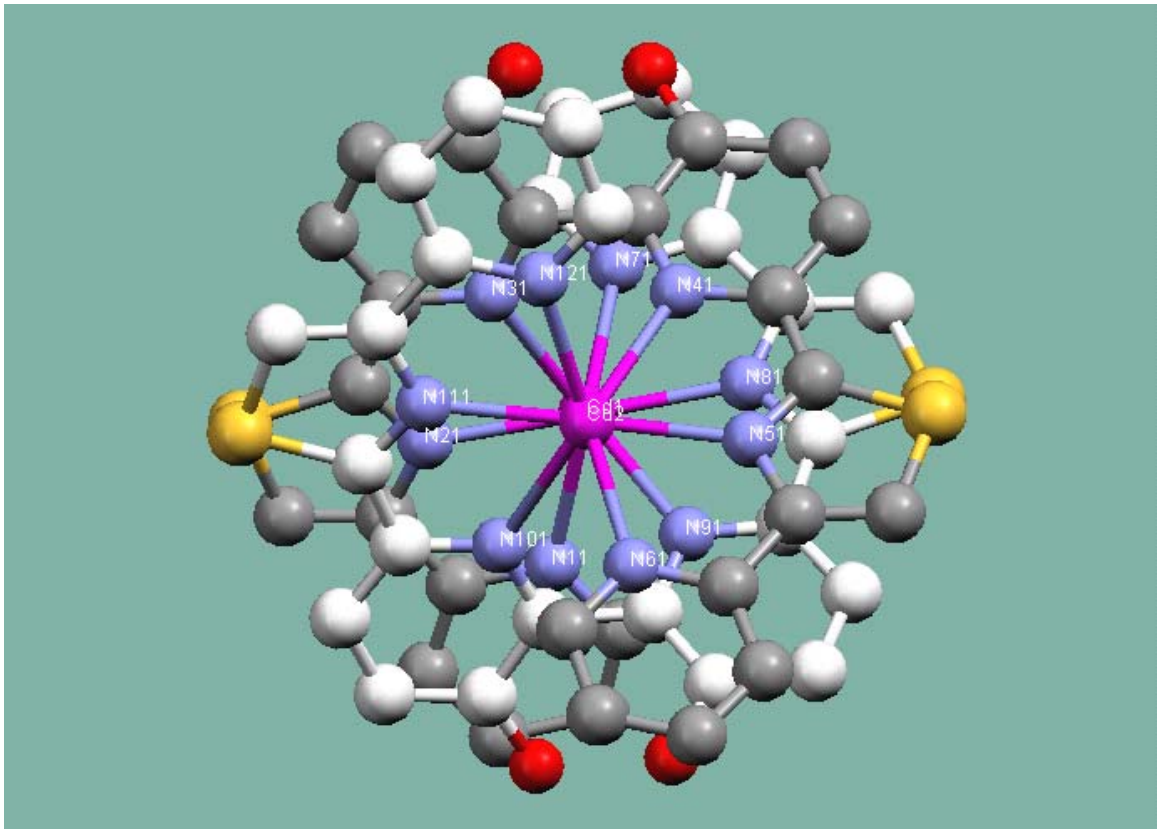

d) Spacefill view

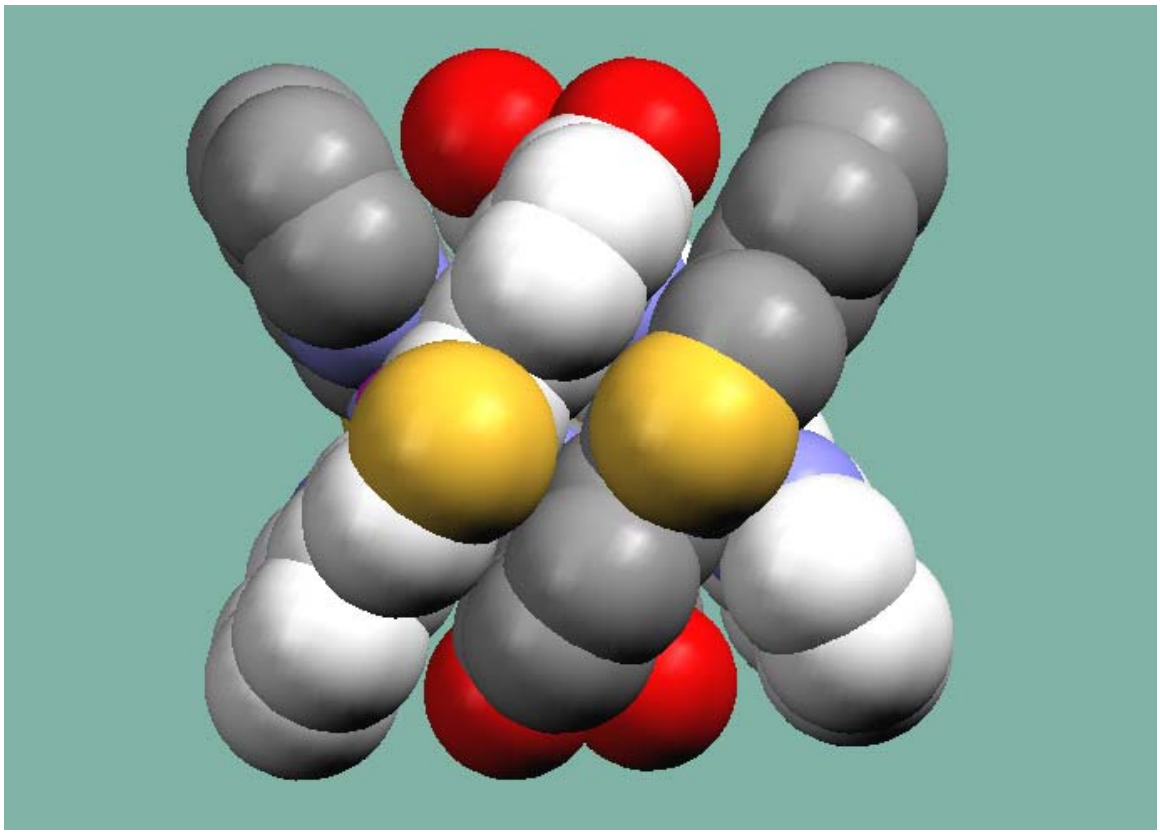

Table 3.2 Selected bond distances (Å) and bond angles (º) for $[Cd_2(L^5)_2]^{4+}$

Bond Lengths			
Cd(1) – N(91)	2.511(6)	Cd(2) – N(61)	2.465(6)
Cd(1) – N(81)	2.232(5)	Cd(2) – N(51)	2.232(5)
Cd(1) – N(11)	2.474(6)	Cd(2) – N(121)	2.453(5)
Cd(1) – N(21)	2.227(5)	Cd(2) – N(111)	2.237(5)
Cd(1) – N(31)	2.536(5)	Cd(2) – N(41)	2.574(5)
Cd(1) – N(71)	2.443(6)	Cd(2) – N(101)	2.588(5)
Bond angles			
N(81) – Cd(1) – N(91)	68.5(2)	N(61) – Cd(2) – N(51)	69.4(2)
N(11) – Cd(1) – N(91)	80.8(2)	N(61) – Cd(2) – N(121)	112.7(2)
N(21) – Cd(1) – N(81)	172.1(2)	N(51) – Cd(2) – N(111)	177.0(2)
N(21) – Cd(1) – N(91)	116.9(2)	N(61) – Cd(2) – N(111)	108.3(2)
N(81) – Cd(1) – N(31)	115.3(2)	N(51) – Cd(2) – N(41)	67.7(2)
N(21) – Cd(1) – N(71)	105.8(2)	N(51) – Cd(2) – N(121)	109.1(2)
N(81) – Cd(1) – N(71)	68.8(2)	N(111) – Cd(2) – N(121)	69.9(2)
N(21) – Cd(1) – N(11)	69.5(2)	N(111) – Cd(2) – N(41)	114.7(2)
N(81) – Cd(1) – N(11)	107.0(2)	N(121) – Cd(2) – N(41)	84.1(2)
N(71) – Cd(1) – N(11)	114.9(2)	N(61) – Cd(2) – N(41)	137.0(2)
N(71) – Cd(1) – N(91)	137.2(2)	N(51) – Cd(2) – N(101)	113.8(2)
N(21) – Cd(1) – N(31)	68.8(2)	N(111) – Cd(2) – N(101)	67.4(2)
N(71) – Cd(1) – N(31)	82.6(2)	N(121) – Cd(2) – N(101)	137.1(2)
N(11) – Cd(1) – N(31)	137.7(2)	N(61) – Cd(2) – N(101)	84.7(2)
N(91) – Cd(1) – N(31)	113.1(2)	N(41) – Cd(2) – N(101)	110.1(2)

3.7 Synthesis and crystal structure of L^6 with $Cd(ClO_4)_2 \cdot 6H_2O$

Reaction of L^6 with $Cd(ClO_4)_2 \cdot 6H_2O$ gave a complex which upon analysis by electrospray mass spectroscopy indicated the formation of a trinuclear double helicate with ions at *m/z* 1616.6 which correspond to $[Cd_3(L^6)_2(ClO_4)_4]^{2+}$. The formation of this trinuclear double helicate was confirmed via X-ray crystallographic analysis.

In the crystal structure each metal ion was found to be in a six-coordinate environment and the coordination geometry surrounding each metal centre can be described as pseudo-octahedral. The two terminal Cd(II) metal ions are coordinated by the three N-donors of the py-thia-thia binding domain of one ligand and the N-donors of the py-thia binding domain of the other ligand as well as a solvent molecule to complete the six-coordinate array. The central Cd(II) metal ion is coordinated by the three N-donors of the bipyridyl-thiazole binding domain of both ligands. The metal-metal separations are 4.123 and 4.197 Å, with the metal…nitrogen bond distances ranging from 2.246 – 2.675 Å. The N-C-C-N torsion angles of this central bipyridyl unit are 40.22˚ and 38.25˚.

In this complex, unlike previous complexes in this series the coordination geometry is formed by the partitioning of the ligand into two tridentate binding domains and one bidentate binding domain. The first terdentate-binding domain consists of a pyridyl-thiazole-thiazole unit and the second consists of a bipyridyl-thiazole unit. The bidentate unit consists of a pyridyl-thiazole unit. The central bipyridine unit has methoxy substituents at the C_3 position and as observed in previous structures these partition the ligand into two separate domains. The irregular six-coordinate environment is formed and comprises (for each terminal Cd metal ion) one tridenate pyridyl-thiazole-thiazole unit of one ligand, a pyridyl-thiazole unit from the other ligand and a monodentate ligand specifically MeCN at Cd(1) and at Cd(3). This ligand is thus arranged in a ‘head to tail’ manner with the bidentate pyridyl-thiazole unit at opposite ends of the helicate.

The formation of this helicate complex with L^6 is controlled by two factors; i) that of the preference of the Cd(II) metal ion to form a six-coordinate pseudo-octahedral environment; ii) the methoxy substituents groups of the central bipyridine unit that are key to the partitioning of the ligand at this central position.

As has been observed in the previous cases the presence of the methoxy substituents groups on the central bipyridine rings of this ligand is the most dominant factor in the formation of this helicate complex.

Figure 3.5 Structure of the complex cation $[Cd_3(L^6)_2(MeCN)(ClO_4)_2]^{4+}$ with a) Capped stick view; b), c) Vertical and horizontal ball and stick view; d) space-fill diagram of the Cd(II) helicate structure.

a) Capped stick view

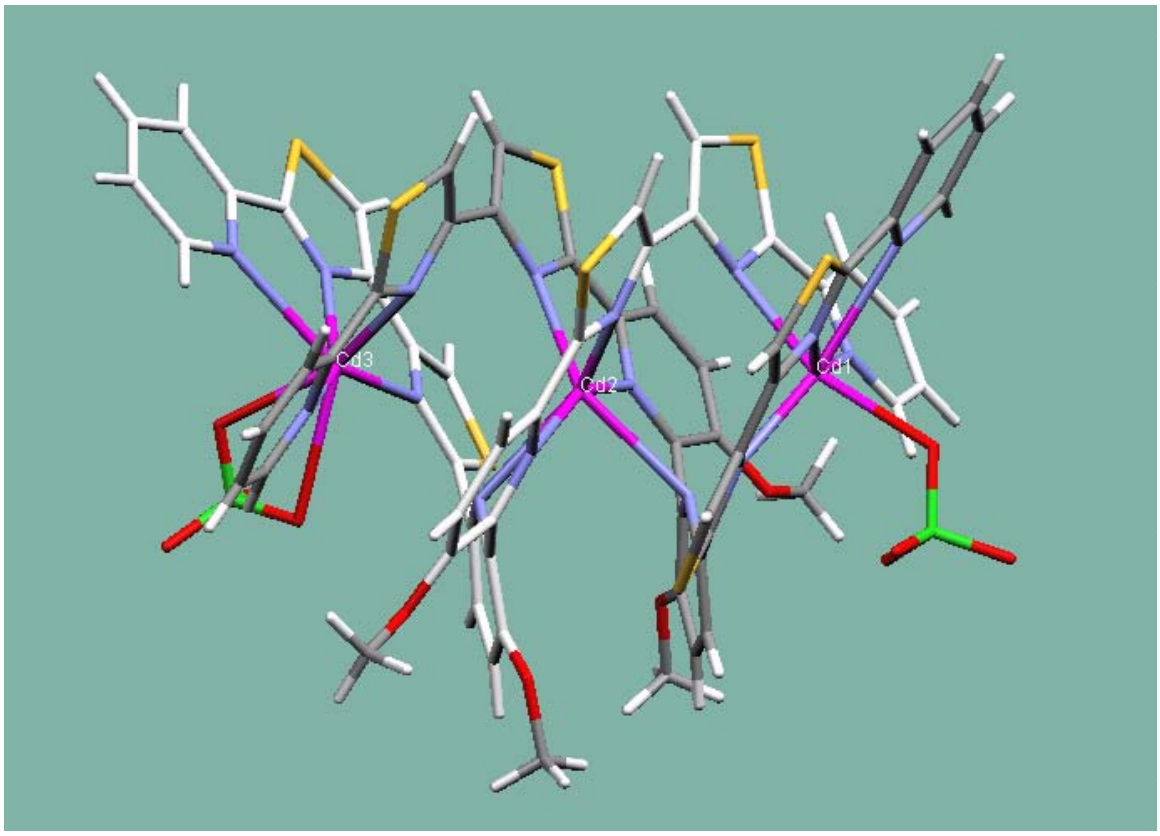

b) Vertical ball and stick view

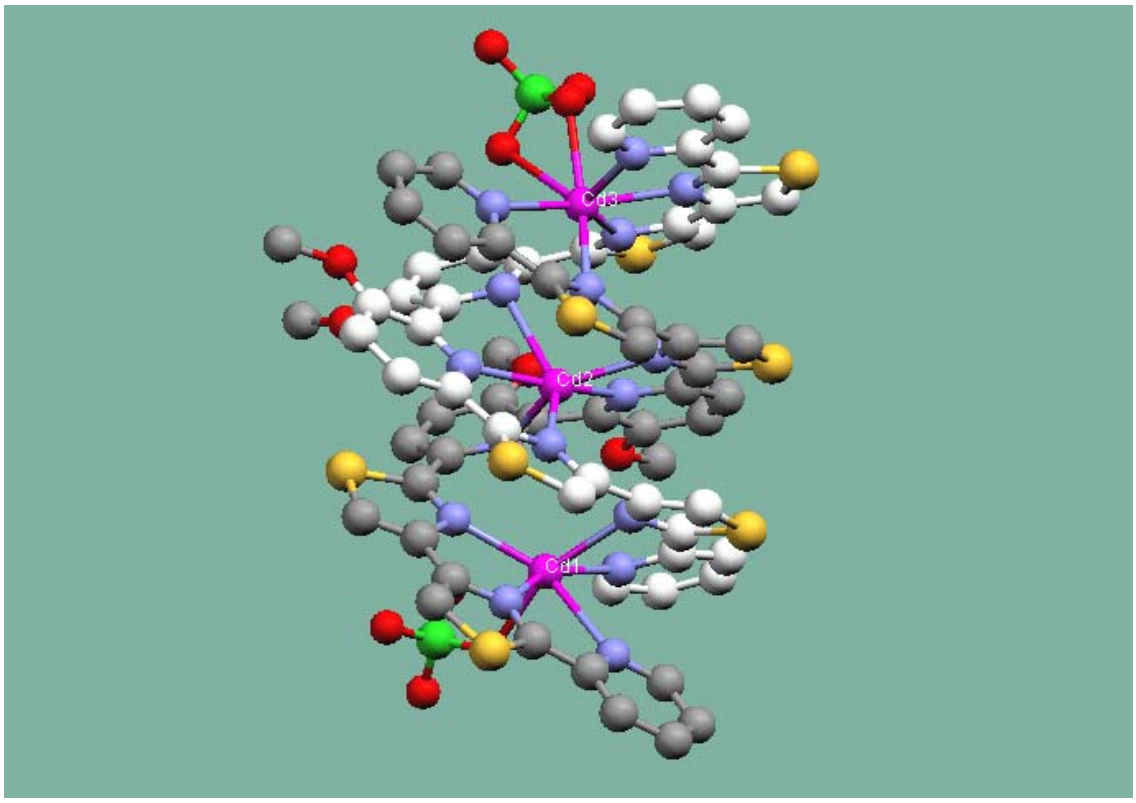

c) View looking down between the helicate complex

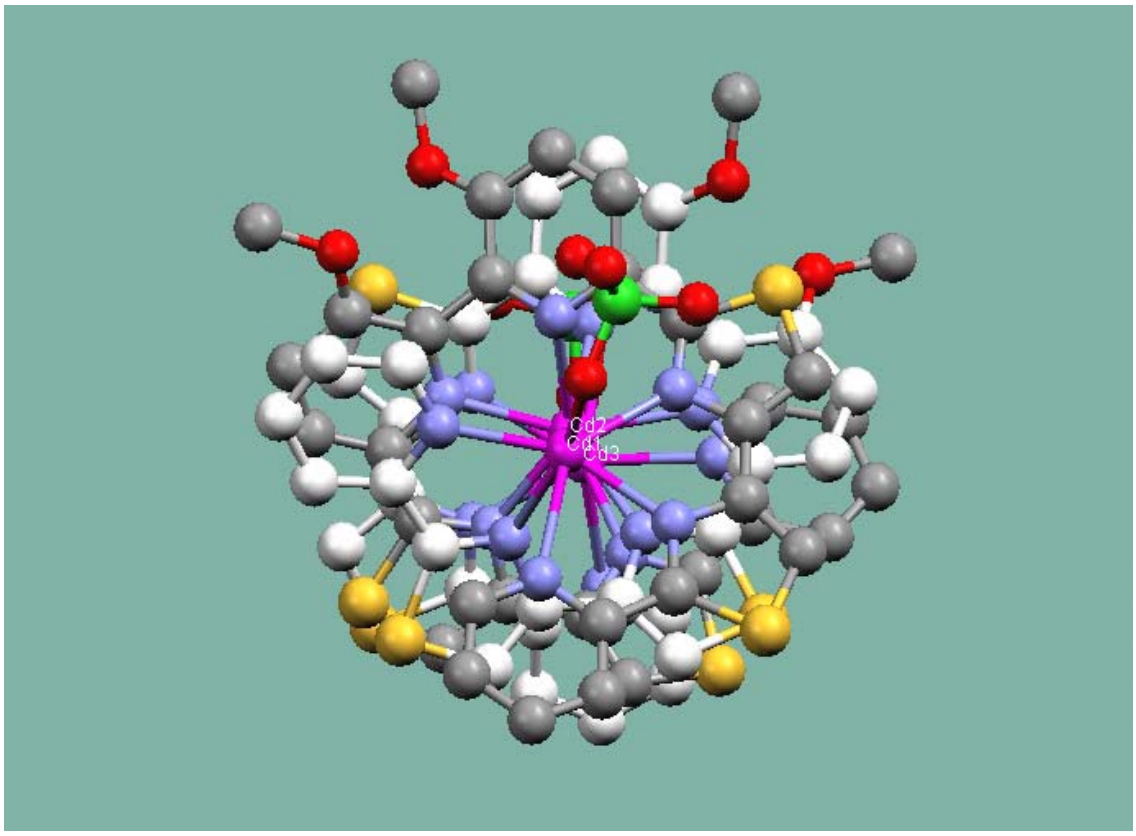

d) Space-fill diagram

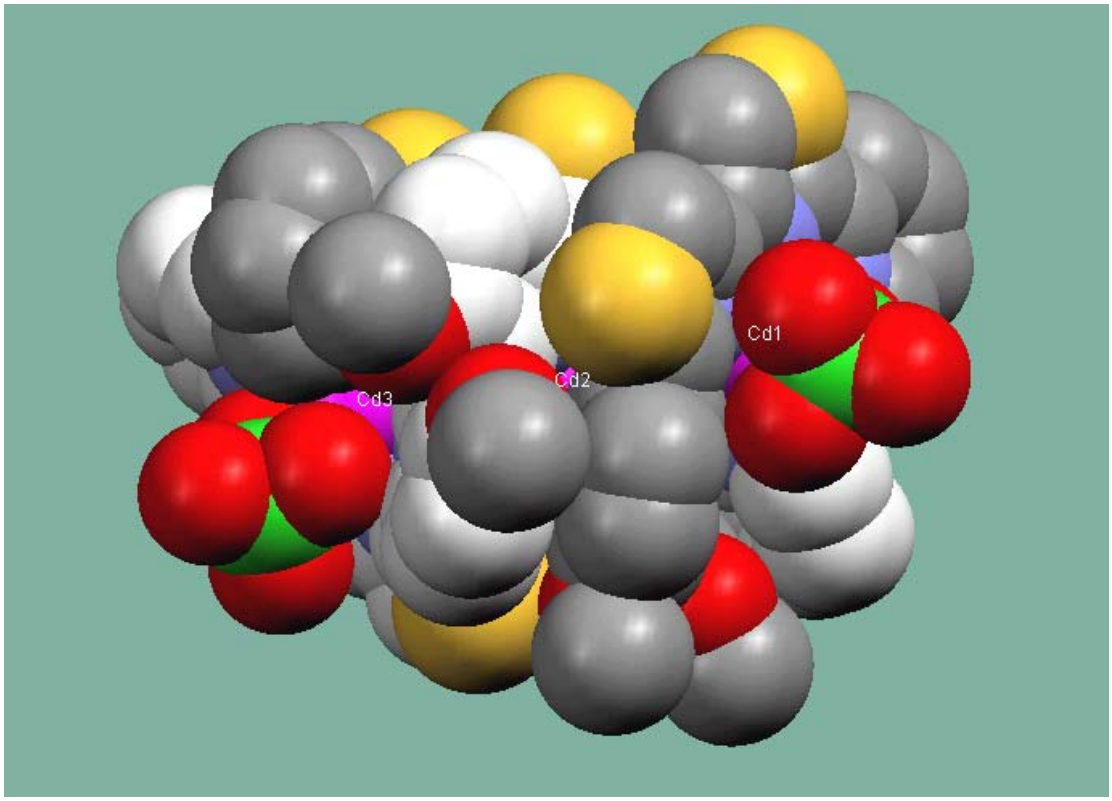

Table 3.3 Selelcted bond distances (Å) and bond angles (˚) for $[Cd_3(L^6)_2(ClO_4)_2]^{4+}$

Bond Lengths			
Cd(1) – N(11)	2.658(4)	Cd(2) – N(111)	2.327(4)
Cd(1) – N(21)	2.247(4)	Cd(2) – N(41)	2.588(4)
Cd(1) – O(1A)	2.369(4)	Cd(2) – N(51)	2.283(4)
Cd(1) – N(101)	2.366(4)	Cd(2) – N(121)	2.281(4)
Cd(1) – N(91)	2.259(4)	Cd(2) – N(131)	2.587(4)
Cd(1) – N(31)	2.342(4)	Cd(2) – N(61)	2.341(4)
Cd(3) – N(141)	2.409(4)	Cd(3) – O(2A)	2.379(5)
Cd(3) – N(151)	2.264(4)	Cd(3) – N(161)	2.672(5)
Cd(3) – N(71)	2.367(4)	Cd(3) – N(81)	2.319(5)
Bond Angles			
N(21) – Cd(1) – N(11)	65.9(1)	N(121) – Cd(2) – N(131)	68.1(1)
N(11) – Cd(1) – O(1A)	88.2(1)	N(111) – Cd(2) – N(131)	137.2(1)
N(21) – Cd(1) – N(101)	97.7(1)	N(121) – Cd(2) – N(61)	128.5(1)
N(11) – Cd(1) – N(101)	76.8(1)	N(111) – Cd(2) – N(61)	89.0(1)
N(21) – Cd(1) – N(91)	153.7(2)	N(51) – Cd(2) – N(131)	93.6(1)
N(91) – Cd(1) – N(31)	135.5(1)	N(61) – Cd(2) – N(131)	106.4(1)
N(91) – Cd(1) – N(101)	72.7(2)	N(51) – Cd(2) – N(41)	68.1(1)
N(21) – Cd(1) – O(1A)	89.8(2)	N(61) – Cd(2) – N(41)	137.6(1)
N(31) – Cd(1) – O(1A)	91.6(1)	N(131) – Cd(2) – N(41)	86.5(1)
N(31) – Cd(1) – N(11)	136.5(1)	N(121) – Cd(2) – N(51)	155.6(1)
N(21) – Cd(1) – N(31)	70.7(1)	N(51) – Cd(2) – N(61)	70.9(2)
N(31) – Cd(1) – N(101)	109.7(1)	N(151) – Cd(3) – N(141)	70.0(2)
N(91) – Cd(1) – O(1A)	91.9(2)	N(151) – Cd(3) – N(71)	96.2(2)
N(101) – Cd(1) – O(1A)	158.6(1)	N(151) – Cd(3) – O(2A)	87.8(2)
N(91) – Cd(1) – N(11)	88.0(1)	N(71) – Cd(3) – O(2A)	156.0(2)
N(111) – Cd(2) – N(41)	108.7(1)	N(81) – Cd(3) – N(141)	140.6(2)
N(51) – Cd(2) – N(111)	129.2(1)	O(2A) – Cd(3) – N(141)	94.9(2)
N(121) – Cd(2) – N(41)	93.9(1)	N(81) – Cd(3) – N(161)	84.2(2)
N(121) – Cd(2) – N(111)	71.1(1)	O(2A) – Cd(3) – N(161)	80.8(2)

3.8 Synthesis of 3,3′-disubstituted ligands L^7 & L^8

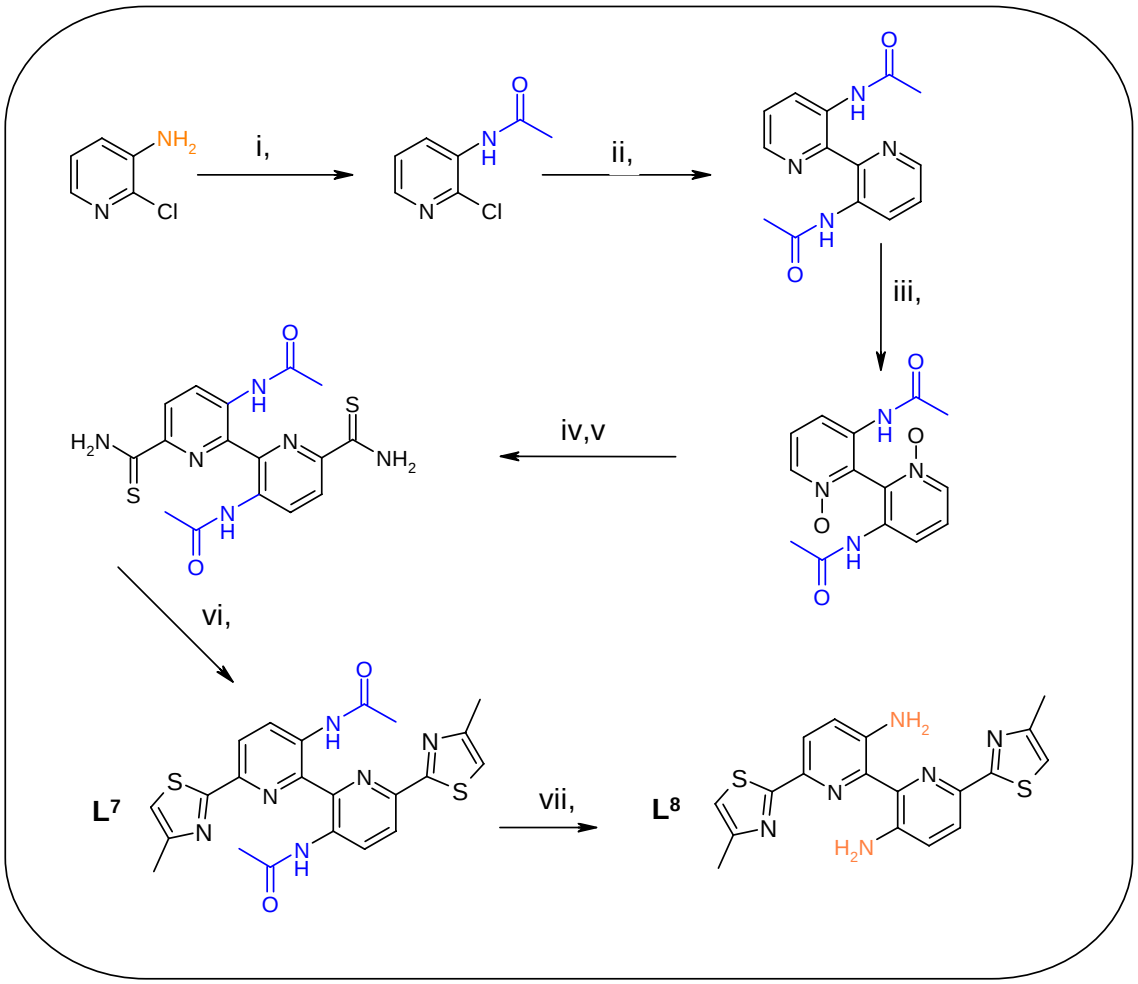

Scheme 3.2 Synthesis of ligands L^7 & L^8

Reagents and conditions: (i) $(CH_3CO)_2O$; (ii) Copper Bronze, DMF ; (iii) $ClC_6H_4CO_3H$, $CHCl_3$; (iv) $(CH_3O)_2SO_2$; (v) NaCN; (vi) $ClCH_2COCH_3$; (vii) HCl, H_2O

3.8 Synthesis of 3,3′-disubstituted ligands L^7 & L^8

The potentially tetradentate ligands L^7 and L^8 were prepared from 3,3′-di-acetylamino-2,2′-bipyridine-1,1′-dioxide via the incorporation of nitrile substituents at the C_6 position of 3,3′-disubstituted bipyridine-dioxide in a similar manner to the previous ligands. Conversion of a nitrile unit to a thioamide was achieved by the reaction with hydrogen sulfide gas. Subsequent reaction of the dithioamide with chloroacetone (in EtOH at reflux) gives ligand L^8.

3.8.1 Synthesis of 3,3′-diacetyl-2,2′-bipyridine precursor ligand

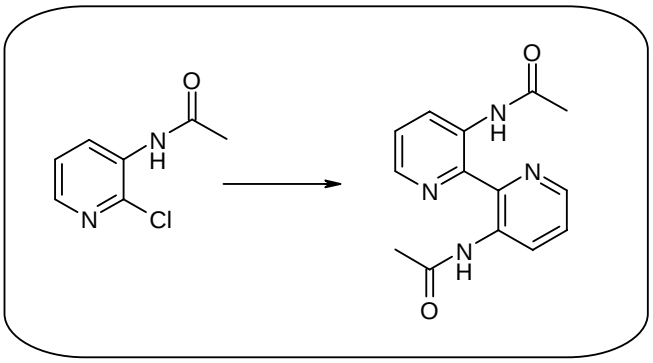

Figure 3.6 Synthesis of 3,3′-diacetyl-2.2′-bipyridine

Preparation of 3,3′-diacetyl-2,2′-bipyridine was performed via a three step synthesis; i) A solution of 3-acetylamino-2-chloropyridine and copper powder in DMF was stirred at an elevated temperature (80˚C) for 12 hr; ii) Filtration followed by neutralised via the addition of ammonia removed the Cu^{2+}; iii) Extraction of the product with dichloromethane. Separation and purification of the product via column chromatography gave 3,3′-di-acetylamino-2,2′-bipyridine as a powdery pale yellow solid. 3,3′-diacetylamino-2,2′-bipyridine was characterised by ^1H NMR (see experimental section). Yields were found to be of the range 50-70%.

3.8.2 *N*-oxidation

N-oxidation of 3,3′-diacetylamino-2,2′-bipyridine with an excess amount of *m*-CPBA affords the 3,3′-diacetylamino-2,2′-bipyridine-1,1′-dioxide. The reaction was monitored by thin layer chromatography over an extended period of time. Here the ^{1}H NMR shows a symmetrical species with three proton signals ranging from δ 7.40 to 9.10 ppm. All three proton signals are substantially shifted when compared to that of the starting material.

3.8.3 Formation of 6,6′-dicyano-3,3′diacetylamino-2,2-bipyridine

Cyanation of 3,3′-di-acetylamino-2,2′-bipyridine-1,1′-dioxide via methylation of the *N*-oxide and subsequent reaction with excess sodium cyanide affords 6,6′-dicyano-3,3′-di-acetylamino-2,2′-bipyridine as a pale tan solid. Here the ^{1}H NMR illustrates that only two signals are observed, those aromatic protons at the C_5 and C_4 position of the pyridine ring. The proton at the C_6 position δ 7.40 ppm is no longer present. Subsequent purification via column chromatography was required prior to further use.

3.8.4 Formation of 3,3′-diacetylamino-2,2′-bipyridine-6,6′-dithioamide

Reaction of the 6,6′-dicyano-3,3′-di-acetylamino-2,2′-bipyridine with hydrogen sulfide gas affords the 3,3′-di-acetylamino-2,2′-bipyridine-6,6′-dithioamide as a yellow precipitate. The ^{1}H NMR shows two signals observed at δ 10.20ppm and 9.75ppm, indicative of the presence of thioamide functional groups, with the ligand retaining its symmetrical nature. The aromatic proton signals remain at δ 8.45 and 8.65 ppm.

3.8.5 Formation of 3,3′-disubstituted ligand L^7

Reaction of 3,3′-diacetylamino-2,2′-bipyridine-6,6′-dithioamide with chloroacetone in DMF affords the 3,3′-disubstituted ligand L^7 as a pale yellow solid.

The ^{1}H NMR shows the presence of the newly formed thiazole ring and methyl substituent with two signals observed at δ 6.97ppm and 2.5ppm respectively.

3.9 Synthesis of 3,3′-disubstituted ligand L^8

The potentially tetradentate ligand L^8 was prepared from hydrolysis of ligand L^7. Reaction of the disubstituted 3,3′-di-acetylamino-2,2′-bipyridine ligand with concentrated hydrochloric acid (HCl) at reflux resulted in the hydrolysis of the amide. The addition of aqueous ammonia afforded the amine-containing ligand via precipitation as the free ligand L^8.

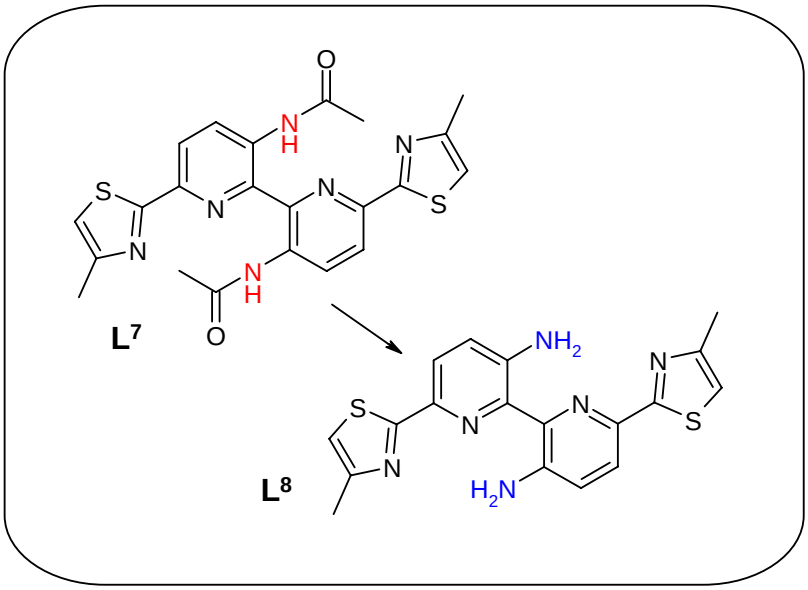

Scheme 3.3 Conversion of ligand L^7 to ligand L^8

3.10 Synthesis and crystal structure of L^8 with $Cd(ClO_4)_2 \cdot 6H_2O$

The reaction of L^8 with $Cd(ClO_4)_2 \cdot 6H_2O$ in an MeCN solution gave complexes that were analysed via electrospray mass spectroscopy and were found to contain the complex cation $[Cd(L^8)_2][ClO_4]^+$ *m/z* 972, and an ion at *m/z* 1285 corresponding to $\{[Cd_2(L)_2(ClO_4)_3]^+\}$ and the formation of a dinuclear double helicate was confirmed via X-ray crystallographic analysis.

Each Cd(II) metal ion was found to be within a six-coordinate environment and the coordination geometry can be described as pseudo-octahedral environment. The metal ions in this complex are coordinated to the two N-donors of the bidentate pyridyl-thiazole unit from each ligand and a perchlorate anion and a MeCN solvent molecule. The Cd…Cd separation in this example is 4.748 Å and the Cd…N bond distances range from 2.312 – 2.398 Å. The longest bond distance 2.398 Å was noted to be that distance between the perchlorate anion and the metal centre.

In this complex the coordination geometry is formed by the partitioning of the ligand into two equivalent bidentate binding domains consisting of a pyridyl-thiazole unit. The central bipyridine unit of the ligand has amine substituents at the C_3 position, groups which due to the unfavourable steric interactions cause the ligand to partition at its centre. L^8, unlike the other ligands described in this chapter is only a potentially tetradentate ligand with four aromatic nitrogen donors on each ligand. Thus, the ligand is forced to partition into two bidentate pyridyl-thiazole units to minimise the steric repulsion between the two amino substituents.

Interestingly a complex formed by the unsubstituted ligand and which contains identical thiazole-bipyridyl-thiazole donor units forms a mononuclear double helicate complex with Cd^{2+}, $[Cd(L)]^{2+}$.[108]

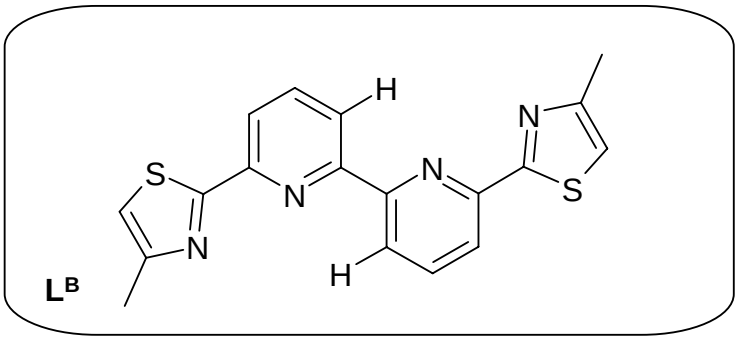

Figure 3.7 Unsubstituted ligand L^B

The principal difference between these two pyridyl/thiazole ligand strands is that unlike L^B, the L^8 ligand contains amine substituents that occupy the 3,3′-position of the central bipyridine group. It is the presence of these substituents that forces the central partitioning of the ligand and does not allow the bipyridine group to act as a bidentate unit, therefore the bipyridine unit assumes a position away from planarity and toward an angle of 90˚ partitioning the ligand into two bidentate domains.

L^B in complete contrast does not contain substituents at the 3.3′-position and as a result, the bipyridine unit is able to approach planarity and the bipyridine group of the ligand is able to behave as a bidentate unit and a mononuclear complex is produced. The formation of this helicate complex is controlled via two independent factors i) that of the stereo-electronic preference of the metal ion to form a six-coordinate environment; ii) but ultimately it is the presence of amine substituents groups on the central bipyridine ring of this ligand chain that is the dominating factor in the formation of this helicate complex.

Figure 3.8 Structure of the complex cation $[Cd(L^8)_2(MeCN)(ClO_4)_2]^+$ with a) Capped stick view; b), c) Ball and stick view; d) Spacefill view of the Cd(II) helicate complex.

a) Capped stick view

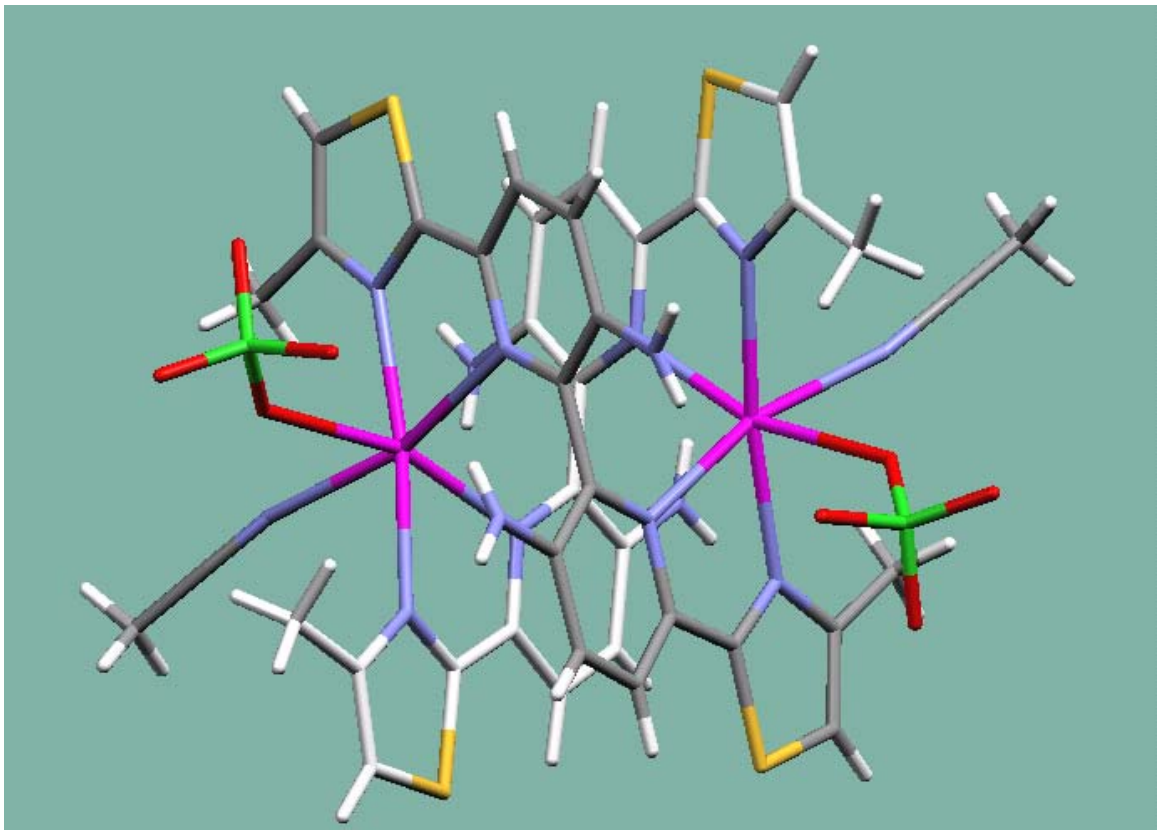

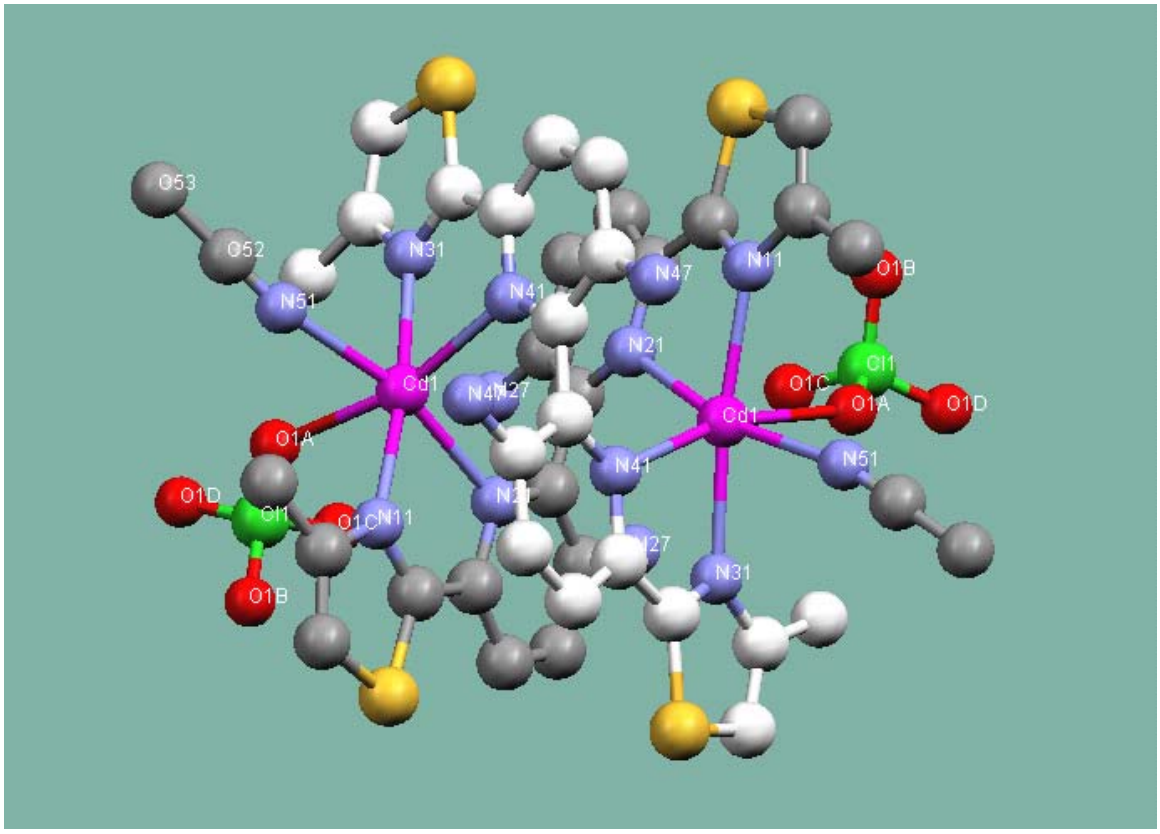

c) Vertical ball and stick view

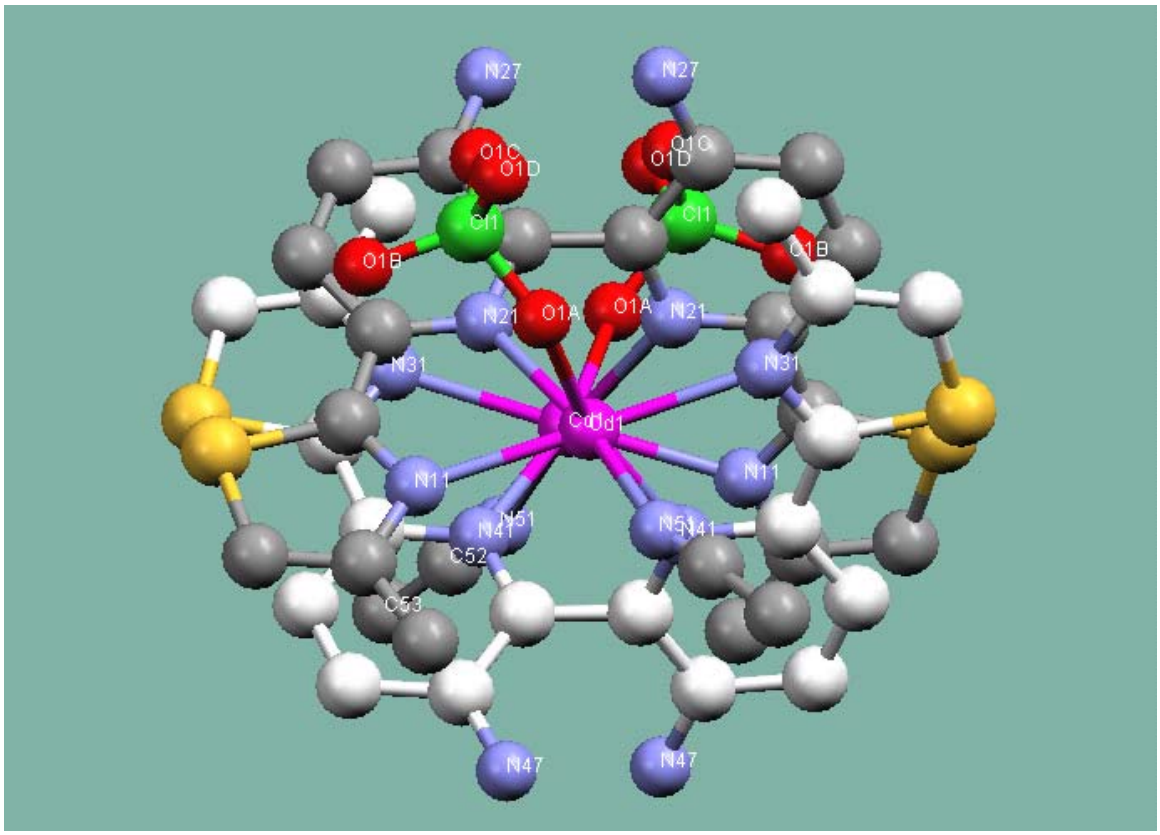

d) Spacefill view

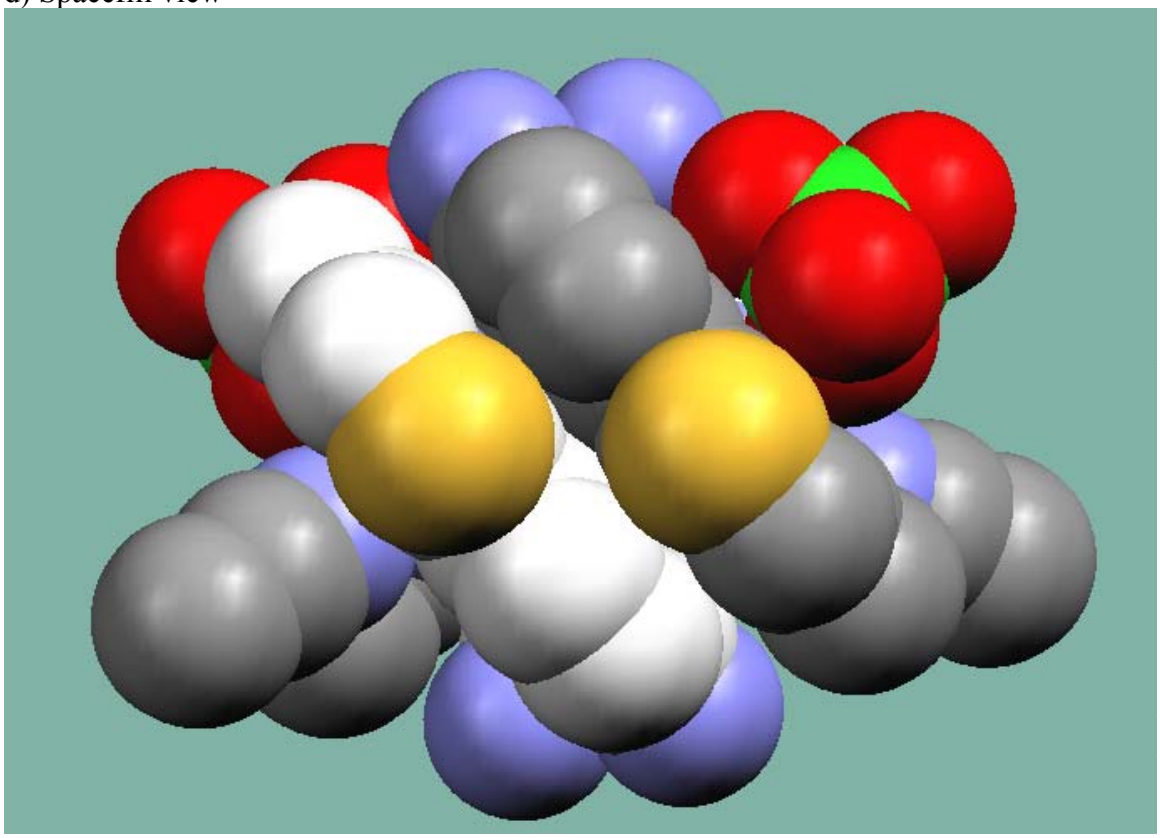

Table 3.4 Selected bond distances (Å) and bond angles (º) for $[Cd_2(L^8)_2]^{4+}$

Bond Lengths	
Cd(1) – N(31)	2.330(1)
Cd(1) – N(51)	2.375(1)
Cd(1) – N(41)	2.348(1)
Cd(1) – N(21)	2.365(1)
Cd(1) – N(11)	2.312(1)
Cd(1) – O(1A)	2.398(1)
Bond angles	
N(31) – Cd(1) – N(51)	79.5(5)
N(31) – Cd(1) – N(41)	73.5(5)
N(51) – Cd(1) – N(41)	90.9(5)
N(31) – Cd(1) – N(21)	110.3(5)
N(51) – Cd(1) – N(11)	95.8(5)
N(11) – Cd(1) – N(31)	173.3(5)
N(11) – Cd(1) – N(41)	111.5(5)
N(11) – Cd(1) – N(21)	73.5(5)
N(41) – Cd(1) – N(21)	101.4(5)
N(21) – Cd(1) – N(51)	165.8(5)
N(11) – Cd(1) – O(1A)	81.6(5)
N(31) – Cd(1) – O(1A)	92.8(6)
N(41) – Cd(1) – O(1A)	164.3(5)
N(21) – Cd(1) – O(1A)	90.2(5)
N(51) – Cd(1) – O(1A)	78.8(5)

3.11 Conclusion

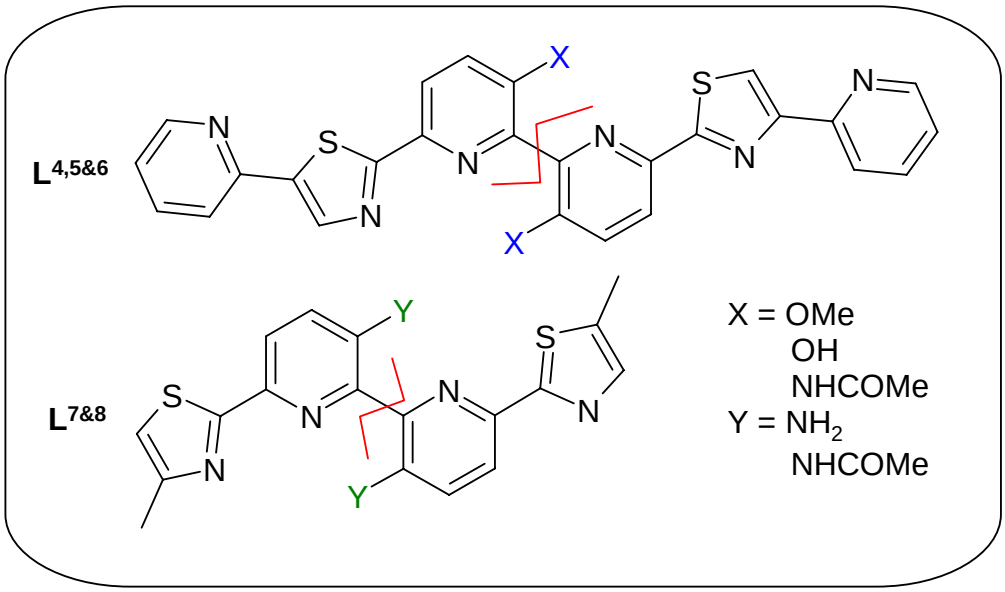

Scheme 3.4 Diagrammatic representation of partitioning in ligand strands L^4 – L^8

The ligands L^4 – L^8 that have been discussed in this chapter are examples of polydentate pyridyl/thiazole ligands that each contain substituents groups at the 3,3′-position of the central bipyridine unit. These substituents are a dominant factor in controlling complex formation (not previously seen in this ligand series). In the previous chapter, the five-membered thiazole ring and its position along the ligand chain was seen to be fairly crucial in the formation of the helicate complexes. Here, the partitioning of the ligand chain was at a position along the ligand chain adjacent to the thiazole rings. The potentially hexadentate ligand L^4, L^5 and L^6 partition centrally between the bipyridine unit purely as a need to separate the substituents present on the bipyridine ring and minimise the unfavourable steric interactions associated.

Previous studies have shown that in-coordination of thiazole units within a ligand strand program the ligand into different binding domains. It has been demonstrated in these chapters that this programming can be easily ‘overwritten’ by the inclusion of sterically demanding substituents.

CHAPTER IV

4. Results & Discussion: Section 1; Ruthenium (II) crown ether complexes

Metal-containing sensors for s-block metal ions have received much attention for example the work of N. S. Finney, S. A. McFarland[90,91] and M. D. Ward[67] *et al* which involved the synthesis of Ru(II) complexes with ligands L^A and L^B that contain a crown ether unit, whose luminescence properties were modulated upon coordination of s-block metal ions, ligands L^A and L^B *Figure 4.1*. Following this we decided to investigate the ability of Ru(II) complexes L^9, L^{10} and L^{11} to act as a sensor for s-block metal ions, *Figure 4.2*.

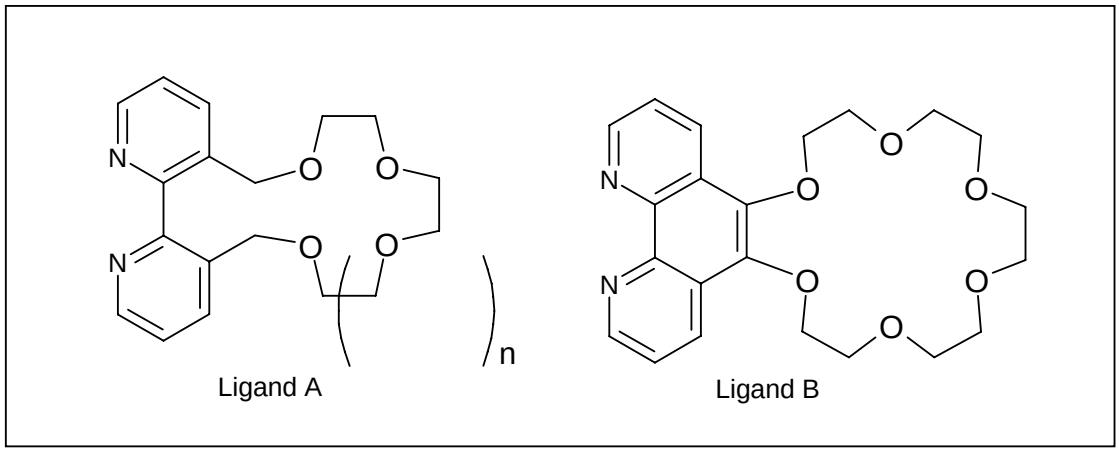

Figure 4.1 Ligand A & B crown ether ligands

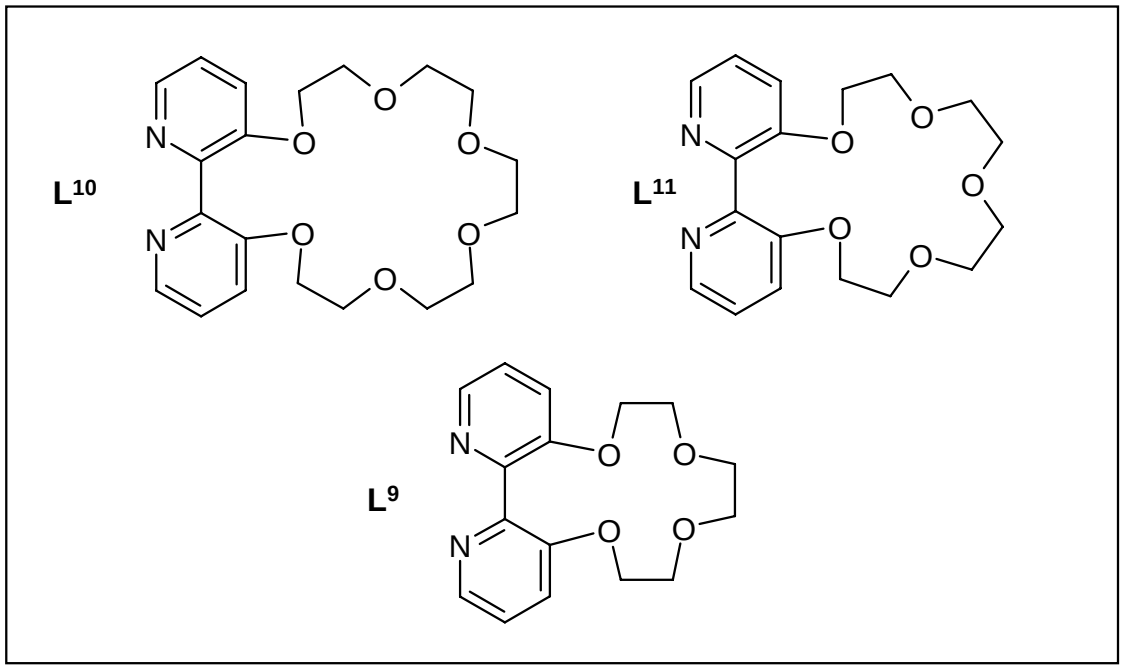

Figure 4.2 Diagrammatic representations of crown ether ligands L^9-L^{11}

The ligands L^9-L^{11} differ from those ligands shown in *Figure* 4.1 as the oxygen atoms are directly attached to the crown ether moiety. It was envisaged that this might have a dramatic effect on the luminescent metal ion coordinated directly to the bipyridine unit due to their close proximity.[87]

4.1 Synthesis of Crown ether ligands $L^9 – L^{11}$

All ligands L^9- L^{11} were synthesised from 3,3′-dihydroxy-2,2′-bipyridine, which was prepared via 3-hydroxy-2-iodopyridine. For each 2,2′-bipyridine-crown ether ligand, 3,3′-dihydroxy-2,2′-bipyridine was de-protonated with excess NaH in DMF at room temperature. Subsequent reaction with tri(ethylene glycol) di-p-tosylate; tetra(ethylene glycol) di-p-tosylate; and penta(ethylene glycol) di-p-tosylate at 80˚C, gave ligands L^9, L^{11} and L^{10} respectively. The reaction was followed by TLC and upon completion the solvent was removed and the crude product partitioned between $NaHCO_3$ (aq) and DCM. Purification by column chromatography gave the pure ligands L^9-L^{11} as pale yellow oils. Analysis by ESI-MS and ^1H NMR were as expected.

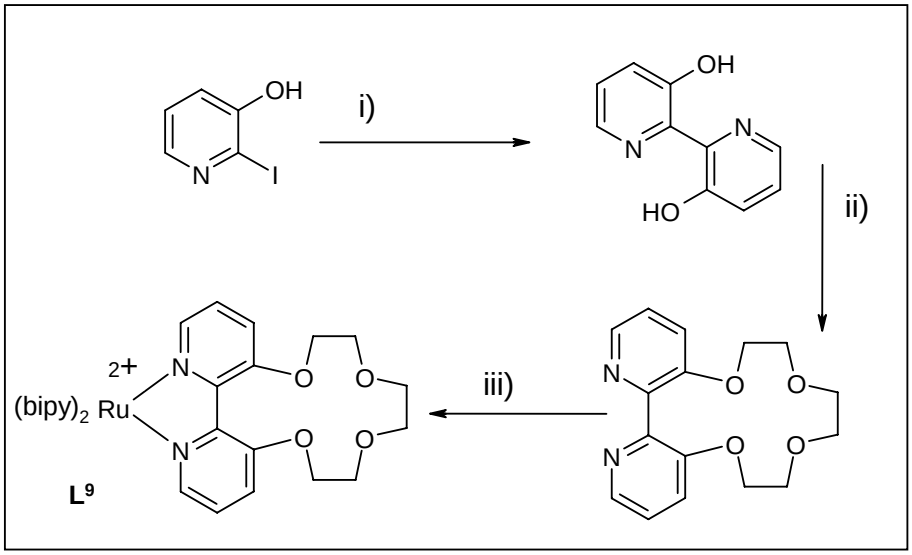

Scheme 4.1 Trisbipyridine-Ruthenium(II)-crown ether complexes $L^9 – L^{11}$ Reagents and conditions; i) $NiCl_2(PPh_3)_3$/DMF/Zn/; ii) NaH/Tri(ethylene glycol)di-*p*-tosylate; iii) $(bipy)_2RuCl_2$/ EtOH

4.2 Synthesis of tris-bipyridine Ruthenium crown ether complexes

In all cases the complexes were synthesised by reaction of the ligand with $(bipy)_2RuCl_2$ in refluxing ethanol. The reaction was monitored via TLC and after completion the complex was purified by column chromatography giving the complexes as an orange/red crystalline solid. Analysis by ESI-MS and ^1H NMR was as expected. *Scheme 4.1* highlights the synthesis of a crown ether complex from its starting material, while *Figure 4.3* shows a diagrammatic representation of all three crown ether complexes produced.

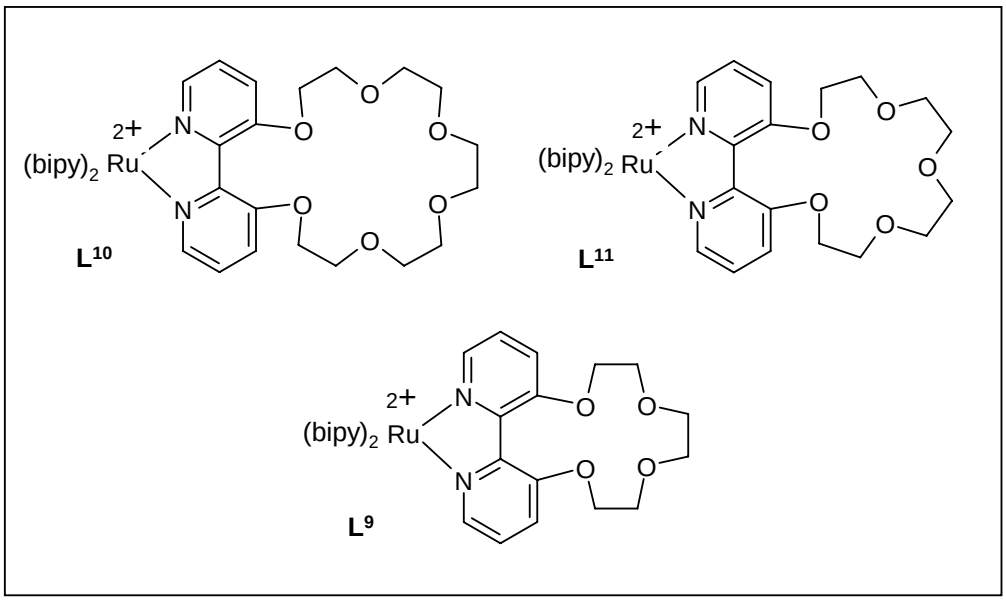

Figure 4.3 Ruthenium(II) crown ether complexes L^9-L^{11}

4.3 Synthesis and crystal structure of L^{11}

The Ru(II)-2,2′-bipyridine-17-crown-5 complex was fairly soluble and readily dissolved in MeCN to form a deep red solution. The $[(bipy)_2Ru\text{-}Crown]^{2+}$ was isolated by addition of $NaPF_6$ to the complex in H_2O (Extracted into DCM). The crystals were grown from MeCN and $[(bipy)_2Ru\text{-}Crown)\ (PF_6)_2$ with addition of $NaClO_4$. Analysis of the crystals by electrospray mass spectrometry indicated the complex cation $[Ru(L^{11})]^{2+}$ *m/z* 904.8. The formation of the Ru(II)-2,2′-bipyridine-[17]-crown-[5]complex confirmed via analysis by X-ray crystallography.

The crystal structure was as expected, with the Ru-N bond lengths unremarkable with all distances being in the typical range for a $[Ru(bipy)_3]^{2+}$ type core (Ru-N 1.995 - 2.064 Å). The N-C-C-N torsion angle of the un-substituted bipyridine units are (0.74 and –1.83˚) whereas the torsion angle of the crown ether containing bipyridine is (24.68˚). This is probably due to the unfavourable interaction between the two oxygen atoms in the 3,3′-position where additional steric constraints are placed on the ligand due to the substitution of the central bipyridine core. Of more significance is the pendant crown ether fragment, which is usually pre-organised for metal ion binding. However, despite the addition of $NaClO_4$ to the crystallising solution the crown itself remains un-coordinated. This is somewhat unexpected, as crown ether units are well known for the coordination of s-block metal cations. However, despite the excess of Na^+ ions a complex of this metal was not observed in the solid state. One possible reason for this is the ability of the oxygen atoms on the 3,3′- position of the bipyridine ring to act as coordinating units. As the geometry of these atoms is constrained by the coordinate bipyridine unit, their lone pairs are unavailable for coordination. As these cannot become involved in interaction of the guest metal ion, the coordination ability of the crown ether unit is substantially reduced.

Figure 4.4 Structures of the complex cation $[Ru(L^{11})][PF_6]_2$ excluding the counter ions; a) Capped stick view; b) Ball and stick view; c) Capped stick view highlighting bipyridine ‘twist’; d) Space-fill view.

a) Capped stick view

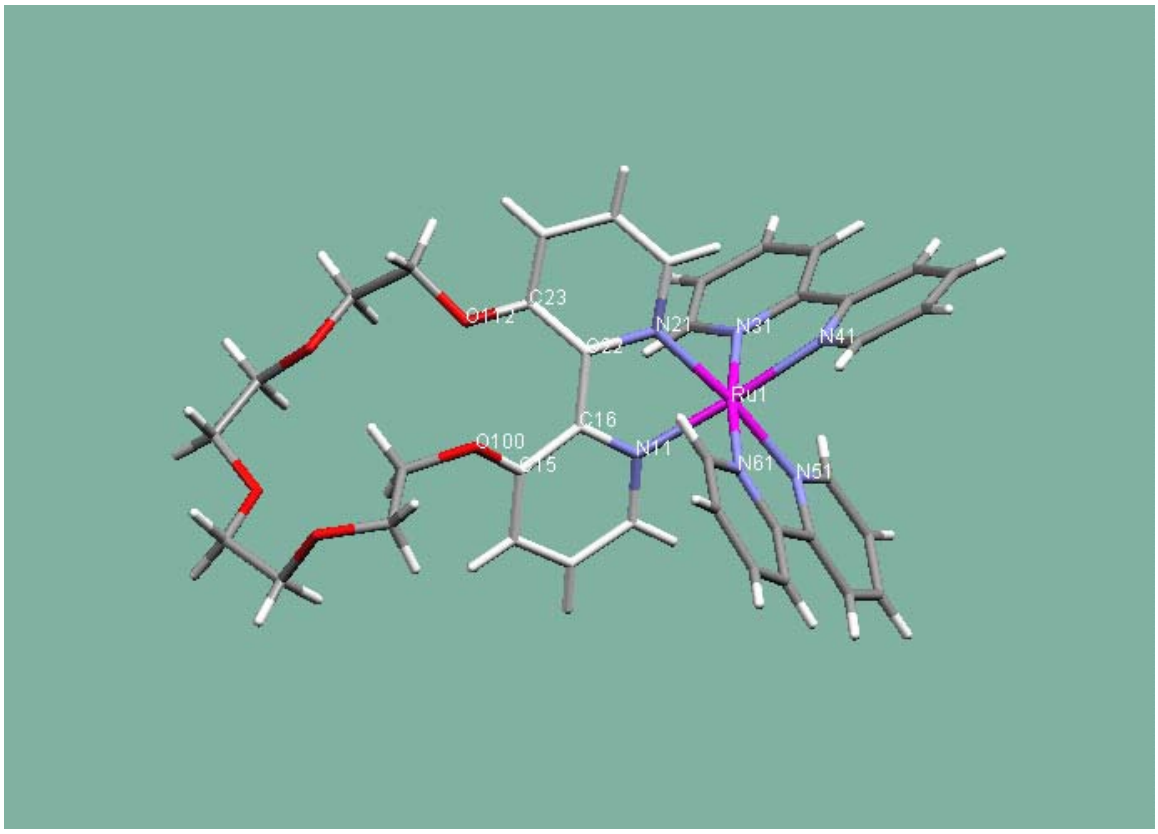

b) Ball and stick view

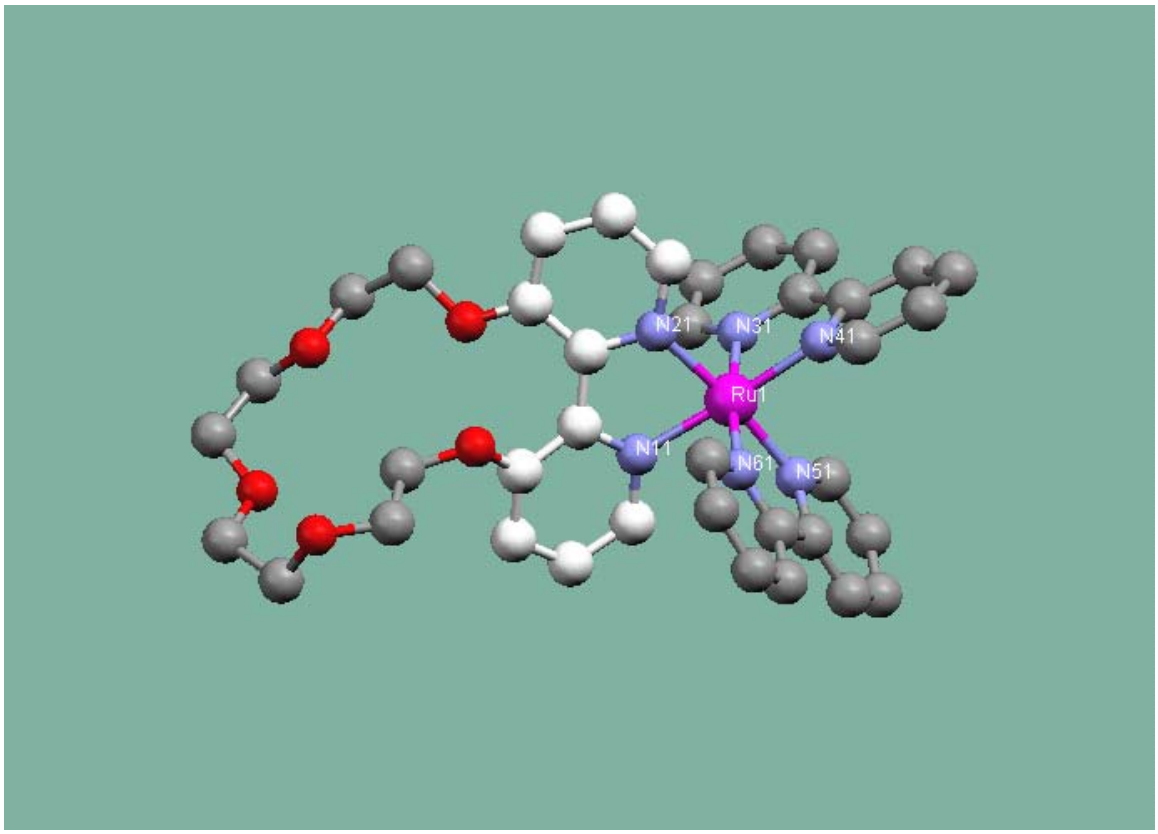

c) i) Capped stick view highlighting the bipyridine ‘twist’

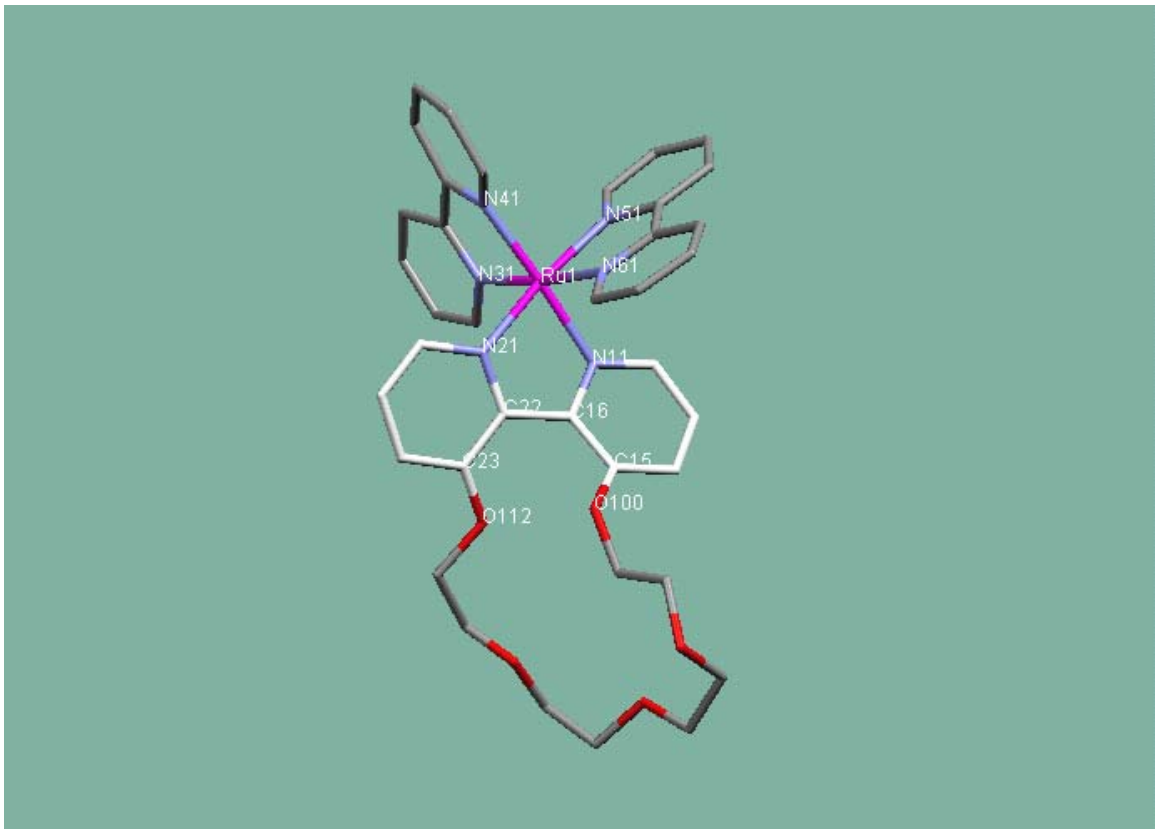

ii)

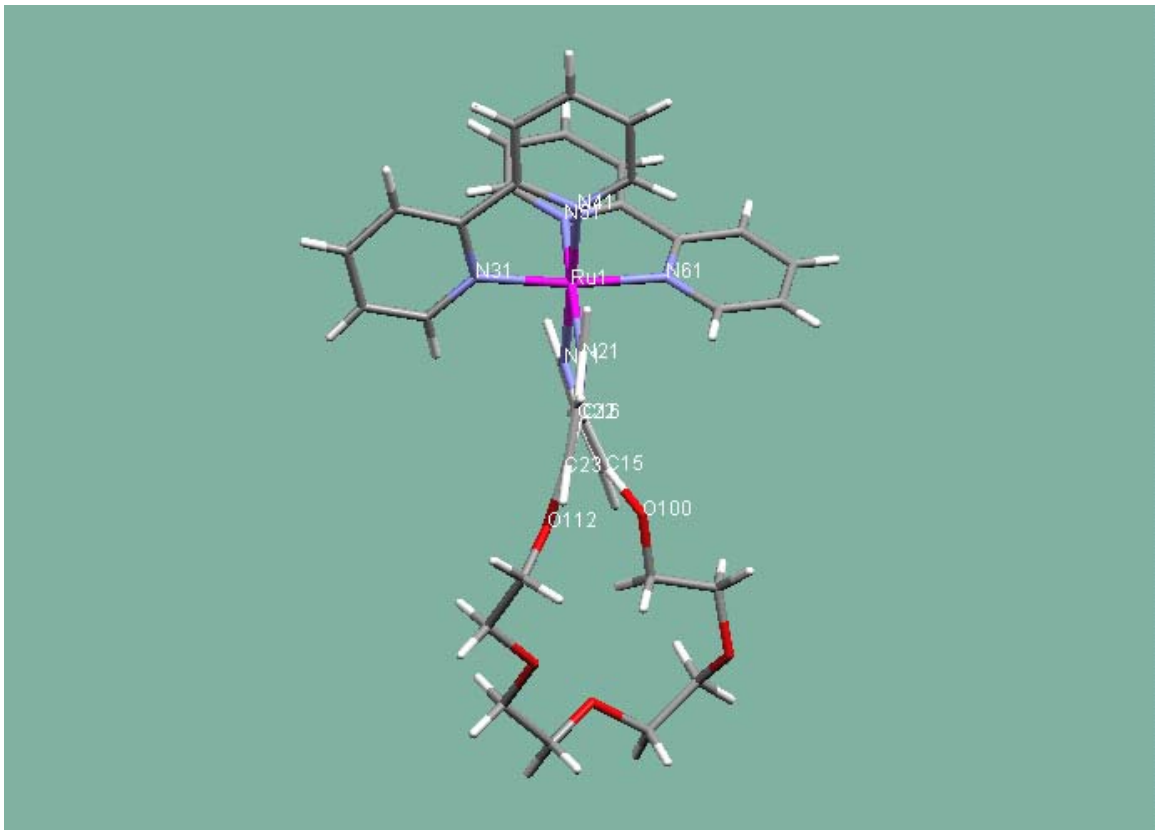

d) Spacefill View

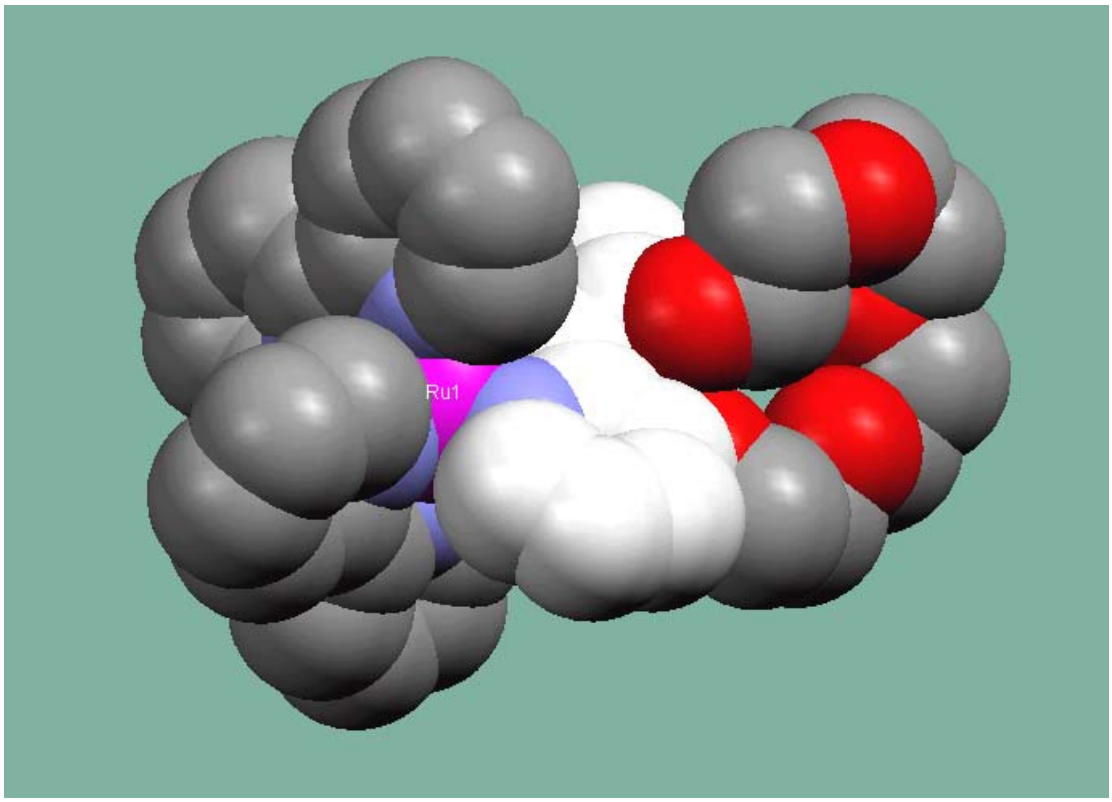

Bond Lengths	
Ru(1) – N(61)	2.056(1)
Ru(1) – N(51)	1.995(1)
Ru(1) – N(11)	2.056(1)
Ru(1) – N(21)	2.026(1)
Ru(1) – N(31)	2.064(1)
Ru(1) – N(41)	2.024(1)
Bond Angles	
N(61) – Ru(1) – N(51)	78.4(5)
N(41) – Ru(1) – N(31)	79.8(5)
N(21) – Ru(1) – N(11)	79.1(5)
N(21) – Ru(1) – N(41)	98.0(5)
N(31) – Ru(1) – N(51)	95.9(4)
N(61) – Ru(1) – N(11)	85.8(4)
N(51) – Ru(1) – N(41)	88.7(4)
N(51) – Ru(1) – N(21)	172.8(4)
N(41) – Ru(1) – N(61)	95.5(5)

N(21) – Ru(1) – N(61)	98.3(4)
N(51) – Ru(1) – N(11)	94.2(4)
N(41) – Ru(1) – N(11)	177.0(5)
N(21) – Ru(1) – N(31)	87.9(4)
N(61) – Ru(1) – N(31)	172.8(5)
N(31) – Ru(1) – N(11)	99.2(5)

Table 4.1 Selected bond distances (Å) and bond angles (˚) for $[Ru(L^{11})][PF_6]_2$.

4.4 Luminescence Studies

The tris-bipyridine ruthenium crown ether complex has a strong absorption spectra at 454 (nm) and a strong emission spectra at 610 (nm).[55]

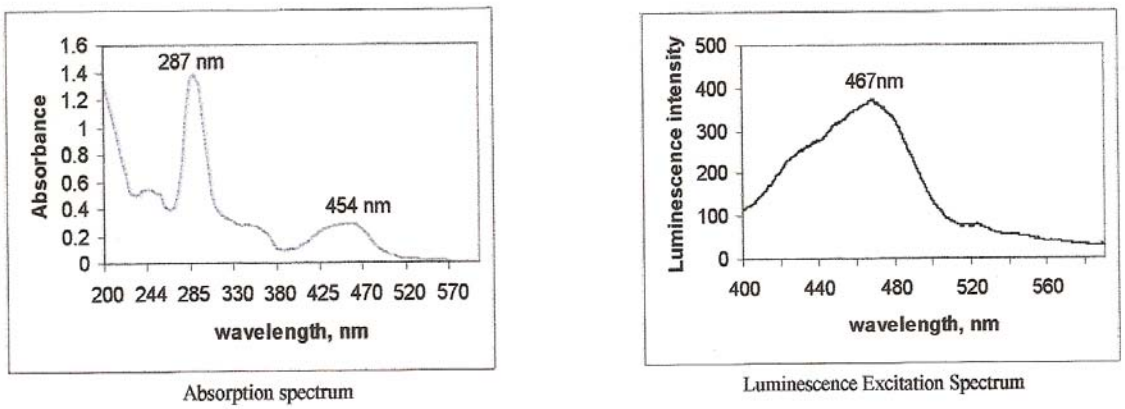

Figure 4.5 Two spectra displaying both the adsorption and excitation of typical Ru(II)-crown ether complexes.

The basis of cation binding studies for the Ru(II)-crown ether complexes is that they lend themselves to this type of investigation due to their inherent luminescent nature and it is this nature that allows study of the changes of luminescent behaviour of these crown ether complexes upon the addition of a wide range of cations.

A number of commonly found cations were initially selected to take part in the titration binding studies of these complexes namely Li^{+}, Ba^{2+}, Na^{+}, Ca^{2+}, Sr^{2+}.

Here below, the emission spectrum for Ru(II)-2,2′-bipyridine-[20]crown-6, *Figure 4.6*.

Emission Spectra

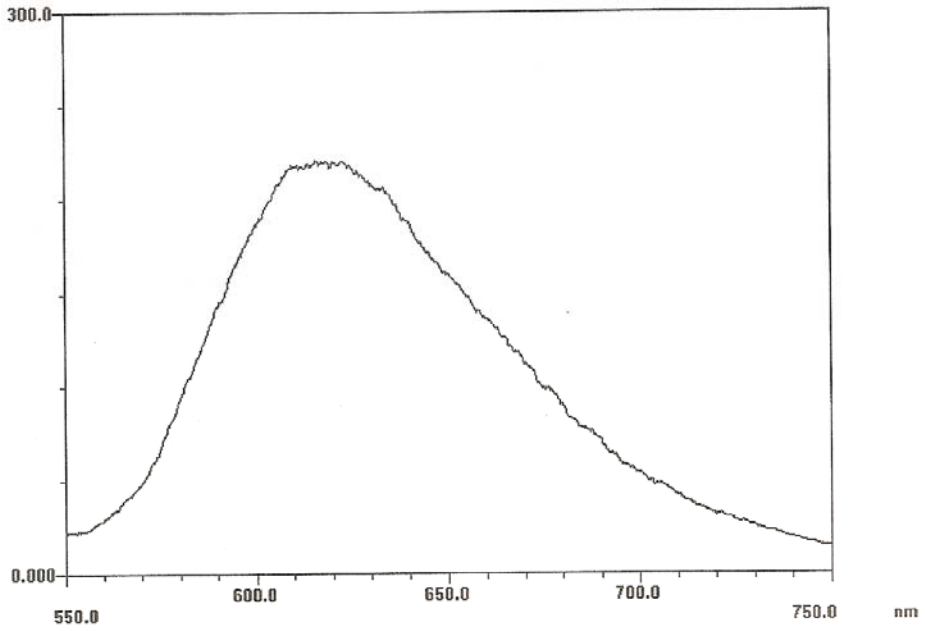

Figure 4.6 Emission spectrum for Ru(II)-2,2′-bipyridine-[20]-crown-6

To investigate the modulation of luminescence, excess addition of a number of cations; Na^{+}, Li^{+}, Ba^{2+}, Ca^{2+}, Sr^{2+}, Mg^{+} were added to a solution of the crown ether complex at a concentration of 5 x 10^{-5} M, (MeCN) and the luminescence spectra was re-recorded. Results are given in *Figure 4.7.*

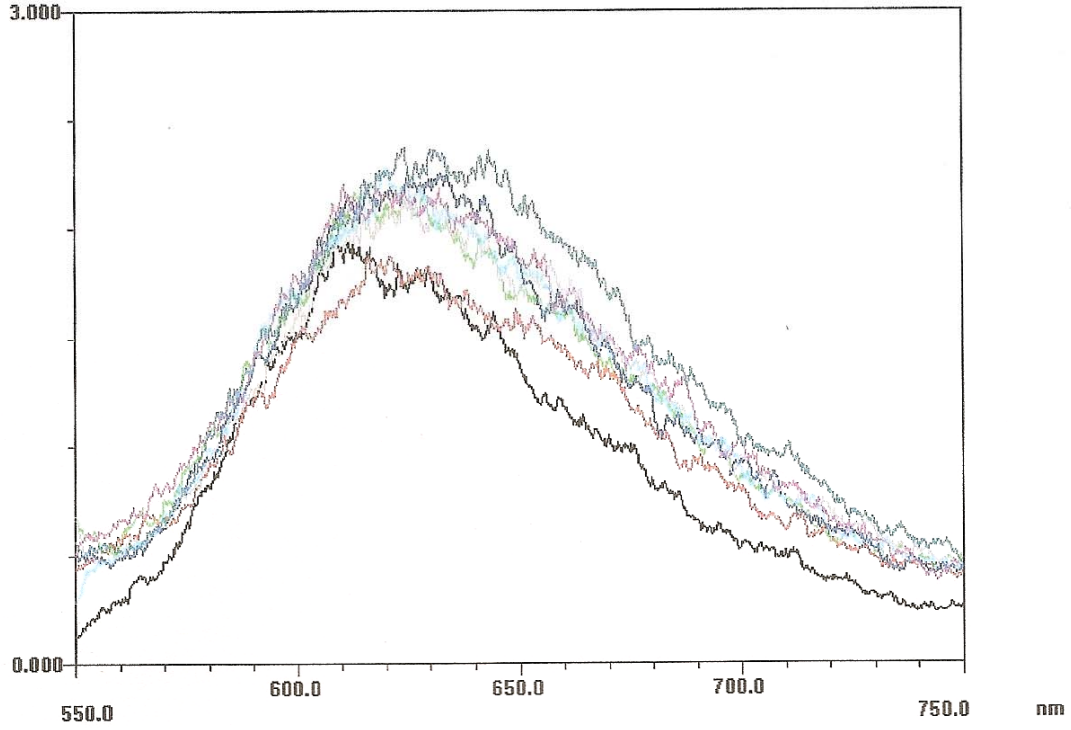

*Figure 4.7.*Emission spectrum for Ru(II)2,2′-bipyridine-[20]-crown-6 with the addition of a number of cations.

As can be seen in *Figure 4.7* little or virtually no effect is observed. There are two possible reasons for this; firstly the s-block metal ion is not coordinated in solution to the crown ether complex. This however seems unlikely as other systems *i.e.* those of Finney, McFarland and Ward *et al* are very similar to the L^9-L^{11} ligand complexes and all these are shown to coordinate to s-block metal ions and there is no logical reason as to why they shouldn't. A second possibility is that the s-block metal only coordinates the 'outer' oxygen atoms as shown in *Figure 4.8*

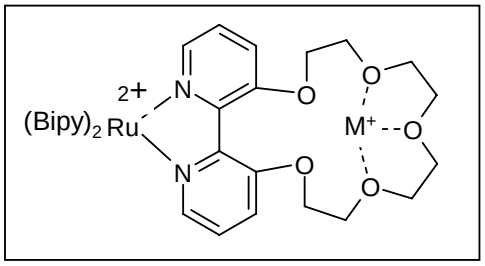

Figure 4.8 Diagrammatic representation of cation association with 'outer' three oxygen atoms of the crown ether ring.

The reason for this is that the two oxygen atoms directly bonded to the bipyridine unit are convergent and therefore coordination of these oxygens would involve the twisting of the crown ether ring as a whole unit. This is unlikely to occur due to the direct connection between the crown ether ring and the bipyridine unit.[87]

This type of behaviour has been observed for similar crown ether systems where this type of pendant crown ether present within a ditopic ligand has been crystallographically shown to coordinate s-block metal ions both with and without transition metals coordinated to the pyridyl ligands.[88,109]

4.5 Results & Discussion: Section 2; Anion binders based on 3,3′-diamino-2,2′-bipyridine

4.6 Synthesis of ligand L^{12}

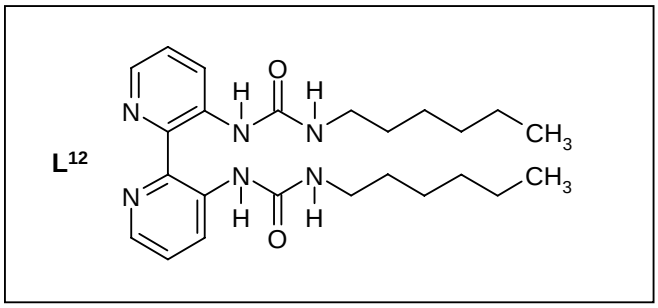

Figure 4.9 Diagrammatical representation of Ligand L^{12}

This ligand was easily synthesised; by refluxing excess RNCO with 3,3′-diamino-2,2′-bipyridine in DCM. Cooling and concentration of the solution gave the pure ligand as pale beige solid. The ^{1}H NMR showed the expected peaks but interestingly one of the amine signals was observed at low field, (11 ppm) indicative of the hydrogen bonding between this proton and the pyridine nitrogen. This type of hydrogen bonding and the presence of a signal at low field is observed when bipyridine contain protons capable of hydrogen bonding in the 3,3′-position.

4.7 Synthesis of Complex X

The complex was synthesised by reaction of the ligand L^{12} with $(bipy)_2RuCl_2$ in refluxing EtOH in the presence of $AgNO_3$. Interestingly without activation of amide groups by $AgNO_3$ the complex could only be isolated in poor yields even after prolonged reaction times. Solvent once evaporated left the product residue, which was purified using column chromatography with a "Maji Mix" solvent system. Extraction with sodium hexafluorophosphate ($NaPF_6$) gave the complex as the PF_6 salt, a deep red/orange fine powder.

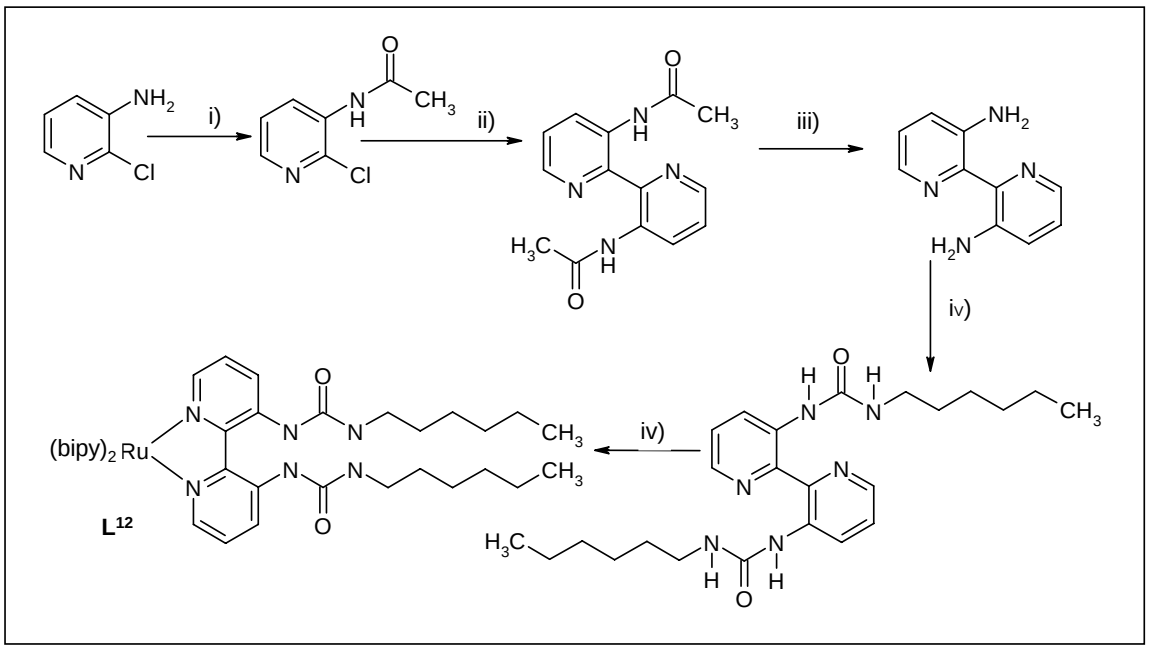

Synthesis scheme 4.2, Synthesis of $(bipy)_2$ruthenium(II)-2,2′-bipyridine-3,3′-di-urea pendant arm. Reagents and conditions; i) Acetic anhydride; ii)Cu/DMF; iii)HCl ; iv) *N*-pentyl-isocyanate/DCM; v) $(bipy)_3RuCl_2$/EtOH

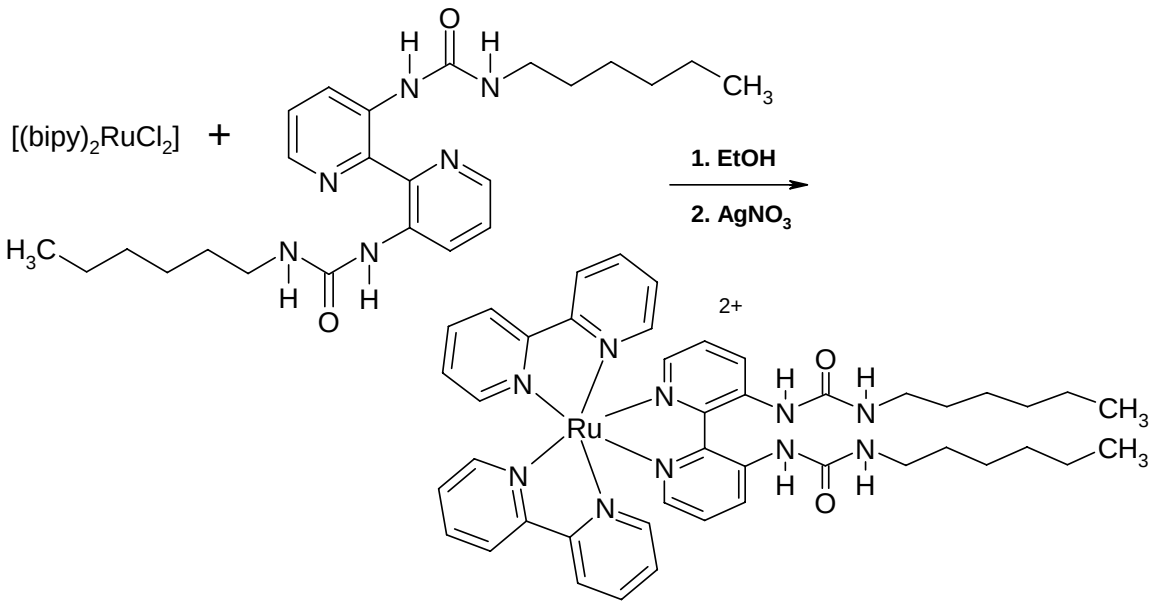

Figure 4.10 Synthesis of Complex X with the use of silver nitrate

4.8 Stability of Complex X

It was noted that the colour of the complex changed over a period of time in nitromethane (MeCN) solution. Monitoring the ^{1}H NMR showed that the complex had decomposed. *Figure 4.11* ^{1}H NMR run initially T0, three days, T3 and after ten days, T10 days.

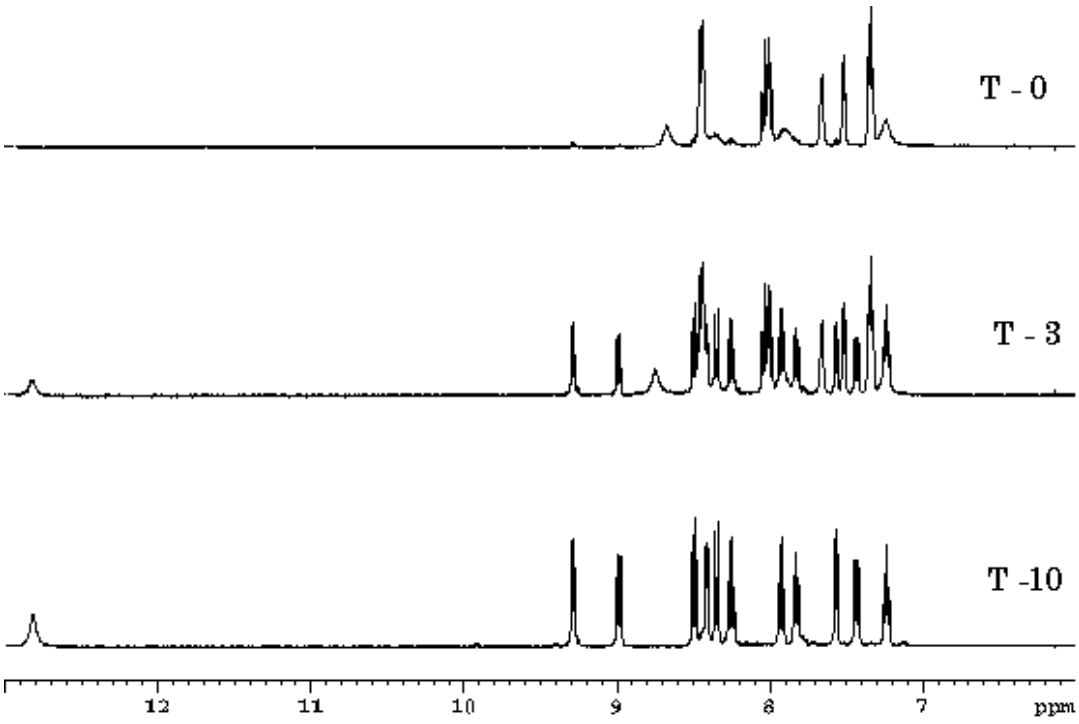

As can be seen over a period of three days the spectra becomes more complex and after 10 days no further change is observed. Comparison of the ^{1}H NMR spectra with the free ligand (Ligand L^{12}) shows that the urea ligand is no longer coordinated to the metal ion and the complex has decomposed to $[(bipy)_2Ru(NCMe)_2]^{2+}$ and free ligand. This is supported by the mass spectrometry studies run alongside that shows an ion corresponding to $[(bipy)_2Ru(NCMe)_2]^{2+}$.

4.9 Luminescence Studies

Complex X is a highly luminescent species and it was envisaged that this property would be modulated upon interaction with anions. This ruthenium complex contains two pendant urea-type functional groups and it is well documented that these form strong interactions with anionic species. Thus experiments were carried out to see if addition of anion(s) to complex X would perturb the luminescence properties.
Figure 4.12 below shows the emission spectrum of the complex X

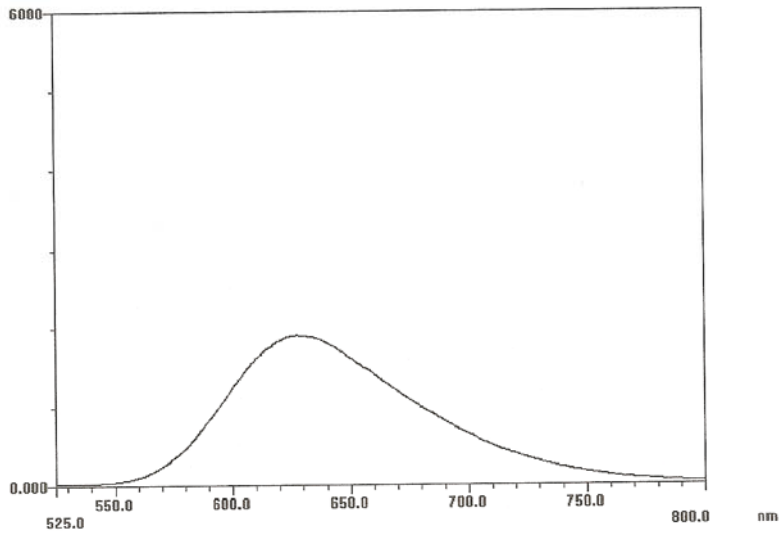

Figure 4.12 Emission spectrum of complex X

Anions F^-,OH^-, Br^-, NO_3^{2-}, AcOH, PO_4^{2-} were chosen and examined for their ability to perturb the luminescence spectra of complex X. The complex was titrated with each anion and the luminescence intensity was recorded relative to the intensity of the complex alone.

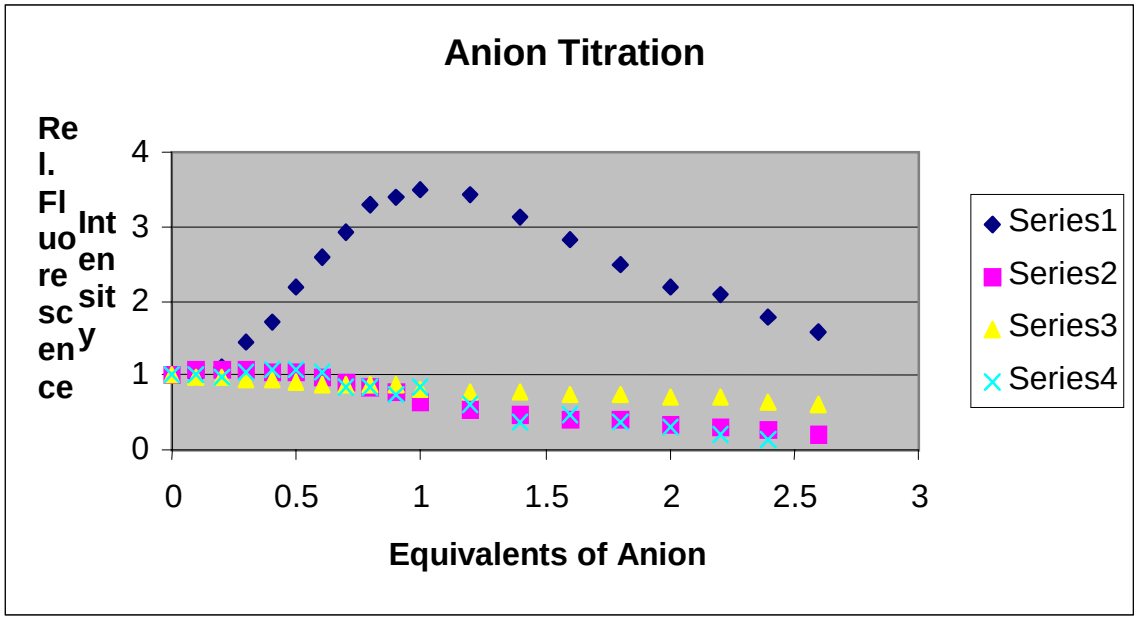

Figure 4.13 shows an overall collation of the titration of complex X with many of the anions. Here it is clearly shown that the $H_2PO_4^-$ anion has a greater affect on the behaviour of complex X and the perturbation of its luminescent properties.

As can be observed, $H_2PO_4^-$ showed the greatest effect upon the complex response compared to the other anion(s). This indicates that the addition of anions and in particular phosphate does indeed have an effect upon the luminescence properties of the complex.

However, close examination of the titration graphs shows that this effect is not quite as simple as was hoped. To look at this complication we investigated the titration graph of the complex with $H_2PO_4^-$.

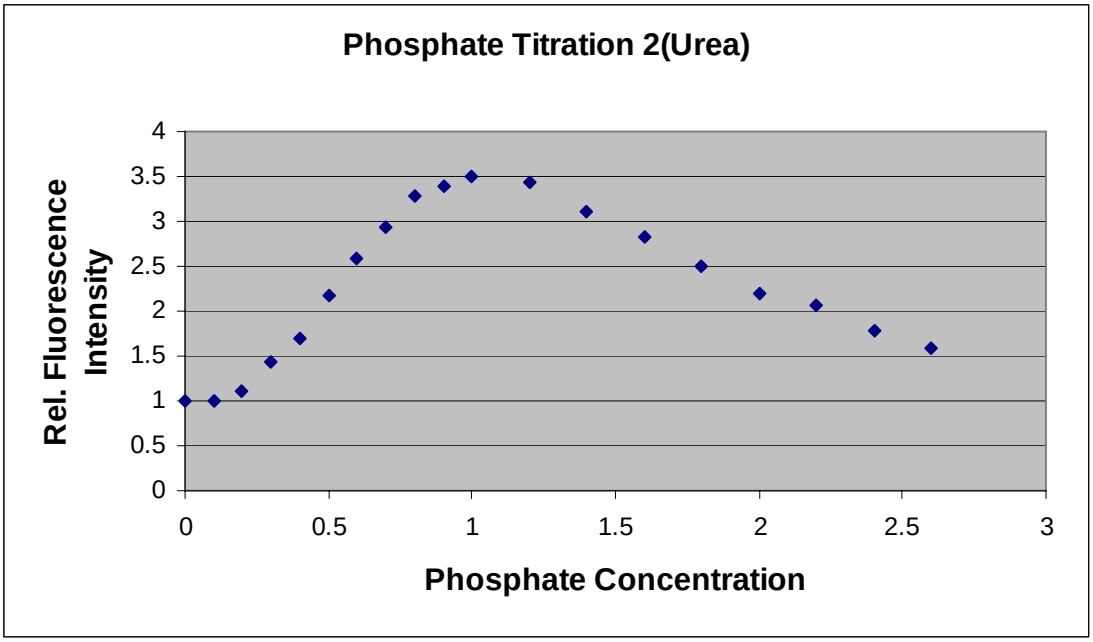

Figure 4.14 Titration of complex X with the phosphate anion.

A marked increase in the relative intensity of luminescence is shown after each addition of phosphate anion, *Figure 4.14*. In this experiment the change in luminescence is observed upon the addition of 0 and 1 equivalent molecule of phosphate anion. It is as expected and the luminescence intensity increases 3-fold however, after this the overall intensity tales off until after 2.5 equivalents of anion has been added, where the intensity has returned to an intensity approaching that of the unbound complex. In fact when we look closely at all the anion titrations that have been performed, even if the luminescence does not increase upon anion addition the luminescence intensity still tails off. Initially it was thought that this could be due to the formation of higher aggregates as the complex contains two urea groups, so a mixture of [Ru + anion] and [Ru + 2(anion)] can be formed and that perhaps it was possible that the complex [Ru + 2(anion)] increases the luminescence, whereas the former complex decreases the luminescence intensity.

In response to the above results a 'reverse' titration was performed, where the initial addition of anion was at high concentration, decreasing the anion concentration with each titration. The result of this titration shows a plateau in the titration where the luminescence is essentially constant.

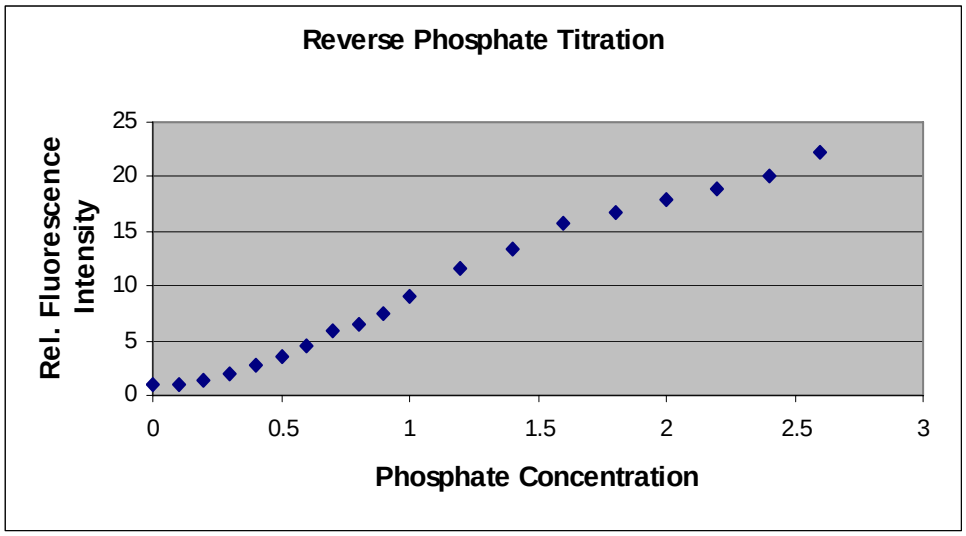

Figure 4.15 'Reverse' titration – phosphate addition to complex X

However, it appears that the actual cause of the decrease is far simpler. A luminescence spectrum of only the complex was obtained at different time intervals (every 10 minutes for 2 hrs). This shows a luminescence decrease of 60% in that period. The decrease in luminescence is probably indicative of decomposition of the complex and the rate of decomposition is unaffected by the anion addition and a similar rate is observed. The ^{1}H NMR and ESI-MS analysis of the complex confirm this over time.

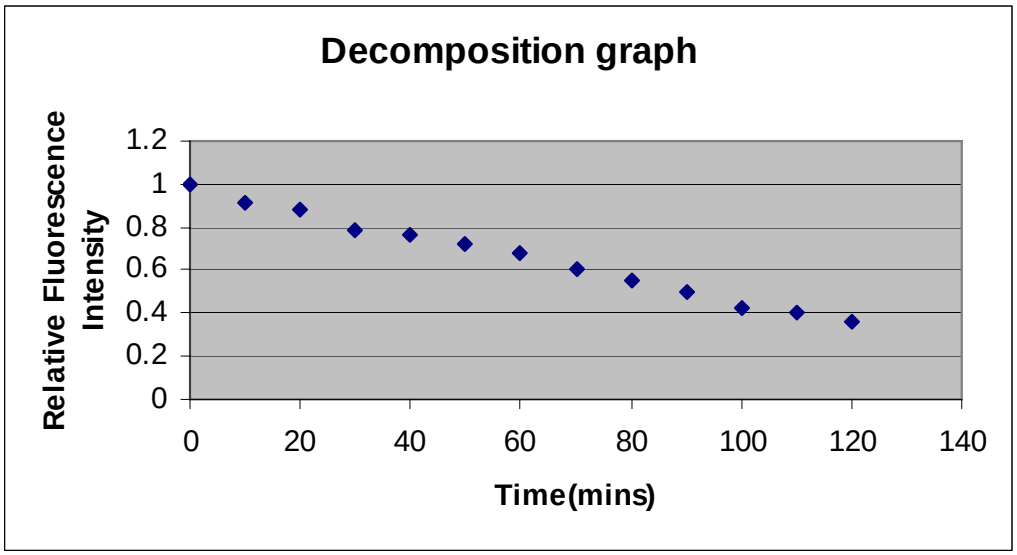

Figure 4.16 Decomposition graph of complex X

The complex X produced was luminescent, however due to the instability of the complex any change in luminescence needs to be interpreted carefully as the concentration of the complex is unknown. *Figure 4.16* shows the spectra recorded indicating the rate of decay of luminescence of the complex over time. None the less addition of NaH_2PO_4 to the complex did show a significant change in the luminescent properties.

4.10 Discussion

The complex shows a clear increase in the luminescence properties upon addition of phosphate anions. This is as expected as it is well known that phosphate anions interact strongly with urea units.

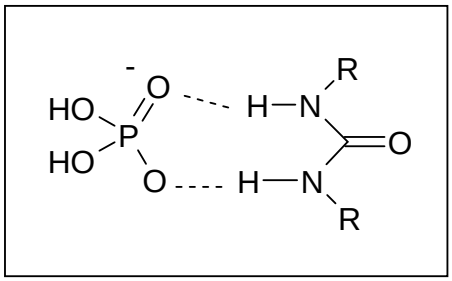

Figure 4.17, diagram of interaction between phosphate anion $H_2PO_4^-$ and urea groups

However, it is clear that from both optical, ^{1}H NMR and UV Vis studies that the complex is decomposing to the free ligand and $[(bipy)_2Ru(NCMe)_2]^{2+}$. The reason for this decomposition is the unfavourable steric interaction between the two urea substituents on the 3,3′- position of the bipyridine unit. Due to the large size of these groups the complex is unstable and decomposes to the starting material. Nevertheless the complex does act as an anion sensor of sorts.

EXPERIMENTAL

5.0 Experimental

5.1 General details

All starting materials and solvents were purchased from Aldrich or Lancaster and used as received. Anhydrous solvents (DMF/THF) were purchased from Aldrich and used as supplied.

The following instruments were used for routine spectroscopic analyses: Bruker DPX400 (^{1}H NMR) and VG Quattro II mass spectrometer with Z-spray source (ESI).

5.2 Terpyridine ligands- pyridyl/ thiazoles

- Synthesis of 6-cyano-2,2′:6′,2″-terpyridine

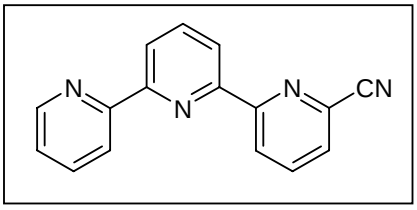

To a stirred solution of 2,2′:6′,2″-terpyridine 1-oxide[30] (0.75 g, 3.0 mmol) and sodium cyanide (0.22 g. 4.5 mmol) in water (15 cm^3) was slowly added a solution of benzyl chloride (0.51 g, 3.6 mmol) in acetone (3 cm^3). During the addition an oily precipitate was formed, the reaction was stirred for a further 35 min, after which time the solid was filtered and washed with water (2 x 2 cm^3). Recrystallisation of the product from MeOH gave 6-cyano-2,2′:6′,2″-terpyridine as a white solid. Yield: 0.38 g, 50%. EI MS: *m/z* (50%, 258 M^+). ^{1}H NMR [400 MHz, $CDCl_3$]: δ (ppm) 8.90 (1H, dd, *J* = 8.1, 1.0 *Hz*), 8.75 (1H, m), 8.60 (1H, m), 8.55 (1H, dd, *J* = 4.3, 1.0 *Hz*), 8.53 (1H, dd, *J* = 4.3, 1.0 *Hz*), 8.03 (1H, dd, *J* = 7.7, 4.3 *Hz*), 8.01 (1H, dd, *J* = 8.1, 4.3 *Hz*), 7.89 (1H, m), 7.75 (1H, dd, *J* = 7.7, 1.0 *Hz*), 7.37 (1H, m). Anal. Found: C, 74.2; H, 3.9; N, 21.6. Calc. For $C_{16}H_{10}N_4$: C, 74.4; H, 3.9; N, 21.7%.

- Synthesis of 2,2′:6′,2″-terpyridine-6-thioamide

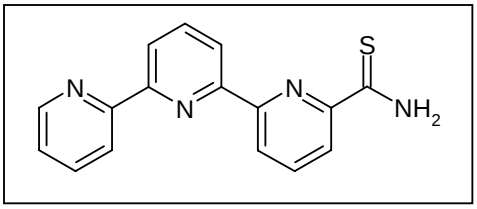

To a suspension of 6-cyano-2,2′:6′,2″-terpyridine (0.8 g, 3.1 mmol) in EtOH (20 cm^3) was added triethylamine (0.1 g, 1.0 mmol). H_2S was slowly bubbled through this solution until the solution turned yellow in colour; the flask was stoppered and left to stand overnight. The solvent was reduced under vacuum to give 2,2′:6′2″-terpyridine-6-thioamide as a light brown solid. Yield: 0.68 g, 86%. Analytically pure samples could be obtained by column chromatography (silica gel, $CHCl_3$-MeOH (9:1)), but the crude material was sufficiently pure for use in subsequent reactions. EI MS: *m/z* (35%, 292 M^+). ^{1}H NMR [400 MHz, $CDCl_3$]: δ (ppm) 9.62 (2H, brs, -NH_2), 8.83 (1H, dd, *J* = 7.9, 1.0 *Hz*), 8.79 (1H, dd, *J* = 7.8, 1.0 *Hz*), 8.72 (1H, m), 8.63 (1H, m), 8.53 (1H, dd, *J* = 7.9, 1.0 *Hz*), 8.43 (1H, dd, *J* = 7.8, 1.0 *Hz*), 8.04 (1H, dd, *J* = 7.9, 7.9 *Hz*), 8.01 (1H, dd, *J* = 7.8, 7.8 *Hz*), 7.89 (1H, m), 7.38 (1H, m). Anal. Found: C, 65.9; H, 3.9; N, 19.5. Calc. For $C_{16}H_{12}N_4S$: C, 65.7; H, 4.1; N, 19.2%.

- Synthesis of 6,6′-dicyano-2,2′:6′,2″-terpyridine

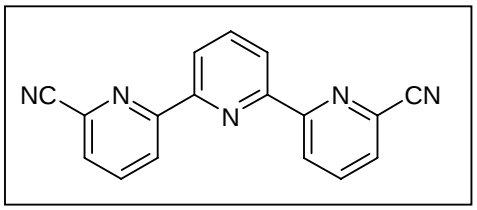

To a solution of 2,2′:6′,2″-terpyridine 1,1′′-dioxide[30] (0.25 g, 0.94 mmol) in dry toluene (30 cm^3) was added trimethylsilyl cyanide (1.0 cm^3, 7.5 mmol) and triethylamine (1.0 cm^3, 7.2 mmol). The solution was refluxed for 8 h after which time a further amount of trimethylsilyl cyanide (1.0 cm^3, 7.5 mmol) and triethylamine (1 cm^3, 7.2 mmol) was added and the solution refluxed for a further 16 hrs. The reaction was then cooled, extracted with $NaHCO_3$ (aq) (2 x 20 cm^3), dried ($MgSO_4$), filtered and evaporated. Purification by column chromatography on silica gel, utilising a

$CHCl_3$-MeOH (9:1) solvent system gave 6,6″-dicyano-2,2′:6′,2″-terpyridine as a white solid. Yield: 0.19 g, 57%. EI MS: *m/z* (20%, 283 M^+). ^{1}H NMR [400 MHz, $CDCl_3$]: δ (ppm) 8.84 (2H, dd, *J* = 7.8, 1.0 *Hz*), 8.60 (2H, d, *J* = 7.8 *Hz*), 8.07 (1H, t, *J* = 7.8 *Hz*), 8.03 (2H, dd, *J* = 7.8, 7.8 *Hz*), 7.77 (2H, *J* = 7.8, 1.0 *Hz*). Anal. Found: C, 72.1; H, 3.6; N, 24.5. Calc. For $C_{17}H_9N_5$: C, 72.1; H, 3.2; N, 24.7%.

- Synthesis of 2,2′:6′,2″-terpyridine-6,6′-dithioamide

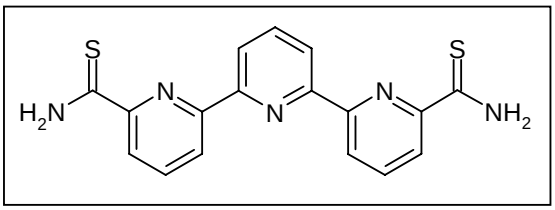

To a suspension of 6,6″-dicyano-2,2′:6′,2″-terpyridine (0.12 g, 0.36 mmol) in EtOH (20 cm^3) was added triethylamine (0.1 g, 1.0 mmol). H_2S was bubbled through for 15 minutes, during which time a pale yellow precipitate forms. Filtration and washing with Et_2O (2 x 1 cm^3) gave 2,2′:6′,2″-terpyridine-6,6″-dithioamide as a yellow solid. Yield: 0.11 g, 89%. EI MS: *m/z* (11%, 351 M^+). ^{1}H NMR [400 MHz, $CDCl_3$]: δ (ppm) 10.30 (1H, s, NH), 10.24 (1H, s, NH), 8.95 (2H, d, *J* = 7.9 *Hz*), 8.86 (2H, d, *J* = 7.5, 1.0 *Hz*), 8.63 (2H, dd, *J* = 1.0 *Hz*), 8.18 (2H, dd, *J* = 7.5, 7.5 *Hz*), 8.14 (1H, t, *J* = 7.9 *Hz*). Anal. Found: C, 58.3; H, 3.9; N, 19.5, Calc. For $C_{17}H_{13}N_5S_2$: C,58.1; H, 3.7; N, 19.9%.

- Synthesis of 1-(2-pyridin-2-yl-1,3-thiazol-4-yl)ethanone

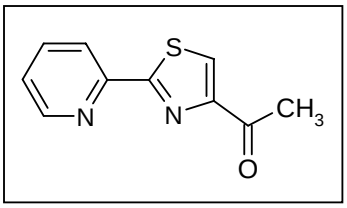

A solution of freshly prepared 1-bromo-2,3-butane-dione (2.6 g, 15.8 mmol) in EtOH (25 cm^3) was slowly added to a solution of pyridine-2-thioamide (2.1 g, 15.2 mmol) in EtOH (50 cm^3), the solution was then refluxed for 4 hrs. After this time the reaction was cooled and concentrated to approximately 20 cm^3, during which time a brown precipitate was formed. Filtration and recrystallisation from H_2O gave 1-(2′-(pyrid-2-

yl)thiazol-4′-yl)ethanone as the HBr salt. Yield 3.25 g, 75%. The salt (3.0 g, 10.5 mmol) was then suspended in H_2O (10 cm^3) and $NaHCO_3$ (aq) added until neutral, the solid was then filtered and washed with water (2 x 2 cm^3). After drying the solid was recrystallised from n-hexane to give 1-(2-pyridin-2-yl-1,3-thiazol-4-yl)ethanone as a cream solid. Yield: 1.72 g, 80%. EI MS: *m/z* (75%, 204 M^+). ^{1}H NMR [400 MHz, $CDCl_3$]: δ (ppm) 8.66 (1H, m, py), 8.29 (1H, m, py), 8.24 (1H, s, tz), 7.85 (1H, m, py), 7.40 (1H, m, py), 2.76 (1H, s, $-CH_3$). Anal. Found: C, 58.9; H, 3.9; N, 13.6, Calc. For $C_{10}H_8N_2OS$: C, 58.8; H, 3.9; N, 13.7%.

- Synthesis of 2-bromo-1-(2-pyridin-2-yl-1,3-thiazol-4-yl-ethanone)

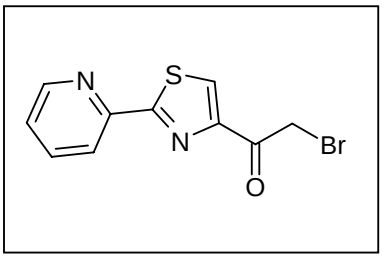

A solution of bromine (0.78 g, 4.9 mmol) in CCl_4 (25 cm^3) was slowly added to a refluxing solution of 1-(2-pyridin-2-yl-1,3-thiazol-4-yl)ethanone (1.0 g, 4.9 mmol) in CCl_4 (50 cm^3) over a period of 1 hr, during which time an orange/yellow precipitate formed. After refluxing for a further hour the solution was cooled and the solid collected by filtration and washed with CCl_4 (2 x 5 cm^3) and Et_2O (2 x 5 cm^3) to give 2-bromo-1-(2-pyridin-2-yl-1,3-thiazol-4-yl)ethanone as the HBr salt. Yield: 1.16 g, 65%. EI MS: *m/z* (60%, 283 M^+). ^{1}H NMR [400 MHz, $CDCl_3$]: δ (ppm) 8.81 (1H, s, tz), 8.68 (1H, m, py), 8.22 (1H, m, py), 8.05 (1H, m, py), 7.57 (1H, m, py), 4.95 (2H, s, $-CH_2Br$).

The crude product was often contaminated with varying amounts of 1-(2′-pyrid-2-yl)thiazol-4′-yl)ethanone·HBr, but was used in the following reaction without purification and without any detrimental effects.

- **Synthesis of L^1-L^3**
- L^1

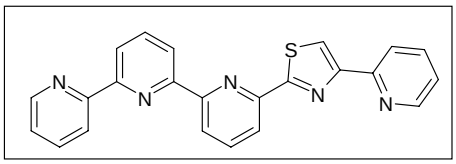

2-(α-Bromoacetyl)-pyridinium hydrobromide (0.38 g, 1.4 mmol) was added to a solution of 2,2′:6′,2″-terpyridine-6-thioamide (0.2 g, 0.7 mmol) in EtOH (50 cm^3) and the solution was refluxed for 4 hrs. After this time the resulting pale yellow precipitate was filtered, washed with EtOH (2 x 2 cm^3) and Et_2O (2 x 3 cm^3) and dried *in vacuo* to give L^1·2HBr. This was then suspended in ammonia (0.88 S.G., 25 cm^3) and left to stand for 12 hrs. Filtration and washing with EtOH (2 x 2 cm^3) and Et_2O (2 x 2 cm^3) gave the free ligand L^1 as a pale yellow solid. Yield: 0.21 g, 78%. EI MS: *m/z* (5%. 393 M^+). ^{1}H NMR [400 MHz, $CDCl_3$]: δ (ppm) 8.84 (1H, dd, *J* = 7.9, 1.0 *Hz*), 8.82 (1H, m, py), 8.75 (2H, m, overlapping), 8.68 (1H,s, tz), 8.60 (1H, dd, *J* = 7.9, 7.9 *Hz*), 8.27 (1H, dd, *J* = 7.9, 7.9 *Hz*), 8.21 (1H, m), 8.19 (1H, m), 7.69 (1H, m), 7.60 (1H, m). Anal, Found: C, 69.0; H, 3.9; N, 17.7. Calc. for $C_{23}H_{15}N_5S$: C, 70.2; H, 3.8; N, 17.8%.

- L^2

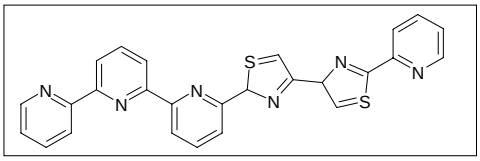

2-Bromo-1-(2′-(pyrid-2-yl)thiazol-4′-yl)ethanone·HBr (0.52 g, 0.014 mmol) was added to a solution of 2,2′:6′,2″-terpyridine-6-thioamide (0.21 g, 0.7 mmol) in EtOH (50 cm^3) and the solution refluxed for 4 hrs. After this time the resulting pale yellow precipitate was filtered, washed with EtOH (2 x 2 cm^3) and Et_2O (2 x 3 cm^3) and dried *in vacuo* to give L^2·2HBr. This was then suspended in ammonia (0.88 S.G., 25 cm^3) and left to stand for 12 hrs. Filtration and washing with EtOH (2 x 2 cm^3) and Et_2O (2 x 3 cm^3) gave the free ligand L^2 as a yellow solid. Yield: 0.27 g, 79%. EI MS: *m/z* (7%, 476 M^+). ^{1}H NMR [400 MHz, $CDCl_3$]: δ (ppm) 8.80 (2H, m, overlapping), 8.59 (1H, dd, *J* = 8.0, 1.0 *Hz*), 8.54 (1H, dd, *J* = 8.0, 1.0 *Hz*, 8.4-8.2 (6H, m, overlapping),

8.15 (1H, m), 8.05 (1H, m) 7.60 (1H, m), 7.55 (1H, m). Anal. Found: C,65.9; H, 3.0; N, 17.4. Calc. for $C_{26}H_{16}N_6S_2$: C,65,5; H, 3.4; N, 17.6%.

- L^3

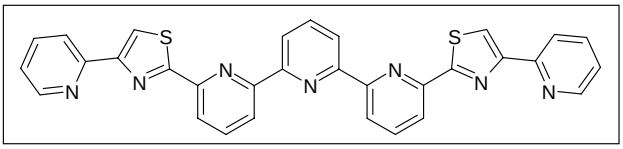

2-(α-Bromoacetyl)-pyridinium hydrobromide (0.32 g, 1.1 mmol) was added to a solution of 2,2′:6′,2″-terpyridine-6,6″-dithioamide (0.10 g, 0.28 mmol) in EtOH (50 cm^3) and the solution refluxed for 4 hrs. After this time the resulting pale yellow precipitate was filtered, washed with EtOH (2 x 2 cm^3) and Et_2O (2 x 3 cm^3) and dried *in vacuo* to give $L^3 \cdot 2HBr$. This was then suspended in ammonia (0.88 S.G., 25 cm^3) and left to stand for 12 hrs. Filtration and washing with EtOH (2 x 2 cm^3) and Et_2O (2 x 2 cm^3) gave the free ligand L^3 as a pale yellow solid. Yield: 0.13 g, 82%. EI MS: *m/z* (7%, 553 M^+). ^1H NMR [400 MHz, $CDCl_3$]: δ (ppm) 8.76 (2H, dd, *J* = 7.9, 1.0 *Hz*), 8.70 (2H, m, py), 8.60 (2H, d, *J* = 7.9 *Hz*), 8.44 (2H, s, tz), 8.38 (2H, dd, *J* = 7.8, 1.0 *Hz*), 8.3-8.2 (5H, m, overlapping), 7.98 (2H, m, py), 7.41 (2H, m, py). Anal. Found: C, 67.5; H, 3.9; N, 17.5. Calc. for $C_{31}H_{19}N_7S_2$: C, 67.2; H, 3.5; N, 17.7%.

Metal Complexes

- $[Cu_2(L^1)][ClO_4]_2$

To a suspension of L^1 (0.010 g, 0.025mmol) in $MeNO_2$ (2.0 cm^3) was added $Cu(ClO_4)_2 \cdot 6H_2O$ (0.009 g, 0.025mmol). The subsequent suspension was immersed in an ultrasound-cleaning bath for 10 minutes resulting in a clear green solution. Filtration followed by slow diffusion of ethyl acetate into the solution gave $[Cu_2(L^1)][ClO_4]_2$ as large green crystals, which were filtered off and dried under vacuum (0.009 g, 54%). EI MS *m/z*: 521 $[Cu_2(L^1)_2]^{4+}$. Anal. Found: C, 41.9; H, 2.5; N, 10.8. Calc. for $C_{46}H_{30}N_{10}S_2Cu_2Cl_4O_{16}$: C, 42; H, 2.3; N, 10.7%.

- $[Ni(L^2)][ClO_4]_2$

To a suspension of L^2 (0.010 g, 0.021mmol) in $MeNO_2$ (2.0 cm^3) was added $Ni(ClO_4)_2 \cdot 6H_2O$ (0.008 g, 0.022mmol). The subsequent suspension was immersed in an ultrasound-cleaning bath for 10 minutes resulting in a colourless solution. Filtration followed by slow diffusion of ethyl acetate into the solution gave $[Ni(L^2)][ClO_4]_2$ as large colourless crystals, which were filtered off and dried under vacuum (0.008 g, 50%). EI MS *m/z*: 1368 $[Ni_2(L^2)_2(ClO_4)_3]^+$. Anal. Found: C, 41.0; H, 2.1; N, 12.4. Calc. for $C_{52}H_{32}N_{12}S_4Ni_2Cl_4O_{16} \cdot 2CH_3NO_2$: C, 40.8; H, 2.4; N, 12.3%.

- $[Co(L^2)][ClO_4]_2$

To a suspension of L^2 (0.010 g, 0.021mmol) in $MeNO_2$ (2.0 cm^3) was added $Co(ClO_4)_2 \cdot 6H_2O$ (0.008 g, 0.022mmol). The subsequent suspension was immersed in an ultrasound cleaning bath for 10 minutes resulting in a colourless solution. Filtration followed by slow diffusion of ethyl acetate into the solution gave $[Co(L^2)][ClO_4]_2$ as large orange crystals, which were filtered off and dried under vacuum (0.010 g, 62%) EI MS *m/z*: 1368 $[Co_2(L^2)_2(ClO_4)_3]^+ M^+$. Anal. Found: C, 41.3; H, 2.2; N, 11.5; Calc. for $C_{52}H_{32}N_{12}S_4Co_2Cl_4O_{16} \cdot CH_3NO_2$: C, 41.6; H, 2.3; N, 11.9%.

- $[Cd_3(L^3)_2][ClO_4]_6$

To a suspension of L^3 (0.010 g, 0.025mmol) in $MeNO_2$ (2.0 cm^3) was added $Cd(ClO_4)_2 \cdot 6H_2O$ (0.016 g, 0.037mmol). The subsequent suspension was immersed in an ultrasound-cleaning bath for 10 minutes resulting in a colourless solution. Filtration followed by slow diffusion of ethyl acetate into the solution gave $[Cd_3(L^3)_2][ClO_4]_6$ as colourless crystals, which were isolated via filtration and dried (0.003 g, mmol). EI MS *m/z*: (Did not show the molecular ion, but the fragment $[Cd_2(L^3)_2][ClO_4]_3^+$. ^1H NMR [400 MHz, CD_3NO_2] : δ (ppm) 8.50 (3H, m, overlapping), 8.48 (2H, d, J = 7.2 *Hz*), 8.32 (2H, dd, J = 7.9, 7.9 *Hz*), 8.25 (2H, d, J = 7.9 *Hz*), 8.00 (2H, m, py), 7.95 (2H, s, tz), 7.92 (2H, m, py), 7.51 (2H, d, J = 7.9 *Hz*), 7.38 (2H, m, py). Anal. Found: C, 35.3; H, 2.1; N, 9.6. Calc. for $C_{62}H_{38}N_{14}S_4Cd_3Cl_6O_{24} \cdot CH_3NO_2 \cdot H_2O$: C, 35.7; H, 2.0; N, 9.9%.

5.3. 3,3′-disubstituted-2,2′-bipyridine

- Synthesis of 3-acetylamino-2-chloropyridine

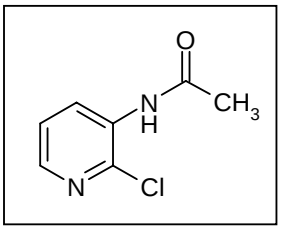

A solution of 3-amino-2-chloropyridine (5.0 g, 38 mmol) in acetic anhydride (25 cm^3) was stirred until dissolved, stoppered and left to stand overnight. The acetic anhydride was evaporated *in vacuo* to give 3-acetylamino-2-chloropyridine as a pink crystalline solid. Yield 4.8 g, 73%. ^{1}H NMR [400 MHz, $CDCl_3$] : δ (ppm) 8.68 (1H, d, J = 9.26 Hz), 8.1 (1H, d, J =6.28 , Hz), 7.65 (1H, br, NH), 7.23 (1H, dd, J =4.68, 4.61 Hz), 2.20 (3H, s, (NHCO**CH_3**)).

- Synthesis of 3,3′-acetylamino-2,2′-bipyridine

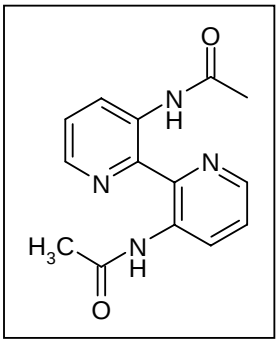

A solution of 3-acetylamino-2-chloropyridine (6.0 g, 35 mmol) and copper powder (6.0 g, 94 mmol) in DMF (40 cm^3) was heated at 80˚C for 12 hrs. When cooled the solvent was evaporated, and the residue was suspended in H_2O (aq) and filtered through celite. Ammonia (0.88 S.G. 300 cm^3) is passed through the celite bed leaving the product as a white solid. The product was extracted with DCM (2 x 20 cm^3), dried ($MgSO_4$), filtered and evaporated giving the product 3,3′-diacetylamino-2,2′-bipyridine as a white solid. Yield 1.0 g, 13%. ^{1}H NMR [400 MHz, $CDCl_3$] : δ (ppm) 13.10 (2H, s, NH), 9.15 (2H, d, J = 9.89, *Hz*), 8.35 (2H, d, J = 6.06 *Hz*), 7.38 (2H, dd, J = 4.57, 4.48 *Hz*), 2.19 (6H, s, CH_3).

- Synthesis of 3,3′-diamino-2,2′-bipyridine

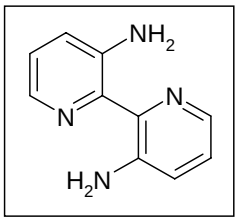

To a stirred solution of 3,3′-diacetylamino-2,2′-bipridine (0.73 g, 2.7 mmol) in water (10 cm^3) HCl was added, at which point the material becomes fully dissolved and the solution is then refluxed for 2 hrs. Once cooled the solution is neutralised with the addition of ammonia (0.88 S.G.). The precipitate formed is then filtered and dried *in vacuo*. The product, 3,3′-diamino-2,2′-bipyridine was isolated as a bright yellow solid. Yield 0.26 g, 52%. ^{1}H NMR [400 MHz, $CDCl_3$] : δ (ppm) 8.0 (4H, overlapping, m), 6.30 (4H, s, NH_2), 7.05 (2H, d, J = 8.4 *Hz*).

- Synthesis of 3,3′-diacetylamino-2,2′-bipyridine-bis-*N*-oxide

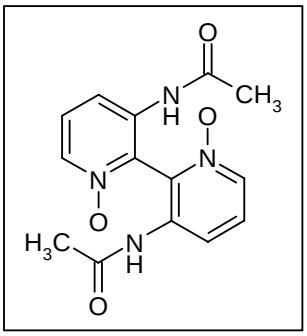

To a solution of 3,3′-diacetylamino-2,2′-bipyridine (3.8 g, 14 mmol) in chloroform (20 cm^3) was added a solution of *m*-CPBA (3-chloro-peroxybenzoic acid, 0.86 g, 5.0mmol) in chloroform (20 cm^3). The solution was stirred at room temperature for 12 hrs, whilst being monitored via TLC and where the product is identified as a bright blue luminescent spot. The solution is cooled (-4˚C), and excess *m*-CPBA is precipitated and filtered off. Concentration of the solvent and purification via column chromatography on silica (CH_2Cl_2 – MeOH) (9:1) ratio gives the product, 3,3′-diacetylamino-2,2′-bipyridine-bis-*N*-oxide as a white solid. Yield 2.1 g, 49%. ^{1}H

NMR [400 MHz, $CDCl_3$]: δ (ppm) 9.48 (2H, s, NH), 8.15 (2H, d, J = 6.39 *Hz*), 7.67 (2H, d, J = 8.43 *Hz*), 7.45 (2H, dd, J = 6.48, 6.40 *Hz*), 2.08 (3H, s, O**C**$\mathbf{H_3}$).

- Synthesis of 6,6′-dicyano-3,3′-diacetylamino-2,2′-bipyridine

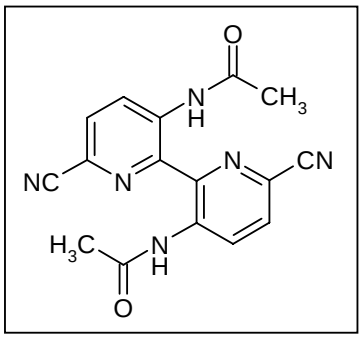

Under an inert atmosphere (N_2) is placed 3,3′-diacetylamino-2,2′-bipyridine-bis-*N*-oxide (0.19 g, 0.6 mmol) and dimethyl sulfate (5 cm^3). The solution is stirred at 50˚C overnight. Ethyl acetate (10 cm^3) is added to the solution this is allowed to settle and the ethyl acetate decanted. Ether (10 cm^3) is then added to the solution and upon settling is decanted. Water (10 cm^3) is then added and the solution is neutralised ($NaHCO_3$). A solution of sodium cyanide (0.12 g, 2.5mmol) in water (3 cm^3) is added and stirred continuously. A precipitate was formed, which is collected via filtration and dried *in vacuo* to give 6,6′-dicyano-3,3′-diacetylamino-2,2′-bipyridine as a pale cream solid. Yield 0.09 g, 45%. ^{1}H NMR [400 MHz, DMSO]: δ (ppm) 10.2 (2H, s, NH), 8.68 (2H, d, J = 8.61 *Hz*), 8.08 (2H, d, J = 8.6 *Hz*), 2.08 (6H, s, CH_3).

- Synthesis of 3,3′-diacetylamino-2,2′-bipyridine-6,6′-dithioamide.

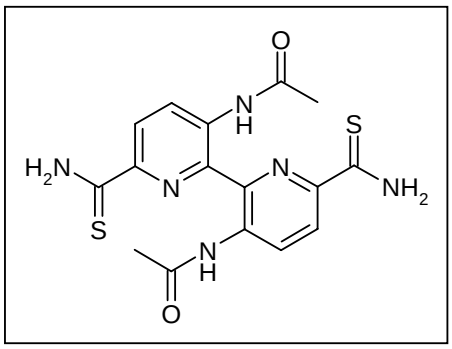

To a solution of 6,6′-dicyano-3,3′-diacetylamide-2,2′-bipyridine (0.2 g, 0.66 mmol) in ethanol (25 cm^3) H_2S gas is bubbled through until the solution colour changes to a yellow colour. The reaction is stoppered and left to stand overnight. The formed precipitate was filtered to give 3,3′-diacetylamino-2,2′-bipyridine-6,6′-dithioamide as a bright yellow solid. Yield 0.22 g, 88%. ^{1}H NMR [400 MHz, DMSO]: δ (ppm) 10.48 (2H, s, NH), 10.15 (2H, s, NH_2), 9.75 (2H, s, NH_2), 8.68 (2H, d, J = 8.77 *Hz*), 8.47 (2H, d, J = 8.68 *Hz*), 2.0 (6H, s, CH_3).

- Synthesis of 3-methoxy-2-iodopyridine

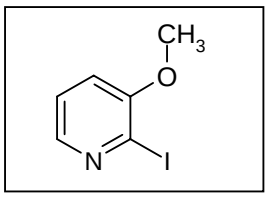

Under an inert atmosphere (N_2) a solution of 3-hydroxy-2-iodopyridine (6.0 g, 27 mmol) and sodium hydride (1.19 g, 50 mmol) in a 50:50 ratio of DMF/THF (2 x 20 cm^3) was stirred at room temperature. To this solution iodomethane (2.0 cm^3, 33mmol) was added and the reaction stirred for a further 4 hrs. After this time a precipitate has formed. Methanol was added to destroy excess NaH and the precipitate filtered *in vacuo* to dryness. The filtrate was extracted with Et_2O and $NaHCO_3$ (aq), the organic fractions collected and evaporated to give the product, 3-methoxy-2-iodopyridine as a pale yellow solid. Yield 5.2 g, 82%. ^{1}H NMR [400 MHz, $CDCl_3$]: δ (ppm) 8.05 (1H, d, J = 6.02 *Hz*), 7.23 (1H, dd, J = 4.58, 4.56 *Hz*), 7.05 (1H, dd, J = 9.56 *Hz*), 3.9 (3H, s, CH_3).

- Synthesis of 3,3-dimethoxy-2,2′-bipyridine

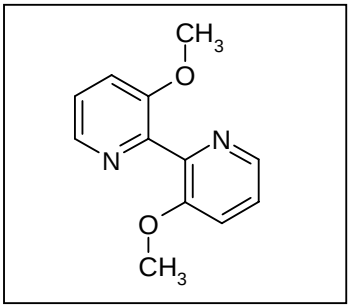

Under an inert atmosphere (N_2) a flask is charged with $NiCl_2(PPh_3)_2$ (1.38 g, 2.1 mmol), $[Et_4N]I$ (5.43 g, 21 mmol) and zinc powder (2.04 g, 31 mmol) in THF (20 cm^3) and the reaction stirred at room temperature for 45 minutes. To this solution was added 3-methoxy-2-iodopyridine (4.96 g, 21 mmol) and the solution refluxed at 70˚C for 12 hrs. Once cool the solvent is evaporated *in vacuo* and ammonia added and the solution is then stirred for an hour. This solution was then extracted using DCM (3 x 75 cm^3), dried ($MgSO_4$) and filtered to give product 3,3-dimethoxy-2,2′-bipyridine as a pale yellow solid. Yield 1.09 g, 24%. ^{1}H NMR [400 MHz, $CDCl_3$]: δ (ppm) 8.35 (2H, dd, J = 2.41, 1.11 *Hz*), 7.34 (4H, m, 2 signals overlapping), 3.8 (6H, s, CH_3).

- Synthesis of 3,3′-dimethoxy-2,2′-bipyridine-bis-*N*-oxide

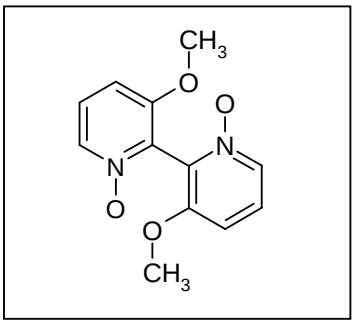

To a solution of 3,3′-dimethoxy-2,2′-bipyridine (0.23 g, 1.1 mmol) in glacial acetic acid (25 cm^3) was added hydrogen peroxide (4.5 cm^3). The solution was stirred at 80˚C for 7 hrs, after which time the acetic acid was reduced to half its original volume. Water (10 cm^3) added and the volume reduced once again. The remaining solution was then neutralised $NaHCO_3$ (aq) and extracted with DCM (2 x 25 cm^3). The organic fractions were collected, dried ($MgSO_4$), filtered and evaporated to dryness. The product 3,3′-dimethoxy-2,2′-bipyridine-bis-*N*-oxide was isolated as a white solid. Yield 0.23 g, 88%. ^1H NMR [400 MHz, $CDCl_3$]: δ (ppm) 8.05 (2H, d, J = 6.44 *Hz*), 7.30 (2H, m, signal overlapping with solvent), 6.94 (2H, d, J = 8.49 *Hz*), 3.80 (6H, s, CH_3).

- Synthesis of 6,6′-dicyano-3,3′-dimethoxy-2,2′-bipyridine

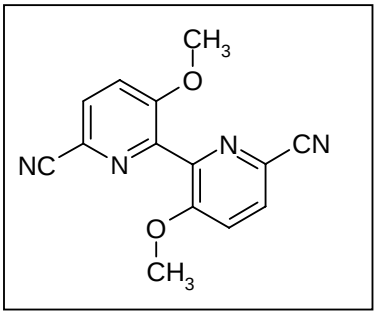

A solution of 3,3′-dimethoxy-2,2′-bipyridine-bis-*N*-oxide (0.23 g, 0.9 mmol) in dimethyl sulfate (5 cm^3) was stirred at 80˚C overnight. Once cool, Et_2O (10 cm^3) was added to the solution, allowed to settle and then carefully decanted. Water (10 cm^3) is added to the resulting oily residue, then neutralised with $NaHCO_3$ (aq). To this a solution of sodium cyanide (0.13 g, 2.6 mmol) in water (5 cm^3) was added and stirred

vigorously. A precipitate forms, which is extracted with DCM (2 x 20 cm^3), dried ($MgSO_4$) filtered and evaporated to give 6,6′-dicyano-3,3′-dimethoxy-2,2′-bipyridine as a pale cream solid. Yield 0.18 g, 72%. ^1H NMR [400 MHz, $CDCl_3$] : δ (ppm) 7.8 (2H, d, J = 8.56 *Hz*), 7.4 (2H, d, J = 8.62 *Hz*), 3.8 (6H, s, CH_3).

- Synthesis of 3,3′-dimethoxy-2,2′-bipyridine-6,6′-dithioamide

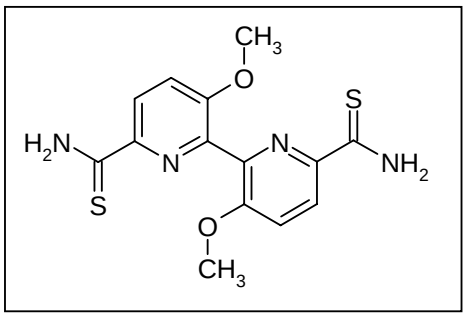

To a solution of 6,6′-dicyano-3,3′-dimethoxy-2,2′-bipyridine (0.15 g, 0.6mmol) in EtOH (35 cm^3) with triethylamine (0.1 g, 0.1mmol) H_2S gas was bubbled through for 15 minutes or until the solution colour turned yellow. The solution was stoppered and left to stand overnight. A precipitate is formed and isolated via filtration *in vacuo* to give 3,3′-dimethoxy-2,2′-bipyridine-6,6′-dithioamide as a bright yellow solid. Yield 0.19 g, 95%. ^1H NMR [400 MHz, $CDCl_3$]: δ (ppm) 9.25 (2H, s, NH_2), 8.8 (2H, d, J = 8.80 *Hz*), 7.48 (2H, s, NH_2), 7.37 (2H, d, J = 8.80 *Hz*), 3.80 (6H, s, CH_3).

- **Synthesis of $L^4 – L^7$**
- Synthesis of L^4

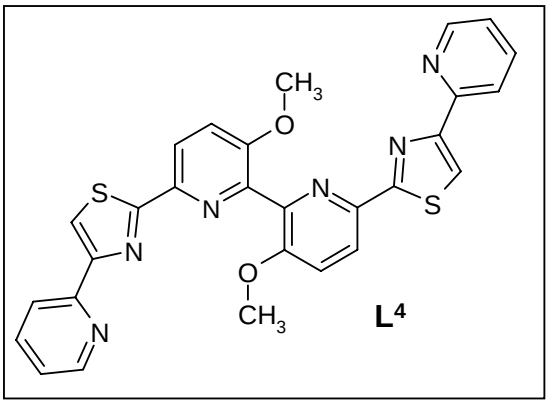

L^4

To a solution of 3,3′-dimethoxy-2,2′-bipyridine-6,6′-dithioamide (0.18 g, 0.5 mmol) in EtOH (35 cm^3) was added α-bromo acetyl pyridine (0.43 g, 2.2 mmol) and the solution was refluxed for 4 hrs. After this time a precipitate forms, which is collected via filtration to give L^4 as a pale yellow solid. Yield 0.22 g, 71%. ^{1}H NMR [400 MHz, DMSO]: δ (ppm) 8.68 (2H, d, J = 4.77 *Hz*), 8.45 (2H, s, thia), 8.38 (2H, d, J = 7.87 *Hz*), 8.1 (2H, t), 7.83 (2H, d, J = 8.85 *Hz*), 7.53 (2H, t), 2.5 (6H, s, CH_3).

- Synthesis of L^5

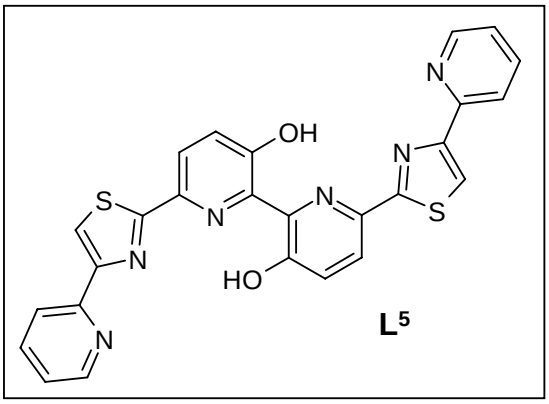

L^5

Under an inert atmosphere (N_2) a solution of pyridine (20 cm^3) and HCl (added until acidic, approximately 20 cm^3) is heated to 200 ˚C for one hour. Ligand L^4 (0.06 g, 0.1 mmol) is then added to the solution, which is continuously stirred for a further 3 hrs. After this time the solution is cooled to 150 ˚C, ice is added to the flask to initiate precipitation of the product. The precipitate is collected via filtration and washed with water (2 x 5 cm^3) to give the product as its HCl salt. The product is suspended in ammonia (0.88 S.G. 5 cm^3), left to stand overnight and filtered to give the free ligand L^5 as a pale yellow solid. Yield 0.05 g, 96%. ^{1}H NMR [400 MHz, DMSO]: δ (ppm) 8.45 (2H, s, thia), 8.08 (2H, d, J = 7.92 *Hz*), 7.98 (4H, m) 7.54 (2H, m), 7.32 (2H,m), 7.18 (2H, m).

- Synthesis of L^6

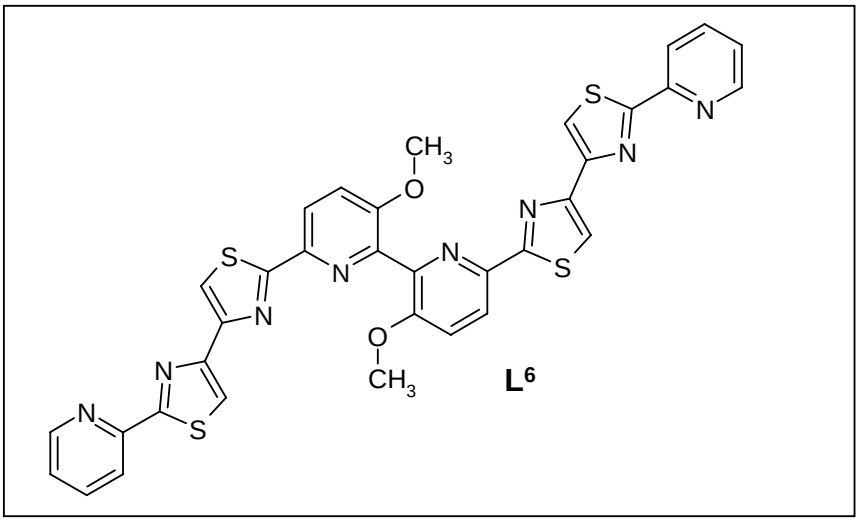

Under an inert atmosphere (N_2) a solution of 3,3′-dimethoxy-2,2′-bipyridine-6,6′-dithioamide (0.12 g, 0.4 mmol) in DMF (5 cm^3) was added 2-bromo-1-(2-pyridin-2-yl-1,3-thiazol-4-yl)ethanone (HBr salt) (0.30 g, 3.0 mmol) and the solution was heated at 80° for 4 hrs. After this time a precipitate forms, which is collected via filtration and dried, EtOH (5 cm^3) and Et_2O (5 cm^3) to give L^6 as a pale yellow solid. Yield 0.1g, 80%. ^{1}H NMR [400 MHz, DMSO]: δ (ppm) 8.68 (2H, d, *J* = 5.01 *Hz*), 8.38 (2H, d, *J* = 8.69 *Hz*), 8.36 (2H, s, thia, C-H), - overlapping with 8.35 (2H, s, py C-H), 8.15 (2H, s, thia C-H), 8.04 (2H, t, *J* = 7.81 *Hz*), 7.85 (2H, d, *J* = 8.76 *Hz*), 7.55 (2H, t, *J* = 4.96 *Hz*), 3.85 (6H, s, CH_3).

- Synthesis of L^7

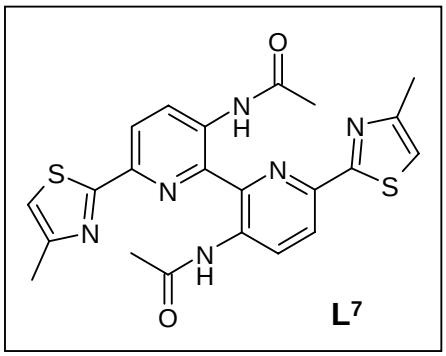

Under an inert atmosphere was added 3,3′-diacetylamino-2,2′-bipyridine-6,6′-dithioamide (0.22 g, 0.6 mmol) and DMF (10 cm^3). To this solution was added chloroacetone (0.11 cm^3. 1.4 mmol) and the reaction stirred overnight at 80 ˚C. A precipitate is formed and filtered to give L^7 as a pale yellow solid. Yield 0.19 g, 73%. ^1H NMR [400 MHz, $CDCl_3$]: δ (ppm) 11.9 (2H, s, NH), 9.1 (2H, d, J = 8.84 *Hz*), 8.17 (2H, d, J = 8.78 *Hz*), 6.97 (2H, s, thia), 2.5 (6H, s, CH_3).

- Synthesis of L^8

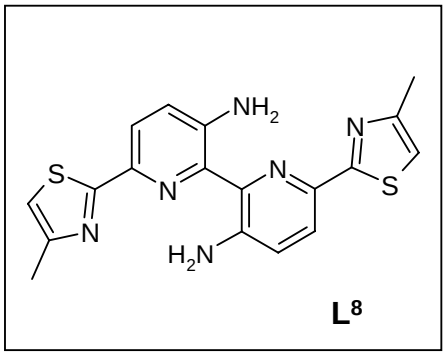

To a solution of L^7 in water (10 cm^3) is added HCl until acidic and the solution refluxed for 2 hrs. Once cool the solution is neutralise with the addition of ammonia (0.88 S.G.) and a precipitate is formed. The precipitate is filtered, washed with Et_2O (2 x 5 cm^3) to give L^8 as a bright yellow solid. Yield 0.10 g, 63%. ^1H NMR [400 MHz, DMSO]: δ (ppm) 7.89 (2H, d, J = 8.55 *Hz*), 7.8 (4H, s, NH_2), 7.35 (2H, d, J = 8.55 *Hz*) 7.26 (2H, s, thia), 2.3 (6H, s, CH_3).

Metal complexes

- $[Zn(L^4)][ClO_4]_2$

To a suspension of L^4 (0.010 g, 0.019 mmol) in $MeNO_2$ (2 cm^3) was added $Zn(ClO_4)_2 \cdot 6H_2O$ (0.0069 g, 0.0185 mmol). The subsequent suspension was immersed in an ultrasound-cleaning bath for 10 minutes resulting in a clear solution. Filtration followed by slow diffusion of ethyl acetate into the solution gave $[Zn(L^4)][ClO_4]_2$ as clear crystals, which were filtered and dried (0.005 g, 19%). EI MS *m/z*: 521, $[Zn(L^4)_2]^{4+}$.

- $[Cd(L^5)][ClO_4]_2$

To a suspension of L^5 (0.010 g, 0.02 mmol) in $MeNO_2$ (2 cm^3) was added $Cd(ClO_4)_2 \cdot 6H_2O$ (0.006 g, 0.02 mmol). The subsequent suspension was immersed in an ultrasound-cleaning bath for 10 minutes resulting in a pale yellow colour solution. Filtration followed by slow diffusion of ethyl acetate into the solution gave $[Cd(L^5)][ClO_4]_2$ as colourless crystals, which were filtered off and dried (0.0046 g, 13%) EI MS *m/z*: 1338.5 $[Cd_2(L^5)_2]^+$.

- $[Co(L^5)][ClO_4]_2$

To a suspension of L^6 (0.010 g, 0.02 mmol) in $MeNO_2$ (2 cm^3) was added $Co(ClO_4)_2 \cdot 6H_2O$ (0.0072 g, 0.02 mmol). The subsequent suspension was immersed in an ultrasound-cleaning bath for 10 minutes resulting in a pale green colour solution. Filtration followed by slow diffusion of ethyl acetate into the solution gave $[Co(L^5)][ClO_4]_2$ as colour crystals, which were filtered and dried (0.0063 g, 17%) EI MS *m/z*: 620 $[Co(L^5)_2]^{2+}$.

$[Cd_3(L^6)_2][ClO_4]_2$

To a suspension of L^6 (0.010 g, 0.014 mmol) in $MeNO_2$ (2 cm^3) was added $Cd(ClO_4)_2 \cdot 6H_2O$ (0.0089 g, 0.03 mmol). The subsequent suspension was immersed in an ultrasound-cleaning bath for 10 minutes resulting in a pale yellow colour solution. Filtration followed by slow diffusion of ethyl acetate into the solution gave $[Cd_3(L^6)_2][ClO_4]_2$ as colourless crystals, which were filtered off and dried g, %) EI MS *m/z*: 1616.6, $[Cd_2(L^6)_2]^{6+}$.

$[Cd_2(L^8)_2][ClO_4]_2$

To a suspension of L^8 (0.005 g, 0.013 mmol) in MeCN (2 cm^3) was added $Cd(ClO_4)_2 \cdot 6H_2O$ (0.004 g, 0.013 mmol). The subsequent suspension was immersed in an ultrasound-cleaning bath for 10 minutes resulting in a yellow solution. Filtration followed by slow diffusion of ethyl acetate into the solution gave $[Cd_2(L^8)_2][ClO_4]_2$ as pale yellow crystals, which were filtered off and dried (0.005 g, 24%) EI MS *m/z*: 972.6 $[Cd(L^8)_2]^+$, M^+.

5.4 $(Bipy)_2Ru(II)$ crown ether derivatives

- Synthesis of 3,3′-dihydroxy-2,2′-bipyridine

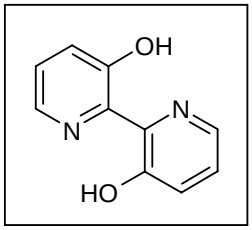

A solution of nickel dichloride hexahydrate ($NiCl_2 \cdot 6H_2O$, 4.0 g, 17 mmol) and triphenylphosphine ($(C_6H_5)_3P$ 17.92 g, 68 mmol) in DMF (75 cm^3) is agitated (using an ultra-sonic water bath) for 5-10 minutes, and then heated to 50˚C, whilst stirred. To this solution zinc powder (6.0 g, 92 mmol) was added and the solution once again agitated for 15 minutes. The solution was then heated at 50 ˚C for one hour. After this time 3-hydroxy-2-iodopyridine (6.0 g, 27 mmol) was added, the reaction continued for a further 2 hrs. Once cool the metal salts are precipitated with the addition of sodium hydroxide (2M, 300 cm^3) with the solid material removed by filtration. The resulting yellow filtrate is acidified with HCl (until pH 4-7 is achieved) and a precipitate is formed. The precipitate was then filtered and dried with the addition of DCM (20 cm^3) and $MgSO_4$. The product was filtered and the solvent evaporated to give 3,3′-dihydroxy-2,2′-bipyridine as a luminous yellow solid. Yield 1.2 g, 23%. ^1H NMR [400 MHz, $CDCl_3$]: δ (ppm) 14.6 (2H, s, OH), 8.08 (2H, d, J = 5.95 *Hz*), 7.45 (2H, d, J = 9.88 *Hz*), 7.32 (2H, dd, J = 4.63, 4.58 *Hz*).

- Synthesis of 2,2′-bipyridine-3,3′-[14]-crown-4

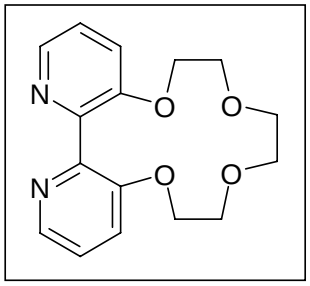

Under an inert atmosphere (N_2) a solution of 3,3′-dihydroxy-2,2′-bipyridine (0.3 g, 1.6 mmol) and sodium hydride (0.15 g, 6.4 mmol) in DMF (30 cm^3) was stirred at room temperature for 10 minutes, then heated to 60°C for 2 hrs allowing full deprotonation of the hydroxyl groups. After this time tri(ethylene glycol) di-*p*-tosylate (0.80 g, 1.6 mmol) was added and the reaction continued at this elevated temperature. The solvent was evaporated and the product extracted with DCM (2 x 20 cm^3) to give 2,2′-bipyridine-3,3′-crown-4 as a pale yellow oil. Yield: 0.29 g, 87%. ^{1}H NMR [400 MHz, $CDCl_3$]: δ (ppm) 8.37 (2H, d, J = 1.86 *Hz*), 8.35 (2H, d, J = 1.91, 1.82 *Hz*), 7.32 (2H, d, J = 1.57 *Hz*), 4.30 – 3.57 (12H, overlapping, -OCH_2CH_2O-).

The synthesis of crown 5 and 6 has been reported previously.[109] The synthesis of each of these ligands is similar to that of 2,2′-bipyridine-3,3′-[14]-crown 4. All were characterised by ^{1}H & ^{13}C NMR.

- Synthesis of 2,2′-bipyridine-3,3′-[17]-crown-5

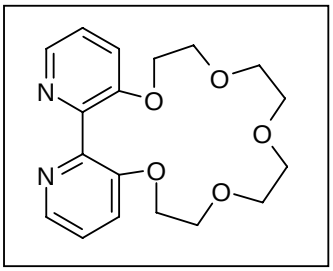

The addition of tetra(ethylene glycol) di-*p*-tosylate (molar equivalent) EI MS *m/z*: (21%, 391.1, M^+). ^{1}H NMR [400 MHz, CD_3NO_2]: δ (ppm) 8.32 (2H, d, J = 4.06 Hz), 7.35 (2H, m, overlapping), 7.20 (2H, m, overlapping), 4.25 (2H, br, CH_2), 4.05 (2H, br, CH_2), 3.8 (2H, br, CH_2), 3.6 (2H, br, CH_2). ^{13}C NMR [80 MHz, $CDCl_3$]: δ (ppm) 153.573, 146.876, 141.394 (CH), 123.726 (CH), 119.231 (CH), 71.045 (CH_2), 70.882 (CH_2), 69.572 (CH_2), 67.978 (CH_2).

- Synthesis of 2,2′-bipyridine-3,3′-[20]-crown-6

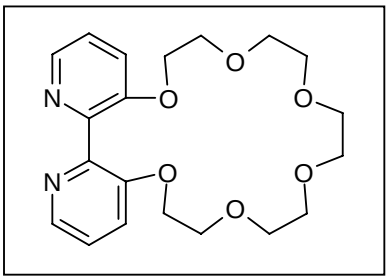

The addition of tetra(ethylene glycol) di-*p*-tosylate (1.1 molar equivalent) EI MS *m/z*: (100%, 347.1, M^+). ^{1}H NMR [400 MHz, CD_3CN]: δ (ppm) 8.32 (2H, d, J = 3.89 Hz), 7.28 (2H, m, overlapping), 7.26 (2H, m, overlapping), 4.1 (2H, br, CH_2), 3.72 (2H, t, J = 5.12, 5.13 Hz), 3.60 (2H, s, CH_2), 3.55 (2H, s, CH_2). ^{13}C NMR [80 MHz, $CDCl_3$]: δ (ppm) 153.5, 147.1, 141.7 (CH), 123.8 (CH_2), 119.7 (CH), 70.68 (CH_2), 70.69 (CH_2), 70.8 (CH_2), 69.5 (CH_2), 68.6 (CH_2).

- Synthesis of L^9 Ru(II) complex

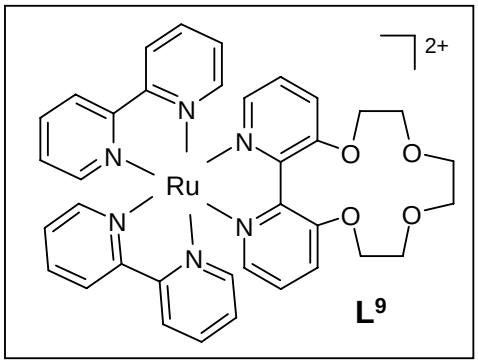

To a solution of *cis*-Bis(2,2′-bipyridine)dichlororuthenium(II) hydrate (0.05 g, 0.1 mmol) in EtOH (50 cm^3) was added 2,2′-bipyridine-3,3′-[14]-crown-4 (0.07 g, 0.29 mmol). The solution was refluxed for 12 hrs, after which time the reaction was allowed to cool to room temperature. Evaporation of the solvent gave a light brown residue, which was purified via column chromatography using a "Maji-Mix" solvent system; MeCN: H_2O: $NaNO_2$ (saturated) (14 : 2 : 1). Collection and evaporation of the organic fractions gave the crude product as red/orange solid. Further extraction of the product with sodium hexafluorophosphate/DCM gave L^{10} complex as the PF_6 salt and as a red/orange crystalline solid. Yield 0.03 g, 25%. EI MS *m/z*: (75%, 860.8, M^+).^{1}H NMR [400 MHz, CD_3CN]: δ (ppm) 7.53 (4H, m- overlapping), 7.10 (4H, m – overlapping), 6.77 (2H, d, J = 5.24 *Hz*), 6.70 (4H, m- overlapping), 6.42 (2H, m), 6.40 (2H, m), 6.34 (2H, d, J = 1.32 *Hz*), 6.32 (2H, d, J = 0.99 *Hz*), 3.42 (4H, m, CH_2), 3.26 (4H, m, CH_2), 2.91 (4H, m, CH_2).

- L^{10} Ru(II) complex

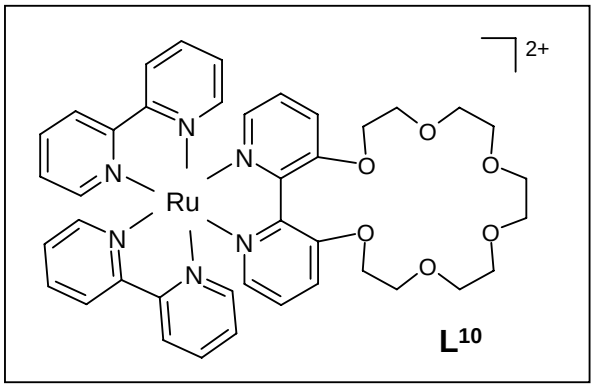

Yield 0.11 g, 13%. EI MS *m/z*: (55%, 948.8, M^+).^{1}H NMR [400 MHz, CD_3NO_2]: δ (ppm) 8.5 (2H, M), 8.1 (2H, M), 8.05 (2H, m), 8.02 (2H, m), 7.75 (2H, m), 7.70 (2H, m), 7.45 (2H, m), 7.38 (2H, m), 7.33 (2H, m), 4.42 (2H, overlapping), 4.40 (2H, m, CH_2), 3.90 (2H, m, CH_2), 3.80 (2H, m, CH_2).

- L^{11} Ru(II) complex

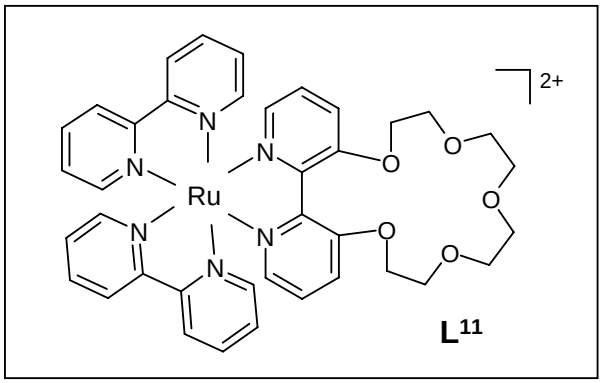

Yield 0.09 g, 61%. EI MS *m/z*: (13%, 904.8, M^+). ^{1}H NMR [400 MHz, CD_3NO_2]: δ (ppm) 8.46 (2H, m, overlapping), 8.44 (2H, m, overlapping), 8.05 (2H, m, overlapping), 8.02 (2H, m, overlapping), 7.7 (2H, d, J = 5.51 *Hz*), 7.65 (2H, m, overlapping), 7.6 (2H, m, overlapping), 7.4 (2H, t, J = 7.05, 6.18 *Hz*), 7.33 (2H, t, J = 7.14, 6.29 *Hz*), 7.25 (2H, d, J = 4.69 *Hz*), 4.31 (2H, m, CH_2), 4.2 (2H, m, CH_2), 3.87 (2H, m, overlapping), 3.84 (2H, m, overlapping).

Metal complexes

- L^{11} – [$(Bipy)_2$-Ru(II) – [17]-crown-5]

To a suspension of L^{11} (0.30 g, 0.49 mmol) in MeCN (3 cm^3) was added $NaPF_6$ (0.82 g, 4.9 mmol). The subsequent suspension was immersed in an ultrasound-cleaning bath for 10 minutes resulting in a deep red/purple solution. Filtration followed by slow diffusion of ethyl acetate into the solution gave $(Bipy)_2$-Ru(II)-[17]-crown-5 as bright red coloured crystals, which were filtered off and dried (0.010 g, 33%) EI MS *m/z*: (13%, 904.8 M^+).

5.5 $(Bipy)_2Ru(II)$-2,2′-bipyridine-3,3′-disubstituted-urea type anion binders

- Synthesis of 3,3′-diamine-2,2′-bipyridine is as previously shown in section 5.3 of the experimental.
- Synthesis of L^{12}

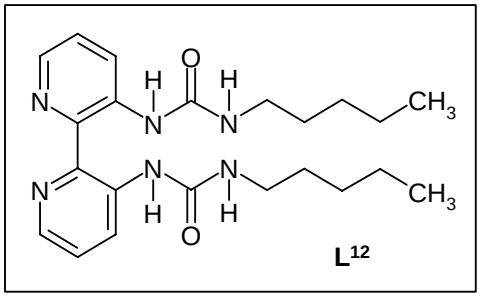

To a solution of 3,3′-diamino-2,2′-bipyridine (0.5 g, 2.7 mmol) in DCM (50 cm^3) was added *N*-pentyl isocyanate (0.76 g, 0.87 cm^3, 6.85 mmol) and the solution refluxed for 12 hrs. After this time the solution was cooled and then concentrated to give a pale yellow precipitate. The solid was filtered and dried *in vacuo* to give L^{12} as a pale yellow solid. Yield: 0.48 g, 44%. ^1H NMR [400 MHz, $CDCl_3$]: δ (ppm) 12.6 (2H, s, NH), 8.93 (2H, d, J = 8.22 *Hz*), 8.15 (2H, d, J = 3.17 *Hz*), 7.30 (2H, dd, J = 4.54, 4.54 *Hz*), 4.55 (2H, s, NH), 3.25 (2H, m, CH_2), 1.47 (2H, m, CH_2), 0.9 (3H, t, J = 3.64 *Hz* CH_3). ^{13}C NMR [80 MHz, $CDCl_3$]: δ (ppm) 155.6, 141.3, 138.4 (py), 129.0 (py), 123.6 (py), 40.9 (CH_2). 29.7 (CH_2), 29.0 (CH_2), 22.4 (CH_2), 14.0 (CH_2).

- Synthesis of $(Bipy)_2Ru(II)$-3,3′-disubstituted anion binding complex (X)

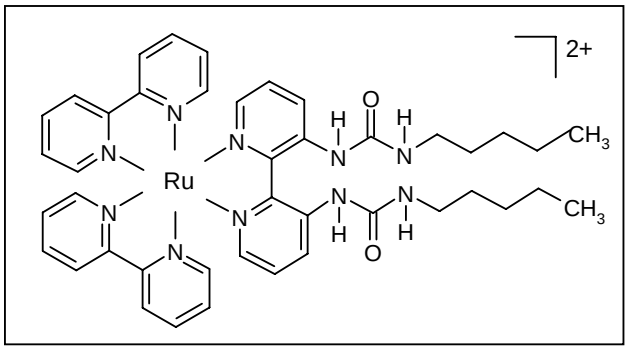

To a solution of *cis*-bis(2,2′-bipyridine)dichlororuthenium(II) hydrate (0.32 g, 0.7 mmol) and silver nitrate (0.11 g, 0.7 mmol) in EtOH (50 cm^3) was added L^{12} (0.27 g, 0.7 mmol) and the solution refluxed for 12 hrs. After this time the solution was cooled, the solvent evaporated to leave the product residue, which was purified using column chromatography with a "Maji Mix" solvent system. Extraction of organic column fractions with sodium hexafluorophosphate gave the complex as the PF_6 salt. Yield: 0.20 g, 34 %. EI MS *m/z*: (50%, 970.8, M^+). ^1H NMR [400 MHz, CD_3NO_2]: δ (ppm) 8.45 (2H, d, J = 6.97 *Hz*), 8.44 (2H, d, J = 6.84 *Hz*), 8.13 (2H, s), 8.05 (2H, d, J = 8.03 *Hz*), 8.0 (2H, d, J = 7.61 *Hz*), 7.98 (2H, d, J = 7.56 *Hz*), 7.65 (2H, d, J = 5.32 *Hz*), 7.38 (2H, d, J = 4.9 *Hz*), 7.36 (2H, d, J = 7.15 *Hz*), 7.3 (2H, d, J = 7.21 *Hz*), 7.15 (2H, m), 5.55 (2H, s, NH), 3.10 (4H, s, CH_2), 0.9 (6H, t, J = 7.03 *Hz*).

REFERENCES

1. J-Marie Lehn, 'Supramolecular Chemistry: Concepts and Perspectives', ed. VCH, 1995.

2. J. W. Steed and J. L. Atwood, 'Supramolecular Chemistry', John Wiley and Sons, 2000.

3. M. J. Hannon and L. J. Childs, *Supramolecular Chemistry*, 2004, **16**, 7-22

4. M. Albrecht, Chem. Soc. Rev., 1998, **27**, 281-287

5. Paul. D. Beer, Philip. A. Gale and David. K. Smith, 'Supramolecular Chemistry', Oxford Chemistry Primer, 1998.

6. J. S. Lindsay, *New J. Chem.,* 1991, **15**, 153-180.

7. C. J. Pedersen, *Angew. Chem. Ind. Ed. Engl*, 1988, **27**, 1021-1027.

8. J. Holliday and C. A. Mirkin, *Angew. Chem. Int. Ed.,* 2001, **40**, 2022-2043.

9. E. C. Constable, Metallosupramolecular chemistry, *Chemistry and Industry*, 1994, 56-59.

10. C. Piquet, G. Bernardinelli and G. Hopfgartner, *Chem. Rev*., 1997, **97**, 2005-2062. a) R. Kramer, J.-M, Lehn, A. DeCian, J. Fischer, *Angew. Chem. Int. Ed. Engl.,* 1993, **32**, 704.

11. G. M. Whitesides and J. P. Mathias, Science, 1992, **254**, 1312-1319

12. T. Beissel, R. E. Powers and K. N. Raymond, *Angew. Chem. Int. Ed. Engl.,* 1996, **35**, 10.

13. G. F. Sweigers and T. J. Malefetse, *Chem. Rev.,* 2000, **100**, 3483-3537.

14. J. P. Plante, P. D. Jones, D. R. Powell and T. E. Glass, *Chem. Commun.,* 2003, 336-337.

15. S. T. Onions, A. M. Franklin, P. N. Horton, M. B. Hursthouse and C. J. Matthews, *Chem. Commun.,* 2003, **23**, 2864-2865.

16. P. N. W. Baxter, J-Marie. Lehn, J. Fischer and M-Therese. Youinou, *Angew. Chem. Int. Ed. Engl.,* 1994, **33**, 2284-2287.

17. C. J. Matthews, S. T. Onions, G. Morata, M. B. Salva, M. R. J. Elsegood and D. J. Price, *Chem. Commun.,* 2003, **3**, 320-321.

18. P. N. W. Baxter, G. S. Hanan and J-Marie. Lehn, *Chem. Commun.,* 1996, 2019-2020.

19. A. J. Blake, N. R. Champness, P. Hubberstey, Wan-Sheung. Li, M. A. Withersby, Martin Schroder, *Coord. Chem. Rev.*, 1999, **183**, 117-138.

20. D. Philip and J. F. Stoddard, *Synlett*, 1991, 445-458.

21. C. O. Dietrich-Buchecker and J-P. Sauvage, *Chem. Rev.,* 1987, **87**, 795.

22. C. O. Dietrich-Buchecker, C. Hemmett, A. Khemiss and J. P. Sauvage, *J. Am. Chem. Soc.,* 1990, **112**, 8002.

23. Solokov, *VI Russ, Chem. Rev.,* 1973, **42**, 252.

24. C. Dietrich-Buchecher and J-P. Sauvage, *Tetrahedron,* 1990, **46**, 503-512.

25. M. Greenwald, D. Wessely, E. Katz, I Willner and Y. Cohen, *J. Org. Chem.,* 2000, **65**, 1050-1058.

26. J. D. Crane, J-P. Sauvage, *New J. Chem*, 1992, **16**, 649-650.

27. R. Kramer, J-Marie. Lehn and A. Marquis-Rigault, *Proc. Natl. Acad. Sci. USA,* 1993, **90**, 5394-5398.

28. U. Ziener, E. Brenning, J-Marie. Lehn, E. Wegelius, K. Rissanieu, G. Baum, D. Fenske and G. Vaughan, *Chem. Eur. Journal*, 2000, **6**, 22.

29. J. D. Crane, J-P. Sauvage, *New. J. Chem.,* 1992, **16**, 649-650.

30. C. R. Rice, C. J. Baylies, H. J. Clayton, J. C. Jeffery, R. L. Paul and M. D. Ward, *Inorganica Chimica Acta,* 2003, **351**, 207-216.

31. M. Greenwald, D. Wesseley, E. Katz, I. Willner and Y. Cohen, *J. Org. Che.,* 2000, **65**, 1050-1058.

32. T. Frisele and L. R. MacGillivray, *Chem. Commun.,* 2003, 1306-1307.

33. C. R. Rice, S. Worl, J. C. Jeffery, R. L. Paul and M. D. Ward, *J. Chem. Soc., Dalton Trans.,* 2001, 550-559.

34. E. C. Constable, T. Kulke, G. Baum and D. Fenske, *Inorganic Chemistry Communications,* 1998, 80-82.

35. G. Baum, E. C. Constable, D. Fenske, C. E. Housecroft, T. Kulke, M. Neuburger and M. Zehnder, *J. Chem. Soc., Dalton Trans.,* 2000, 945-959.

36. B. Hasenknopf, J-Maire. Lehn, N. Bournediene, A. Dupont-Gervais, A. Van Dorsselaer, B. Griesel and D. Fenske, *J. Am. Chem. Soc.,* 1997, **119**, 10956-10961.

37. G. Baum, E. C. Constable, D. Fenske, C. E. Housecroft and T. Kulke, *Chem. Commun.,* 1999, 195-196.

38. G. R. L. Cousins, S. Poulson and J. K. M. Sanders, *Chem. Commun.,* 1999, 1575-1576.

39. R. L. E. Furlan, G. R. L. Cousins and J. K. M. Sanders, *Chem. Commun.,* 2000, 1761-1762.

40. E. Stulz, Yiu-Fai Ng, S. M. Scott and J. M. Sanders, *Chem. Commun.,* 2002, **5**, 524-525.

41. V. G. Machado, P. N. W. Baxter and J.-Marie. Lehn, *Inorganic Chemistry*, 2001, 1-61. a) E. C. Constable, *Tetrahedron*, 1992, **48**, 10013-10059.

42. F. Krohnke, *Synthesis*, 1976, 1-24.

43. E.C. Constable, S. M. Elder, J. Healy, D. A. Tocher and M. D. Ward, *J. Am. Chem. Soc.,* 1990, **112**, 4590-4592.

44. C. Janiak, L. Uehlin, He-Ping Wu, P. Klufers, H. Piotrowski and T. G. Scharmann, *J. Chem. Soc., Dalton Trans.,* 1999, 3121-3131.

45. E. C. Constable, A. J. Edwards, P. R. Raithby and J. V. Walker, *Angew. Chem. Int. Ed. Engl*., 1993, **32**, (10) 1465-1467.

46. M. Albrecht, *Chemistry Reviews*, 2001, **101**, 3458-3497. a) *J. Org. Chem*. 1985, **50**, 3636-3638. b) A. J. Amoroso, M. W. Burrows, A. A. Dickinson, C. Jones, D. J. Wiillock and Wing-Tak Wong, *J. Chem. Soc., Dalton Trans*., 2001, **3**, 225-227.

47. He-Ping Wu, C. Janiak, G. Rheinwald and H. Lang, *J. Chem. Soc., Dalton Trans.,* 1999, 183-190. a) P. N. W. Baxter, J. A. Connor, W. B. Schweiser and J. D. Wallis, *J. Chem. Soc., Dalton Trans*., 1992, 3015-3019.

48. B. Wu, Xiao-Juan Yang, C. Janiak and P. G. Lassahn, *Chem. Commun.,* 2003, 902-903. a) C. R. Rice, K. M. Anderson, *Polyhedron*, 2000, *19*, 495-498.

49. C. R. Rice, S. Onions, N. Vidal, J. D. Wallis, M-C. Senna, M. Pilkington and H. Stoechli-Evans, *Eur. J. Inorg. Chem.*, 2002, 1985-1997.

50. N. K. Solanki, A. E. H. Wheatley, S. Radojevic, M. McPartlin and M. A. Halcrow, *J. Chem. Soc., Dalton Trans.,* 1999, 521-523.

51. A. M. W. Cargill Thompson, J. C. Jeffery, D. J. Liard and M. D. Ward, *J. Chem. Soc., Dalton Trans.*, 1996, 879-884.

52. C. R. Rice, S. Onions, N. Vidal, J. D. Wallis, Maria-Cristina. Senna, M. Pilkington and H. Stockli-Evans, *Eur. J. Chem.,* 2002, 1985-1997.

53. M. J. Hannon, C. L. Painting, E. A. Plummer, L. J. Childs and N. W. Alcock, *Chem. Eur. J.* 2002, **8**, 2226-2238. a) B. Galland, D. Limosin, H. Laguitton-Pasquier and A. Deronzier, *Inorganic Chemistry Communications*, 2002, **5**, 5-8.

54. E. C. Constable, A. J. Edwards, G. R. Haire, M. J. Hannon and P. R. Raithby, *Polyhedron, 1998,* **17**, 243-253. a) U. Ziener, E. Brreuning, J-Marie. Lehn, E. Wegelius, K. Rissanen, G. Baum, D. Fenske and G. Vaughan, *Chem. Eur. J., 2000,* **6**, 4132-4139.

55. M. A. Halcrow, E. K. Brechin, E. J. L. Mcinnes, F. E. Mabbs and J. E. Davies, *J. Chem. Soc., Dalton Trans.,* 1998, 2477-2482.

56. G. Baum, E. C. Constable, D. Fenske and T. Kulke, *Chem. Commun.,* 1997, 2043-2044. a) E. C. Constable, S. M. Elder and J. Healy, *J. Soc. Chem. Dalton Trans.,* 1990, 1669-1674.

57. E. C. Constable, S. M. Elder, M. J. Hannon, A. Martin, P. R. Raithby and D. A. Tocher, *J. Chem. Soc., Dalton Trans.,* 1996, 2423-2433.

58. E. C. Constable and J. V. Walker, *J. Chem. Soc., Chem. Commun.*, 1992, 884-886.

59. P. Kwok-Keung Ho, Kung-Kai Cheung and Chi-Ming Che, *Chem. Commun.,* 1996, 1197-1198.

60. C. R. Rice, C. J. Baylis, L. P. Harding, J. C. Jeffery, R. L. Paul and M. D. Ward, *Polyhedron,* 2003, **22**, 755-762. a) H. J. Clayton, L. P. Harding, J. C. Jeffery, T. Riis-Johannessen, A. P. Laws, C. R. Rice and M. Whithead, *Chem. Commun*., 2008, 108-110.

61. C. R. Rice, C. J. Baylis, L. P. Harding, J. C. Jeffery, R. L. Paul and M. D. Ward, *J. Chem. Soc., Dalton Trans.,* 2001, 3039-3044.

62. C. R. Rice, S. Worl, J. C. Jeffery, R. L. Paul and M. D. Ward, *Chem. Commun.,* 2000, 1529-1530.

63. T. R- Johannessen, J. C. Jeffery, A. P. K. Robson, C. R. Rice and L. P. Harding, *Inorganica Chimica Acta,* 2005, **358**, 2781-2798.

64. C. R. Rice, C. J. Baylis, H. J. Clayton, J. C, Jeffery, R. L. Paul and M. D. Ward, *Inorganica Chimica Acta*, 2003, **351**, 207-216.

65. J. F. Callan, A. Prasanna de Silva and D. C. Magri, *Tetrahedron,* 2005, **61**, 8551-8588. a) J-Marie. Lehn, *Angew. Chem. Int. Ed. Engl*, 1990, **29**, 1304-1319.

66. P. D. Beer, P. A. Gale and G. Z. Chen, *J. Chem. Soc., Dalton Trans.,* 1999, 1897-1909.

67. M. D. Ward, *Chem. Soc. Rev.*, 1997, **26**, 365-375. a) T. Akasaka, H. Inoue, M. Kuwabara, T. Mutai, j. Otsuki and K. Araki, *Dalton Transactions.*, 2003, 1-14.

68. A. Prasana de Silva, H. Q. Nimal Gunaratne, T. Gunnlaugsson, A. J.M. Huxley, C. P. McCoy, J. T. Rademacher and T. E. Rice, *Chem. Rev*., 1997, **97**, 1515-1566.

69. R. Pohl, D. Aldakov, P. Kubat, K. Jursikova, M. Marquez and P. Anzenbacher, Jr. *Chem Commun*., 2004, 1282-1283. a) N. C. Fletcher, T. C. Robinson, A. Behrendt, J. C. Jeffery, Z. R. Reeves and M. D. Ward, *J. Chem. Soc., Dalton Trans.*, 1999, 2999-3006.

70. B. Linton and A. D. Hamilton, *Chem. Rev.*, 1997, **97**, 1669-1680.

71. P. D. Beer and J. Cadman, *Coordination Chemistry Reviews*, 2000, **205**, 131-155.

72. K. Rurach, V. Resch-Geyer, *Chem. Soc. Rev*., 2002, **31**, 116-127.

73. P. A. Gale, *Coordination Chemistry Reviews*, 2000, **199**, 181-233. a) J.-Marie. Lehn, *Angew. Chem. Int. Ed. Engl*., 1998, **27**, 89-112.

74. V. Balzani, F. Barigelletti and L. De Cola, '*Metal Complexes as Light Absorption and Light Emission Sensitisers'*, Topics in Current Chemistry, 1990, **158**, 32-71.

75. L. Sun, L. Hammarstrom, B. Akermark and S. Styring, *Chem. Soc. Rev*., 2001, **30**, 36-49.

76. Chun-Man. Chan, Chun-Sing. Fung, Kwok-Yin. Wong and W. Lo, *Analyst*, 1998, **123**, 1843-1847.

77. N. Armaroli, F. Barigelletti, G. Calogero, L. Flamigni, C. M. White and M. D. Ward, *Chem, Commun*., 1997, 2181-2182.

78. D. Bruce and M. Richter, *Analyst*, 2002, **127**, 1492-1494.

79. S. Encinas, A. M. Barthram, M. D. Ward, F. Barigelletti and S. Campagna, *Chem. Commun*., 2001, 277-278.

80. A. Juris, V. Balzani, *Coord. Chem. Rev.*, 1988, **84**, 85-277.

81. H.-J. Schneider and A. Yatsimirsky, *Principles & Methods in Supramolecular Chemistry*, Wiley.

82. M. Schmittel, Heng-Wei Lin, E. Thiel, A. J. Meixner and H. Ammon, *Dalton Trans*., 2006, 4020-4028.

83. D. A. Laidler and J. F. Stoddart, *The 'Chemistry of ethers, crown ethers, hydroyl groups and their sulphur analogues' – Part 1, 1980*, John Wiley & Sons.

84. J. S. Bradshaw, R. M. Izatt, A. V. Bordunov, C. Y. Zhu and J. K. Hathaway, *'Crown Ethers'* Brigham Young University, Provo. UT. USA.

85. N. C. Fletcher, M. D. Ward, S. Encinas, N. Armaroli, L. Flamigni and F. Barigelletti*, Chem. Commun*., 1999, 2089-2090.

86. C. J. Baylies, J. C. Jeffery, T. A. Miller, R. Moon, C. R. Rice and T. Riis-Johannessen, *Chem. Commun*., 2005, 4158-4160.

87. G. Bokolinis, T. Riis-Johannessen, L. P. Harding, J. C. Jeffery, N. McLay and C. R. Rice, *Chem. Commun.*, 2006, 1980-1982.

88. J. Rebek, Jr., J.E. Trend, R. V. Wattley and S. Chakravorti, *J. Am. Chem. Soc.,* 1979, 4333-4336.

89. C. R. Rice, A. Guerrero, Z. R, Bell, R. L. Paul, G. R. Motson, J. C. Jeffery and M. D. Ward, *New J. Chem*., 2001, **25**, 185-187.

90. S. A. McFarland, D. Magde and N. S. Finney, *Inorg. Chem*., 2005, **44**, 4066-4076.

91. S.A. McFarland and N. S. Finney, *Chem. Commun.,* 2003, 388-389.

92. L. H. Uppadine, J. E. Redman, S. W. Dent, M. G. B. Drew and P. D. Beer, *Inorg. Chem*., 2001, **40**, 2860-2869.

100. P.D. Beer and J. Cadman, *New J. Chem*., 1999, **23**, 347-349. a) C.R. Rice, *Coordination Chemistry Reviews*, 2006, **250**, 3190-3199.

101. V. Wing-Wah Yam and V. Wing-Man Lee, *Inorg, Chem*. 1997, **36**, 2124-2129. a) P. A. Gale, S. Camiolo, G. J. Tizzard, C. P. Chapman, M. E. Light, S. J. Coles and M. B. Hursthouse, *J. Org. Chem.*, 2001, **66**, 7849-7853.

102. *'New Rhenium(I) Bipyridine Crown Ether Receptors' Inorganic Chemistry*, 2001, **40**, 2864-2869.

103. P.D. Beer, V. Timoshenko, M. Maestri, P. Passaniti and V. Balzani, *Chem. Commun*., 1999, 1755-1756. a) D. Jimenez, R. Martinez-Manez, F. Sancenon and J. Soto, *Tetrahedron*, 2002, **43,** 2823-2825.

104. A. M. W. Cargill Thompson, M. C. C. Smailes, J. C. Jeffery and M. D. Ward, J. Chem. Soc., Dalton Trans, 1997, 737-743. a) R. Pohl, D. Aldakov, P. Kubat, K. Jursikova, M. Marquez and P. Anzenbacher, Jr. *Chem. Commun*., 2004, 1282-1283.

105. L. P. Harding, J. C. Jeffery, T-Riis Johannessen, C. R. Rice and Zuotao Zeng. *Chem Commun*., 2004, 654-655. a) J. L. Sessler, P. I. Sansom, A. Andrievsky and V. Kral, *'Supramolecular Chemistry of Anions'* 1997, Wiley-VCH.

106. J. C. Jeffery, E. Schatz and M. D. Ward, *J. Chem. Soc., Dalton Trans.*, 1992, 1921-1927.

107. C. Dietrich- Buchecker and J. P. Sauvage, *Tetrahedron*, 1990, **46**, 503.

108. T-Riis Johannessen, The Synthesis and Structural Characterisation of Metallosupramolecular Complexes based on Neutral Polydentate N-donor Ligands, University of Bristol, 2006.

109. C. J. Baylies, T. Riis-Johannessen, L. P. Harding, J. C. Jeffery, R. Moon, C. R. Rice and M. Whitehead, *Angew. Chem., Int. Ed.,* 2005, **44**, 2-6. a) C. J. Baylies, J. C. Jeffery, T. A. Miller, R. Moon, C. R. Rice and T. Riis-Johannessen, *Chem. Commun*., 2005, 4158-4160.

APPENDIX I – CRYSTAL DATA TABLES

Table 1. Pyridyl/thiazole crystallographic data.[a]

Compound	$[Cu_2(L^1)][ClO_4]_2$
Formula	C 23, H 15, Cl 2, Cu, N 5, O 8, S
M	655.90
System, space group	Monoclinic, C2/C
a / Å	19.490(3)
b / Å	13.592(2)
c / Å	20.232(3)
α / °	90.0
β / °	114.118(2)
γ / °	90.0
U / *Å*^{3}	4891.9(12)
Z	8
μ / mm^{-1}	0.0277
Reflections collected: Total, independent, R_{int}	5630
Final R_1, wR_2 [b,c]	0.0502, 0.0877

[a] Details in common: diffractometer, Siemens SMART using Mo-Kα radiation (0.71073 Å); temperature of data collection 173 K.
[b] Structure was refined on F_o^2 using all data; the value of R_1 is given for comparison with older refinements based on F_o with a typical threshold of F >_ 4 σ(F).
[c] $wR_2 = [\Sigma[w(F_o^2-F_c^2)^2]]^{1/2}$ where $w^{-1} = \sigma^2(F_o^2) + (aP)^2 + (bP)$ and $P = [\max(F_o^2,0) + 2F_c^2]/3$

Table 2. Pyridyl/thiazole crystallographic data.[a]

Compound	$[Ni(L^2)][ClO_4]_2$
Formula	C 54, H 39, Cl 4, N 14, Ni 2, O 20.5, S 4
M	1599.45
System, space group	Triclinic, P-1
a / Å	11.118(2)
b / Å	12.860(2)
c / Å	23.270(4)
α / °	82.198(3)
β / °	78.550(3)
γ / °	72.113(3)
U / $Å^3$	3093.1(10)
Z	2
μ / mm^{-1}	0.0513
Reflections collected: Total, independent, R_{int}	10843
Final R_1, wR_2 [b,c]	0.1189, 0.1984

[a] Details in common: diffractometer, Siemens SMART using Mo-Kα radiation (0.71073 Å); temperature of data collection 173 K.
[b] Structure was refined on F_o^2 using all data; the value of R_1 is given for comparison with older refinements based on F_o with a typical threshold of F >_ 4 σ(F).
[c] $wR_2 = [\Sigma[w(F_o^2-F_c^2)^2]]^{1/2}$ where $w^{-1} = \sigma^2(F_o^2) + (aP)^2 + (bP)$ and $P = [\max(F_o^2,0) + 2F_c^2]/3$

Table 3. Pyridyl/thiazole crystallographic data.[a]

Compound	$[Co(L^2)][ClO_4]_2$
Formula	C 54, H 38, Cl 4, Co 2, N 14, O 20, S 4,
M	1590.88
System, space group	Triclinic, P-1
a / Å	11.186(2)
b / Å	12.931(3)
c / Å	23.072(5)
α / °	82.920(3)
β / °	78.726(3)
γ / °	72.260(3)
U / $Å^3$	3110.0(11)
Z	2
μ / mm^{-1}	0.1138
Reflections collected: Total, independent, R_{int}	14032
Final R_1, wR_2 [b,c]	0.1917, 0.2676

[a] Details in common: diffractometer, Siemens SMART using Mo-Kα radiation (0.71073 Å); temperature of data collection 173 K.
[b] Structure was refined on F_o^2 using all data; the value of R_1 is given for comparison with older refinements based on F_o with a typical threshold of F >_ 4 σ(F).
[c] $wR_2 = [\Sigma[w(F_o^2-F_c^2)^2]]^{1/2}$ where $w^{-1} = \sigma^2(F_o^2) + (aP)^2 + (bP)$ and $P = [\max(F_o^2,0) + 2F_c^2]/3$

Table 4. Pyridyl/thiazole crystallographic data.[a]

Compound	$[Cd_3(L^3)_2][ClO_4]_6$
Formula	C 32.33, H 28.33, Cd 1.5, Cl 3, N 8.33, O 17.33, S 2
M	1150.04
System, space group	Monoclinic, C2/C
a / Å	35.597(19)
b / Å	17.593(10)
c / Å	15.131(8)
α / °	90.0
β / °	102.478(10)
γ / °	90.0
U / $Å^3$	9253(9)
Z	8
μ / mm^{-1}	1.036
Reflections collected: Total, independent, R_{int}	8259
Final R_1, wR_2 [b,c]	0.1763, 0.3343

[a] Details in common: diffractometer, Siemens SMART using Mo-Kα radiation (0.71073 Å); temperature of data collection 173 K.
[b] Structure was refined on F_o^2 using all data; the value of R_1 is given for comparison with older refinements based on F_o with a typical threshold of F >_ 4 σ(F).
[c] $wR_2 = [\Sigma[w(F_o^2-F_c^2)^2]]^{1/2}$ where $w^{-1} = \sigma^2(F_o^2) + (aP)^2 + (bP)$ and $P = [\max(F_o^2,0) + 2F_c^2]/3$

Table 5. Pyridyl/thiazole crystallographic data.[a]

Compound	$[Zn(L^4)][ClO_4]_2$
Formula	C 60, H 53, Cl 4, N 16, 0 28.5, S 4, Zn 2
M	1854.96
System, space group	Triclinic, P-1
a / Å	12.2605(3)
b / Å	14.5063(3)
c / Å	21.9684(5)
α / °	74.773(2)
β / °	85.929(2)
γ / °	75.954(2)
U / $Å^3$	3657.18(14)
Z	2
μ / mm^{-1}	4.062
Reflections collected: Total, independent, R_{int}	28088
Final R_1, wR_2 [b,c]	0.0407, 0.0530, 0.1494

[a] Details in common: diffractometer, Siemens SMART using Mo-Kα radiation (0.71073 Å); temperature of data collection 173 K.
[b] Structure was refined on F_o^2 using all data; the value of R_1 is given for comparison with older refinements based on F_o with a typical threshold of F >_ 4 σ(F).
[c] $wR_2 = [\Sigma[w(F_o^2-F_c^2)^2]]^{1/2}$ where $w^{-1} = \sigma^2(F_o^2) + (aP)^2 + (bP)$ and $P = [\max(F_o^2,0) + 2F_c^2]/3$

Table 6. Pyridyl/thiazole crystallographic data.[a]

Compound	$[Cd(L^5)][ClO_4]_2$
Formula	C 56, H 44, Cd 2, Cl 4, N 16, O 28, S 4
M	1883.91
System, space group	Triclinic, P-1
a / Å	15.094(3)
b / Å	15.627(3)
c / Å	16.199(3)
α / °	74.78(3)
β / °	84.40(3)
γ / °	87.40(3)
U / $Å^3$	3668.5(13)
Z	2
μ / mm^{-1}	0.932
Reflections collected: Total, independent, R_{int}	34131
Final R_1, wR_2 [b,c]	0.0459, 0.0793, 0.1800

[a] Details in common: diffractometer, Siemens SMART using Mo-Kα radiation (0.71073 Å); temperature of data collection 173 K.
[b] Structure was refined on F_o^2 using all data; the value of R_1 is given for comparison with older refinements based on F_o with a typical threshold of F >_ 4 σ(F).
[c] $wR_2 = [\Sigma[w(F_o^2-F_c^2)^2]]^{1/2}$ where $w^{-1} = \sigma^2(F_o^2) + (aP)^2 + (bP)$ and $P = [\max(F_o^2,0) + 2F_c^2]/3$

Table 7. Pyridyl/thiazole crystallographic data.[a]

Compound	$[Cd_3(L^6)_2][ClO_4]_2$
Formula	C 76, H 68, Cd 3, Cl 6, N 24, O 43.5, S 8
M	2819.92
System, space group	Triclinic, P-1
a / Å	13.979(3)
b / Å	14.361(3)
c / Å	29.232(6)
α / °	102.70(3)
β / °	103.15(3)
γ / °	90.15(3)
U / *Å*^{3}	5566.3(19)
Z	2
μ / mm^{-1}	0.958
Reflections collected: Total, independent, R_{int}	58947
Final R_1, wR_2 [b,c]	0.0703, 0.0876, 0.2041

[a] Details in common: diffractometer, Siemens SMART using Mo-Kα radiation (0.71073 Å); temperature of data collection 173 K.
[b] Structure was refined on F_o^2 using all data; the value of R_1 is given for comparison with older refinements based on F_o with a typical threshold of F >_ 4 σ(F).
[c] $wR_2 = [\Sigma[w(F_o^2-F_c^2)^2]]^{1/2}$ where $w^{-1} = \sigma^2(F_o^2) + (aP)^2 + (bP)$ and $P = [\max(F_o^2,0) + 2F_c^2]/3$

Table 8. Pyridyl/thiazole crystallographic data.[a]

Compound	$[Cd_2(L^8)_2][ClO_4]_2$
Formula	C 29.33, H 29.33, Cd 1.33, Cl 2.67, N 10.67, O10.67, S 2.67
M	1031.86
System, space group	Monoclinic, C2/C
a / Å	22.217(4)
b / Å	11.429(2)
c / Å	23.837(5)
α / °	90.0
β / °	112.17(3)
γ / °	90.0
U / $Å^3$	5605.4(19)
Z	6
μ / mm^{-1}	1.182
Reflections collected: Total, independent, R_{int}	31699
Final R_1, wR_2 [b,c]	0.0162, 0.0222, 0.0551

[a] Details in common: diffractometer, Siemens SMART using Mo-Kα radiation (0.71073 Å); temperature of data collection 173 K.
[b] Structure was refined on F_o^2 using all data; the value of R_1 is given for comparison with older refinements based on F_o with a typical threshold of F >_ 4 σ(F).
[c] $wR_2 = [\Sigma[w(F_o^2-F_c^2)^2]]^{1/2}$ where $w^{-1} = \sigma^2(F_o^2) + (aP)^2 + (bP)$ and $P = [\max(F_o^2,0) + 2F_c^2]/3$

Table 9. Pyridyl/thiazole crystallographic data.[a]

Compound	$[Ru(L^{11})][PF_6]_2$
Formula	C 38, H 38, Cl 2, N 6, O 13, Ru
M	958.71
System, space group	Triclinic, P-1
a / Å	12.054(2)
b / Å	12.566(3)
c / Å	13.122(3)
α / °	101.38(3)
β / °	91.89(3)
γ / °	91.01(3)
U / $Å^3$	1946.8(7)
Z	2
μ / mm^{-1}	0.616
Reflections collected: Total, independent, R_{int}	3631
Final R_1, wR_2 [b,c]	0.1222, 0.2265

[a] Details in common: diffractometer, Siemens SMART using Mo-Kα radiation (0.71073 Å); temperature of data collection 173 K.
[b] Structure was refined on F_o^2 using all data; the value of R_1 is given for comparison with older refinements based on F_o with a typical threshold of F >_ 4 σ(F).
[c] $wR_2 = [\Sigma[w(F_o^2-F_c^2)^2]]^{1/2}$ where $w^{-1} = \sigma^2(F_o^2) + (aP)^2 + (bP)$ and $P = [\max(F_o^2,0) + 2F_c^2]/3$

APPENDIX II – PUBLICATIONS